The Role of the Bundle Sheath in the Leaf Development of C_3 plants

Inaugural-Dissertation

zur Erlangung des Doktorgrades
der Mathematisch-Naturwissenschaftlichen Fakultät der
Heinrich-Heine-Universität Düsseldorf

vorgelegt von

Christian Rosar
aus Düsseldorf

Düsseldorf, Oktober 2012

aus dem Institut für Biochemie der Pflanzen
der Heinrich-Heine-Universität Düsseldorf

Gedruckt mit der Genehmigung der
Mathematisch-Naturwissenschaftlichen Fakultät der
Heinrich-Heine-Universität Düsseldorf

Referent: Prof. Dr. A. P. M. Weber
Koreferent: Prof. Dr. R. Simon

Tag der mündlichen Prüfung: 6.12.2012

Erklärung

Ich habe die vorliegende Dissertation eigenständig und ohne unerlaubte Hilfe angefertigt. Die Dissertation habe ich in der vorgelegten oder in ähnlicher Form noch bei keiner anderen Institution eingereicht. Ich habe bisher keine erfolglosen Promotionsversuche unternommen.

Düsseldorf, 29.10.2012

Christian Rosar

Contents

Abbreviations

5`MP	5`-monophosphate
7G	7-glucoside
9G	9-glucoside
AA	amino acid
AB	antibody
ABA	abscisic acid
AB_{RE}	antibody against RE
ACC	1-aminocyclopropane-1-carboxylic acid
ade	adenine
ado	adenosine
ADP	adenosine diphosphate
ADP	adenosine-5`-diphosphate
ala	alanine
alb	albino
alx	altered APX2 expression
am	albomaculans
AMP	adenosine-5`-monophosphate
AOX	alternative oxidase
AP	alkaline phosphatase
APX	ascorbate peroxidase
arb. units	arbitrary units
ARR5	Arabidopsis response regulator5
asn	asparagine
asp	aspartate
ATase	glutamine aminotransferase
atd	amidophosphoribosyl-transferase deficient
ATP	adenosine triphosphate
ATP	adenosine-5`-triphosphate
aver.	average
BA	6-benzyladenine, 6-benzylaminopurine
BF	bright field
BL	brassinolide
BMFZ	Biologisch Medizinisches Forschungszentrum der HHU Düsseldorf
bp	base pair
BS	bundle sheath
BSA	bovine serum albumin
C	carbon or carbohydrate
car	carbamoylphosphate synthase
cas	cycloartenol-synthase
cDNA	complementary DNA/copy DNA
chl	chlorophyll
chm	chloroplast mutator
chs	chilling sensitive
cia	chloroplast import apparatus
cla	cloroplastos alterados

cm	centimeter
col-0	columbia-0
CPS	carbamoylphosphate synthase
cTP	chloroplast targeting transit peptide
cue1	chlorophyll a/b binding protein (CAB) gene underexpressed1
cycB	cyclin B
cys	cysteine
cZ	cis zeatin
DCG	dehydrodoconiferyl alcohol glucoside
dcl	defective chloroplasts and leaf-mutable
DHZ	dihydrozeatin
DiT	dicarboxylate translocator
DNA	desoxy-ribonucleid acid
dov	differential development of vasculature associated cells
dpg	days post germination
DR5	direct repeat 5
DTT	dithiothreitol
DUF	domain of unknown function
DXP	1-deoxy-D-xylulose 5-phosphate synthase
E. coli	Escherichia coli
EDTA	ethylenediaminetetraacetic acid
EMS	ethyl methane sulfonate
En-2	Enkheim-2
F	filial generation
FA	fatty acid
FP	forward primer
FtsH	filamentation temperature sensitive
F_v/F_m	ratio of variable fluorescence to maximum fluorescence
FW	fresh weight
GABA	γ-amino butyric acid
GDC	glycine decarboxylase
gDNA	genomic DNA
GFP	green fluorescence protein
GlnaseD	glutaminase domain
glu	glutamate
gly	glycine
GMP	guanosine-5`-monophosphate
GPT	glucose-6-phosphate/phosphate translocator
gua	guanine
GUN	genome uncoupled
guo	guanosine
GUS	beta-glucuronidase
h	hour
HHU	Heinrich-Heine Universität
his	histidine
HMA	heavy metal P_{1b}-ATPase
hsp	heat shock promoter
hyp	hypoxanthine

IAA	indole-3 acetic acid
IAAGlu	indole-3-acetyl-glutamate
IAAsp	indole-3-acetyl-aspartate
IE	inner envelope
IF	infiltration buffer
ile	isoleucine
im	immutans
IMP	Inosine-5`-monophosphate
ino	inosine
iP	N_6-(Δ^2-isopently)adenine
iPGAM	2-3-bisphosphoglycerate-independent phosphoglycerate mutase
kas	ß-keto[acyl carrier protein] synthase
kbp	kilo base pair
KCl	sodium chloride
kDa	kilo Dalton
KOH	sodium hydroxide
L1, L2, L3	cell layers of the SAM
lcd	lower cell density
LD	long day
Ler	Landsberg erecta
leu	leucine
LMD	laser microdissection
lvr	lovastatin-resistent
M	mesophyll or marker
mcd	mesophyll cell defective
mdl	maternal distorted leaf
MEP	2-C-methyl-erythritol-4-phosphate
MES	2-(*N*-morpholino)ethanesulfonic acid
met	methionine
$MgCl_2$	magnesium chloride
min	minute
MJas	methyl jasmonates
mL	milliliter
mM	millimolar
mRNA	messenger RNA
MS	Murashige Skoog
msh	mutS homolog
mtDNA	mitochondrial DNA
N	nitrogen
n	number of replicates
n.a.	not assigned
Na_3PO_4	sodium phosphate
NaCl	sodium chloride
$NADP^+$	nicotinamide adenine dinucleotide phosphate
NaH_2PO_4	sodiumhydrogen phosphate
NCED	nine-cis-epoxy carotenoid diooxygenase
nd	not determined
nm	nanometer

ntrc	NADPH-thioredoxin reductase
OE	outer envelope
OEP	outer envelope protein
OG	O-glucoside
ORF	open reading frame
osb	organellar single strand binding protein
OX	overexpressor
p	p-value (statistics)
pac	pale cress
PCR	polymerase chain reaction
PDS	phytoene desaturase
PEN	polyethylene naphthalate
PEP	phosphoenolpyruvate
PGA	phosphoglyceric acid
phe	phenylalanine
$PMA1_{Pro}$	promoter of the plasma membrane H^+-ATPase
PPDK	pyruvate/orthophosphate dikinase
PPT	phosphoenolpyruvate/phosphate translocator
PQ	plastoquinone
PR5	pathogenesis related 5
PRA	5-phosphoribosylamine
PRPP	5-phosphoribosyl-1-pyrophosphate
PRSAD	5-phosphoribosylamine (PRA) synthase domain
PS	photosystem
$P_{short,RE}$	short promoter of RE
PTOX	plastid terminal oxidase
puf	protein of unknown function
Q_b	plastoquinone B
qRT-PCR	quantitative real time PCR
R	riboside
re	reticulata
RE_{long}	long splice isoform of RE
RE_{short}	short splice isoform of RE
RF	recombination frequency
RGR	relative growth rate
RIN	RNA integrity number
RNA	ribonucleid acid
RNAi	RNA interference
ROS	reactive oxygen species
RP	reverse primer
rRNA	ribosomal RNA
RS	restriction site
RT	room temperature
RuBisCo	ribulose-1,5-bisphosphate-carboxylase/oxygenase
S	Svedberg
S.D.	standard deviation
S.E.	standard error
SAM	shoot apical meristem

SC-U	synthetic complete medium without uracil
ser	serine
sig. lev.	significance level
smo	small organ
SSPL	simple sequence length polymorphism
T-DNA	transfer DNA
TAE	tris-acetate-EDTA
Thf	thylakoid formation
thr	threonine
TM	transmembrane
TPT	triosephosphate phosphate/phosphate translocator
tris	tris(hydroxymethyl)aminomethane
trp	tryptophan synthetase or tryptophan
tyr	tyrosine
tZ	trans zeatin
ub	ubiquitin
UTR	untranslated region
UV	ultraviolett
val	valine
var	yellow variegated
vdl	variegated and distorted leaf
ven	venosa
VIPP	vesicle-inducing protein in plastids
vs.	versus
w/v	weight per volume
w/w	weight/weight
wco	white cotyledons
WGE	wheat germ extract
xan	xanthine
xao	xanthosine
XPT	pentose-phosphate/phosphate translocator
XVE	estradiol activated promoter
YFP	green fluorescence protein
YNB	yeast nitrogen base
ys	yellow stripe
z2	rice zebra2
µE	µ Einstein

I. Preface

This PhD thesis is divided into independent sections, written as manuscripts. The *introduction* to this work is given in form of the *Manuscript 1*, the review “Leaf development of reticulated and variegated mutants: metabolic vs. cellular syndromes and the role of the bundle sheath”. The review gives an overview of the reticulated mutants, including a section about *dov1* and *re*, which are described in *Manuscript 2* (Rosar et al., 2012) and in *Manuscript 3*, respectively. *Manuscripts 1* and *3* are presented as submission-ready versions. Further experiments that were not described in the *Manuscripts* are included in the *Addendum*. The PhD thesis was organized this way to create publishable units.

II. Aim of the PhD thesis

The aim of the PhD thesis is to understand leaf development in the C_3-plant *Arabidopsis thaliana*. While in C_4-plants, photosynthesis is compartmentalized between mesophyll (M) and bundle sheath (BS), this is not the case for C_3-photosynthesis. A series of reticulated *Arabidopsis* leaf mutants has a well differentiated vasculature and BS but an aberrant M, which is mirrored as a dark vein on a pale leaf lamina. The classical reticulated mutants are *reticulata* (*re*) (González-Bayón et al., 2006), *chlorophyll a/b binding protein (CAB) gene underexpressed1* (*cue1*) (Streatfield et al., 1999), *differential development of vasculature associated cells1* (*dov1*) (Kinsman and Pyke, 1998), and *venosa3* and *6* (*ven3* and *ven6*) (Mollá-Morales et al., 2011). By the start of the project, only the function of *cue1* was identified. *Cue1* is defective in the plastidic import of phospho*enol*pyruvate (PEP) (Streatfield et al., 1999), a key substrate for the synthesis of aromatic amino acids and thereof derived secondary compounds. These metabolites were hypothesized to generate a signal that drives M differentiation (Streatfield et al., 1999). Our group hypothesizes that this signal is derived from the BS and a restriction of the signal causes the reticulated leaf phenotype (*Manuscripts 1*, *2*, and *3*). *Ven3* and *ven6* are defective in arginine metabolism (Mollá-Morales et al., 2011).

It was the goal to decipher the role of the BS in *Arabidopsis* with regard to the development of the inner leaf architecture. Two approaches complementing each other were performed. Two single gene approaches aimed at establishing the function of the gene products defective in (i) *dov1* and (ii) *re*. A global un-biased approach aimed to determine the comparative transcriptional profiles of BS, vasculature and M in wild-type plants, using laser microdissection (LMD) coupled to downstream transcriptional profiling (iii).

(i) As a hallmark mutant, *dov1* was used to dissect the differential development of BS and M cells. Studies with *dov1* essentially contributed to the knowledge that the vasculature develops prior to the M (Kinsman and Pyke, 1998). The genetic nature of *dov1*, however, remained elusive. Hence, we aimed at genetically cloning the affected gene. The gene was mapped to encode for ATase2, the first enzyme in *de novo* purine biosynthesis. The effect of the purine-derived phytohormone cytokinin on plant performance was assessed by growth kinetic analysis, cytokinin profiling, and cytokinin activity determination (Rosar et al., 2012).

(ii) *Re*, first described more than fifty years ago (Rédei and Hironyo, 1964), was morphologically described, mapped and found to be allelic to *lower cell density1-1* (*lcd1-1*) (González-Bayón et al., 2006). The function of *RE*, however, remains elusive. Using a combination of cluster analysis of publicly available data, microarray analysis, metabolic profiling and biochemical mutant complementation assays we narrowed down RE to be involved in basic amino acid metabolism (*Manuscript 3*). Experimental evidence promoted

that RE is a novel class of plastidic amino acid transporters (*Addendum*). Further work is required to ultimately assign a function to the RE protein.

(iii) The role of the BS in C_3-plants has been largely neglected, while it`s role in C_4-plants is well established. A comparative transcriptional profile of the BS, the vasculature, and the M of *Arabidopsis* was initiated in order to get insights into the transcripts repertoire of the different cell types. RNA in leaf sectors was fixed with ethanol/acetic acid, dehydrated in an ethanolic dilution series, and embedded in paraffin. Microtome cut cross sections of embedded tissues were fixed on glass slides and deparaffinized. RNA of whole cross sections was isolated in a quality allowing subsequent cDNA synthesis and deep sequencing. Time limitation due to starting the project at the end of the second PhD year did not allow the sampling of enough tissue specific material for sequencing (*Addendum*).

References

González-Bayón R, Kinsman EA, Quesada V, Vera A, Robles P, Ponce MR, Pyke KA, Micol JL (2006) Mutations in the *RETICULATA* gene dramatically alter internal architecture but have little effect on overall organ shape in *Arabidopsis* leaves. Journal of Experimental Botany **57:** 3019-3031

Kinsman EA, Pyke KA (1998) Bundle sheath cells and cell-specific plastid development in *Arabidopsis* leaves. Development **125:** 1815-1822

Mollá-Morales A, Sarmiento-Mañús R, Robles P, Quesada V, Pérez-Pérez JM, González-Bayón R, Hannah MA, Willmitzer L, Ponce MR, Micol JL (2011) Analysis of *ven3* and *ven6* reticulate mutants reveals the importance of arginine biosynthesis in *Arabidopsis* leaf development. The Plant Journal **65:** 335-345

Rédei GP, Hironyo Y (1964) Linkage studies. Arabidopsis Information Service **1:** 9-10

Rosar C, Kanonenberg K, Nanda AM, Mielewczik M, Bräutigam A, Novák O, Strnad M, Walter A, Weber APM (2012) The leaf reticulate mutant *dov1* is impaired in the first step of purine metabolism. Molecular Plant doi: 10.1093/mp/sss045

Streatfield SJ, Weber A, Kinsman EA, Häusler RE, Li JM, Post-Beittenmiller D, Kaiser WM, Pyke KA, Flügge UI, Chory J (1999) The *phosphoenolpyruvate/phosphate translocator* is required for phenolic metabolism, palisade cell development, and plastid-dependent nuclear gene expression. Plant Cell **11:** 1609-1621

III.1 Summary

Reticulate *Arabidopsis* leaf mutants are defective in processes governing the development of the inner leaf architecture. These mutants are aberrant in the mesophyll (M) but have an intact vasculature and bundle sheath (BS). While the role of the BS in C_4 plants is well established, knowledge about the BS in C_3 plants is scarce. Reticulate mutants are defective in primary metabolism. While the molecular identity of the reticulated mutants *cue1* (Streatfield et al., 1999) and *ven3/6* (Mollá-Morales et al., 2011) was established, the nature of *dov1* (Kinsman and Pyke, 1998) and *re* (González-Bayón et al., 2006) was unknown at the beginning of the PhD project. In this study, we genetically mapped *DOV1* and identified the function of the gene product as a key enzyme in purine biosynthesis (Rosar et al., 2012, *Manuscript 2*). In a comparative approach with *cue1*, we showed that *RE* is involved in amino acid metabolism (*Manuscript 3*). Due to strong experimental evidence RE is further hypothesized to transport amino acids across plastid envelopes (*Addendum*).

By positional cloning, it was demonstrated that *dov1* is defective in the ATase2 gene, encoding the glutamine phosphoribosyl aminotransferase 2 (ATase2), an enzyme of the first step of *de novo* purine biosynthesis (*Manuscript 2*). Enzyme activity tests demonstrated lowered activity for the mutated protein. The purine-derived cytokinins, phytohormones promoting plant growth, are present at lower levels in the mutant. Cytokinin feeding and hormone reporter assays showed that likely lowered purine levels and not decreased cytokinin concentrations are primarily responsible for the *dov1* phenotype. The influence of purine metabolism was assessed with systematic growth screens.

Re was first described more than fifty years ago (Rédei and Hironyo, 1964), morphologically described and genetically mapped about forty years later (González-Bayón et al., 2006). Transcriptional profiling, extensive metabolite analysis, hormone level determination and hormone response patterns, and a comparison to the characterized *cue1* mutant, suggested that *re* is affected in leaf amino acid metabolism (*Manuscript 3*). *Cue1*, *ven3*, *ven6*, and other reticulated mutant are affected in amino acid metabolism. RE´s function, however, remains elusive.

The basis of the reticulated phenotype is discussed as either caused by a limited supply of primary metabolites or an affected signaling event. These hypotheses and a hypothesis of a partitioned synthesis of amino acids between M and vasculature/BS are presented in *Manuscript 1*, a review. In this review, reticulated and variegated mutants are compared and underlying hypotheses are critically discussed. Further experimental evidence prompted us to hypothesize that RE is a novel plastidic amino acid transporter (*Addendum*).

The thus far established experimental setup for tissue specific transcriptional profiling is summarized in the *Addendum*. High quality cross-sections of fixed and paraffinized leaf tissue were achieved, harboring RNA of high integrity for further transcriptional analysis.

References

González-Bayón R, Kinsman EA, Quesada V, Vera A, Robles P, Ponce MR, Pyke KA, Micol JL (2006) Mutations in the *RETICULATA* gene dramatically alter internal architecture but have little effect on overall organ shape in *Arabidopsis* leaves. Journal of Experimental Botany **57:** 3019-3031

Kinsman EA, Pyke KA (1998) Bundle sheath cells and cell-specific plastid development in *Arabidopsis* leaves. Development **125:** 1815-1822

Mollá-Morales A, Sarmiento-Mañús R, Robles P, Quesada V, Pérez-Pérez JM, González-Bayón R, Hannah MA, Willmitzer L, Ponce MR, Micol JL (2011) Analysis of *ven3* and *ven6* reticulate mutants reveals the importance of arginine biosynthesis in *Arabidopsis* leaf development. The Plant Journal **65:** 335-345

Rédei GP, Hironyo Y (1964) Linkage studies. Arabidopsis Information Service **1:** 9-10

Rosar C, Kanonenberg K, Nanda AM, Mielewczik M, Bräutigam A, Novák O, Strnad M, Walter A, Weber APM (2012) The leaf reticulate mutant *dov1* is impaired in the first step of purine metabolism. Molecular Plant doi: 10.1093/mp/sss045

Streatfield SJ, Weber A, Kinsman EA, Häusler RE, Li JM, Post-Beittenmiller D, Kaiser WM, Pyke KA, Flügge UI, Chory J (1999) The *phosphoenolpyruvate/phosphate translocator* is required for phenolic metabolism, palisade cell development, and plastid-dependent nuclear gene expression. Plant Cell **11:** 1609-1621

III.2 Zusammenfassung

Retikulierte *Arabidopsis*-Mutanten sind in der Entwicklung der inneren Blattarchitektur gestört, denn sie weisen ein desintegriertes Mesophyll (M) aber intaktes Leitgewebe und eine intakte Bündelscheide (BS) auf. Im Gegensatz zu C_4-Pflanzen ist die Rolle der BS in C_3-Pflanzen kaum untersucht. Retikulierte Mutanten sind im Primärmetabolismus stark beeinträchtigt. Während die molekulare Identität der klassischen retikulierten Mutante *cue1* (Streatfield et al., 1999), *ven3* und *ven6* (Mollá-Morales et al., 2011) auf Proteinebene aufgeklärt wurde, war der defekte Genlokus der Mutante *dov1* (Kinsman and Pyke, 1998) zu Beginn des Projektes unbekannt. Zwar war *RE* genetisch lokalisiert, die Proteinfunktion jedoch unbekannt (González-Bayón et al., 2006).

In der vorliegenden Arbeit wurde die Funktion des DOV1-Proteins als Schlüsselenzym der Purin-Biosynthese identifiziert (Rosar et al., 2012, *Manuscript 2*) und die Funktion von RE in einer komparativen Studie auf den Aminosäurestoffwechsel eingeschränkt (*Manuscript 3*). Ferner liegen experimentelle Befunde vor, die RE als einen plastidären Aminosäuretransporter erscheinen lassen (*Addendum*).

Es konnte gezeigt werden, dass *dov1* im ATase2 Gen mutiert ist, das für die Glutaminphosphoribosylaminotransferase 2 (ATase2) kodiert. Dieses Enzym katalysiert die erste Reaktion in der *de novo* Purinbiosynthese. Enzymaktivitätsmessungen zeigten, dass das mutierte Protein DOV1 in seiner Aktivität herabgesetzt ist. Die Konzentration von Zytokininen – Purinderivaten – war in *dov1*-Pflanzen erniedrigt. Zytokinine sind Pflanzenhormone, die das Wachstum positiv beeinflussen. Fütterung von Zytokinin und Hormon-Reporter-Experimente zeigten, dass sehr wahrscheinlich die erniedrigten Puringehalte und nicht die erniedrigten Zytokininkonzentrationen primär ursächlich für den *dov1* Phänotyp sind. Der Einfluss des Purinstoffwechsels auf das Pflanzenwachstum wurde in systematisierten Wachstumsexperimenten gezeigt (Rosar et al., 2012, *Manuscript 2*).

Re-Mutanten wurden vor mehr als fünfzig Jahren das erste Mal beschrieben (Rédei and Hironyo, 1964), später genetisch kartiert und morphologisch charakterisiert (González-Bayón et al., 2006). Transkriptionsstudien, intensive Metabolitanalysen, Hormonkonzentrationsbestimmungen, Hormon-Antworten in Reporter-Pflanzenlinien und ein Vergleich mit der gut charakterisierten *cue1*-Mutante zeigte, das *re* im Aminosäurestoffwechsel beeinflusst ist (*Manuskript 2*). Auch *cue1*, *ven3* und *ven6* sind im Aminosäurestoffwechsel beeinflusst. Die genaue Funktion von RE bleibt jedoch unbekannt.

Die Ursache des retikulierten Blattphänotyps wird im Zusammenhang einer limitierten Verfügbarkeit von Primärmetaboliten oder einem gestörten Signalweg diskutiert. Diese Hypothesen, und die einer Kompartimentierung des Aminosäurestoffwechsels zwischen Leitgewebe/BS und M, werden im *Manuscript 1* diskutiert, welches als *Review* formuliert ist.

In diesem *Review* werden retikulierte und variegierte Mutanten verglichen und die zugrundeliegenden Hypothesen kritisch diskutiert.

Die soweit etablierten experimentellen Befunde und geschaffenen Grundlagen für das gewebsspezifische transkriptionelle Profil von M und BS werden im *Addendum* zusammengefasst. Es konnten in Paraffin fixierte Gewebeschnitte hoher Qualität erzeugt werden, die eine Isolation reiner RNA für transkriptionelle Analysen erlauben.

Literatur

González-Bayón R, Kinsman EA, Quesada V, Vera A, Robles P, Ponce MR, Pyke KA, Micol JL (2006) Mutations in the *RETICULATA* gene dramatically alter internal architecture but have little effect on overall organ shape in *Arabidopsis* leaves. Journal of Experimental Botany **57:** 3019-3031

Kinsman EA, Pyke KA (1998) Bundle sheath cells and cell-specific plastid development in *Arabidopsis* leaves. Development **125:** 1815-1822

Mollá-Morales A, Sarmiento-Mañús R, Robles P, Quesada V, Pérez-Pérez JM, González-Bayón R, Hannah MA, Willmitzer L, Ponce MR, Micol JL (2011) Analysis of *ven3* and *ven6* reticulate mutants reveals the importance of arginine biosynthesis in *Arabidopsis* leaf development. The Plant Journal **65:** 335-345

Rédei GP, Hironyo Y (1964) Linkage studies. Arabidopsis Information Service **1:** 9-10

Rosar C, Kanonenberg K, Nanda AM, Mielewczik M, Bräutigam A, Novák O, Strnad M, Walter A, Weber APM (2012) The leaf reticulate mutant *dov1* is impaired in the first step of purine metabolism. Molecular Plant doi: 10.1093/mp/sss045

Streatfield SJ, Weber A, Kinsman EA, Häusler RE, Li JM, Post-Beittenmiller D, Kaiser WM, Pyke KA, Flügge UI, Chory J (1999) The *phosphoenolpyruvate/phosphate translocator* is required for phenolic metabolism, palisade cell development, and plastid-dependent nuclear gene expression. Plant Cell **11:** 1609-1621

IV.
Manuscript 1

Leaf development of reticulated and variegated mutants:
metabolic vs. cellular syndromes and
the role of the bundle sheath

Leaf development of reticulated and variegated mutants: metabolic vs. cellular syndromes and the role of the bundle sheath

Christian Rosar[a], Andrea Bräutigam[a], Andreas P. M. Weber [a,b]

a Institute for Plant Biochemistry and Cluster of Excellence on Plant Sciences (CEPLAS), Heinrich-Heine-Universität, Universitätsstraße 1, D-40225 Düsseldorf
b to whom the correspondence should be addressed. Email: aweber@uni-duesseldorf.de; fax: +49-211-8113706; phone: +49-211-8112347

Abstract

Leaves are specialized planar organs for photosynthesis that act as solar panels. Light is converted into chemical energy, and organic metabolites are generated. Research has focused on the chloroplast as a key player in photosynthetic processes. However, less is known about the role of plastids in leaf development. Leaf development has been largely investigated at it`s early events, mainly in the shoot apical meristem (SAM) and leaf primordia. There are mutants that are defective in the overall organization of the leaf shape and in the organization of the internal leaf structure. The latter mutants were categorized as reticulated and variegated leaf mutants, which share an aberrant mesophyll (M). While most reticulated mutants have dark veins on a pale leaf lamina, variegated mutants show leaves with white and green patches spanning the vasculature. Nearly all reticulated and variegated mutants characterized to date are affected in proteins associated with a function in plastids. Because leaves are meaningful models for organ morphogenesis, these mutants are powerful tools to investigate leaf development. Reticulated mutants are either disturbed in plastidic amino acid-, nucleotide- or protein biosynthesis. The majority of variegated mutants is affected in thylakoid located proteins, affected in carotenoid biosynthesis, photoprotective mechanisms, or thylakoid formation. The discrimination of variegation and reticulation is not always distinct as compiled for ATase2 mutants in this review. Hypotheses explaining the mechanisms of variegation and reticulation will be presented and differences elaborated. The focus will be on the *threshold model*, *supply* and *signaling* hypotheses. The role of the bundle sheath (BS) in leaf development, as inferred from studies of reticulated mutants, is critically discussed. We concentrate on mutants of *Arabidopsis thaliana*, but also include other plant species.

Leaf morphogenesis and growth

Plants differentiate on their mother plant from a zygote, which grows and differentiates into the embryo. In dicotyledenous plants the embryo harbors the basal root meristem, a central region hypocotyl, and the SAM, which is flanked by two cotyledons (Barton, 2010). The SAM consists of a central and a peripheral zone that delivers founder cells (Furner and Pumfrey, 1992; Irish and Sussex, 1992; Schnittger et al., 1996; Barton, 2010). Founder cells on the flanks of the SAM differentiate into leaf primordia, histologically identifiable bulbs that grow out to lateral organs such as leaves, stems, and the floral structures during the plant`s whole lifespan (Fleming, 2006; Barton, 2010; Byrne, 2012). In this developmental process most plants, including *Arabidopsis*, establish symmetric leaves. This symmetry consists of three components: (i) proximodistal (base to tip), (ii) dorso-ventral, i.e. adaxial (upper) and abaxial (lower) site, and (iii) mediolateral symmetry (from left to right).

In a typical leaf, the photosynthetic active M, i.e. spongy and palisade parenchyma, is wedged between the cuticulated upper and lower epidermis. The M cells are arranged adjacent to each other without large air spaces, which are restricted to the leaf inner space around the stomata. Embedded in the M, the vasculature, consisting of phloem, xylem and associated cells, forms a pipeline system that transports water, solutes and assimilates. The vasculature is surrounded by the BS, which is made of one, as for *Arabidopsis*, or multiple cell layers (Leegood, 2008).

To understand leaf development, mutants have been isolated and characterized in *Arabidopsis* (Rédei, 1963; Röbbelen, 1968). Among these are those with aberrant leaf shape and size, and those with aberrant internal leaf architecture (Rosar et al., 2012). The differentiation and growth of leaves is subdivided into three different stages: (i) leaf initiation, (ii) the development of the leaf lamina, and (iii) further modifications of the leaf lamina (Byrne, 2012). The ultimate size of a leaf depends on meristematic growth, which fixes the upper boundary of leaf size. Leaf size is then realized by cell expansion (Fleming, 2006; Tsukaya, 2006; Anastasiou and Lenhard, 2007). It was hypothesized that overall leaf size is regulated rather by epidermal cell growth than by M cell proliferation (González-Bayón et al., 2006; Bemis and Torii, 2007; Savaldi-Goldstein et al., 2007; Javelle et al., 2011; Pérez-Pérez et al., 2011; Powell and Lenhard, 2012).

During leaf initiation (i), the three cell layers L1, L2 and L3 of the SAM become transcriptionally distinct, and give rise to the leaf primordium (Fleming, 2002; Tsiantis and Hay, 2003; Byrne, 2005; Canales et al., 2005; Fleming, 2006; Byrne, 2012). This initial differentiation drives the spatial and temporal control of leaf development (Byrne, 2005; Fleming, 2006). The L1 layer gives rise to the epidermis, the multilayer of L3 cells to the vasculature, and L2 cells to the rest of the leaf, e.g. palisade and spongy parenchyma (Furner and Pumfrey, 1992; Irish and Sussex, 1992; Poethig, 1997; Barton, 2010).

Differentiation is based on transcription factors interacting with phytohormones, such as cytokinins (Yanai et al., 2005; Zhao et al., 2010; Yoshida et al., 2011), auxins (Reinhardt et al., 2003; Scanlon, 2003; Heisler et al., 2005; Zhao et al., 2010; Yoshida et al., 2011), and gibberellic acids (Jasinski et al., 2005). The role of phytohormones has been reviewed in detail (Byrne, 2012). It has been hypothesized that variegated phenotypes with undifferentiated or missing plastids are comparable to mosaic phenotypes of mammals and are thus fixed at the leaf initiation stage (Yu et al., 2007).

The leaf lamina is established through polar growth and lateral expansion. Internal tissues differentiate and dorso-ventral symmetry is established by transcription factors, trans-acting small interfering RNAs, and phytohormones (Byrne, 2012). The M of reticulated plants is altered by either a decreased cell number and/or cell size (Kinsman and Pyke, 1998; Streatfield et al., 1999; González-Bayón et al., 2006; Jing et al., 2009; Lepistö et al., 2009; Rosar et al., 2012). These parameters are governed by two successive processes, which are mainly controlled by cytokinins and auxins, respectively: cell proliferation and expansion (Mizukami, 2001; Anastasiou and Lenhard, 2007; Tsukaya, 2008). Reticulated and variegated mutants are affected in the differentiation of internal leaf structure and in leaf shape. Thus, the connection of lamina shape and internal tissue differentiation can be studied with these mutants as tools.

Reticulated leaf mutants

Three morphological classes of reticulated mutants have been described (González-Bayón et al., 2006), i.e. leaves with (i) dark green veins on a green lamina, (ii) green veins on a pale lamina, and (iii) a pale vasculature on a green lamina, with (i) and (ii) being similar. Most reticulated mutants belong to the classes (i) and (ii). The inverse reticulated pattern of the class (iii) is found in *Arabidopsis* mutants, in which RNAi-mediated cell-to-cell communication is affected (Dunoyer et al., 2010) and chlorophyll synthesis in the BS is silenced (Janacek et al., 2009). In classes (i) and (ii), the interveinal M cells are reduced in size and/or number, which causes the pale green color. The vasculature and the BS are well differentiated.

Amino acids are crucial for leaf development and growth (Schurr et al., 2000; Ruuhola et al., 2003) and inhibition of their synthesis is fatal for plants (Muralla et al., 2007). The alteration of metabolic pathways, such as amino acid metabolism, affects leaf morphology (Fleming, 2006; Jing et al., 2009). Some amino acid biosynthesis mutants, e.g. in threonine synthesis (Bartlem et al., 2000), are retarded in growth but have green leaves. *Cue1*, *ven3*, *ven6*, and *trp2* are affected in amino acid metabolism. *Cue1* is defective in the shikimate

pathway, and thus in the synthesis of aromatic amino acids and derived secondary phenolic compounds (Streatfield et al., 1999; Voll et al., 2003). *Ven3* and *ven6* are impaired in arginine (Mollá-Morales et al., 2011) and *trp2* in tryptophan (trp) synthesis (Last et al., 1991; Barczak et al., 1995; Jing et al., 2009). Overexpression of a phenylpropanoid enzyme in tobacco causes interveinal chlorosis and a disturbed M structure (Merali et al., 2012), corresponding to the definition of reticulation. Similar phenotypes are observed if phenylpropanoid metabolic pathways are altered (Elkind et al., 1990; Piquemal et al., 1998).

ATase2 mutants are disturbed in purine metabolism and have patchy reticulated leaves. That is, while white patches contain green major veins, the white leaf areas span minor veins. This is in stark contrast to the evenly reticulated mutants *cue1*, *ven3*, *ven6*, *ntrc*, and *re*. Several ATase2 alleles have been described: *dov1*, *atd2*, *cia1*, and *alx13* (Kinsman and Pyke, 1998; Hung et al., 2004; Woo et al., 2011; Rosar et al., 2012). A tobacco mutant repressed in carbamoylphosphate synthase activity, and thus impaired in the *de novo* pyrimidine synthesis, is reticulated (Lein et al., 2008). Suppression of all known pyrimidine *de novo* synthesis genes in tobacco did not cause a visible phenotype besides growth reduction (Schröder et al., 2005). However, biochemical inhibition of the pyrimidine *de novo* pathway led to growth reduction and chlorosis but neither reticulation nor variegation (Bassett et al., 2003). A mutant defective in uracil phosphoribosyltransferase, an enzyme of the pyrimidine *salvage pathway*, has chlorotic pale green leaves with decreased grana stacking (Mainguet et al., 2009).

Furthermore, reticulated and variegated mutants with deficiencies in the plastidic RNA synthesis and translational machinery have been described in *Arabidopsis* (Hricová et al., 2006; Horiguchi et al., 2011; Tiller et al., 2012) and other species (Börner and Sears, 1986; Hagemann, 1986; Hess et al., 1994; Yaronskaya et al., 2003). If ribosomal proteins do not accumulate correctly, an impact on leaf shape and growth was described (Van Lijsebettens et al., 1994). Studies in animals prompted to an essential function of ribosomal proteins in organ growth (Fleming, 2006). Similarly, plants treated with antibiotics interfering with the plastid-translation machinery display an aberrant M structure (Wycliffe et al., 2005), and both cell size and number is decreased (Feng et al., 2007; Jing et al., 2009). A mutated regulator of multiple metabolic processes, *ntrc* (Lepistö et al., 2009), causes reticulation. Finally, a tobacco photorespiratory mutant defective in the glycine decarboxylase shows an inverse reticulate phenotype (Lein et al., 2008).

Taken together, all characterized reticulated mutants are defective in either amino acid, purine synthesis or in plastid ribosomal activity. All processes are linked to each other and ultimately converge in the production of essential components of the cell. Amino acids are building blocks of proteins, which are synthesized by ribosomes, and need nucleic acids

for synthesis (Figure 1). This observation increases the chance of pleiotropic effects in the reticulated mutants, and drives the challenge to identify the primary cause of the phenotype.

Cue1 (chlorophyll a/b binding protein (CAB) gene underexpressed1)

Cue1 is a hallmark reticulate mutant, which is used as a phenotypical reference in this review. All other mutants will be described starting with their molecular identities. All mutants are briefly described in Table 1.

Cue1, of which six alleles are known, has reticulated cotyledons, rosette-, cauline-, young- and old leaves (Streatfield et al., 1999). This leaf pattern is caused by a decreased number of aberrant, smaller, and spherical rather than columellar palisade cells, which contain fewer and smaller chloroplasts (Li et al., 1995; Streatfield et al., 1999). The BS in *cue1* is normally developed, i.e. neither affected in size nor morphology nor in it´s chloroplast morphology and number (Li et al., 1995; Streatfield et al., 1999). *Cue1* is delayed in chloroplast and whole plant development, in line with much smaller leaves, a severe biomass (Li et al., 1995), and protein reduction (Voll et al., 2003). The penetrance of the phenotype is light intensity dependent. While *cue1* is reticulated under high-light, it is rather green under low-light (Streatfield et al., 1999). *Cue1* mutants have decreased chlorophyll and carotenoid levels (Li et al., 1995; Voll et al., 2003) along with a decreased photosystem II (PSII) capacity (López-Juez et al., 1998; Streatfield et al., 1999).

The *cue1* mutant was isolated in a genetic screen for decreased transcript levels of chlorophyll a/b binding proteins (Li et al., 1995; López-Juez et al., 1998). *Cue1* is defective in the phospho*enol*pyruvate/phosphate translocator (PPT1) of the chloroplast envelope membrane (Streatfield et al., 1999; Figure 1). PPT1 imports phospho*enol*pyruvate (PEP) into the chloroplast stroma (Fischer et al., 1997; Streatfield et al., 1999; Voll et al., 2003), an essential process, because PEP cannot be generated from 3-phosphogylcerate (3-PGA) via glycolysis due to a lack of phosphoglycerate mutase and/or enolase (Bagge and Larsson, 1986; Voll et al., 2003). PEP is required in the following processes: (i) fatty acid biosynthesis (Kleinig and Liedvogel, 1980; Benning, 2009); (ii) after conversion to pyruvate in branched chain amino acid synthesis (Schulze-Siebert et al., 1984; Kochevenko and Fernie, 2011), (iii) isoprenoid synthesis (Lichtenthaler et al., 1997), and (iv) the shikimate pathway for production of aromatic amino acids (Herrmann, 1995; Schmid and Amrhein, 1995; Herrmann and Weaver, 1999; Rippert et al., 2009; Maeda and Dudareva, 2012). Downstream reactions in phenylalanine metabolism produce phenolic secondary compounds (Schmid and Amrhein, 1995; Fischer et al., 1997; Knappe et al., 2003; Voll et al., 2003; Tzin and Galili, 2010).

While fatty acid contents are not lowered in *cue1* leaves (Streatfield et al., 1999), amino acid levels are deregulated with allover higher amino acid concentrations. Particularly,

arginine, glutamine, asparagine, urea, and nitrate are increased three to four fold in *cue1* (Streatfield et al., 1999). *Cue1* has decreased relative amounts of aromatic amino acids to total amino acids (Streatfield et al., 1999). However, quantitation showed that aromatic amino acids, apart from a 50% reduction of phenylalanine, are not dramatically lowered (Voll et al., 2003). Consequently, only phenylalanine-derived phenylpropanoids including flavonoids, anthocyanins, hydroxycinnamic acids and simple phenolics are diminished (Streatfield et al., 1999; Voll et al., 2003). If phenolic metabolism and monolignol biosynthesis in tobacco is impaired by overexpression of the transcription factor AmMY308, plants are reticulated (Tamagnone et al., 1998; Tamagnone et al., 1998). Phenylpropanoids exert a plethora of functions in plants (Vogt, 2010): they act as UV protectants (Schmelzer et al., 1988; Sheahan, 1996), antioxidants (Yamasaki et al., 1997; Grace and Logan, 2000; Pollastri and Tattini, 2011), constitute scaffold compounds like lignin or suberin (Holloway, 1983; Lewis and Yamamoto, 1990), are modulators of phytochrome responses (Murphy et al., 2000; Brown et al., 2001) and are involved in defense mechanisms (Kunkel and Brooks, 2002). In *cue1*, protective flavonoids are not produced, even under high-light conditions. Tyrosine is a precursor of tocopherol, vitamin K, and plastoquinone (Garcia et al., 1999; Hofius and Sonnewald, 2003). Due to a restriction of the shikimate pathway the plastoquinone (PQ) pool size is smaller and highly reduced (Streatfield et al., 1999). Possibly, a reduced PQ pool could generate a plastidic retrograde signal that leads to chlorosis in paraveinal regions.

The *cue1* leaf phenotype was rescued by addition of phenylalanine, tryptophan, and tyrosine (all amino acids together) to the growth medium (Streatfield et al., 1999; Voll et al., 2003). The PEP generation in *cue1* plastids by transgenic overexpression of PPT restored the visual and biochemical phenotype (Voll et al., 2003). Similar results were obtained when targeting the pyruvate/orthophosphate dikinase (PPDK) from the C_4 plant *Flaveria trinervia* to *cue1* plastids (Voll et al., 2003). Both experiments indicate that the shortage of PEP in the plastid stroma is the primary cause of the *cue1* phenotype (Voll et al., 2003). The resulting lowered aromatic amino acid or downstream secondary metabolites levels likely cause the phenotype (Streatfield et al., 1999; Voll et al., 2003). *Cue1* was also linked to a defect in cryptochrome mediated signaling (Voll et al., 2003). The *Arabidopsis* genome harbors two homologues: PPT1, expressed along the veins and PPT2, expressed in the whole leaf (Knappe et al., 2003). The PPT2 knockout *cue2* has no visible phenotype (Li et al., 1995).

***ipgam* double mutants (*ipgam1/ipgam2*)**

An *Arabidopsis ipgam1/ipgam2* double knock out of two isoforms of 2-3-bisphosphoglycerate-independent phosphoglycerate mutases (iPGAMs) is reticulated (Zhao and Assmann, 2011). These plastidic enzymes catalyze the formation of 3-PGA form 2-PGA, and are hampered in the provision of PEP to the plastid (Figure 1). The reticulated phenotype was credited to an altered amino acid metabolism (Zhao and Assmann, 2011), similarly to *cue1* (Voll et al., 2004). The double mutant was investigated in the context of disturbed stomatal movement (Zhao and Assmann, 2011). Additionally, they do not develop pollen and are male-sterile, a fact linked to a decreased energy provision (Li et al., 2010; Zhao and Assmann, 2011). PEP import into the plastid is essential for gametophyte and sporophyte development (Prabhakar et al., 2010). All other described reticulated and variegated mutants are fertile and do not show any constraints in reproduction.

***Ven3 and ven6* (*Venosa3 and venosa6*)**

A genetic screen for altered leaf phenotypes yielded the reticulated mutants *ven1* to *6*, with *ven2* allelic to *reticulata* (Berná et al., 1999). The nature of *ven1*, *ven3*, *ven4*, and *ven5* remain elusive. *Ven3* and *ven6*, however, were recently deciphered at the molecular level (Mollá-Morales et al., 2011). *VEN3* and *VEN6* encode for the small and the large subunit of the ornithine carbamoylphosphate synthase (CPS), synonymous to CarA and CarB, respectively (Mollá-Morales et al., 2011; Figure 1). Both genes are expressed in a vein-associated manner (Potel et al., 2009). Ornithine is converted by CPS to citrulline, which is further metabolized to arginine. Thus, in *ven3* and *6* the formation of citrulline and arginine is hampered, proven by diminished arginine levels (Mollá-Morales et al., 2011). Biochemical inhibition of CPS led to ornithine accumulation and a chlorotic phenotype (Patil et al., 1972; Turner and Mitchell, 1985). Since each *ven3* and *6* are not null alleles, they produce basal levels of arginine and survive (Mollá-Morales et al., 2011). The mutants` reticulated leaf phenotype is suppressed by exogenous application of citrulline and arginine. However, other phenotypic traits, such as a reduced leaf size, are partially restored (Mollá-Morales et al., 2011). In *Nicotiana tabacum*, the repression of the CPS large subunit leads to a reticulated phenotype, which was discussed with a focus on an affected pyrimidine metabolism (Lein et al., 2008). *Ven3* and *ven6* could also be linked to a defect in the pyrimidine metabolism. In plants, a single CPS is involved in both arginine and pyrimidine biosynthesis, which thus requires tight coordination (Slocum, 2005). Pyrimidine levels were not determined in *ven3* and *ven6* (Mollá-Morales et al., 2011).

While VEN3 and VEN6 are single copy genes, and are not masked by their homologs (Mollá-Morales et al., 2011), the recessive mutants *cue1, re, trp2*, and ATase2 mutants have

at least two homologues (Last et al., 1991; Knappe et al., 2003; Hung et al., 2004; González-Bayón et al., 2006; Zhang et al., 2008; Jing et al., 2009; Rosar et al., 2012). VEN3 and VEN6 are semi-dominant, meaning that heterozygotes have phenotypes that are intermediate between homozygous parental lines and wild-type (Mollá-Morales et al., 2011). *Ven3* and *ven6* have a reduced number of smaller palisade cells (Mollá-Morales et al., 2011). Only *ven6-1* did not show a reduction of the palisade cell size (Mollá-Morales et al., 2011). Particularly, *ven3-3* displayed strong indentations (Mollá-Morales et al., 2011). The *ven3/ven6* double mutants showed a very strong synergistic phenotype (Mollá-Morales et al., 2011).

***trp2* (*tryptophan2*)**

All *Arabidopsis* mutants that have a defect in trp biosynthesis have small, reticulated leaves, including the alleles *trp2* and *trp3* (Barczak et al., 1995; Radwanski et al., 1996; Jing et al., 2009). Root development was not affected in *trp2* (Jing, Cui et al. 2009). *Trp* mutants are either defective in the α- or in the ß-subunit of trp-synthase (Figure 1). The α-subunit has two and the ß-subunit at least two homologues (Last et al., 1991; Zhang et al., 2008; Jing et al., 2009). *Trp2* mutants have dramatically decreased trp levels (Ouyang et al., 2000; Jing et al., 2009). The T-DNA line *trp2-301* is designated as *small organ1* (*smo1*), with *smo1/trp2-301* being a backcross without T-DNA insertion (Jing et al., 2009). Trp addition complemented the phenotype by normal palisade parenchyma development but caused a slight reduction in growth (Jing et al., 2009).

The plastid borne trp is a precursor of the plant hormone auxin, which is involved in plant growth and development (Delarue et al., 1998; Zhao et al., 2001; Zhao et al., 2002; Cheng et al., 2006; Tao et al., 2008). Despite decreased trp contents, auxin levels were elevated in *trp2* alleles (Normanly et al., 1993; Ouyang et al., 2000; Jing et al., 2009). *Trp2* did neither show an auxin responsive related phenotype nor did the application of auxin revert the phenotype. Thus, auxin is not causal for the phenotype (Jing et al., 2009). The auxin increase was attributed to a severely affected homeostasis in this mutant (Jing et al., 2009). Since trp is essential in protein biosynthesis, which itself is linked to cell proliferation, protein levels were investigated in *smo1/trp2*, but not found to be diminished (Jing et al., 2009). To conclude if protein biosynthesis *per se* could lead to a reticulated leaf phenotype, the translation inhibitor cyclohexemide was applied to wild-type plants. The drug, however, led to both smaller and less palisade cells, unlike *smo1/trp2,* which were only decreased in M cell size. Thus, (Jing et al., 2009) conclude that the *trp2* phenotype was not caused by a reduction of protein biosynthesis. The ultimate answer, if reduction of protein biosynthesis causes the reticulation is still to be resolved. Hence, the *trp2* phenotype was causally linked

to the lack of trp. This metabolic shortcut provoked a delay in chloroplast development in *trp2* with underdeveloped M thylakoids, with less chlorophyll, and a decreased photosynthetic performance at early stages (Jing et al., 2009). This coincides with reticulated cotyledons and young leaves, with a less penetrant, even partially restored wild-type like phenotype in older leaves (Jing et al., 2009). A less penetrant phenotype was found in old *re* leaves (González-Bayón et al., 2006). The number of chloroplasts with less and smaller starch granules, however, seemed to be the same in *smo1/trp2* and wild-type (Jing et al., 2009).

ATase2* mutants: *dov1, cia1, atd2, and alx13

The recessive *ATase2* mutants are defective in glutamine phosphoribosyl pyrophosphate aminotransferase2 (ATASE2), the enzyme catalyzing the first step of the *de novo* purine biosynthesis (Zrenner et al., 2006; Rosar et al., 2012; Figure 1). *Arabidopsis* harbors the three homologues ATASE1, 2 and 3 (Hung et al., 2004; Rosar et al., 2012). ATASE enzymes are conserved within and across species (Hung et al., 2004; Van der Graaff et al., 2004; Rosar et al., 2012). Several allelic ATase2 mutants have been described: *dov1*, *cia1*, *atd2*, and *alx13*. *Dov1* was identified in a screen for reticulate leaf mutants of *Arabidopsis*, termed *differential development of vasculature associated cells1* (Kinsman and Pyke, 1998). *Cia1* (*chloroplast import apparatus1*) was discovered in a screen for mutants with defects in chloroplast protein (Sun et al., 2001; Hung et al., 2004), *alx13* (*altered APX2 expression13)* in a screen for high-light induced gene expression (Ball et al., 2004; Rossel et al., 2004).

Much like PPT (Streatfield et al., 1999), TRP (Jing et al., 2009), VEN3/VEN6 (Mollá-Morales et al., 2011), and RE (González-Bayón et al., 2006) are plastid localized, ATASE2 is found in the chloroplast stroma (Hung et al., 2004). The *de novo* purine biosynthesis is shared between the plastid (Van der Graaff et al., 2004) and the cytosol in *Arabidopsis* (Witz et al., 2012). *Cia1*, which has lowered leaf purine levels, as indicated by decreased ATP/GTP levels, was biochemically complemented with purines, i.e. AMP and IMP (Hung et al., 2004), and *atd*2 by IMP (Hung et al., 2004; Van der Graaff et al., 2004). The purine building blocks aspartate and glycine were increased in *dov1*, likely due to a reduced purine production (Rosar et al., 2012). Purines are precursors of cytokinins (Mok and Mok, 2001), which drive metabolic events (Redig et al., 1996) and are abundant in meristematic tissues (Zhang et al., 1996; Van der Graaff et al., 2004). In line with lowered purine levels (Hung et al., 2004; Van der Graaff et al., 2004), total cytokinin contents in *dov1* leaves were decreased (Rosar et al., 2012). External cytokinin application to *dov1* and *cia1*, however, did not revert the phenotype (Hung et al., 2004; Rosar et al., 2012). *De novo* purine biosynthesis genes are highly expressed in meristematic and mitotically active tissues (Senecoff et al., 1996; Zhang et al.,

1996; Van der Graaff et al., 2004; Zrenner et al., 2009). Cytokinin response activity assays revealed that cytokinin activity in *dov1* is diminished, which is in agreement with growth retardation and lowered mitotic events (Rosar et al., 2012).

While in *dov1* leaves, total ATASE activity was lowered (Van der Graaff et al., 2004; Rosar et al., 2012), it was higher in green and white leaf sectors of *alx13* (Woo et al., 2011). The increased activity was attributed to the import deficient chloroplasts in *alx13*: ATASE2 enzymes are not or less efficiently imported into the plastids and accumulate in the cytosol (Woo et al., 2011). We suppose that the deviant results are due to the leaf age at which the ATASE activity was determined. Rosar et al., 2012 used young leaves at the six leaf stage while Woo et al., 2011 used older leaves at the fourteen leaf stage. Since ATase2 is expressed preferentially in younger tissues (Ito et al., 1994; Hung et al., 2004), it`s activity is supposedly higher and the mutation in the gene affects the enzyme activity more severely in young tissues.

ATase2 mutants are delayed in whole plant development and growth. The reticulation is restricted to rosette leaves (Kinsman and Pyke, 1998; Woo et al., 2011; Rosar et al., 2012). An ATase mutant of tobacco has a similar phenotype as the *Arabidopsis* mutants (Van der Graaff et al., 2004). ATASE2 is expressed in cotyledons (Hung et al., 2004), leaves, flowers, and roots (Ito et al., 1994; Hung et al., 2004). The M cell number is severely decreased but size only marginally lowered in *dov1* (Kinsman and Pyke, 1998) and *cia1* (Hung et al., 2004). In *dov1,* BS cells and their chloroplasts appear normal, while the mostly pale chloroplasts of palisade and spongy M cells are reduced in number per cell, and lack internal thylakoid membrane structures (Kinsman and Pyke, 1998). *Atd2* has residual thylakoid membranes and shows vesicle formation (Van der Graaff et al., 2004). Some M cells in white sectors are heteroplastidic, i.e. they contain normal chloroplasts (Kinsman and Pyke, 1998), a trait also found in variegated mutants (Tilney-Bassett, 1975; Hagemann, 1986). *Arabidopsis ATase1* mutants have no visible phenotype (Hung et al., 2004).

The leaf phenotype was described as strongly reticulated (Kinsman and Pyke, 1998), as “albino/pale-green mosaic”-like (Hung et al., 2004), and as variegated with occasionally reticulated patterns (Woo et al., 2011). These observations fit to the variable penetrance of the phenotype depending on growth and environmental conditions, seen in *dov1* (Kinsman and Pyke, 1998; Rosar et al., 2012), *cia1* (Hung et al., 2004), *atd2* (Van der Graaff et al., 2004), and *alx13* (Woo et al., 2011). When grown under low-light, *atd2* and *alx13* leaves remain green (Van der Graaff et al., 2004; Woo et al., 2011), which is attributed to less photo-oxidative damage (Van der Graaff et al., 2004). However, Woo et al., 2011 concluded through growing plants in different light regimes and performing shift experiments, that green and white sectors are determined by the time of cell division and not caused by photo-oxidative damage. Chlorotic sectors arise from green cells during leaf growth, when cells

divide rapidly and plastids are generated (Woo et al., 2011). This indicates that chlorosis is not a cell line heritable trait. Such heritability of progenitor cells, however, is attributed to many variegated mutants (Aluru and Rodermel, 2004; Rosso et al., 2006; Rosso et al., 2009). It must be noted that the discovery of fully differentiated chloroplasts in the SAM (Charuvi et al., 2012) may challenge this hypothesis. Vascular patterning and density in *dov1* is not affected (Kinsman and Pyke, 1998). During development, photosynthesis was massively lowered at all stages in rosette leaves. However, photosynthesis increased in younger leaves of older plant rosettes (Woo et al., 2011; Rosar et al., 2012). This observation was explained by an increased uptake of or access to pools of purines generated via the salvage pathway (Rosar et al., 2012), which still occurs in ATase2 mutants (Hung et al., 2004).

In summary, the *ATase2* phenotype is likely primarily caused by the lack of the primary metabolites purines and not by cytokinin deficiency (Rosar et al., 2012). However, other and/or secondary mechanisms cannot be excluded. GUN1- and/or photoreceptor mediated pathways were discussed to be impaired in *alx13* (Woo et al., 2011).

***ntrc* (*NADPH-thioredoxin reductase*)**

Ntrc is defective in the plastid NADPH-thioredoxin reductase (Serrato et al., 2004; Lepistö et al., 2009), which belongs to the redox-active thioredoxin superfamily (Lepistö et al., 2009). Although their exact physiological role is poorly understood (Buchanan and Balmer, 2005; Gelhaye et al., 2005; Holmgren et al., 2005; Meyer et al., 2005; Meyer et al., 2006; Reichheld et al., 2010), these proteins modulate the activity of target proteins in a photoperiod and redox-state dependent manner. NTRC, unique to oxygenic photosynthetic organisms and *Mycobacterium leprae*, regulates metabolic processes, such as the Calvin-Benson cycle, chlorophyll biosynthesis, the shikimate pathway, and enzymes of the aromatic amino acids, such as 3-deoxy-D-arabino-heptulosonate-7-phosphate synthase and trp synthase (Lepistö et al., 2009; Figure 1). The shikimate-derived aromatic amino acid pool size is increased in *ntrc*, while auxin and cytokinin levels are decreased under short-day conditions (Lepistö et al., 2009). Supplementation with aromatic amino acids reverts the phenotype and plant growth, likely due to the restoration of the aromatic amino biosynthesis homeostasis (Lepistö et al., 2009). Thus, we hypothesize that the *ntrc* phenotype may be caused by secondary means, i.e. via a constraint in the regulation of aromatic amino acid metabolism. *Ntrc,* decreased in the number of M cells with less chloroplast per cell, was linked to be affected in ROS-mediated signaling (Lepistö et al., 2009). Despite reduced chlorophyll levels, primary photosynthetic reactions are not affected, but carbon assimilation rate is decreased in *ntrc* (Lepistö et al., 2009). Additionally, *ntrc* plants were repressed in

expression of cryptochromes and phytochromes, which act in photoperiodic and photomorphogenic growth (Lepistö et al., 2009). An upregulation of genes related to chlorophyll biosynthesis was hypothesized to influence signals attenuating chloroplast biogenesis (Lepistö et al., 2009).

***re* (*reticulata*) / *lcd1* (*lower cell density1*)**

The molecular function of *RE* has not been deciphered to date, although *re* mutants were first described almost fifty years ago (Rédei and Hironyo, 1964). *Re* has been used for decades as a visible marker for genetic mapping due to a low degree of pleiotropy (Rédei and Hironyo, 1964; González-Bayón et al., 2006). Thus far, nine alleles have been described: *re-1* to *re-7* (González-Bayón et al., 2006), *re-8* (Overmyer et al., 2008), and *lcd1* (*lower cell density1*) (Barth and Conklin, 2003; González-Bayón et al., 2006). *Ven 2-1*, *ven 2-2* and *ven 2-3* (Berná et al., 1999) are allelic to *re-3*, *re-4*, and *re-5*, respectively (González-Bayón et al., 2006). *Re/lcd1* displays a reduced number of spongy and particularly palisade cells, but the number of chloroplasts per cell and plastid morphology is not affected (Barth and Conklin, 2003; González-Bayón et al., 2006). The vascular bundle and BS is normally developed, with a larger number of chloroplasts in BS of *re-1* (González-Bayón et al., 2006). *Re* has reticulated cotyledons, rosette and cauline leaves, but neither a phenotype in inflorescence, floral organs, fruit, seeds nor in the root was observed (Barth and Conklin, 2003; González-Bayón et al., 2006). The leaves show a simpler venation pattern, with shorter vascular bundles only in fully expanded leaves (González-Bayón et al., 2006). Along with a slightly decreased biomass per leaf area in *lcd1* (Barth and Conklin, 2003), the leaf area of *re* is slightly decreased (Gonzalez-Bayon, Kinsman et al. 2006). The rate of photosynthesis was slightly lower in *lcd1* on an area, but not on a fresh weight basis (Barth and Conklin, 2003). RE may be regulated by light, as mutants do not exhibit the pale interveinal phenotype when grown under very low-light (Barth and Conklin, 2003; Overmyer et al., 2008). The reticulate phenotype becomes less apparent when leaves are aging (González-Bayón et al., 2006). The expression of *RE* is highest in young and meristematic leaf- and root tissues, and restricted to the leaf veins (González-Bayón et al., 2006). RE is predicted to be plastid localized (González-Bayón et al., 2006), as confirmed by proteomic analysis of the plastid envelope (Zybailov et al., 2008; Bräutigam and Weber, 2009; Ferro et al., 2010). Despite decreased chlorophyll contents, with no alteration of photosynthetic pigment composition, *lcd1* is not affected in it`s photosynthetic performance (Barth and Conklin, 2003). *Lcd1* is susceptible to pathogens, such as *Pseudomonas syringae* (Barth and Conklin, 2003). However, the ROS-scavening system, which is involved in mediating pathogen responses, is not affected in *lcd1* (Barth and Conklin, 2003).

Two hypotheses were provided to explain the *re* phenotype. Firstly, RE/LCD1 plays a role in cell division particularly of M cell (Barth and Conklin, 2003), resulting in leaves with a lower cell density. Secondly, RE/LCD1 is involved in several functions, and if mutated, has pleitropic effects besides that of lower cell density (Barth and Conklin 2003)(González-Bayón et al., 2006).

PEND

When BnPEND, a plastid localized protein from rape seed (*Brassica napus*), is overexpressed in tobacco, leaves become patchy white-green to reticulate (Wycliffe et al., 2005). BnPEND, and its homologues in other plant species have a N-terminal DNA-binding domain similar to bZIP transcription factors. The C-terminus is likely anchored to the plastid inner envelope (Wycliffe et al., 2005; Kodama, 2007). The PEND protein of *Pisum sativum* seedlings binds the plastid DNA to the inner envelope during replication and transcription, particularly during plastid development in young plants and leaves (Wycliffe et al., 2005). Thus, an overexpression disturbs processes in chloroplast development and causes the distorted organization of M cells (Wycliffe et al., 2005). BnPEND is also thought be involved in retrograde signaling (Wycliffe et al., 2005).

Photorespiratory phenotypes

Photorespiration starts with the oxygenase activity of ribulose-1,5-bisphosphate-carboxylase/oxygenase (RuBisCO) forming phosphogylcolate. Phosphoglycolate is recycled to the Calvin-Benson cycle intermediate phosphogylcerate in a coordinated process between cytosol, mitochondria, and peroxisomes (Maurino and Peterhänsel, 2010; Peterhansel et al., 2010). When a subunit of the glycine decarboxylase (GDC) complex is downregulated in tobacco, leaves become chlorotic along their veins (Lein et al., 2008), corresponding to an inverse reticulated phenotype.

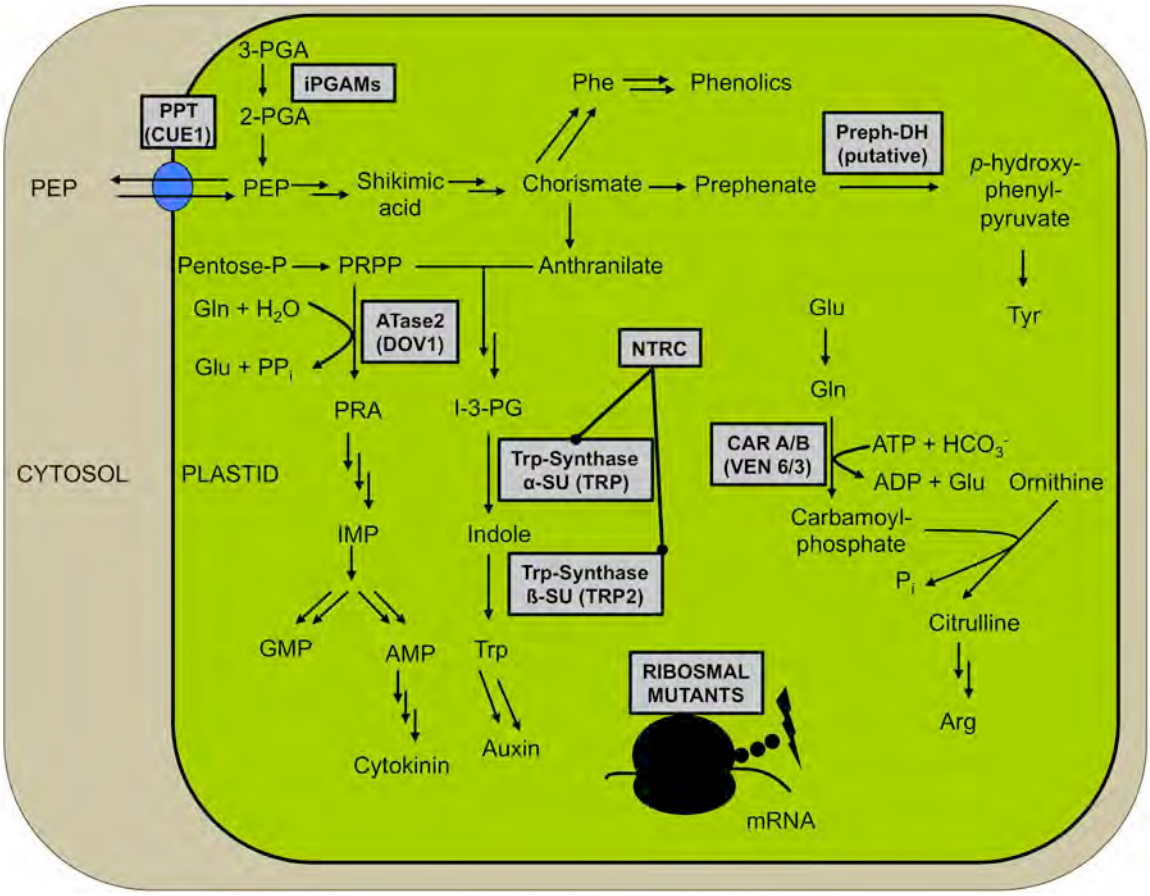

Figure 1: Affected pathways in reticulated mutants. All molecularly characterized reticulate mutants are defective in purine, amino acids or plastid ribosomal subunits. *Dov1* is defective in ATase2 and thus in *de novo* purine metabolism. *Cue1*, deficient in the PPT1, cannot import PEP in the plastid. PEP is a precursor for aromatic amino acid biosynthesis and thereof derived secondary metabolites, such as phenolics. *Ipgam* double mutants are defective in plastidic PEP generation. *Ven3* and *ven6* are disturbed in arginine biosynthesis via defective CAR B and CAR A subunits, respectively. A mutant of the prephenate-DH is likely affected in tyrosine biosynthesis. NTRC regulates a plethora of metabolic processes, among them trp synthesis. Some ribosomal mutants are defective in plastidic protein synthesis. AMP: adenosine-5`-monophosphate; ADP: adenosine-5`-diphosphate; ATP: adenosine-5`-triphosphate; Glu: glutamate; Gln: glutamine; $HCO_3^-$: Hydrogencarbonate; iPGAM: 2-3-bisphosphoglycerate-independent phosphoglycerate mutase; IMP: Inosine-5`-monophosphate; I-3-PG: indole-3-phosphoglycerate; IPGA: phosphoglyceric acid; PPT: phosphoenolpyruvate-phosphate translocator; PRA: 5-phosphoribosylamine; PRPP: 5-phosphoribosyl-1-pyrophosphate; GMP: guanosine-5`-monophosphate; PEP: phospho*enol*pyruvate; Phe: phenylalanine; P_i: phosphate.

Variegated mutants

The variegated phenotype is characterized by distinct green and white sectors that are most prominent in leaves but can be observed in the stem (Kirk and Tilney-Bassett, 1978; Rodermel, 2001; Sakamoto, 2003; Miura et al., 2007; Rodermel, 2008). The green sectors contain fully and normally developed chloroplasts while the white sectors contain aberrant chloroplasts, which frequently lack an organized internal membrane structure, chlorophyll, and/or carotenoids (Miura et al., 2007; Rodermel, 2008). However, variegated and reticulated phenotypes cannot always be unambiguously distinguished, as outlined for *ATase2* mutants in this review.

Variegation mutants are widespread in dicots and monocots, C_3- and C_4-plants. Variegation is found in nature and thus should have benefits for the plants (Tsukaya et al., 2004; Kato et al., 2007; Sheue et al., 2012). Variegation in monocots is often referred to as striping (Sakamoto, 2003). There is a plethora of ca. 200 to several hundred *Arabidopsis* variegation mutants in the Arabidopsis stock centers at Nottingham and Ohio state (Yu et al., 2007). Although many of these mutants were isolated and described (Rédei, 1963; Röbbelen, 1968), most of them have not been genetically or molecularly identified to date (Yu et al., 2007). Variegation mutants have been used in linkage studies and as morphological markers (Jenkins, 1924; Robertson, 1967; Sakamoto, 2003).

Two types of variegation mutants are distinguished: green and white sectors with (i) different genotypes and (ii) with the same genotype (Sakamoto, 2003; Yu et al., 2007). Case (i) is due to chimerism, transposable elements, RNA silencing, plastome mutators, plastome mutations, mitochondrial genome mutations, or plastid-nucleus incompatibility (Newton and Coe, 1986; Chatterjee et al., 1996; Keddie et al., 1996; Stoike and Sears, 1998; Bellaoui et al., 2003; Yu et al., 2007). Mutants defective in either plastid or mitochondrial genes do not obey to Mendel`s law and helped to discover the non-nuclear inheritance (Granick, 1955; Tilney-Bassett, 1975; Connett, 1986; Yu et al., 2007). One group of molecularly characterized nuclear-recessive variegated mutants is defective in the photo-protective machinery leading to white sectors. These mutants are often associated with carotenoid biosynthesis, such as *im*, *var1*, *var2*, and *var3* (Wetzel et al., 1994; Aluru et al., 2006; Kato et al., 2007; Miura et al., 2007; Aluru et al., 2009; Rosso et al., 2009). Another group is impaired likely directly in proper thylakoid and thus chloroplast biogenesis, such as *thf1* (Keren et al., 2005; Huang et al., 2006). The variegated phenotype is probably pleiotropic because different metabolic pathways are affected. In this review, we will refer to nuclear recessive mutations.

im (immutans*) and *spotty

The nuclear recessive *Arabidopsis* mutant *im* was isolated more than fifty years ago (Rédei, 1963, 1967). *Spotty*, allelic to *im*, was isolated in an EMS screen, and was designated *im* (Wetzel et al., 1994; Rosso et al., 2009). *Im*, ubiquitously expressed throughout development (Aluru et al., 2001) is defective in the plastid terminal oxidase (PTOX) (Figure 2), a redox protein similar to the alternative oxidase (AOX) of the alternative (cyanide-resistent) pathway of mitochondrial respiration (Carol et al., 1999; Wu et al., 1999; Fu et al., 2012) where AOX oxidizes ubiquinol and reduces oxygen to water (Siedow and Umbach, 1995; Vanlerberghe and McIntosh, 1997). Similar reactions are involved in carotenoid biosynthesis: phytoene desaturase (PDS) oxidizes phytoene, and reduces PQ (Wetzel et al., 1994; Aluru et al., 2006). By recycling, i.e. oxidizing the PQ-pool and reducing oxygen, IM thus facilitates PDS function (Josse et al., 2000; Joët et al., 2002; Josse et al., 2003, Figure 2). Hence, *im* is impaired in carotenoid biosynthesis, indicated by the accumulation of the non-colored phytoene in white tissues (Wetzel et al., 1994). Carotenoids protect plants from generated ROS-species. Thus, the white carotenoid-less sectors are triggered by photobleaching resulting from an increase in plastidic ROS (Wetzel et al., 1994; Wu et al., 1999; Aluru et al., 2009; Rosso et al., 2009).

Additionally to carotenoid biosynthesis, PTOX is involved in growing numbers of plastidic pathways, such as photosystem I (PSI) cyclic electron transport (Okegawa et al., 2010; McDonald et al., 2011), central regulation of photosystem II (PSII) excitation pressure in early chloroplast biogenesis (Rosso et al., 2009), and chlororespiration mediating the oxidation of the plastidial PQ pool in the dark and reducing oxygen (Josse et al., 2000; Hirschberg, 2001; Joët et al., 2002; Peltier and Cournac, 2002; Fu et al., 2005; Shahbazi et al., 2007; Yu et al., 2007). IM is suggested to be an electron transport safety valve by acting as an alternative electron sink to detoxify excess electrons during photosynthetic overcapacity and thus lowering ROS production under unfavorable environmental conditions (Niyogi, 2000; Rizhsky et al., 2002; Yu et al., 2007; Rosso et al., 2009; McDonald et al., 2011). However, under non-stressed steady-state photosynthesis, IM is suggested to have a role in development (Rosso et al., 2006). By combining both results, it was concluded that IM protects against photo-oxidation during the development of chloroplasts, amyloplasts and etioplasts (Aluru et al., 2001; Aluru et al., 2009). Despite intensive research on IM, it`s precise physiological function remains unclear (Inaba and Ito-Inaba, 2010).

The variegated *im* phenotype is restricted to leaves and not found in cotyledons and other organs (Aluru et al., 2001). Green sectors are thicker than wild-type, due to an increase in air space, epidermal and M cell size. Chloroplasts are morphologically normal, while white sectors harbor vacuolated plastids lacking lamellar structures (Wetzel et al., 1994). In white leaf sectors, wild-type like leaf thickness was observed, and palisade cells failed to expand

properly (Aluru et al., 2001). The variegated *ghost* mutant in tomato (*Lycopersicon esculentum*) (Barr et al., 2004) lacks the IM-orthologue GH (Rick et al., 1959; Wetzel et al., 1994). GH is important in chloroplast and chromoplast differentiation (Barr et al., 2004). However, amyloplasts, etioplasts, and chromoplasts are well developed in *im* (Aluru et al., 2001) and *ghost* (Barr et al., 2004).

***var2* (*yellow variegated2)* and *var1* (*yellow variegated 1*)**

The recessive *yellow variegated2 (var2)* mutant is defective in the ATP-dependent metalloprotease FtsH2 (Kato et al., 2007) and the *yellow variegated1 (var1)* in FtsH5 (Aluru et al., 2006; Miura et al., 2007; Figure 2). FtsH2 and FtsH5 are components of the thylakoid membrane localized FtsH heterocomplex (Zaltsman et al., 2005; Kato et al., 2007). FtsH degrades, among various chloroplast proteins (Ostersetzer and Adam, 1997; Lindahl et al., 2000; Zelisko et al., 2005; Adam et al., 2006; Komenda et al., 2006; Sakamoto, 2006), the D1 protein of PSII, e.g. in the case of photodamage (Aluru et al., 2006; Miura et al., 2007). Variegation is likely caused by an imbalance between biosynthesis and degradation of the D1 protein (Miura et al., 2007). The D1 protein is the plastoquinone B (Q_b) binding pocket of PSII where electrons are transferred to the PQ pool (Miura et al., 2007). FtsH participates in the PSII repair cycle (Lindahl et al., 2000; Bailey et al., 2002; Sakamoto et al., 2004).

Var2 mutants, first isolated by Redei in the 1950s (Yu et al., 2007), have normally developed cotyledons. While the first true leaves are white, the next appearing rosette leaves become variegated. Variegation in *var2* affects all green organs, i.e. leaves, stems, sepals, and siliques (Koornneeff et al., 1982). An EMS-mutagenized allele of *var2* (Koornneeff et al., 1982; Martínez-Zapater, 1993) and a T-DNA tagged allele were genetically identified (Takechi et al., 2000). *Var4* is allelic to *var2* (Koornneeff et al., 1982). The *var1* variegation is restricted to leaves (Martínez-Zapater, 1993). The white sectors of *var2* consist of viable cells, which are defective in chloroplast differentiation (Kato et al., 2007).

The enhanced phenotype of the *var1/2* double mutant indicates that both mutants are involved in the same process (Sakamoto et al., 2002). However, despite high similarity to each other, FtsH2 (VAR2)- and FtsH5 (VAR1)-proteins, were proposed to have different roles (Yu et al., 2005; Zaltsman et al., 2005).

***var3* (*variegated3*)**

The nuclear recessive *Arabidopsis var3* is a transposon-insertion mutant (Næsted et al., 2004). Three *VAR3* homologs are encoded in the genome, of which VAR3 and another homologue is likely chloroplast envelope localized (Naested et al., 2004). VAR3 interacts *in*

vitro and in yeast with nine-*cis*-epoxy carotenoid dioxygenase4 (NCED4) (Iuchi et al., 2001; Figure 2), suggesting that VAR3 is involved in the regulation of carotenoid biosynthesis (Naested et al., 2004). All determined carotenoids in *var3* were reduced (Naested et al., 2004). *Var3* has green cotyledons and yellow variegated rosette leaves. In yellow sectors, the number of palisade cells, whose chloroplasts lack the thylakoid membrane structure, is reduced. In green sectors the chloroplast is wild-type like (Næsted et al., 2004). The variegation is already visible during early chloroplast biogenesis, shortly before leaves emerge.

***pac* (*pale cress*)**

The exact molecular function of PAC has not been corroborated to date. However, the chloroplast localized light-regulated PAC protein (Reiter et al., 1994; Tirlapur et al., 1999) is hypothesized to be involved in plastid-encoded mRNA maturation/processing (Meurer et al., 1998), and thereby in synthesis or stability of carotenoids (Holding et al., 2000; Figure 2). In analogy to *im*, the *pac* phenotype is likely partially caused by a carotenoid deficiency (Holding et al., 2000). *Pac* has decreased abscisic acid (ABA) levels, a plant hormone derived from carotenoids (DellaPenna and Pogson, 2006) and involved in stomata movement. In accordance, the PAC protein was located exclusively to epidermal guard cells (Reiter et al., 1994; Holding et al., 2000) where ABA is primarily involved in stomata movement (Raschke and Hedrich, 1985; Schroeder et al., 2001; Kim et al., 2010). Since ABA is required for proper determination of leaf identity in heterophyllous aquatic leaves (Ueno, 1998), the changed leaf cell morphology in *pac* could be due to inhibited ABA function (Holding et al., 2000). Pac was rescued by exogenous application of cytokinin (Grevelding et al., 1996). Two T-DNA tagged *pac* alleles are isolated: *pac-1* and *pac-2* (Feldmann, 1991; Reiter et al., 1994; Grevelding et al., 1996). The pale green *pac-1* has a poorly differentiated palisade parenchyma, enlarged epidermal cells and almost thylakoid-less plastids (Reiter et al., 1994). Contrarily, *pac-2* is variegated with normal green chloroplasts in green and abnormal plastids in white sectors (Grevelding et al., 1996). Despite both alleles are putative null, the phenotypes are quite different likely due to leaky expression and/or the different mutant ecotypes (Yu et al., 2007). *Pac* plants accumulate more chlorophyll and have greener leaves when grown under low-light (Holding et al., 2000).

cla1 (cloroplastos alterados1*) and *cas1* (*cycloartenol-synthase)

Three *cla1* alleles were isolated in *Arabidopsis*: *cla1* as a T-DNA line (Mandel et al., 1996; Estévez et al., 2000), *lovostatin-resistant111* (*lvr111*) (Crowell et al., 2003), and *chilling sensitive5* (*chs5*) (Araki et al., 2000). While the null-allele *cla1* is albino*, lvr111* shows a variegated dwarf phenotype. *Chs5* is chlorotic when grown at 15°C. The affected gene encodes 1-deoxy-D-xylulose 5-phosphate synthase (DXP), the rate-limiting enzyme of the plastidic 2-C-methyl-erythritol-4-P (MEP) pathway for isoprenoid biosynthesis, such as carotenoids and quinones (Lichtenthaler et al., 1997; Lichtenthaler et al., 1997; Araki et al., 2000; Estévez et al., 2000; Estévez et al., 2001; Figure 2). Total isoprenoids were massively decreased in *cla1-1* and *lvr111* (Crowell et al., 2003). *Cla1-1* harbors white thylakoid less plastids that accumulate vesicles. The white and variegated phenotype is linked to photoinhibition due to the lack of photoprotective carotenoids (Crowell et al., 2003). *CLA1* has a homologous gene (Araki et al., 2000). Mutants of the cycloartenol-synthase (*cas1*), defective in an enzyme of the sterol biosynthesis, have an albino stem and petiole (Babiychuk et al., 2008).

thf1* (*thyalkoid formation1*) and *ispf

The THF1 protein interacts with PSII and is suggested to regulate PSII biogenesis (Keren et al., 2005). THF1 was detected in the stroma, the outer envelope, and in stromules (Keren et al., 2005). Stromules are plastidic extensions that likely mediate intracellular signaling (Kwok and Hanson, 2004). Additionally, THF1 interacts with a plasma membrane bound G-protein at sites of stromule/plasma membrane interaction, favoring a role of THF1 in G-protein-linked D-glucose sugar signaling (Huang et al., 2006). *Thf1* is stunted and variegated, while antisense plants are of variant penetrance, depending on line and light conditions (Wang et al., 2004). White and yellow sectors of *thf1* accumulate vesicles in their thylakoid lacking chloroplasts, suggesting that *thf1* is defective in thylakoid biogenesis (Wang et al., 2004). Thylakoids likely develop from vesicles from the inner envelope (Westphal et al., 2001; Andersson and Sandelius, 2004). Thylakoid vesicle formation is prominent in *ispf1*, a variegated mutant defective in the plastidic non-mevalonate isoprenoid biosynthesis (Hsieh and Goodman, 2006), giving rise to the phytol side chain of chlorophyll and carotenoids. The non-mevalonate pathway is likely arrested in early leaf and plastid biogenesis (Hsieh and Goodman, 2006). THF1 is homologous to the *Synechocystis* protein PSB29 (Keren et al., 2005).

hma1 (heavy metal P_{1B}-ATPase)

The variegated *Arabidopsis* mutant *hma1* is defective in the copper transporter HMA1, a heavy metal P_{1B}-ATPase, that imports iron across the plastid membrane (Seigneurin-Berny et al., 2006). Copper is a cofactor in various plastid enzymes involved in ROS scavenging (Seigneurin-Berny et al., 2006). The variegation, most prominent under high-light, is attributed to photobleaching. The striping maize mutant *yellow stripe1* (*ys1*) is defective in the uptake of iron and other heavy metal ions across the plasmamembrane into the cytosol (Von Wirén et al., 1994; Schaaf et al., 2004).

kas1* (*ß-Keto-[Acyl Carrier Protein] Synthase1)

The *Arabidopsis kas1* mutant has multiple morphological impairments, including chlorotic, netted patches on small leaves (Wu and Xue, 2010), similar to reticulated leaves. ß-Keto-[Acyl Carrier Protein] Synthase1 (KAS1) elongates fatty acids. The gene is expressed at high levels during early developmental stages and in the whole rosette leaf (Shimakata and Stumpf, 1982; Wu and Xue, 2010).

***albino3 (alb3)* and *white cotyledons* (*wco*)**

Although being *Arabidopsis* albino mutants, *alb3* and *wco* are often described in the context of variegation. *Alb3* is defective in ALB3, which builds a pore in the thylakoid membrane for protein import (Figure 2). ALB 3 interacts with diverse proteins (Cai et al., 2010; Dünschede et al., 2011; Ingelsson and Vener, 2012). *Alb3* has both white cotyledons and true leaves (Sundberg et al., 1997). The nuclear recessive *Arabidopsis* mutant *white cotyledons* (*wco*) has white/pale cotyledons and green leaves, but is not variegated (Yamamoto et al., 2000). Plastids in white tissues contain plastoglobuli and have only rudimentary thylakoids (Yamamoto et al., 2000). Likely, this mutant is primarily affected in cotyledon specific 16 sRNA maturation (Yamamoto et al., 2000).

chm* (*chloroplast mutator*), *mdl* (*maternal distorted leaf*), *osb1* (*organellar single strand binding protein1*), *msh1* (*mutS homolog1*), and *am (albomaculans)

The variegated *chloroplast mutator* alleles *chm1* and *chm2* of *Arabidopsis* were isolated in an EMS screen (Rédei, 1967; Rédei and Plurad, 1973) and *chm3* was isolated by (Martínez-Zapater et al., 1992). The leaves of homozygous recessive plants have a reticulated rough-leaf phenotype (Mourad and White, 1992). CHM encodes AtMSH1, a mitochondrial protein that is involved in DNA mismatch repair and recombination and likely

controls mitochondrial genome copy number (Abdelnoor et al., 2003; Figure 2). The defective mitochondria affect chloroplasts secondarily. *Mdl* mutants, derived as a cross between *chm* and wild-type, confirm the role in mitochondrial gene rearrangement (Sakamoto et al., 1996). The mechanism of variegation is considered to be similar to that of *non-chromosomal stripe* (*ncs)* maize mutants (Newton and Coe, 1986; Gabay-Laughnan and Newton, 2005; Yu et al., 2007). Organellar single strand binding protein1 (OSB1) was identified to be responsible for regulation of the plant mitochondrial genome via correct stoichiometric mtDNA transmission (Figure 2). In the case of instable mtDNA, plants appeared variegated. OSB1 expression is restricted to gametophytic cells (Zaegel et al., 2006), in line with the hypothesis that the variegated phenotype is caused in very early developmental stages. *Msh1* is defective in it´s putative function in mitochondrial replication (Abdelnoor et al., 2003; Arrieta-Montiel et al., 2009). The recessive *am* mutants of *Arabidopsis* were generated almost 50 years ago (Röbbelen, 1966). The plastids are permanently defective and maternally inherited. White sectors contain heteroplastidic cells with normal green chloroplasts and abnormal, non-pigmented vesiculated, thylakoid less and plastoglobuli-rich white plastids. The heteroplastidity is likely a consequence of incomplete sorting out. It was suggested that *am* is a form of plastome mutator, i.e. a nuclear mutation leading to a plastidic mutation (Tilney-Bassett, 1975; Hagemann, 1986).

Variegated mutants in dicotyledonous non-*Arabidopsis* species

dcl* (*defective chloroplasts and leaf-mutable*) and *vdl (variegated and distorted leaf)

The tomato *dcl* variegated phenotype is defective in the DCL protein, which is required for rRNA processing and plastid ribosome assembly (Bellaoui et al., 2003; Bellaoui and Gruissem, 2004). The *Arabidopsis dcl* allele is pale green but not variegated (Bellaoui and Gruissem, 2004). The nuclear recessive *vdl* mutant is defective in a putative plastid targeted DEAD-box RNA helicase (Wang et al., 2000). DEAD-box RNA helicases are involved in ribosomal synthesis (Cordin et al., 2006). *Arabidopsis* mutants of ribosomal subunits also display altered leaf morphology (Börner and Sears, 1986; Hagemann, 1986; Hess et al., 1994; Yaronskaya et al., 2003; Hricová et al., 2006; Horiguchi et al., 2011; Tiller et al., 2012). *Vdl* is characterized by variegated leaves, aberrant inflorescences and roots. The white leaf sectors are distorted, lack palisade cells and have undifferentiated plastids lacking internal membrane structure (Wang et al., 2000).

***mcd1* (*mesophyll cell defective1*)**

Despite the molecular function has not been identified, the recessive variegated *mcd1* of sunflower is discussed as being similar to *var3* (Næsted et al., 2004; Fambrini et al., 2010). *Mcd1* displays aberrant, poorly shaped palisade and spongy M cells with prominent intracellular spaces, in some areas without M cells (Fambrini et al., 2010). Palisade cells are highly vacuolated and reduced in number of chloroplasts. Also cotyledons are affected. Photosynthetic capacity is largely decreased in white/yellow leaf sectors while it is at wild-type level in green patches (Fambrini et al., 2010).

Mutants in monocots

This chapter briefly gives an overview of striped mutants of both C_4- and C_3-monocotyledonous plants. Despite they are often referred to be analogous to variegated mutants, we think that they correspond to reticulated phenotypes. If these corresponded to variegated dicot mutants, the sectoring should also be chaotic and should not include veinal structures.

Maize *iojap*, and barley *albostrians* and *saskatoon* mutants

The white stripes of the recessive *iojap* mutants are caused by missing components of the plastid 50S-ribosome (Han et al., 1992). Additionally, plastidic RNA editing is disturbed (Halter et al., 2004). The barley *albostrians* and *saskatoon* mutants lack the 70S ribosome due to a nuclear recessive mutation (Börner and Sears, 1986; Hagemann, 1986; Hess et al., 1994; Yaronskaya et al., 2003).

***z2* (*rice zebra2*)**

The *z2* mutant of rice (*Oryza sativa*), first reported more than 70 years ago (Chai et al., 2011), has leaves with transverse white/yellow and green stripes. The mutant is defective in carotenoid isomerase, which is expressed in root M and vascular bundles (Chai et al., 2011). *Z2* plants are likely corroborated in photoprotective mechanisms due to low levels of lutein (Chai et al., 2011). However, the *z2* phenotype is suppressed by continuous light under which no excess levels of ROS species accumulate. Under short day conditions, the plants show the phenotype and accumulate high ROS levels (Han et al., 2012). The deficiency of the carotenoids was thus not causal for the phenotype. In *z2* leaves, the substrate of carotenoid isomerase, tetra-*cis*-lycopene, accumulated under short day and not under continuous light (Han et al., 2012). Since this substance is positively correlated with ROS

accumulation and subsequent expression of cell death related genes, the phenotype was linked to a photoperiodic accumulation of tetra-*cis*-lycopene (Han et al., 2012). These observations may also shed a new light on variegated *Arabidopsis* mutants that are defective in carotenoid biosynthesis.

Uncharacterized reticulated and variegated mutants

A lot of variegated and reticulated mutants have not been mapped and/or molecularly identified to date. Phenome databases using publicly available seed stocks were established (Kuromori et al., 2006; Kuromori et al., 2009; Myouga et al., 2010; Yamaguchi et al., 2012). Allelic and thus redundant listing of mutants cannot be excluded. We screened these databases for variegated and reticulated phenotypes.

(Feldmann, 1991) categorized T-DNA insertional mutations morphologically, among them variegated and reticulated plants. However, no exact description or identity is provided.

(Kuromori et al., 2006) selected 4000 transposon-insertion lines and observed the visible phenotype, including both novel and previously reported mutants. Four variegated and four reticulated leaf mutants were detected. The mutants listed in this chapter were inferred from the database *http://rarge.psc.riken.jp/phenome*, and are not exclusively listed in the publication by Kuromori et al., 2006. The reticulated lines are listed as pale green leaves in the database. Thus, we defined the reticulation after inspection of the photographs in the database. The lines are listed in Table 1 (reticulated: At1g15710, At1g65260, At1g32080, At5g27010; At1g75030; variegated leaves: At4g21060, At4g01690, At2g20860; variegated seedlings/pale leaves: At4g27600; At1g32080 is listed as pale green, appears, however, reticulated; At1g75030 is listed as pale green, looks reticulated/variegated). A reticulated insertion line in a gene of a prephenate dehydrogenase family protein (At1g15710) is likely defective in the plastidic trp biosynthesis (Figure 1), like *trp2* (Last et al., 1991; Zhang et al., 2008; Jing et al., 2009). VIPP1 (At1g65260) is a vesicle inducing protein in thylakoid and plastid formation (Kroll et al., 2001; Westphal et al., 2001). The six remaining mutants were not molecularly characterized at the date of publication (Kuromori et al., 2006). At1g32080 is predicted to encode for LRGB, a plastidic protein involved in chloroplast development (Yang et al., 2012). At1g75030 encodes a PR5-like protein, whose function is unknown (Hu and Reddy, 1997). At5g27010 has not been identified yet. The variegated mutant with an insertion in At4g21060 is assigned to be defective in a putative ß-1,3-galactosyltransferase (Qu et al., 2008). The line inserted into At4g01690 is deficient in protoporphyrinogen oxidase (PPOX) (Lermontova and Grimm, 2006; Tanaka et al., 2011). The T-DNA line in At4g27600 is likely corrupted in phosphofructokinase B-type carbohydrate kinase family protein NARA5,

which is expressed in the plastid (Ogawa et al., 2009). The function of NARA5, however, is unknown. At2g20860 encodes the lipoic acid synthase1 (LIP1) (Yasuno and Wada, 2002; Li-Beisson et al., 2010).

(Myouga et al., 2010) established a database of tagged insertion lines from seed stock centers and from their own laboratory stocks. Insertions for 1369 plastid-localized nuclear encoded genes were taken into account. Five defective genes for variegated, 24 for pale leaf mutants and six for weak pale mutants were described. Among the five variegated mutants, one was allelic to *thf1* and one to *cia1*. The class of pale and weakly pale mutants was not subdivided and not categorized as reticulated.

Through screening the database established by Yamaguchi et al., 2012 we found six variegated T-DNA insertion mutants in the following genes: At4g34740 (Atase2), At4g27600 (pfkB-like carbohydrate kinase family protein), At4g34830 (pentatricopeptide repeat protein), At4g18750 (pentatricopeptide repeat protein), At2g20890 (THF1), and At1g32080 (AtLrgb).

(Lloyd and Meinke, 2012) established a database of yet described and published but also mutants from their lab stock. Most of the mutants described in this review are also listed by (Lloyd and Meinke, 2012): *cue1*, *ven3*, *ven6*, *trp2*, *ATase2*-mutants, *ntrc*, *re*, *im*, *var1*, *var2*, *pac*, *cla1*, *thf1*, *hma1*, *kas1*, *alb3*, *chm*, *osb1*, and *msh1*.

Antirrhinum majus mutants were described as displaying leaf coloration (Hammer et al., 1990). These descriptions correspond to the definitions of variegation and reticulation phenotypes. The molecular identity of the mutants, however, has not been corroborated yet.

Hypotheses explaining variegation and reticulation

The most challenging task is to explain the variegated and reticulated phenotype based on the molecular constraints. Different hypotheses have been presented by various research groups to link the molecular defect to the phenotype. The hypotheses are not always excluding each other. We try to integrate the hypotheses to draw a bigger picture and will also present our point of view. The overview of reticulated mutants depicted in Figure 3.

Variegated and reticulated mutants cannot always be distinguished unambiguously, as depicted for ATase2 mutants in this review. It will be challenging to categorize novel mutants in the future. Variegated mutants are mostly defective in thylakoid localized proteins and/or in proteins involved in carotenoid biosynthesis and/or are defective in scavenging excitation energy/ROS. These defects end in deficiencies of thylakoid and chloroplast differentiation, as it is also observed for M chloroplasts of ATase2 mutants (Kinsman and

Pyke, 1998; Hung et al., 2004). Reticulated mutants are either associated with primary/secondary metabolic, regulatory or protein biosynthesis defects, all due to unfunctional stroma or plastid envelope proteins. At least the evenly reticulated *trp2* mutant is not changed in M chloroplast ultrastructure (Jing et al., 2009), indicating that chloroplast development is unaffected. Mutations initially identified due to their similarity in leaf morphology, are affected in a single pathway or molecular mechanism, making gene-morphological relations reproducible (Pérez-Pérez et al., 2011). Thus, variegated and reticulated mutants are powerful tools to investigate metabolic defects.

Retrograde signaling

Plastids are semi-autonomous organelles, i.e. they harbor plastid and nuclear encoded proteins. Thus, a communication between the nucleus and the plastid is essential to ensure the coordinated interlocking of metabolic and developmental programs. This communication occurs from the nucleus to the plastid (anterograde signaling) and from the plastid to the nucleus (retrograde signaling) (Nott et al., 2006; Pogson et al., 2008). Reactive oxygen species (ROS) are key signaling molecules in retrograde signaling, which serves two functions: (i) signals for developmental control and (ii) signals involved in integration of environmental stimuli (Pogson et al., 2008; Woodson and Chory, 2008; Pfannschmidt, 2010).

In particular, the first mechanism is likely affected in variegated and reticulated mutants. In *im* and *var2* the impairment in chloroplast biogenesis is correlated with the retrograde suppression of nuclear encoded photosynthetic genes (Wetzel et al., 1994; Aluru et al., 2001; Kato et al., 2007; Miura et al., 2010), specifically in white sectors of *var2* (Kato et al., 2007). Plastid-encoded genes accumulate to wild-type levels in *var2* (Takechi et al., 2000). The lack of palisade M in *cla1* (Estevez et al., 2000) and the *var3* phenotype (Yu et al., 2007) are linked to disturbed retrograde signaling.

Cue1, isolated in a screen for suppressed nuclear encoded photosynthesis genes, is hypothesized to be defective in retrograde developmental signals that specify M development (Knappe et al., 2003). D*ov1* is likely affected in retrograde signaling (Yu et al., 2007). It`s allele *alx13*, however, does not have decreased nuclear encoded transcripts of photosynthesis genes, indicating that the retrograde signaling is not affected (Woo et al., 2011). *Ntrc* is linked to a deficiency in antioxidant activities (Lepistö et al., 2009), because n*trc* and also it´s rice homologue show hypersensitive responses to abiotic stresses (Serrato et al., 2004; Pérez-Ruiz et al., 2006), similar to the ozone-susceptible *lcd1* (Overmyer et al., 2008). Accumulation of ROS leads to chlorosis, restricted to interveinal regions. However, superoxide or hydrogen peroxide is not accumulated in *ntrc* (Lepistö et al., 2009). *Lcd1* is discussed as being affected in retrograde signaling. The impaired defense responses are

interpreted as being secondary (Barth and Conklin, 2003): *lcd1* leaves contain more apoplast, in which ozone dissolves preferentially into ROS, leading to higher ROS concentrations. These increased ROS concentrations in turn attack the decreased number of M cells, which are prone to pronounced tissue damage. Ribosome deficient plastids are hypothesized to be downregulated in plastid-derived signals, i.e. affected in retrograde signaling (Hess et al., 1994).

The threshold model of variegated phenotypes

The *threshold model of photooxidation* links the molecular defects to the variegated phenotype (Rosso et al., 2009). The model was refined later by the same group (Fu et al., 2012). The *threshold model* states that, if IM is present above a threshold, proplastids will develop to green chloroplasts, giving rise to green leaf sectors. If IM is below this threshold, the plastid will be damaged by photoinhibition and will not develop correctly, giving rise to white sectors (Rosso et al., 2006; Rosso et al., 2009). The redoxactive plastid terminal oxidase IM is active in carotenoid synthesis primarily in early chloroplast biogenesis. If IM lacks, phytoene accumulates due to an overreduction of the PQ-pool (Baerr et al., 2005; Rosso et al., 2006). Thus, carotenoids are not synthesized and ROS species are not scavenged. The plastids are vulnerable to photooxidation particularly under high-light by newly accumulating chlorophyll. In the revised *threshold model*, above threshold levels of IM correspond to below threshold levels in terms of excitation pressure, a means of the reduction state of the PQ pool (Fu et al., 2012). Developing chloroplasts are subjected to different excitation pressures due to intrinsic differences in their biochemistry, which in turn are caused by leaf gradients of light and determinants of light capture and use (Smith et al., 1997). It is argued that cells in the leaf primordia are exposed to different light regimes by shading through neighboring tissues. Superimposed, individual cells in the meristematic tissues of the primordia undergo individual circadian rhythms independently from each other (Velez-Ramirez et al., 2011; Fu et al., 2012). Outputs of the circadian clock are reflected in regulating ROS scavenging, even under the same light regime (Velez-Ramirez et al., 2011). If a cell or cell population is below the excitation pressure threshold, it develops green intact plastids in its cell lineage, and thus green sectors. If it is above the excitation threshold, the early plastids do not develop internal membrane structures, stay white and form white sectors as the outcome of the cell lineage. Thus, the chaotic patterning in *im* is a magnified version of different cell patterns already established in early leaf development, such as in the primoridia. If grown in low-light, *im* variegation is alleviated and thus photooxidative pressure lowered, giving rise to green tissue (Rédei, 1963; Wetzel et al., 1994; Aluru and Rodermel, 2004; Rosso et al., 2006; Yu et al., 2007; Rosso et al., 2009). When *im* is grown under low-

light and transferred to high-light, the plants stay green, indicating that the developmental stage is crucial for establishing variegation (Rosso et al., 2006; Rosso et al., 2009). At low temperatures and relatively high irradiance, leaves became variegated (Rosso et al., 2009). Light shift experiments indicate that the excitation pressure is positively correlated with extent of variegation in *var2*, *var1*, and *spotty* (Rosso et al., 2009).

In analogy to *im*, a threshold model is proposed for *var2* and *var1* (Yu et al., 2004, 2005; Yu et al., 2007). The thylakoid and the light triggered chloroplast development is believed to be a cell-autonomous process determined by overall FtsH levels. The differentiation of proplastids into chloroplasts only occurs if the two pairs of FtsH-proteins - AtFtsH1 and 5 and AtFtsH2 and 8 – oligomerize above a threshold level (Yu et al., 2005; Zaltsman et al., 2005; Kato et al., 2007). If a certain FtsH level is not reached, the plastids become arrested at later developmental stages, meaning they stay white and create white sectors (Kato et al., 2007). These plastids lack the thylakoid structure but show no further abnormalities (Chen et al., 2000; Takechi et al., 2000; Sakamoto et al., 2002; Kato et al., 2007). White sectors are not associated with senescence (Kato et al., 2007) and the sector formation was, unlike reported by (Sakamoto et al., 2002), not seen as resulting from impaired D1 turnover induced photobleaching (Zaltsman et al., 2005; Kato et al., 2007). Photobleaching as a sensitive response to high-light is interpreted as solely characteristic for green and not for white tissue of *var2* (Kato et al., 2007). Sector boundaries are fixed at full expansion in *var2*, i.e. the variegation pattern is irreversible once developed.

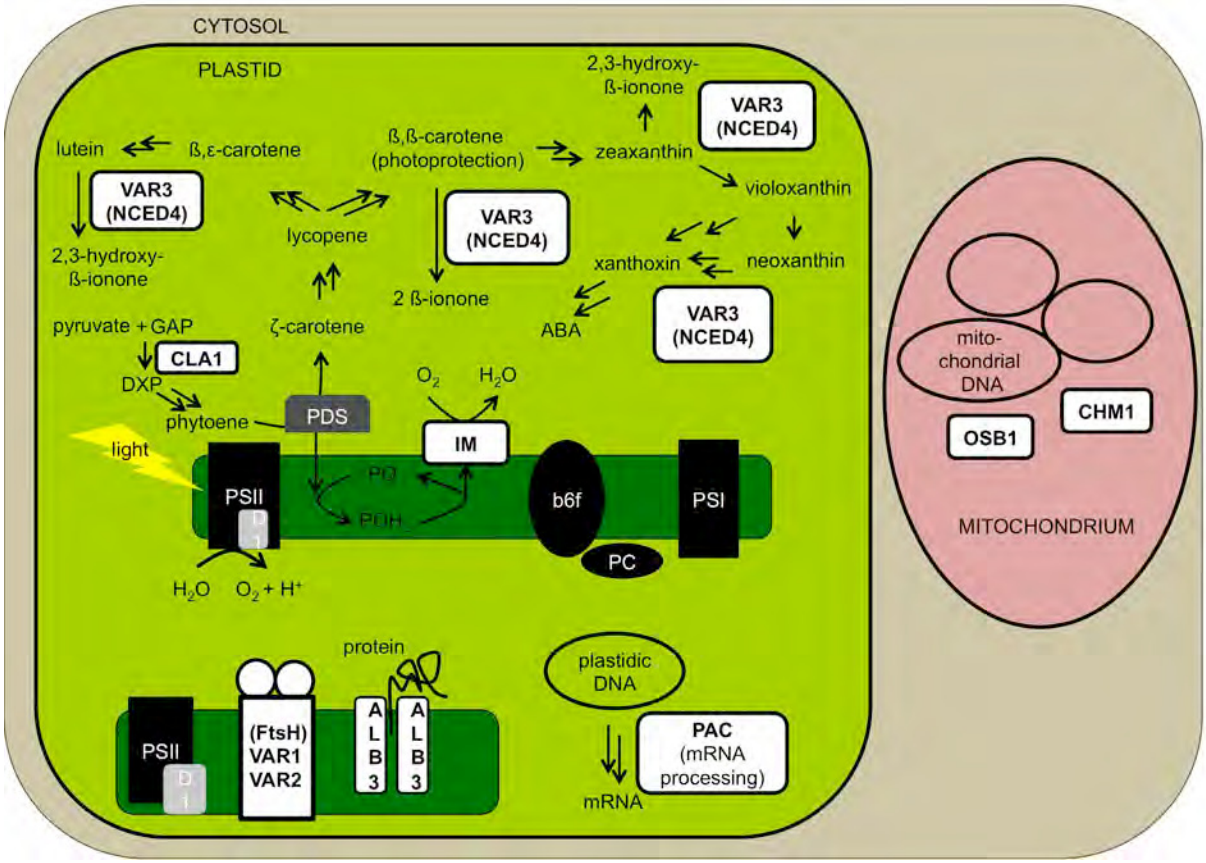

Figure 3: Affected pathways in variegated mutants. All molecularly characterized variegated mutants are defective in carotenoid biosynthesis, proteins in thylakoid membrane formation, replication, and mRNA processing. The *var3* mutant is defective in NCED4, i.e. in 2,3-hydroxy-ß-ionone and 2 ß-ionone synthesis, and thus in ß-carotene degradation. *Cla1* mutants are defective in the synthesis of the ß-carotene precursor phytoene. IM is indirectly involved as a redox-enzyme in the ζ -carotene synthesis. *Var1* and *var3*, defective in FtsH-subunits, are disturbed in thylakoid biogenesis as much as *alb3* mutants are. If plastidic mRNA processing is disturbed in *pac* mutants, leaves are variegated. The mitochondrial genome replication mutants *osb1* and *chm1* are variegated. ABA: abscisic acid; alb3: albino 3; chm1: chloroplast mutator1; cla1: cloroplastos alterados; DXP: 1-deoxy-D-xylulose 5-phosphate synthase; FtsH: filamentation temperature sensitive; nced 4:nine-*cis*-epoxy carotenoid diooxygenase 4; osb1: organellar single strand binding protein 1; pac: pale cress; PDS: phytoene desaturase; PS I: photosystem I, PS II: photosystem II, var: variegated.

How the mesophyll development affects leaf size

Reticulated mutants have smaller leaves with prominent leaf teeth (Kinsman and Pyke, 1998; Berná et al., 1999; Hung et al., 2004; Van der Graaff et al., 2004; González-Bayón et al., 2006; Lepistö et al., 2009; Horiguchi et al., 2011; Mollá-Morales et al., 2011; Byrne, 2012; Rosar et al., 2012). These indentations are likely due to the disturbed M structure in interveinal fields (González-Bayón et al., 2006). The reticulated phenotype is established early during development. *Re* was affected in early stages of leaf primordial development but not in the SAM (González-Bayón et al., 2006), and *cue1* discussed as affected in leaf primordia (Streatfield et al., 1999). The exact time point of leaf morphology

establishment was not assessed. Despite epidermal cell size contributes most, M cells also contribute to leaf size (Bemis and Torii, 2007; Powell and Lenhard, 2012). The growth of a leaf to its final size depends on two successive processes: (i) cell proliferation and (ii) cell expansion, with the number of cells and cell size as outcomes, respectively. Both processes are differentially regulated by cytokinins and auxins, respectively (Mizukami and Fischer, 2000; Mizukami, 2001; Anastasiou and Lenhard, 2007; Tsukaya, 2008; Jing et al., 2009). Reticulation can be either caused by decreased cell number and/or cell size. Thus, the phenotype can be either mediated by impaired cell proliferation or cell expansion.

Trp2 plants have smaller M cells but are not decreased in cell number. Determination of *trp2* growth kinetics reveal that leaf size increased at comparatively late stages of early leaf development, consistent with an alteration of cell expansion and/or prolongation of cell proliferation (Jing et al., 2009). Conclusively with this finding, *trp2* has a lower polyploidy level resulting from less endo-reduplication (Jing et al., 2009). Endo-reduplication and polyploidy levels correlate with plant cell size (Sugimoto-Shirasu and Roberts, 2003; Jing et al., 2009). Since cell elongation and proliferation are separately controlled processes (Mizukami and Fischer, 2000), trp is growth limiting only during elongation process (Jing et al., 2009). A both reduced M cell number and size in *ven3* and *6*, with the exception of *ven6-1* being not reduced in cell size (Mollá-Morales et al., 2011), indicates a decelerated proliferation and expansion. *Dov1* and *cia1* have a severely decreased M cell number but only marginally lowered cell size (Kinsman and Pyke, 1998; Hung et al., 2004). This observation is in line with growth kinetics of *dov1*, which is affected in rather early leaf expansion (Rosar et al., 2012). Thus, we conclude that the affected purine and cytokinin metabolism (Rosar et al., 2012) affects *dov1* early in development, before cell expansion occurs. The slightly reduced M cell size indicates that cell elongation is not severely affected, which is line with auxin response activities being at least partially active in *dov1* (Rosar, Kanonenberg et al. 2012). We propose that the metabolic constraints in *cue1* might be effective very early in development, similar to *dov1*, because *cue1* plants are decreased in M cell number but not in size (Streatfield et al., 1999). *Ntrc* is likely affected in early and late leaf development because cell number and size is decreased (Lepistö et al., 2009). *Re* plants, strongly lowered in M number but rarely decreased in size (González-Bayón et al., 2006), might thus be affected in very early events, similar to *dov1* but contrarily to *trp2*.

Supply and signaling hypothesis

A *threshold model*, as proposed for variegated mutants, seems not to be applicable to reticulated mutants. While variegation is patchy and chaotic, reticulation is coordinated and evenly distributed, i.e. pale sectors are constrained to interveinal fields with a well differentiated vasculature and BS. Thus, it is more likely, that a defect in leaf development is established in a certain cell population that develops either into the M, BS or vasculature. Two hypotheses have been published to explain the reticulated phenotype: the *signaling* and the *supply* hypothesis

The *supply hypothesis* states that reticulated mutants are defective in providing the plant with metabolites (Streatfield et al., 1999; Rosar et al., 2012). While *cue1*, *trp2*, *ven3* and *6* have lowered levels of the respective amino acid, ATase2 mutants are lowered in purine levels. Exogenous application of appropriate metabolites reverts the phenotypes. The joint interpretation of these results points to a limited supply of metabolites, such as amino acids and purines, to the M, which does not develop properly.

The *signaling hypothesis*, first presented by Streatfield et al., 1999, states that metabolic signals are generated in BS or vein and/or associated cells. If the signal is interrupted, the M will not able to follow leaf growth and will become aberrant (Figure 3). Veins and the BS likely differentiate together, since they form during early leaf development and differentiate prior to the M because it`s differentiation precludes minor vein formation (Pyke et al., 1991; Kinsman and Pyke, 1998; Candela et al., 1999; Hoffmann and Poorter, 2002). Some reticulated mutants have at least one homologue of which one is expressed along the veins. If this gene is defective, such as in in *cue1*, *ven3* and *6*, and *re*, plants exhibit a reticulate phenotype (Knappe et al., 2003; González-Bayón et al., 2006; Rosar et al., 2012). The nature of the metabolic signal is unknown. As discussed for *cue1*, aromatic amino acids *per se* might be a signal or derived secondary phenylpropanoid compounds, such as dehydrodiconiferyl alcohol glucoside (DCG) (Voll et al., 2003). Amino acids and nucleotides have a signaling function (Dennison and Spalding, 2000; Jeter et al., 2004; Joshi et al., 2010; Chivasa and Slabas, 2012; Sun et al., 2012). Hormones cannot be excluded as signal molecules, despite direct evidence is missing to date. Auxin, derived from trp, is possibly involved in vascular differentiation and the adjacent BS (Kinsman and Pyke, 1998). Phytohormones, found in the phloem sap, travel through the plant to exert their functions at the site of unloading (Komor et al., 1993; Kamboj et al., 1998; Lough and Lucas, 2006). Yet unidentified primary or secondary metabolites could act as signaling molecules. Small peptides are involved in regulating cell proliferation and organ growth. The knowledge about these processes is largely confined to the early leaf development in the SAM (Fukuda and Higashiyama, 2011). Proteins, such as the leaf development transcription factor KNOTTED1, can move across plasmodesmata (Schobert et al., 2004). Thus, proteins might interfere with

M development, and could establish a morphological gradient (Fleming, 2006). The biochemical complementation of phenotypes does not preclude a *signaling hypothesis*. The metabolites are thus taken up by the plant, and substitute the missing metabolite and thus the signal.

Both the *signaling* and the *supply hypothesis* are interwoven with the role of the BS and/or associated tissue in C_3-plants. However, only little is known about this tissue type (Leegood, 2008). Reticulated mutants are thus candidates not only for understanding internal leaf development but also for deciphering the physiological role of the BS.

The emerging role of the bundle sheath in mesophyll development

In both the *supply* and the *signaling hypothesis* the BS and/or the vasculature plays a crucial role. The BS of *Arabidopsis* is a chlorenchymatic cell layer surrounding the xylem, phloem and some adjacent cell such as companion cells. BS cells constitute ca. 15% of chloroplast-containing cells in *Arabidopsis* (Kinsman and Pyke, 1998), are found in BS of further dicotyledonous plants (Crookston and Moss, 1970), and are photosynthetically active in barley, including dark reactions (Williams et al., 1989; Koroleva et al., 2000; Fryer et al., 2003). Despite being smaller and occurring in a lower density than M chloroplasts, BS chloroplasts have the same ultrastructure as M chloroplasts with a well developed thylakoid structure and grana stacking (Kinsman and Pyke, 1998). The BS likely differentiates in a position-dependent manner, rather than from a cell lineage since they already form during leaf initiation along the xylem and phloem (Kinsman and Pyke, 1998). The BS is involved in both loading and unloading of phloem and xylem, and prevents air entering the xylem (Sage, 2001; Leegood, 2008). Already Haberlandt concluded from the presence of chloroplasts in the BS that these cells may have an additional function other than being just an efferent tissue and an unimportant addition to the photosynthetic apparatus (Haberlandt, 1914)(Leegood and Walker, 2003). Due to its central position within the leaf, the BS is prone to control the flux of information within a leaf, for example as discussed in the context of light-dependent acclimation (Kangasjärvi et al., 2009). The BS has been hypothesized to be relevant for leaf development (Kinsman and Pyke, 1998; Streatfield et al., 1999; González-Bayón et al., 2006; Rosar et al., 2012) by generating a signal that triggers M differentiation (see above).

By now, there is increasing evidence, that metabolism and thus potential signaling processes are differentially compartmentalized between different leaf tissues (Bechtold et al., 2008; Leegood, 2008; Kangasjärvi et al., 2009). The carbohydrate and nitrogen metabolism of xylem, phloem, and the BS is different from that of the M (Leegood, 2008). The phloem, containing plastids (Schobert et al., 2004), plays an important role in carbohydrate

metabolism (Nolte and Koch, 1993). Cells around the vein of C_3-plants play a crucial role in the synthesis of metabolites associated with carbohydrate metabolism (Janacek et al., 2009). The barley BS likely removes assimilates from the M and the apoplast, and thus buffers carbohydrates and malate between M cells and phloem (Leegood, 2008). In C_3-plants, high activities of three decarboxylases, which are also found in the C_4-BS, are abundant in vein-associated tissues (Hibberd and Quick, 2002). Pyruvate orthophosphate dikinase (PPDK) has a higher activity in the vasculature of tobacco and celery stems (Hibberd and Quick, 2002). PPDK converts pyruvate into PEP, which is fed into the shikimate pathway (Hibberd and Quick, 2002).

Not only is there evidence of a compartmentalized carbohydrate metabolism, also amino acid metabolism seems to be compartmentalized. Threonine aldolase2, catalyzing the degradation of threonine into glycine, is expressed around the vasculature (Joshi et al., 2006). The shikimate pathway for aromatic amino acid biosynthesis is more prominent in vein associated tissues (Janacek et al., 2009). Enzymes of amino acid biosynthesis are expressed along the veins, and if defective, result in a reticulated phenotype: CUE1 (Knappe et al., 2003), VEN3 and VEN6 (Potel et al., 2009). Particular amino acid transporters are expressed along the veins in *Arabidopsis*, preferentially in the BS (Kwart et al., 1993; Fischer et al., 1995; Rentsch et al., 1996; Hirner et al., 1998). In cucumber, the M and phloem sap composition differs during day/night cycle, suggesting that amino acid metabolism is occurring in the vast majority within vasculature or cells around it (Mitchell et al., 1992). Additionally, the transport metabolites arginine and citrulline occur in different concentrations around the veins in curcubits. The nitrogen in the phloem sap mainly consists of amino acids, with arginine and glutamine being the most abundant amino acids (Schobert et al., 2004). In a recent review it was argued that amino acid composition of the M and phloem differ (Turgeon, 2010). Nitrogen assimilation is differently compartmentalized between vascular tissue and M in wheat and tobacco during transition from sink to source leaves (Brugière et al., 2000; Kichey et al., 2005). It was proposed that glutamine is produced in higher amounts in vascular cells (BS, xylem parenchyma, mestome sheath and epidermis) of wheat and transported via those cells into the M (Kichey et al., 2005). However, similar amino acid compositions of phloem and M sap in spinach, barley, and sugar beet were detected (Riens et al., 1991; Winter et al., 1992; Lohaus et al., 1994), indicating that no amino acid metabolism between both cell types occurs and that amino acid metabolism is not compartmentalized between these cell types. Amino acids may use apoplastic and/or symplastic routes for final phloem loading (Schobert et al., 2004), depending on the nitrogen availability. The xylem is involved in amino acid uptake (Okumoto et al., 2002).

Additionally, the phloem contributes to secondary product biosynthesis (Burlat et al., 2004), particularly in the plastidic MEP pathway, giving rise to isoprenoids. These cell types

are also involved in wound signaling in rice via lignification of the xylem wall (Hilaire et al., 2001) and via the prosystemin protein in tomato (Hilaire et al., 2001; Narváez-Vásquez and Ryan, 2004). Lignin biosynthesis bases on phenylpropanoid metabolism and thus on the shikimate pathway (Lewis and Yamamoto, 1990).

Similarities in BS and M enzyme distribution between C_3-and C_4-plants are in agreement with a pre-adaption to C_4-photosynthesis, in which photosynthesis is compartmentalized between M and BS (Christin et al., 2010; Langdale, 2011; Sage et al., 2011). Carbon is fixed into a C_4-acid in the RuBisCo lacking M, and decarboxylated in the BS. The released CO_2 is consumed in the Calvin-Benson cycle. The sulfate metabolism, predominantly occurring in the C_4-BS, is also predominant in the C_3-BS (Leegood, 2008). Light dependent acclimation processes in C_3-plants, mainly mediated by ROS as central players, are likely compartmentalized between M and BS. The BS plays a pivotal role in generating ROS signals that are involved in plant development. These topics are reviewed elsewhere (Kangasjärvi et al., 2009). ABA, whose plastidic and cytosolic synthesis is concentrated in the vasculature parenchyma cells (Cheng et al., 2002; Koiwai et al., 2004; Christmann et al., 2005; Nambara and Marion-Poll, 2005; Kanno et al., 2012), is involved in BS specific ROS signaling (Galvez-Valdivieso et al., 2009). ABA transporters are found in the vasculature (Kanno et al., 2012). ABA is a key player in initiating a redox-retrograde signal from BSC chloroplasts to activate APX2 expression (Ascorbate peroxidase2) (Galvez-Valdivieso et al., 2009). APX2 is expressed specifically and ascorbate synthesis initiated in the BS (Fryer et al., 2003; Mullineaux et al., 2006). *Arabidopsis* BS cells differ from neighboring cells in hydrogen peroxide and antioxidant metabolism. Thus, hydrogen peroxide from BS cell chloroplasts may be part of wider signaling network (Fryer et al., 2003; Kangasjärvi et al., 2009). However, ABA signaling in veins was observed under high-light conditions and not under physiological conditions. Consequently, an involvement of ROS signaling in the sense of the signaling hypothesis is at least less unlikely. The ATase2 allele *alx13* was found in screen for mutations that alter regulation of the high-light inducible APX2 gene.

In summary, we conclude that the variegated phenotype originates from a disturbed chloroplast biogenesis *per se* and starts very early during leaf development already in the SAM or primordia formation. A defect in plastid development in certain cells/tissues thus is magnified on the adult leaves by patchy white/green leaves. The reticulated phenotype, in contrast, is either caused early in development or later during leaf initiation by being specific to a genetically inherited trait in certain cell types. We think that the inhibition of amino acid and/or purine biosynthesis around the veins is causal for the reticulated phenotype. If the signaling or supply hypothesis is more likely, has to be tested. The *signaling hypothesis* assumes that the intact BS chloroplasts generate a metabolic signal that triggers M

differentiation. If BS chloroplasts are, however, rendered specifically unfunctional by respressing the BS-chloroplast chlorophyll biosynthesis, the M still develops normally. This observation, at least, makes the *signaling hypothesis* less likely To deepen the understanding of the BS`s role in C_3-plants, tissue specific profiling techniques, such as laser microdissection (LMD) (Asano et al., 2002; Kehr, 2003; Kerk et al., 2003; Nakazono et al., 2003; Inada and Wildermuth, 2005; Galbraith and Birnbaum, 2006; Wuest et al., 2010; Schmid et al., 2012) will be of importance.

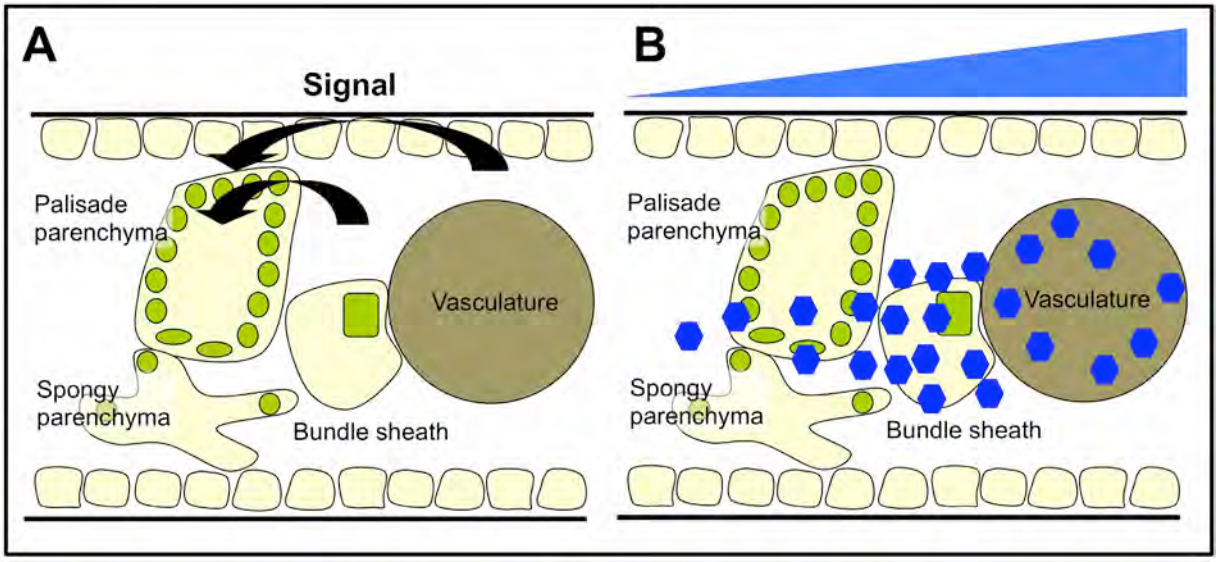

Figure 3: Signaling and supply hypothesis. The schematic cross-sections show the central vasculature, the bundle sheath (BS), and the mesophyll (M). **(A)** The *signaling hypothesis* states that a metabolic signal is generated in the vasculature/and or the BS. This signal triggers differentiation of the M. If the signal is disturbed, as hypothesized for the reticulated mutants, the M does not develop correctly and becomes aberrant with smaller and/or less cells. **(B)** The *supply hypothesis* states that metabolites transported through the vasculature are shuffled to the developing M in young plants. If the supply with metabolites is disturbed, the M becomes aberrant.

Table 1. Reticulated and variegated mutants. Table 1 is split and shown on the next five pages. *A.t.*: *Arabidopsis thaliana*; *Z.m.*: *Zea mays*; N.t. *Nicotiana tabacum*; B.: *Begonia*; *S.l.*: *Solanum lycopersicum*, *A.m.*: *Anthirrrhinum majus; O.s.*: *Oryza sativa*; *H.a.*: *Helianthus annus*. M: mesophyll; BS: bundle sheath; E: epidermis; P: palisade parenchyma; EM: electron microscopy; WT: wild-type; ?: either no information was found or the information was not established; Database (Kuromori et al., 2006): /http://rarge.psc.riken.jp/phenome; database (Yamaguchi et al., 2012) :http://rarge.psc.riken.jp/chloroplast.

Mutant	Full name	Gene	Alleles	Mutagen	Protein function	Process	Plastid morphology	Leaf morphology	Cells	References
Reticulated mutants of *Arabidopsis thaliana*										
cue1	*chlorophyll a/b binding protein (CAB) gene underexpressed1*	At5g33320	*cue1-1*	X-ray	Phosphoenol-pyruvate/ phosphate translocator1 (PPT1)	import of phosphoenol-pyruvate (PEP) across plastid envelope	M chloroplast: smaller (particularly in palisade cells), normal granal stacking (EM) BS chloroplast: normal size and number normal granal stacking (EM)	reticulated cotyledons, rosette, cauline leaves; very small leaves; prominent leaf teeth	M: less cells, normal size; palisade cells spherical with fewer and smaller chloroplasts; normal chloroplast number per cell; airspace volume between M-cells increased; BS: normal size, normal chloroplast size and number	Li et al., 1995; López-Juez et al., 1998; Streatfield et al., 1999
			cue1-2	X-ray						
			cue1-3	EMS						
			cue1-4	unknown						
			cue1-5	unknown						
			cue1-6	unknown						
			cue1-7	unknown						
			cue1-8	T-DNA						
ipgam double mutant (ipgam1/ipgam2)	2-3-*bisphospho glycerate-independent phosphor-glycerate mutase*	At1g09780/ At3g08590	?	?	2-3-bisphospho-glycerate-independent phospho-glycerate mutase	conversion of 3-PGA to 2-PGA	?	?	?	Zhao and Assmann, 2011
ven3	*venosa3*	At1g29900	?	EMS	CAR-B (CPS large SU)	arginine biosynthesis	?	reticulated, small, leaf teeth	M: less cells; smaller palisade cells	Berná et al., 1999; Molá-Morales et al., 2011
ven6	*venosa6*	At3g27740	?	EMS	CAR-A (CPS small SU)		?	reticulated, small, leaf teeth	M: less cells	
trp2 smo1/trp2-301	*tryptophan synthase2*	At5g54810	*trp2*	EMS; *trp2-301* (T-DNA)	TSB1 (Tryptophan synthase ß1)	tryptophan biosynthesis	number of chloroplasts same as in WT; young leaves: fewer starch granules and under-developed chloroplasts; older leaves: size and structure as in WT	smaller, reticulated, also smaller and reticulated cotyledons	M: smaller size, normal number, epidermal cells at WT-like	Last et al., 1991; Barczak et al., 1995; Jing et al., 2009
			trp3	EMS						
			smo-1							
ATase2 mutants	Glutamine phosphor-ribosyl-pyrophos-phate amino-transferase2	At4g34740	*dov1-1* (differential development of vasculature associated cells 1-1)	EMS	ATASE2	first step of *de novo* purine biosynthesis	BS: normal chloroplast: M: abnormal chloroplasts, some normal chloroplasts	delay in growth, smaller true leaves, strongly reticulated leaves, cotyledons not affected	M: decreased number, slightly smaller cells BS: normal chloroplasts, normal size	Kinsman and Pyke, 1998; Van der Graaff et al., 2004; Rosar et al., 2012
			cia1-2 (*chloroplast import apparatus 1-2*)	T-DNA			?	smaller leaves, „albino/pale-green mosaic leaves"	M: cells reduced in numer (ca. 50% of WT level); cell size only slightly reduced	Hung et al., 2004; Sun et al., 2009
			atd2 (ATase deficient2)	T-DNA			M: abnormal chloroplasts, no thylakoid structure; vesiculation of thylakoid; Some M cells with residual thylakoid membrane structures near to vasculature	strong growth retardation and leaf chlorosis, or formation of white leaves but green cotyledons; green upon first emergence, but become rapidly white	M: no palisade cells; additional layer of spongy M; larger airpaces in M (not mentioned by authors, but seen in cross-sections)	Van der Graaff et al., 2004
			alx13 (*altered APX2 expression 13*)	point mutation			?	variegated phenotype, reticulated pattern occasionally observed; leaf serration slightly increased	?	Woo et al., 2011

Mutant	Full name	Gene	Alleles	Mutagen	Protein function	Process	Plastid morpholgy	Leaf morpholgy	Cells	References
Reticulated mutants of *Arabidopsis thaliana*										
ntrc	*NADPH-thioredoxin reductase*	At2g41680	?	T-DNA	NADPH-thioredoxin reductase	regulation of metabolic processes	?	reticulated leaves; prominent leaf teeth	M: decreased number; decreased size	Serrato et al., 2004; Lepistö et al., 2009
re	*reticulata*	At2g37860	*re-1*	deletion	unknown; localized to the plastid	unknown	M chloroplast: ultrastructure unknown (no EM) BS chloroplast: ultrastructure unknown (no EM)	reticulated leaves; prominent leaf teeth; leaves thinner than WT (*re-1*), but increased thickness next to veins	M: slightly smaller size, reduced number of palisade and spongy M with palisade cell loss more pronounced; Palisade cells more vacuolated; BS: more chloroplasts per cell E: cell size and morphology normal (all in *re-1*)	González-Bayón et al., 2006
			re-2	EMS						Berná et al., 1999; González-Bayón et al., 2006
			re-3, ven2-1	EMS						
			re-4, ven2-2	EMS						González-Bayón et al., 2006
			re-5, ven3-3	T-DNA						
			re-6	T-DNA						González-Bayón et al., 2006; Overmyer et al., 2008
			re-7	T-DNA						
			re-8, rcd2	unknown (point mutation)						Overmyer et al., 2008
			lcd1-1 (lower cell density1-1)	EMS						Barczak et al., 1995; Conklin et al., 1996; Barth and Conklin, 2003
SUC-P19HA	?	?	?	?	disturbed cell-cell communication	cell-cell communicatio	?	white veins and green intercostal leaf lamina (inverse reticulated)	?	Dunoyer et al., 2010
BS specific inactivation of CS	?	?	?	?	silincing of BS photosynthesis	silincing of BS photosynthesis	BS: reduced granal stacking, penetrating into BS near M cells	white veins and green incostal leaf lamina (inverse reticulated)	?	Janacek et al., 2009
BnPEND	?	?	?	Overex-pressor of *Brassica napus* PEND protein	localized to plastid	unknown	chloropast internal structure lost	pale to chlorotic	M: structure lost	Wycliffe et al., 2005
Mutant	**Full name**	**Gene**	**Alleles**	**Mutagen**	**Protein function**	**Process**	**Plastid morpholgy**	**Leaf morpholgy**	**Cells**	**References**
Variegated mutants of *Arabidopsis thaliana*										
pac	*pale cress (pac)*	At2g48120	*pac-1*	T-DNA	?	unknown; likely disturbed in mRNA-maturation	plastids: almost thylakoid-less	Pale	M: palisade parenchyma poorly differentiated, epidermal cells enlarged (*pac-1* and *pac-2* have different phenotypes)	Reiter et al., 1994
			pac-2	T-DNA	?		green sectors: normal chloroplasts; white sectors: abnormal chloroplasts	variegated		Grevelding et al., 1996
cla1	*cloroplastos alterados1*	At4g15560	*cla1-1*	T-DNA	1-Deoxyxylulose 5-Phosphate Synthase (localized to chloroplast)	MEP pathway for isoprenoid biosynthesis	white plastids without thylakoids and with vesicles	albino	M: without palisade parenchyma	Estévez et al., 2000; Mandel et al., 1996
			lvr111 (lovostatin-resistant111)	EMS			?	Variegated dwarf phenotype	?	Crowell et al., 2003
			chs5 (chilling sensitive5)	EMS			?	Chlorotic when grwon at 15°C	?	Araki et al., 2000

Mutant	Full name	Gene	Alleles	Mutagen	Protein function	Process	Plastid morpholgy	Leaf morpholgy	Cells	References
Variegated mutants of *Arabidopsis thaliana*										
sca3	*scabra3*	At2g24120	*sca3-2*	T-DNA	Plastid RNA polymerase	RNA polymerase	chloroplast number reduced and chloroplast not properly developed, less developed thylakoid organization	pale green cotyledons and leaves; reticulated (cell surrounding midvein more similar to WT than M cells); leaf veins almost unaltered	M: decreased number; larger airspaces (morphology described for *sca3-2*)	Berná et al., 1999; Hricová et al., 2006
			sca3-1	EMS						
			sca3-3	EMS						
im	*immutans*	At4g22260	*im*	EMS	IM, plastidic terminal oxidase (PTOX)	disturbed carotenoid biosynthesis	normal in green sectors; Plastids without thylkoids in white/yellow sectors, some cells in white sectors with green intact plastids (heteroplastididc)	white sector dominates leaf, green sectors appears to be spotty; green spots affected by light; variegation restricted to leaves	green sectors: thicker than WT white sectors: palisades not developed properly	Rédei, 1963; Rédei, 1967; Wetzel et al., 1994; Meehan et al., 1996; Sakamoto, 2003; Aluru et al., 2001; Rosso et al., 2009; Fu et al., 2012
			spotty	EMS						
chm	*chloroplast mutator*	At3g24320	*chm1* *chm2*	EMS	CHM: mitochondrial protein	involved in DNA mismtach repair and in controlling mitochondrial genome copy number	?	large white sectors mostly at either side of leaf; rough leaves	?	Rédei and Plurad, 1973; Martínez-Zapater, 1993; Abdelnoor et al., 2003; Sakamoto, 2003
			chm3	*?*						
var1	*(yellow) variegated1*	At5g42270	?	?	FTSH: role in membrane modeling events during thylakoid biosynthesis; degradation of photodamaged D1	disturbed balance between PSII synthesis and degradation	?	Uniform white and green sectors	?	Martínez-Zapater, 1993; Sakamoto et al., 2002
var2	*(yellow) variegated2*	At2g30950	*var4*	?			normal in green sectors; heteroplastic and vacuolated in white/yellow sectors	cotyledons normal; first true leaves are white, variegated leaves, stems, sepals and siliques; uniform white and green sectors in leaves	?	Martínez-Zapater, 1993; Chen et al., 1999; Chen et al., 2000; Lindahl et al., 2000; Kato et al., 2007; Miura et al., 2010
			?	EMS						
			var2	T-DNA						
var3	*(yellow) variegated3*	At5g17790	?	T-DNA	VAR3 protein	VAR3 interacts with nine-*cis*-epoxy carotenoid dioxygenase4 (NCED4), affected carotenoid biosynthesis	Yelllow sectors: thylakoid structure lacks; green sectors: normal chloroplasts	Variegated leaves	yellow patches: few if any palisade cells; green sectors: normal M	Næsted et al., 2004
thf1	*thylakoid formation1*	At2g20890	Line detected by (Yamaguchi et al., 2012)	T-DNA	THF1 protein	unknown	white sectors: thylkoids are lacking	?	variegated leaves	Wang et al., 2004; Keren et al., 2005; Huang et al., 2006; Yamaguchi et al., 2012
msh1	*mutS homolog1*	At3g24320	-	?	putative function in mitochondrial replication	?	?	variegated leaves	?	Abdelnoor et al., 2003
hma1	*heavy metal P_{1B}-ATPase*	At4g37270	-	T-DNA	heavy metal ATPase	transports iron over the plastid membrane	?	variegated leaves	?	Seigneurin-Berny et al., 2006
kas1	*ß-Keto-[Acyl Carrier Protein] Synthase1*	At5g46290	-	T-DNA	ketoacyl-synthase	plastdic fatty acid elongation	yellow sectors: enlarged chloroplasts; grana not developed (EM); green sectors: normal sized chloroplasts, normal number	small, variegated leaves with green, netted patches	green sectors: normal M cells; Yellow sectors: aberrant M structure	Wu and Xue, 2010
osb1	*Organellar single strand binding protein1*	At1g47720	*osb1-1* *osb1-2*	T-DNA	OSB1 protein	involved in correct stoichiometric mtDNA transmission	?	Variegated leaves	Some M cells abnormal	Zaegel et al., 2006

Mutant	Full name	Gene	Alleles	Mutagen	Protein function	Process	Plastid morpholgy	Leaf morpholgy	Cells	References
***Arabidopsis thaliana* mutants found in databases, either having a reticulated or variegated phenotype**										
?	?	At1g15710	?	T-DNA	prephenate dehdrogenase family protein; chloroplast	likely in tyrosine biosynthesis	?	reticulated; listed as pale green leaves	?	Kuromori et al., 2006; Yamaguchi et al., 2012
lrgA	?	At1g32080	?	T-DNA	protein in chloroplast membrane; MEP1	Function unknown	Less thylakoid stacking	described as variegated leaves; leaves appear, however, more reticulated on picture, veinal chlorosis	?	Kuromori et al., 2006; Yang et al., 2012
vipp1	Vesicle inducing protein in plastids 1	At1g65260	?	T-DNA	VIPP1	protein required for thylakoid formation	?	sligtly reticulated; listed as pale green	?	Kroll et al., 2001; Kuromori et al., 2006
?	?	At5g27010	?	T-DNA	CYTOCHROME P450 family	unknown	?	reticulated; listed as pale green leaves	?	Kuromori et al., 2006
?	?	At4g21060	?	T-DNA	putative beta-1,3-galactosyltransferase	unknown	?	described as variegated leaves	?	Kuromori et al., 2006
?	?	At4g01690	?	T-DNA	encodes protoporphyrinogen oxidase (PPOX)	unknown	?	described as variegated leaves	?	Kuromori et al., 2006; Lermontova and Grimm, 2006; Tanaka et al., 2011
?	?	At4g27600	?	T-DNA	phosphofructokinase B-type carbohydrate kinase family protein, NARA5. Regulates photosynthetic gene expression	unknown	?	variegated; Listed as pale green leaves and variegated seedling	?	Kuromori et al., 2006; Ogawa et al., 2009; Yamaguchi et al., 2012
?	?	At2g20860	?	T-DNA	unknown	unknown	?	Variegated leaves	?	Kuromori et al., 2006
?	?	At1g75030	?	T-DNA	ATLP-3 (ARABIDOPSIS THAUMATIN-LIKE PROTEIN 3)	unknown	?	Plant leaves look slightly Variegated/reticulated; listed as pale green leaves	?	Kuromori et al., 2006
?	?	At4g34830	?	T-DNA	Pentatrico-peptide repeat (PPR) superfamily protein	unknown	?	variegated, pale-green	?	Yamaguchi et al., 2012
?	?	At4g18750	?	T-DNA	Pentatrico-peptide repeat (PPR) superfamily protein	unknown	?	variegated	?	Yamaguchi et al., 2012

Mutants in non-*Arabidopsis* specis (*Zea mays, Nicotiana spec., barley)*											
Mutant	**Full name**	**species**	**Gene**	**Alleles**	**Mutagen**	**Protein function**	**Process**	**Plastid mopholgy**	**Leaf morpholgy**	**Cells**	**References**
ys1	*yellow stripe 1*	Z.m.	?	?	?	plasma membrane iron transporter	iron and heavy metal transport into cell	?	striped	?	Von Wirén et al., 1994; Schaaf et al., 2004;
z2	*rice zebra 2*	O.s.	?	?	?	carotenoid isomerase	carotenoid biosynthesis	?	yellow/white and green stiped	?	Chai et al., 2011; Han et al., 2012
AT, ntpurf	?	*N.t.*	NtPurf	?	antisense	ATase2 (Glutamine phosphoribosy pyrophosphat e amidotransfer ase 2)	first step of *de novo* purine biosynthesis	?	similar phenotype observed as for *atd2*	?	Van der Graaff et al., 2004
dag	*Anthirrrhinum majus differentiation and greening*	*A.m.*	unknown	?	insertion	unknown	unknown	reduced grana stacking	variegated	palisade cells reduced in number	Sommer et al., 1985; Chatterjee et al., 1996
dcl	*defective chloroplasts and leaves*	*S. l.*	Unknown	?	*Ds* insertion	rRNA processing/pla stid ribosome assembly	likely required for rRNA processing and plastid ribosome assembly	palisade M: reduced grana stacking, vesicles in chloroplasts	variegated; no visible phenotype in *A. thaliana* homologue mutant	palisade cells with reduced number of chloroplasts	Keddie et al., 1996; Bellaoui et al., 2003; Bellaoui and Gruissem, 2004
mcd1	*mesophyll cell defective1*	*H.a.*	unknown	?	imbred line	unknown	unknown	smaller leaves, patchy yellow/green (variegated)	variegated/chlorotic	palisade and spongy M cells with large intracellular spaces, in some areas without M cells; Palisade cells with reduced number of chloroplasts	Fambrini et al., 2010

Acknowledgement and funding:

This work was funded by grants of the Deutsche Forschungsgemeinschaft (DFG CRC 590 to APMW and iRTG 1525 to APMW). CR thanks the "Studienstiftung des deutschen Volkes" for support.

References

Abdelnoor RV, Yule R, Elo A, Christensen AC, Meyer-Gauen G, Mackenzie SA (2003) Substoichiometric shifting in the plant mitochondrial genome is influenced by a gene homologous to MutS. Proceedings of the National Academy of Sciences of the United States of America **100:** 5968-5973

Adam Z, Rudella A, van Wijk KJ (2006) Recent advances in the study of Clp, FtsH and other proteases located in chloroplasts. Current Opinion in Plant Biology **9:** 234-240

Aluru MR, Bae H, Wu DY, Rodermel SR (2001) The *Arabidopsis immutans* mutation affects plastid differentiation and the morphogenesis of white and green sectors in variegated plants. Plant Physiology **127:** 67-77

Aluru MR, Rodermel SR (2004) Control of chloroplast redox by the IMMUTANS terminal oxidase. Physiologia Plantarum **120:** 4-11

Aluru MR, Yu F, Fu A, Rodermel S (2006) *Arabidopsis* variegation mutants: new insights into chloroplast biogenesis. Journal of Experimental Botany **57:** 1871-1881

Aluru MR, Zola J, Foudree A, Rodermel SR (2009) Chloroplast photooxidation-induced transcriptome reprogramming in Arabidopsis *immutans* white leaf sectors. Plant Physiology **150:** 904-923

Anastasiou E, Lenhard M (2007) Growing up to one's standard. Current Opinion in Plant Biology **10:** 63-69

Andersson M, Sandelius A (2004) A chloroplast-localized vesicular transport system: a bio-informatics approach. BMC Genomics **5:** 40

Araki N, Kusumi K, Masamoto K, Niwa Y, Iba K (2000) Temperature-sensitive *Arabidopsis* mutant defective in 1-deoxy-D-xylulose 5-phosphate synthase within the plastid non-mevalonate pathway of isoprenoid biosynthesis. Physiologia Plantarum **108:** 19-24

Arrieta-Montiel MP, Shedge V, Davila J, Christensen AC, Mackenzie SA (2009) Diversity of the Arabidopsis Mitochondrial Genome Occurs via Nuclear-Controlled Recombination Activity. Genetics **183:** 1261-1268

Asano T, Masumura T, Kusano H, Kikuchi S, Kurita A, Shimada H, Kadowaki K (2002) Construction of a specialized cDNA library from plant cells isolated by laser capture microdissection: toward comprehensive analysis of the genes expressed in the rice phloem. Plant Journal **32:** 401-408

Babiychuk E, Bouvier-Navé P, Compagnon V, Suzuki M, Muranaka T, Van Montagu M, Kushnir S, Schaller H (2008) Albinism and cell viability in cycloartenol synthase deficient *Arabidopsis*. Plant signaling and behavior **3:** 978-980

Baerr JN, Thomas JD, Taylor BG, Rodermel SR, Gray GR (2005) Differential photosynthetic compensatory mechanisms exist in the *immutans* mutant of *Arabidopsis thaliana*. Physiologia Plantarum **124:** 390-402

Bagge P, Larsson C (1986) Biosynthesis of aromatic amino acids by highly purified spinach chloroplasts - compartmentation and regulation of the reactions. Physiologia Plantarum **68:** 641-647

Bailey S, Thompson E, Nixon PJ, Horton P, Mullineaux CW, Robinson C, Mann NH (2002) A critical role for the Var2 FtsH homologue of *Arabidopsis thaliana* in the photosystem II repair cycle *in vivo*. Journal of Biological Chemistry **277:** 2006-2011

Ball L, Accotto GP, Bechtold U, Creissen G, Funck D, Jimenez A, Kular B, Leyland N, Mejia-Carranza J, Reynolds H, Karpinski S, Mullineaux PM (2004) Evidence for a direct link between glutathione biosynthesis and stress defense gene expression in *Arabidopsis*. Plant Cell **16:** 2448-2462

Barczak AJ, Zhao JM, Pruitt KD, Last RL (1995) 5-fluoroindole resistance identifies tryptophan synthase beta subunit mutants in *Arabidopsis thaliana*. Genetics **140:** 303-313

Barr J, White WS, Chen L, Bae H, Rodermel S (2004) The GHOST terminal oxidase regulates developmental programming in tomato fruit. Plant Cell and Environment **27:** 840-852

Barth C, Conklin PL (2003) The lower cell density of leaf parenchyma in the *Arabidopsis thaliana* mutant *lcd1-1* is associated with increased sensitivity to ozone and virulent *Pseudomonas syringae*. Plant Journal **35:** 206-218

Bartlem D, Lambein I, Okamoto T, Itaya A, Uda Y, Kijima F, Tamaki Y, Nambara E, Naito S (2000) Mutation in the threonine synthase gene results in an over-accumulation of soluble methionine in *Arabidopsis*. Plant Physiology **123:** 101-110

Barton MK (2010) Twenty years on: The inner workings of the shoot apical meristem, a developmental dynamo. Developmental Biology **341:** 95-113

Bassett EV, Bouchet BY, Carr JM, Williamson CL, Slocum RD (2003) PALA-mediated pyrimidine starvation increases expression of aspartate transcarbamoylase (*pyrB*) in *Arabidopsis* seedlings. Plant Physiology and Biochemistry **41:** 695-703

Bechtold U, Richard O, Zamboni A, Gapper C, Geisler M, Pogson B, Karpinski S, Mullineaux PM (2008) Impact of chloroplastic- and extracellular-sourced ROS on high light-responsive gene expression in Arabidopsis. Journal of Experimental Botany **59:** 121-133

Bellaoui M, Gruissem W (2004) Altered expression of the *Arabidopsis* ortholog of *DCL* affects normal plant development. Planta **219:** 819-826

Bellaoui M, Keddie JS, Gruissem W (2003) DCL is a plant-specific protein required for plastid ribosomal RNA processing and embryo development. Plant Molecular Biology **53:** 531-543

Bemis SM, Torii KU (2007) Autonomy of cell proliferation and developmental programs during *Arabidopsis* aboveground organ morphogenesis. Developmental Biology **304:** 367-381

Benning C (2009) Mechanisms of lipid transport involved in organelle biogenesis in plant cells. *In* Annual Review of Cell and Developmental Biology, Vol 25, pp 71-91

Berná G, Robles P, Micol JL (1999) A mutational analysis of leaf morphogenesis in *Arabidopsis thaliana*. Genetics **152:** 729-742

Börner T, Sears B (1986) Plastome mutants. Plant Molecular Biology Reporter **4:** 69-92

Bräutigam A, Weber APM (2009) Proteomic analysis of the proplastid envelope membrane provides novel insights into small molecule and protein transport across proplastid membranes. Molecular Plant **2:** 1247-1261

Brown DE, Rashotte AM, Murphy AS, Normanly J, Tague BW, Peer WA, Taiz L, Muday GK (2001) Flavonoids act as negative regulators of auxin transport *in vivo* in *Arabidopsis*. Plant Physiology **126:** 524-535

Brugière N, Dubois F, Masclaux C, Sangwan RS, Hirel B (2000) Immunolocalization of glutamine synthetase in senescing tobacco (*Nicotiana tabacum* L.) leaves suggests that ammonia assimilation is progressively shifted to the mesophyll cytosol. Planta **211:** 519-527

Buchanan BB, Balmer Y (2005) Redox regulation: A broadening horizon. *In* Annual Review of Plant Biology, Vol 56, pp 187-220

Burlat V, Oudin A, Courtois M, Rideau M, St-Pierre B (2004) Co-expression of three MEP pathway genes and *geraniol 10-hydroxylase* in internal phloem parenchyma of *Catharanthus roseus* implicates multicellular translocation of intermediates during the biosynthesis of monoterpene indole alkaloids and isoprenoid-derived primary metabolites. Plant Journal **38:** 131-141

Byrne ME (2005) Networks in leaf development. Current Opinion in Plant Biology **8:** 59-66

Byrne ME (2012) Making leaves. Current Opinion in Plant Biology **15:** 24-30

Cai W, Ma J, Chi W, Zou M, Guo J, Lu C, Zhang L (2010) Cooperation of LPA3 and LPA2 is essential for photosystem II assembly in *Arabidopsis*. Plant Physiology **154:** 109-120

Canales C, Grigg S, Tsiantis M (2005) The formation and patterning of leaves: recent advances. Planta **221:** 752-756

Candela H, Martínez-Laborda A, Micol JL (1999) Venation pattern formation in *Arabidopsis thaliana* vegetative leaves. Developmental Biology **205:** 205-216

Carol P, Stevenson D, Bisanz C, Breitenbach J, Sandmann G, Mache R, Coupland G, Kuntz M (1999) Mutations in the *Arabidopsis* gene *IMMUTANS* cause a variegated phenotype by inactivating a chloroplast terminal oxidase associated with phytoene desaturation. Plant Cell **11:** 57-68

Chai C, Fang J, Liu Y, Tong H, Gong Y, Wang Y, Liu M, Wang Y, Qian Q, Cheng Z, Chu C (2011) *ZEBRA2*, encoding a carotenoid isomerase, is involved in photoprotection in rice. Plant Molecular Biology **75:** 211-221

Charuvi D, Kiss V, Nevo R, Shimoni E, Adam Z, Reich Z (2012) Gain and loss of photosynthetic membranes during plastid differentiation in the shoot apex of *Arabidopsis*. Plant Cell **24:** 1143-1157

Chatterjee M, Sparvoli S, Edmunds C, Garosi P, Findlay K, Martin C (1996) DAG, a gene required for chloroplast differentiation and palisade development in *Antirrhinum majus*. Embo Journal **15:** 4194-4207

Chen M, Choi YD, Voytas DF, Rodermel S (2000) Mutations in the *Arabidopsis* VAR2 locus cause leaf variegation due to the loss of a chloroplast FtsH protease. Plant Journal **22:** 303-313

Cheng WH, Endo A, Zhou L, Penney J, Chen HC, Arroyo A, Leon P, Nambara E, Asami T, Seo M, Koshiba T, Sheen J (2002) A unique short-chain dehydrogenase/reductase in *Arabidopsis* glucose signaling and abscisic acid biosynthesis and functions. Plant Cell **14:** 2723-2743

Cheng YF, Dai XH, Zhao YD (2006) Auxin biosynthesis by the YUCCA flavin monooxygenases controls the formation of floral organs and vascular tissues in *Arabidopsis*. Genes and Development **20:** 1790-1799

Chivasa S, Slabas AR (2012) Plant extracellular ATP signalling: new insight from proteomics. Molecular Biosystems **8:** 445-452

Christin P-A, Freckleton RP, Osborne CP (2010) Can phylogenetics identify C_4 origins and reversals? Trends in Ecology and Evolution **25:** 403-409

Christmann A, Hoffmann T, Teplova I, Grill E, Müller A (2005) Generation of active pools of abscisic acid revealed by in vivo Imaging of water-stressed *Arabidopsis*. Plant Physiology **137:** 209-219

Connett MB (1986) Mechanisms of maternal inheritance of plastids and mitochondria: Developmental and ultrastructural evidence. Plant Molecular Biology Reporter **4:** 193-205

Cordin O, Banroques J, Tanner NK, Linder P (2006) The DEAD-box protein family of RNA helicases. Gene **367:** 17-37

Crookston RK, Moss DN (1970) Relation of carbon dioxide compensation and chlorenchymatous vascular bundle sheaths in leaves of dicots. Plant Physiology **46:** 564-567

Crowell DN, Packard CE, Pierson CA, Giner JL, Downes BP, Chary SN (2003) Identification of an allele of *CLA1* associated with variegation in *Arabidopsis thaliana*. Physiologia Plantarum **118:** 29-37

Delarue M, Prinsen E, Van Onckelen H, Caboche M, Bellini C (1998) *Sur2* mutations of *Arabidopsis thaliana* define a new locus involved in the control of auxin homeostasis. Plant Journal **14:** 603-611

DellaPenna D, Pogson BJ (2006) Vitamin synthesis in plants: tocopherols and carotenoids. Annual Review of Plant Biology **57:** 711-738

Dennison KL, Spalding EP (2000) Glutamate-gated calcium fluxes in *Arabidopsis*. Plant Physiology **124:** 1511-1514

Dunoyer P, Schott G, Himber C, Meyer D, Takeda A, Carrington JC, Voinnet O (2010) Small RNA duplexes function as mobile silencing signals between plant cells. Science **328:** 912-916

Dünschede B, Bals T, Funke S, Schünemann D (2011) Interaction studies between the chloroplast signal recognition particle subunit cpSRP43 and the full-length translocase Alb3 reveal a membrane-embedded binding region in Alb3 protein. Journal of Biological Chemistry **286:** 35187-35195

Elkind Y, Edwards R, Mavandad M, Hedrick SA, Ribak O, Dixon RA, Lamb CJ (1990) Abnormal-plant development and down-regulation of phenylpropanoid biosynthesis in transgenic tobacco containing a heterologous phenylalanine ammonia-lyase gene. Proceedings of the National Academy of Sciences of the United States of America **87:** 9057-9061

Estévez JM, Cantero A, Reindl A, Reichler S, Leon P (2001) 1-deoxy-D-xylulose-5-phosphate synthase, a limiting enzyme for plastidic isoprenoid biosynthesis in plants. Journal of Biological Chemistry **276:** 22901-22909

Estévez JM, Cantero A, Romero C, Kawaide H, Jiménez LF, Kuzuyama T, Seto H, Kamiya Y, León P (2000) Analysis of the expression of *CLA1*, a gene that encodes the 1-deoxyxylulose 5-phosphate synthase of the 2-C-methyl-D-erythritol-4-phosphate pathway in *Arabidopsis*. Plant Physiology **124:** 95-103

Fambrini M, Degl'Innocenti E, Cionini G, Pugliesi C, Guidi L (2010) *Mesophyll cell defective1*, a mutation that disrupts leaf mesophyll differentiation in sunflower. Photosynthetica **48:** 135-142

Feldmann KA (1991) T-DNA insertion mutagenesis in *Arabidopsis*: mutational spectrum. The Plant Journal **1:** 71-82

Feng H, Chen Q, Feng J, Zhang J, Yang X, Zuo J (2007) Functional characterization of the *Arabidopsis* eukaryotic translation initiation factor 5A-2 that plays a crucial role in plant growth and development by regulating cell division, cell growth, and cell death. Plant Physiology **144:** 1531-1545

Ferro M, Brugiere S, Salvi D, Seigneurin-Berny D, Court M, Moyet L, Ramus C, Miras S, Mellal M, Le Gall S, Kieffer-Jaquinod S, Bruley C, Garin J, Joyard J, Masselon C, Rolland N (2010) AT_CHLORO, a comprehensive chloroplast proteome database with subplastidial localization and curated information on envelope proteins. Molecular and Cellular Proteomics **9:** 1063-1084

Fischer K, Kammerer B, Gutensohn M, Arbinger B, Weber A, Häusler RE, Flügge UI (1997) A new class of plastidic phosphate translocators: A putative link between primary and secondary metabolism by the *phosphoenolpyruvate/phosphate* antiporter. Plant Cell **9:** 453-462

Fischer WN, Kwart M, Hummel S, Frommer WB (1995) Substrate specificity and expression profile of amino acid transporters (AAPss) in *Arabidopsis*. Journal of Biological Chemistry **270:** 16315-16320

Fleming AJ (2002) The mechanism of leaf morphogenesis. Planta **216:** 17-22

Fleming AJ (2006) The integration of cell proliferation and growth in leaf morphogenesis. Journal of Plant Research **119:** 31-36

Fryer MJ, Ball L, Oxborough K, Karpinski S, Mullineaux PM, Baker NR (2003) Control of *Ascorbate Peroxidase 2* expression by hydrogen peroxide and leaf water status during excess light stress reveals a functional organisation of *Arabidopsis* leaves. Plant Journal **33:** 691-705

Fu A, Liu H, Yu F, Kambakam S, Luan S, Rodermel S (2012) Alternative Oxidases (AOX1a and AOX2) Can Functionally Substitute for Plastid Terminal Oxidase in *Arabidopsis* Chloroplasts. The Plant Cell Online **24:** 1579-1595

Fu AG, Park S, Rodermel S (2005) Sequences required for the activity of PTOX (IMMUTANS), a plastid terminal oxidase - *In vitro* and *in planta* mutagenesis of iron-binding sites and a conserved sequence that corresponds to exon 8. Journal of Biological Chemistry **280:** 42489-42496

Fukuda H, Higashiyama T (2011) Diverse functions of plant peptides: Entering a new phase. Plant and Cell Physiology **52:** 1-4

Furner IJ, Pumfrey JE (1992) Cell fate in the shoot apical meristem of *Arabidopsis thaliana*. Development **115:** 755-764

Gabay-Laughnan S, Newton KJ (2005) Mitochondrial mutations in maize. Maydica **50:** 349-359

Galbraith DW, Birnbaum K (2006) Global studies of cell type-specific gene expression in plants. *In* Annual Review of Plant Biology, Vol 57, pp 451-475

Galvez-Valdivieso G, Fryer MJ, Lawson T, Slattery K, Truman W, Smirnoff N, Asami T, Davies WJ, Jones AM, Baker NR, Mullineaux PM (2009) The high light response in *Arabidopsis* involves ABA signaling between vascular and bundle sheath cells. Plant Cell **21:** 2143-2162

Garcia I, Rodgers M, Pepin R, Hsieh TF, Matringe M (1999) Characterization and subcellular compartmentation of recombinant 4-hydroxyphenylpyruvate dioxygenase from *Arabidopsis* in transgenic tobacco. Plant Physiology **119:** 1507-1516

Gelhaye E, Rouhier N, Navrot N, Jacquot JP (2005) The plant thioredoxin system. Cellular and Molecular Life Sciences **62:** 24-35

González-Bayón R, Kinsman EA, Quesada V, Vera A, Robles P, Ponce MR, Pyke KA, Micol JL (2006) Mutations in the *RETICULATA* gene dramatically alter internal architecture but have little effect on overall organ shape in *Arabidopsis* leaves. Journal of Experimental Botany **57:** 3019-3031

Grace SC, Logan BA (2000) Energy dissipation and radical scavenging by the plant phenylpropanoid pathway. Philosophical Transactions of the Royal Society of London Series B-Biological Sciences **355:** 1499-1510

Granick S (1955) Die Plastiden und Chondriosomen. *In* W Ruhland, ed, Encyclopedia of Plant Physiology, Vol 1. Springer Verlag, Berlin, Germany, pp 507-564

Grevelding C, Suter-Crazzolara C, von Menges A, Kemper E, Masterson R, Schell J, Reiss B (1996) Characterisation of a new allele of *pale cress* and its role in greening in *Arabidopsis thaliana*. Molecular & General Genetics **251:** 532-541

Haberlandt G (1914) Physiological plant anatomy. London, MacMillan

Hagemann R (1986) A special type of nucleus-plastid interactions: nuclear gene induced plastome mutants. *In* G Akoyunoglou, H Senger, eds, Regulation of Chloroplast Differentiation. Alan R. Liss., New York, NY, pp 455-466

Halter CP, Peeters NM, Hanson MR (2004) RNA editing in ribosome-less plastids of *iojap* maize. Current Genetics **45:** 331-337

Hammer K, Knüpffer S, Knüpffer H (1990) Das Gaterslebener *Antirrhinum*-Sortiment. Genetic Resources and Crop Evolution **38:** 91-117

Han CD, Coe EH, Martienssen RA (1992) Molecular-cloning and characterization of *iojap* (*ij*), a pattern striping gene of maize. Embo Journal **11:** 4037-4046

Han S-H, Sakuraba Y, Koh H-J, Paek N-C (2012) Leaf variegation in the rice *zebra2* mutant is caused by photoperiodic accumulation of tetra-*cis*-lycopene and singlet oxygen. Molecules and Cells **33:** 87-97

Heisler MG, Ohno C, Das P, Sieber P, Reddy GV, Long JA, Meyerowitz EM (2005) Patterns of auxin transport and gene expression during primordium development revealed by live imaging of the *Arabidopsis* inflorescence meristem. Current Biology **15:** 1899-1911

Herrmann KM (1995) The shikimate pathway: early steps in the biosynthesis of aromatic compounds. Plant Cell **7:** 907-919

Herrmann KM, Weaver LM (1999) The shikimate pathway. Annual Review of Plant Physiology and Plant Molecular Biology **50:** 473-503

Hess WR, Müller A, Nagy F, Börner T (1994) Ribosome-deficient plastids affect transcription of light-induced nuclear genes: genetic evidence for a plastid-derived signal. Molecular and General Genetics MGG **242:** 305-312

Hibberd JM, Quick WP (2002) Characteristics of C_4 photosynthesis in stems and petioles of C_3 flowering plants. Nature **415:** 451-454

Hilaire E, Young SA, Willard LH, McGee JD, Sweat T, Chittoor JM, Guikema JA, Leach JE (2001) Vascular defense responses in rice: Peroxidase accumulation in xylem parenchyma cells and xylem wall thickening. Molecular Plant-Microbe Interactions **14:** 1411-1419

Hirner B, Fischer WN, Rentsch D, Kwart M, Frommer WB (1998) Developmental control of H^+/amino acid permease gene expression during seed development of *Arabidopsis*. Plant Journal **14:** 535-544

Hirschberg J (2001) Carotenoid biosynthesis in flowering plants. Current Opinion in Plant Biology **4:** 210-218

Hoffmann WA, Poorter H (2002) Avoiding bias in calculations of relative growth rate. Annals of Botany **90:** 37-42

Hofius D, Sonnewald U (2003) Vitamin E biosynthesis: biochemistry meets cell biology. Trends in Plant Science **8:** 6-8

Holding DR, Springer PS, Coomber SA (2000) The chloroplast and leaf developmental mutant, *pale cress*, exhibits light-conditional severity and symptoms characteristic of its ABA deficiency. Annals of Botany **86:** 953-962

Holloway PJ (1983) some variations in the composition of suberin from the cork layers of higher plants. Phytochemistry **22:** 495-502

Holmgren A, Johansson C, Berndt C, Lönn ME, Hudemann C, Lillig CH (2005) Thiol redox control via thioredoxin and glutaredoxin systems. Biochemical Society Transactions **33:** 1375-1377

Horiguchi G, Mollá-Morales A, Pérez-Pérez JM, Kojima K, Robles P, Ponce MR, Micol JL, Tsukaya H (2011) Differential contributions of ribosomal protein genes to *Arabidopsis thaliana* leaf development. Plant Journal **65:** 724-736

Hricová A, Quesada V, Micol JL (2006) The *SCABRA3* nuclear gene encodes the plastid RpoTp RNA polymerase, which is required for chloroplast biogenesis and mesophyll cell proliferation in *Arabidopsis*. Plant Physiology **141:** 942-956

Hsieh MH, Goodman HM (2006) Functional evidence for the involvement of *Arabidopsis* IspF homolog in the nonmevalonate pathway of plastid isoprenoid biosynthesis. Planta **223:** 779-784

Hu X, Reddy ASN (1997) Cloning and expression of a PR5-like protein from *Arabidopsis*: inhibition of fungal growth by bacterially expressed protein. Plant Molecular Biology **34:** 949-959

Huang J, Taylor JP, Chen JG, Uhrig JF, Schnell DJ, Nakagawa T, Korth KL, Jones AM (2006) The plastid protein THYLAKOID FORMATION1 and the plasma membrane G-protein GPA1 interact in a novel sugar-signaling mechanism in *Arabidopsis*. Plant Cell **18:** 1226-1238

Hung WF, Chen LJ, Boldt R, Sun CW, Li HM (2004) Characterization of *Arabidopsis* glutamine phosphoribosyl pyrophosphate amidotransferase-deficient mutants. Plant Physiology **135:** 1314-1323

Inaba T, Ito-Inaba Y (2010) Versatile roles of plastids in plant growth and development. Plant and Cell Physiology **51:** 1847-1853

Inada N, Wildermuth MC (2005) Novel tissue preparation method and cell-specific marker for laser microdissection of *Arabidopsis* mature leaf. Planta **221:** 9-16

Ingelsson B, Vener AV (2012) Phosphoproteomics of *Arabidopsis* chloroplasts reveals involvement of the STN7 kinase in phosphorylation of nucleoid protein pTAC16. Febs Letters **586:** 1265-1271

Irish VF, Sussex IM (1992) A fate map of the *Arabidopsis* embryonic shoot apical meristem. Development **115:** 745-753

Ito T, Shiraishi H, Okada K, Shimura Y (1994) Two amidophosphoribosyltransferase genes of *Arabidopsis thaliana* expressed in different organs. Plant Molecular Biology **26:** 529-533

Iuchi S, Kobayashi M, Taji T, Naramoto M, Seki M, Kato T, Tabata S, Kakubari Y, Yamaguchi-Shinozaki K, Shinozaki K (2001) Regulation of drought tolerance by gene manipulation of 9-*cis*-epoxycarotenoid dioxygenase, a key enzyme in abscisic acid biosynthesis in *Arabidopsis*. Plant Journal **27:** 325-333

Janacek SH, Trenkamp S, Palmer B, Brown NJ, Parsley K, Stanley S, Astley HM, Rolfe SA, Quick WP, Fernie AR, Hibberd JM (2009) Photosynthesis in cells around veins of the C_3 plant *Arabidopsis thaliana* is important for both the shikimate pathway and leaf senescence as well as contributing to plant fitness. Plant Journal **59:** 329-343

Jasinski S, Piazza P, Craft J, Hay A, Woolley L, Rieu I, Phillips A, Hedden P, Tsiantis M (2005) KNOX action in *Arabidopsis* is mediated by coordinate regulation of cytokinin and gibberellin activities. Current Biology **15:** 1560-1565

Javelle M, Vernoud V, Rogowsky PM, Ingram GC (2011) Epidermis: the formation and functions of a fundamental plant tissue. New Phytologist **189:** 17-39

Jenkins MT (1924) Heritable characters of maize. journal of Herdity **15:** 467-472

Jeter CR, Tang WQ, Henaff E, Butterfield T, Roux SJ (2004) Evidence of a novel cell signaling role for extracellular adenosine triphosphates and diphosphates in *Arabidopsis*. Plant Cell **16:** 2652-2664

Jing YJ, Cui DY, Bao F, Hu ZB, Qin ZX, Hu YX (2009) Tryptophan deficiency affects organ growth by retarding cell expansion in *Arabidopsis*. Plant Journal **57:** 511-521

Joët T, Genty B, Josse EM, Kuntz M, Cournac L, Peltier G (2002) Involvement of a plastid terminal oxidase in plastoquinone oxidation as evidenced by expression of the *Arabidopsis thaliana* enzyme in tobacco. Journal of Biological Chemistry **277:** 31623-31630

Joshi V, Joung J-G, Fei Z, Jander G (2010) Interdependence of threonine, methionine and isoleucine metabolism in plants: accumulation and transcriptional regulation under abiotic stress. Amino Acids **39:** 933-947

Joshi V, Laubengayer KM, Schauer N, Fernie AR, Jander G (2006) Two *Arabidopsis* threonine aldolases are nonredundant and compete with threonine deaminase for a common substrate pool. Plant Cell **18:** 3564-3575

Josse EM, Alcaraz JP, Labouré AM, Kuntz M (2003) *In vitro* characterization of a plastid terminal oxidase (PTOX). European Journal of Biochemistry **270:** 3787-3794

Josse EM, Simkin AJ, Gaffé J, Labouré AM, Kuntz M, Carol P (2000) A plastid terminal oxidase associated with carotenoid desaturation during chromoplast differentiation. Plant Physiology **123:** 1427-1436

Kamboj JS, Blake PS, Baker DA (1998) Cytokinins in the vascular saps of *Ricinus communis*. Plant Growth Regulation **25:** 123-126

Kangasjärvi S, Nurmi M, Tikkanen M, Aro EM (2009) Cell-specific mechanisms and systemic signalling as emerging themes in light acclimation of C_3 plants. Plant Cell and Environment **32:** 1230-1240

Kanno Y, Hanada A, Chiba Y, Ichikawa T, Nakazawa M, Matsui M, Koshiba T, Kamiya Y, Seo M (2012) Identification of an abscisic acid transporter by functional screening using the receptor complex as a sensor. Proceedings of the National Academy of Sciences **109:** 9653-9658

Kato Y, Miura E, Matsushima R, Sakamoto W (2007) White leaf sectors in *yellow variegated2* are formed by viable cells with undifferentiated plastids. Plant Physiology **144:** 952-960

Keddie JS, Carroll B, Jones JDG, Gruissem W (1996) The *DCL* gene of tomato is required for chloroplast development and palisade cell morphogenesis in leaves. Embo Journal **15:** 4208-4217

Kehr J (2003) Single cell technology. Current Opinion in Plant Biology **6:** 617-621

Keren N, Ohkawa H, Welsh EA, Liberton M, Pakrasi HB (2005) Psb29, a conserved 22-kD protein, functions in the biogenesis of photosystem II complexes in *Synechocystis* and *Arabidopsis*. Plant Cell **17:** 2768-2781

Kerk NM, Ceserani T, Tausta SL, Sussex IM, Nelson TM (2003) Laser capture microdissection of cells from plant tissues. Plant Physiology **132:** 27-35

Kichey T, Le Gouis J, Sangwan B, Hirel B, Dubois F (2005) Changes in the cellular and subcellular localization of glutamine synthetase and glutamate dehydrogenase during flag leaf senescence in wheat (*Triticum aestivum* L.). Plant and Cell Physiology **46:** 964-974

Kim TH, Bohmer M, Hu HH, Nishimura N, Schroeder JI (2010) Guard cell signal transduction network: Advances in understanding abscisic acid, CO_2, and Ca^{2+} signaling. *In* S Merchant, WR Briggs, D Ort, eds, Annual Review of Plant Biology, Vol 61, Vol 61. Annual Reviews, Palo Alto, pp 561-591

Kinsman EA, Pyke KA (1998) Bundle sheath cells and cell-specific plastid development in *Arabidopsis* leaves. Development **125:** 1815-1822

Kirk JTO, Tilney-Bassett RAE (1978) The Plastids, 2nd edn. Elsevier/North-Holland, Amsterdam, the Netherlands

Kleinig H, Liedvogel B (1980) Fatty acid synthesis by isolated chromoplasts from the daffodil. Energy sources and distribution patterns of the acids. Planta **150:** 166-169

Knappe S, Flügge UI, Fischer K (2003) Analysis of the plastidic *phosphate translocator* gene family in Arabidopsis and identification of new *phosphate translocator*-homologous transporters, classified by their putative substrate-binding site. Plant Physiology **131:** 1178-1190

Knappe S, Löttgert T, Schneider A, Voll L, Flügge UI, Fischer K (2003) Characterization of two functional *phosphoenolpyruvate/phosphate translocator (PPT)* genes in *Arabidopsis*-AtPPT1 may be involved in the provision of signals for correct mesophyll development. Plant Journal **36:** 411-420

Kochevenko A, Fernie AR (2011) The genetic architecture of branched-chain amino acid accumulation in tomato fruits. Journal of Experimental Botany **62:** 3895-3906

Kodama Y (2007) Plastidic proteins containing motifs of nuclear transcription factors. Plant Biotechnology **24:** 165-170

Koiwai H, Nakaminami K, Seo M, Mitsuhashi W, Toyomasu T, Koshiba T (2004) Tissue-specific localization of an abscisic acid biosynthetic enzyme, AAO3, in *Arabidopsis*. Plant Physiology **134:** 1697-1707

Komenda J, Barker M, Kuviková S, de Vries R, Mullineaux CW, Tichý M, Nixon PJ (2006) The FtsH protease slr0228 is important for quality control of photosystem II in the thylakoid membrane of *Synechocystis* sp. PCC 6803. Journal of Biological Chemistry **281:** 1145-1151

Komor E, Liegl I, Schobert C (1993) Loading and translocation of various cytokinins in phloem and xylem of the seedlings of *Ricinus communis* L. Planta **191:** 252-255

Koornneeff M, Dellaert LWM, van der Veen JH (1982) EMS- and relation-induced mutation frequencies at individual loci in *Arabidopsis thaliana* (L.) Heynh. Mutation Research/Fundamental and Molecular Mechanisms of Mutagenesis **93:** 109-123

Koroleva OA, Tomos AD, Farrar J, Roberts P, Pollock CJ (2000) Tissue distribution of primary metabolism between epidermal, mesophyll and parenchymatous bundle sheath cells in barley leaves. Functional Plant Biology **27:** 747-755

Kroll D, Meierhoff K, Bechtold N, Kinoshita M, Westphal S, Vothknecht UC, Soll J, Westhoff P (2001) VIPP1, a nuclear gene of *Arabidopsis thaliana* essential for thylakoid membrane formation. Proceedings of the National Academy of Sciences **98:** 4238-4242

Kunkel BN, Brooks DM (2002) Cross talk between signaling pathways in pathogen defense. Current Opinion in Plant Biology **5:** 325-331

Kuromori T, Takahashi S, Kondou Y, Shinozaki K, Matsui M (2009) Phenome analysis in plant species using loss-of-function and gain-of-function mutants. Plant and Cell Physiology **50:** 1215-1231

Kuromori T, Wada T, Kamiya A, Yuguchi M, Yokouchi T, Imura Y, Takabe H, Sakurai T, Akiyama K, Hirayama T, Okada K, Shinozaki K (2006) A trial of phenome analysis using 4000 *Ds*-insertional mutants in gene-coding regions of *Arabidopsis*. Plant Journal **47:** 640-651

Kwart M, Hirner B, Hummel S, Frommer WB (1993) Differential expression of two related amino acid transporters with differing substrate specificity in *Arabidopsis thaliana*. The Plant Journal **4:** 993-1002

Kwok EY, Hanson MR (2004) Stromules and the dynamic nature of plastid morphology. Journal of Microscopy-Oxford **214:** 124-137

Langdale JA (2011) C-4 Cycles: Past, Present, and Future Research on C_4 Photosynthesis. Plant Cell **23:** 3879-3892

Last RL, Bissinger PH, Mahoney DJ, Radwanski ER, Fink GR (1991) Tryptophan mutants in *Arabidopsis*: the consequences of dublicated tryptophan synthase ß genes. Plant Cell **3:** 345-358

Leegood RC (2008) Roles of the bundle sheath cells in leaves of C_3 plants. Journal of Experimental Botany **59:** 1663-1673

Leegood RC, Walker RP (2003) Regulation and roles of phospho*enol*pyruvate carboxykinase in plants. Archives of Biochemistry and Biophysics **414:** 204-210

Lein W, Usadel B, Stitt M, Reindl A, Ehrhardt T, Sonnewald U, Börnke F (2008) Large-scale phenotyping of transgenic tobacco plants (*Nicotiana tabacum*) to identify essential leaf functions. Plant Biotechnology Journal **6:** 246-263

Lepistö A, Kangasjärvi S, Luomala EM, Brader G, Sipari N, Keränen M, Keinänen M, Rintamäki E (2009) Chloroplast NADPH-thioredoxin reductase interacts with photoperiodic development in *Arabidopsis*. Plant Physiology **149:** 1261-1276

Lermontova I, Grimm B (2006) Reduced activity of plastid protoporphyrinogen oxidase causes attenuated photodynamic damage during high-light compared to low-light exposure. The Plant Journal **48:** 499-510

Lewis NG, Yamamoto E (1990) Lignin: occurence, biogenesis and biodegradation. Annual Review of Plant Physiology and Plant Molecular Biology **41:** 455-496

Li HM, Culligan K, Dixon RA, Chory J (1995) *CUE1*: a mesophyll cell-specific positive regulator of light-controlled gene-expression in *Arabidopsis*. Plant Cell **7:** 1599-1610

Li W-Q, Zhang X-Q, Xia C, Deng Y, Ye D (2010) *MALE GAMETOPHYTE DEFECTIVE 1*, encoding the FAd subunit of mitochondrial F1F0-ATP synthase, is essential for pollen formation in *Arabidopsis thaliana*. Plant and Cell Physiology **51:** 923-935

Li-Beisson Y, Shorrosh B, Beisson F, Andersson MX, Arondel V, Bates PD, Baud S, Bird D, Debono A, Durrett TP, Franke RB, Graham IA, Katayama K, Kelly AA, Larson T, Markham JE, Miquel M, Molina I, Nishida I, Rowland O, Samuels L, Schmid KM, Wada H, Welti R, Xu C, Zallot R, Ohlrogge J (2010) Acyl-lipid metabolism. The Arabidopsis book / American Society of Plant Biologists **8:** e0133-e0133

Lichtenthaler HK, Rohmer M, Schwender J (1997) Two independent biochemical pathways for isopentenyl diphosphate and isoprenoid biosynthesis in higher plants. Physiologia Plantarum **101:** 643-652

Lichtenthaler HK, Schwender J, Disch A, Rohmer M (1997) Biosynthesis of isoprenoids in higher plant chloroplasts proceeds via a mevalonate-independent pathway. Febs Letters **400:** 271-274

Lindahl M, Spetea C, Hundal T, Oppenheim AB, Adam Z, Andersson B (2000) The thylakoid FtsH protease plays a role in the light-induced turnover of the photosystem II D1 protein. Plant Cell **12:** 419-431

Lloyd J, Meinke D (2012) A comprehensive dataset of genes with a loss-of-function mutant phenotype in *Arabidopsis*. Plant Physiology **158:** 1115-1129

Lohaus G, Burba M, Heldt HW (1994) Comparison of the contents of sucrose and amino acids in the leaves, phloem sap and taproots of high and low sugar-producing hybrids of sugar beet (*Beta vulgaris* L.). Journal of Experimental Botany **45:** 1097-1101

López-Juez E, Paul Jarvis R, Takeuchi A, Page AM, Chory J (1998) New *Arabidopsis cue* mutants suggest a close connection between plastid- and phytochrome regulation of nuclear gene expression. Plant Physiol. **118:** 803-815

Lough TJ, Lucas WJ (2006) Integrative plant biology: Role of phloem long-distance macromolecular trafficking. *In* Annual Review of Plant Biology, Vol 57, pp 203-232

Maeda H, Dudareva N (2012) The shikimate pathway and aromatic amino acid biosynthesis in plants. Annual Review of Plant Biology **63:** 73-105

Mainguet SE, Gakière B, Majira A, Pelletier S, Bringel F, Guérard F, Caboche M, Berthomé R, Renou JP (2009) Uracil salvage is necessary for early *Arabidopsis* development. Plant Journal **60:** 280-291

Mandel MA, Feldmann KA, Herrera-Estrella L, Rocha-Sosa M, León P (1996) *CLA1*, a novel gene required for chloroplast development, is highly conserved in evolution. Plant Journal **9:** 649-658

Martínez-Zapater JM (1993) Genetic analysis of variegated mutants in *Arabidopsis*. Journal of Heredity **84:** 138-140

Martínez-Zapater JM, Gil P, Capel J, Somerville CR (1992) Mutations at the Arabidopsis CHM locus promote rearrangements of the mitochondrial genome. The Plant Cell Online **4:** 889-899

Maurino VG, Peterhänsel C (2010) Photorespiration: current status and approaches for metabolic engineering. Current Opinion in Plant Biology **13:** 249-256

McDonald AE, Ivanov AG, Bode R, Maxwell DP, Rodermel SR, Hüner NPA (2011) Flexibility in photosynthetic electron transport: The physiological role of plastoquinol terminal oxidase (PTOX). Biochimica Et Biophysica Acta-Bioenergetics **1807:** 954-967

Merali Z, Mayer MJ, Parker ML, Michael AJ, Smith AC, Waldron KW (2012) Expression of a bacterial, phenylpropanoid-metabolizing enzyme in tobacco reveals essential roles of phenolic precursors in normal leaf development and growth. Physiologia Plantarum **145:** 260-274

Meurer J, Grevelding C, Westhoff P, Reiss B (1998) The PAC protein affects the maturation of specific chloroplast mRNAs in *Arabidopsis thaliana*. Molecular and General Genetics **258:** 342-351

Meyer Y, Reichheld JP, Vignols F (2005) Thioredoxins in *Arabidopsis* and other plants. Photosynthesis Research **86:** 419-433

Meyer Y, Riondet C, Constans L, Abdelgawwad MR, Reichheld JP, Vignols F (2006) Evolution of redoxin genes in the green lineage. Photosynthesis Research **89:** 179-192

Mitchell DE, Gadus MV, Madore MA (1992) Patterns of assimilate production and translocation in muskmelon (*Cucumis melo* L) I. Diurnal Patterns. Plant Physiology **99:** 959-965

Miura E, Kato Y, Matsushima R, Albrecht V, Laalami S, Sakamoto W (2007) The balance between protein synthesis and degradation in chloroplasts determines leaf variegation in *Arabidopsis yellow variegated* mutants. Plant Cell **19:**1313-1328

Miura E, Kato Y, Sakamoto W (2010) Comparative transcriptome analysis of green/white variegated sectors in *Arabidopsis yellow variegated2*: responses to oxidative and other stresses in white sectors. Journal of Experimental Botany **61:** 2433-2445

Mizukami Y (2001) A matter of size: developmental control of organ size in plants. Current Opinion in Plant Biology **4:** 533-539

Mizukami Y, Fischer RL (2000) Plant organ size control: *AINTEGUMENTA* regulates growth and cell numbers during organogenesis. Proceedings of the National Academy of Sciences of the United States of America **97:** 942-947

Mok DWS, Mok MC (2001) Cytokinin metabolism and action. Annual Review of Plant Physiology and Plant Molecular Biology **52:** 89-118

Mollá-Morales A, Sarmiento-Mañús R, Robles P, Quesada V, Pérez-Pérez JM, González-Bayón R, Hannah MA, Willmitzer L, Ponce MR, Micol JL (2011) Analysis of *ven3* and *ven6* reticulate mutants reveals the importance of arginine biosynthesis in *Arabidopsis* leaf development. The Plant Journal **65:** 335-345

Mourad GS, White JA (1992) The isolation of apparently homoplastidic mutants induced by a nuclear recessive gene in *Arabidopsis thaliana*. TAG Theoretical and Applied Genetics **84:** 906-914

Mullineaux PM, Karpinski S, Baker NR (2006) Spatial dependence for hydrogen peroxide-directed signaling in light-stressed plants. Plant Physiology **141:** 346-350

Muralla R, Sweeney C, Stepansky A, Leustek T, Meinke D (2007) Genetic dissection of histidine biosynthesis in *Arabidopsis*. Plant Physiol. **144:** 890-903

Murphy A, Peer WA, Taiz L (2000) Regulation of auxin transport by aminopeptidases and endogenous flavonoids. Planta **211:** 315-324

Myouga F, Akiyama K, Motohashi R, Kuromori T, Ito T, Iizumi H, Ryusui R, Sakurai T, Shinozaki K (2010) The Chloroplast Function Database: a large-scale collection of *Arabidopsis Ds*/Spm-or T-DNA-tagged homozygous lines for nuclear-encoded chloroplast proteins, and their systematic phenotype analysis. Plant Journal **61:** 529-542

Næsted H, Holm A, Jenkins T, Nielsen HB, Harris CA, Beale MH, Andersen M, Mant A, Scheller H, Camara B, Mattsson O, Mundy J (2004) Arabidopsis *VARIEGATED 3* encodes a chloroplasttargeted, zinc-finger protein required for chloroplast and palisade cell development. Journal of Cell Science **117:** 4807-4818

Nakazono M, Qiu F, Borsuk LA, Schnable PS (2003) Laser-capture microdissection, a tool for the global analysis of gene expression in specific plant cell types: Identification of genes expressed differentially in epidermal cells or vascular tissues of maize. Plant Cell **15:** 583-596

Nambara E, Marion-Poll A (2005) Abscisic acid biosynthesis and catabolism. *In* Annual Review of Plant Biology, Vol 56, pp 165-185

Narváez-Vásquez J, Ryan CA (2004) The cellular localization of prosystemin: a functional role for phloem parenchyma in systemic wound signaling. Planta **218:** 360-369

Newton KJ, Coe EH (1986) Mitochondrial DNA changes in abnormal growth (nonchromosomal stripe) mutants of maize. Proceedings of the National Academy of Sciences of the United States of America **83:** 7363-7366

Newton KJ, Coe EH (1986) Mitochondrial DNA changes in abnormal growth (nonchromosomal stripe) mutants of maize. Proceedings of the National Academy of Sciences **83:** 7363-7366

Niyogi KK (2000) Safety valves for photosynthesis. Current Opinion in Plant Biology **3:** 455-460

Nolte KD, Koch KE (1993) Companion-cell specific localization of sucrose synthase in zones of phloem loading and unloading. Plant Physiology **101:** 899-905

Normanly J, Cohen JD, Fink GR (1993) *Arabidopsis thaliana* auxotrophs reveal a tryptophan-independent biosynthetic pathway for indole-3-acetic acid. Proceedings of the National Academy of Sciences **90:** 10355-10359

Nott A, Jung H-S, Koussevitzky S, Chory J (2006) Plastid-to-nucleus retrograde signaling. *In* Annual Review of Plant Biology, Vol 57, pp 739-759

Ogawa T, Nishimura K, Aoki T, Takase H, Tomizawa K-I, Ashida H, Yokota A (2009) A Phosphofructokinase B-Type Carbohydrate Kinase Family Protein, NARA5, for massive expressions of plastid-encoded photosynthetic genes in *Arabidopsis*. Plant Physiology **151:** 114-128

Okegawa Y, Kobayashi Y, Shikanai T (2010) Physiological links among alternative electron transport pathways that reduce and oxidize plastoquinone in *Arabidopsis*. Plant Journal **63:** 458-468

Okumoto S, Schmidt R, Tegeder M, Fischer WN, Rentsch D, Frommer WB, Koch W (2002) High affinity amino acid transporters specifically expressed in xylem parenchyma and developing seeds of *Arabidopsis*. Journal of Biological Chemistry **277:** 45338-45346

Ostersetzer O, Adam Z (1997) Light-stimulated degradation of an unassembled Rieske FeS protein by a thylakoid-bound protease: The possible role of the FtsH protease. Plant Cell **9:** 957-965

Ouyang J, Shao X, Li J (2000) Indole-3-glycerol phosphate, a branchpoint of indole-3-acetic acid biosynthesis from the tryptophan biosynthetic pathway in *Arabidopsis thaliana*. The Plant Journal **24:** 327-333

Overmyer K, Kollist H, Tuominen H, Betz C, Langebartels C, Wingsle G, Kangasjarvi S, Brader G, Mullineaux P, Kangasjärvi J (2008) Complex phenotypic profiles leading to ozone sensitivity in *Arabidopsis thaliana* mutants. Plant Cell and Environment **31:** 1237-1249

Patil SS, Tam LQ, Sakai WS (1972) Mode of action of toxin from *Pseudomonas phaseolicola* 1. toxin specificity, chlorosis, and ornithine accumulation. Plant Physiology **49:** 803-&

Peltier G, Cournac L (2002) Chlororespiration. Annual Review of Plant Biology **53:** 523-550

Pérez-Pérez JM, Rubio-Díaz S, Dhondt S, Hernández-Romero D, Sánchez-Soriano J, Beemster GTS, Ponce MR, Micol JL (2011) Whole organ, venation and epidermal cell morphological variations are correlated in the leaves of *Arabidopsis* mutants. Plant, Cell & Environment **34:** 2200-2211

Pérez-Ruiz JM, Spínola MC, Kirchsteiger K, Moreno J, Sahrawy M, Cejudo FJ (2006) Rice NTRC is a high-efficiency redox system for chloroplast protection against oxidative damage. Plant Cell **18:** 2356-2368

Peterhansel C, Horst I, Niessen M, Blume C, Kebeish R, Kurkcuoglu S, Kreuzaler F (2010) Photorespiration. The Arabidopsis book / American Society of Plant Biologists **8:** e0130

Pfannschmidt T (2010) Plastidial retrograde signalling - a true "plastid factor" or just metabolite signatures? Trends in Plant Science **15:** 427-435

Piquemal J, Lapierre C, Myton K, O'Connell A, Schuch W, Grima-Pettenati J, Boudet AM (1998) Down-regulation of cinnamoyl-CoA reductase induces significant changes of lignin profiles in transgenic tobacco plants. Plant Journal **13:** 71-83

Poethig RS (1997) Leaf morphogenesis in flowering plants. Plant Cell **9:** 1077-1087

Pogson BJ, Woo NS, Förster B, Small ID (2008) Plastid signalling to the nucleus and beyond. Trends in Plant Science **13:** 602-609

Pollastri S, Tattini M (2011) Flavonols: old compounds for old roles. Annals of Botany **108:** 1225-1233

Potel F, Valadier MH, Ferrario-Méry S, Grandjean O, Morin H, Gaufichon L, Boutet-Mercey S, Lothier J, Rothstein SJ, Hirose N, Suzuki A (2009) Assimilation of excess ammonium into amino acids and nitrogen translocation in *Arabidopsis thaliana* - roles of glutamate synthases and carbamoylphosphate synthetase in leaves. Febs Journal **276:** 4061-4076

Powell AE, Lenhard M (2012) Control of Organ Size in Plants. Current Biology **22:** R360-R367

Prabhakar V, Lottgert T, Geimer S, Dormann P, Kruger S, Vijayakumar V, Schreiber L, Gobel C, Feussner K, Feussner I, Marin K, Staehr P, Bell K, Flugge UI, Hausler RE (2010) Phosphoenolpyruvate provision to plastids is essential for gametophyte and sporophyte development in *Arabidopsis thaliana*. Plant Cell **22:** 2594-2617

Pyke KA, Marrison JL, Leech RM (1991) Temporal and spatial development of the cells of the expanding first leaf of *Arabidopsis thaliana* (l) heynh. Journal of Experimental Botany **42:** 1407-1416

Qu Y, Egelund J, Gilson P, Houghton F, Gleeson P, Schultz C, Bacic A (2008) Identification of a novel group of putative *Arabidopsis thaliana* β-(1,3)-galactosyltransferases. Plant Molecular Biology **68:** 43-59

Radwanski ER, Barczak AJ, Last RL (1996) Characterization of tryptophan synthase alpha subunit mutants of *Arabidopsis thaliana*. Molecular and General Genetics **253:** 353-361

Raschke K, Hedrich R (1985) Simultaneous and independent effects of abscisic acid on stomata and the photosynthetic apparatus in whole leaves. Planta **163:** 105-118

Rédei GP (1963) Somatic instability caused by a cysteine-sensitive gene in Arabidopsis. Science **139:** 767-&

Rédei GP (1967) Biochemical Aspects Of A Genetically Determined Variegation In *Arabidopsis*. Genetics **56:** 431-&

Rédei GP, Hironyo Y (1964) Linkage studies. Arabidopsis Information Service **1:** 9-10

Rédei GP, Plurad SB (1973) Hereditary structural alterations of plastids induced by a nuclear mutator gene in *Arabidopsis*. Protoplasma **77:** 361-380

Redig P, Shaul O, Inze D, Van Montagu M, Van Onckelen H (1996) Levels of endogenous cytokinins, indole-3-acetic acid and abscisic acid during the cell cycle of synchronized tobacco BY-2 cells. Febs Letters **391:** 175-180

Reichheld JP, Riondet C, Delorme V, Vignols F, Meyer Y (2010) Thioredoxins and glutaredoxins in development. Plant Science **178:** 420-423

Reinhardt D, Pesce ER, Stieger P, Mandel T, Baltensperger K, Bennett M, Traas J, Friml J, Kuhlemeier C (2003) Regulation of phyllotaxis by polar auxin transport. Nature **426:** 255-260

Reiter RS, Coomber SA, Bourett TM, Bartley GE, Scolnik PA (1994) Control of leaf and chloroplast development by the *Arabidopsis* gene *pale cress*. Plant Cell **6:** 1253-1264

Rentsch D, Hirner B, Schmelzer E, Frommer WB (1996) Salt stress-induced proline transporters and salt stress-repressed broad specificity amino acid permeases identified by suppression of a yeast amino acid permease-targeting mutant. Plant Cell **8:** 1437-1446

Rick CM, Thompson AE, Brauer O (1959) genetics and development of an unstable chlorophyll deficiency in *Lycopersicon esculentum*. American Journal of Botany **46:** 1-11

Riens B, Lohaus G, Heineke D, Heldt HW (1991) Amino acid and sucrose content determined in the cytosolic, chloroplastic, and vacuolar compartments and in the phloem sap of spinach leaves. Plant Physiology **97:** 227-233

Rippert P, Puyaubert J, Grisollet D, Derrier L, Matringe M (2009) Tyrosine and phenylalanine are synthesized within the plastids in *Arabidopsis*. Plant Physiology **149:** 1251-1260

Rizhsky L, Hallak-Herr E, Van Breusegem F, Rachmilevitch S, Barr JE, Rodermel S, Inzé D, Mittler R (2002) Double antisense plants lacking ascorbate peroxidase and catalase are less sensitive to oxidative stress than single antisense plants lacking ascorbate peroxidase or catalase. Plant Journal **32:** 329-342

Röbbelen G (1966) Chloroplastendiffernzierung nach geninduzierter Plastommutation bei *Arabidopsis thaliana*. Zeitschrift für Pflanzenphysiologie **55:** 387-403

Röbbelen G (1968) Genbedingte Rotlichtempfindlichkeit der Chloroplastendifferenzierung bei *Arabidopsis*. Planta **81:** 237-254

Robertson DW (1967) Linkage studies of various barley mutations (*Hordeum* species). Crop Science **7:** 41-42

Rodermel S (2001) Pathways of plastid-to-nucleus signaling. Trends in Plant Science **6:** 471-478

Rodermel S (2008) *Arabidopsis* variegation mutants. *In* The Arabidopsis Book, Vol null. The American Society of Plant Biologists, pp 1-28

Rosar C, Kanonenberg K, Nanda AM, Mielewczik M, Bräutigam A, Novák O, Strnad M, Walter A, Weber APM (2012) The leaf reticulate mutant *dov1* is impaired in the first step of purine metabolism. Molecular Plant doi:10.1093/mp/sss045

Rossel J, Cuttriss A, Pogson B (2004) Identifying photoprotection mutants in *Arabidopsis thaliana*. *In* C R, ed, Photosynthesis research protocols, Totowa, NJ, USA, pp 287 - 299

Rosso D, Bode R, Li W, Krol M, Saccon D, Wang S, Schillaci LA, Rodermel SR, Maxwell DP, Hüner NPA (2009) Photosynthetic redox imbalance governs leaf sectoring in the *Arabidopsis thaliana* variegation mutants *immutans*, *spotty*, *var1*, and *var2*. Plant Cell **21:** 3473-3492

Rosso D, Ivanov AG, Fu A, Geisler-Lee J, Hendrickson L, Geisler M, Stewart G, Krol M, Hurry V, Rodermel SR, Maxwell DP, Hüner NPA (2006) IMMUTANS does not act as a stress-induced safety valve in the protection of the photosynthetic apparatus of *Arabidopsis* during steady-state photosynthesis. Plant Physiology **142:** 574-585

Ruuhola T, Ossipov V, Lempa K, Haukioja E (2003) Amino acids during development of mountain birch leaves. Chemoecology **13:** 95-101

Sage RF (2001) Environmental and evolutionary preconditions for the origin and diversification of the C_4 photosynthetic syndrome. Plant Biology **3:** 202-213

Sage RF, Christin P-A, Edwards EJ (2011) The C_4 plant lineages of planet Earth. Journal of Experimental Botany **62:** 3155-3169

Sakamoto W (2003) Leaf-variegated mutations and their responsible genes in *Arabidopsis thaliana*. Genes and Genetic Systems **78:** 1-9

Sakamoto W (2006) Protein degradation machineries in plastids. *In* Annual Review of Plant Biology, Vol 57, pp 599-621

Sakamoto W, Kondo H, Murata M, Motoyoshi F (1996) Altered mitochondrial gene expression in a maternal distorted leaf mutant of *Arabidopsis* induced by *chloroplast mutator*. Plant Cell **8:** 1377-1390

Sakamoto W, Miura E, Kaji Y, Okuno T, Nishizono M, Ogura T (2004) Allelic characterization of the leaf-variegated mutation *var2* identifies the conserved amino acid residues of FtsH that are important for ATP hydrolysis and proteolysis. Plant Molecular Biology **56:** 705-716

Sakamoto W, Tamura T, Hanba-Tomita Y, Murata M (2002) The *VAR1* locus of *Arabidopsis* encodes a chloroplastic FtsH and is responsible for leaf variegation in the mutant alleles. Genes to Cells **7:** 769-780

Savaldi-Goldstein S, Peto C, Chory J (2007) The epidermis both drives and restricts plant shoot growth. Nature **446:** 199-202

Scanlon MJ (2003) The polar auxin transport inhibitor *N*-1-naphthylphthalamic acid disrupts leaf initiation, KNOX protein regulation, and formation of leaf margins in maize. Plant Physiology **133:** 597-605

Schaaf G, Ludewig U, Erenoglu BE, Mori S, Kitahara T, von Wirén N (2004) ZmYS1 functions as a proton-coupled symporter for phytosiderophore- and nicotianamine-chelated metals. Journal of Biological Chemistry **279:** 9091-9096

Schmelzer E, Jahnen W, Hahlbrock K (1988) *In situ* localization of light-induced chalcone synthase mRNA, chalcone synthase, and flavonoid end products in epidermal cells of parsley leaves. Proceedings of the National Academy of Sciences **85:** 2989-2993

Schmid J, Amrhein N (1995) Molecular organization of the shikimate pathway in higher plants. Phytochemistry **39:** 737-749

Schmid MW, Schmidt A, Klostermeier UC, Barann M, Rosenstiel P, Grossniklaus U (2012) A powerful method for transcriptional profiling of specific cell types in eukaryotes: Laser-assisted microdissection and RNA sequencing. Plos One **7:** e29685

Schnittger A, Grini PE, Folkers U, Hulskamp M (1996) Epidermal fate map of the *Arabidopsis* shoot meristem. Developmental Biology **175:** 248-255

Schobert C, Lucas W, Franceschi V, Frommer W (2004) Intercellular transport and phloem loading of sucrose, oligosaccharides and amino acids. *in* R Leegood, T Sharkey, S Caemmerer, eds, Photosynthesis, Vol 9. Springer Netherlands, pp 249-274

Schröder M, Giermann N, Zrenner R (2005) Functional analysis of the pyrimidine *de novo* synthesis pathway in solanaceous species. Plant Physiology **138:** 1926-1938

Schroeder JI, Allen GJ, Hugouvieux V, Kwak JM, Waner D (2001) Guard cell signal transduction. Annual Review of Plant Physiology and Plant Molecular Biology **52:** 627-658

Schulze-Siebert D, Heineke D, Scharf H, Schultz G (1984) Pyruvate-derived amino acids in spinach chloroplasts - synthesis and regulation during photosynthetic carbon metabolism. Plant Physiology **76:** 465-471

Schurr U, Heckenberger U, Herdel K, Walter A, Feil R (2000) Leaf development in *Ricinus communis* during drought stress: dynamics of growth processes, of cellular structure and of sink-source transition. Journal of Experimental Botany **51:** 1515-1529

Seigneurin-Berny D, Gravot A, Auroy P, Mazard C, Kraut A, Finazzi G, Grunwald D, Rappaport F, Vavasseur A, Joyard J, Richaud P, Rolland N (2006) HMA1, a new Cu-ATPase of the chloroplast envelope, is essential for growth under adverse light conditions. Journal of Biological Chemistry **281:** 2882-2892

Senecoff JF, McKinney EC, Meagher RB (1996) *De novo* purine synthesis in *Arabidopsis thaliana* II. The PUR7 gene encoding 5'-phosphoribosyl-4-(*N*-succinocarboxamide)-5-aminoimidazole synthetase is expressed in rapidly dividing tissues. Plant Physiology **112:** 905-917

Serrato AJ, Pérez-Ruiz JM, Spínola MC, Cejudo FJ (2004) A novel NADPH thioredoxin reductase, localized in the chloroplast, which deficiency causes hypersensitivity to abiotic stress in *Arabidopsis thaliana*. Journal of Biological Chemistry **279:** 43821-43827

Shahbazi M, Gilbert M, Labouré A-M, Kuntz M (2007) Dual role of the plastid terminal oxidase in tomato. Plant Physiology **145:** 691-702

Sheahan JJ (1996) Sinapate esters provide greater UV-B attenuation than flavonoids in *Arabidopsis thaliana* (*Brassicaceae*). American Journal of Botany **83:** 679-686

Sheue C-R, Pao S-H, Chien L-F, Chesson P, Peng C-I (2012) Natural foliar variegation without costs? The case of *Begonia*. Annals of Botany **109:** 1065-1074

Shimakata T, Stumpf PK (1982) Isolation and function of spinach leaf ß-ketoacyl-[acyl-carrier-protein] synthases. Proceedings of the National Academy of Sciences **79:** 5808-5812

Siedow JN, Umbach AL (1995) Plant mitochondrial electron transfer and molecular biology. Plant Cell **7:** 821-831

Slocum RD (2005) Genes, enzymes and regulation of arginine biosynthesis in plants. Plant Physiology and Biochemistry **43:** 729-745

Smith WK, Vogelmann TC, DeLucia EH, Bell DT, Shepherd KA (1997) Leaf form and photosynthesis. Bioscience **47:** 785-793

Stoike LL, Sears BB (1998) *Plastome mutator*-induced alterations arise in *Oenothera* chloroplast DNA through template slippage. Genetics **149:** 347-353

Streatfield SJ, Weber A, Kinsman EA, Häusler RE, Li JM, Post-Beittenmiller D, Kaiser WM, Pyke KA, Flügge UI, Chory J (1999) The *phosphoenolpyruvate/phosphate translocator* is required for phenolic metabolism, palisade cell development, and plastid-dependent nuclear gene expression. Plant Cell **11:** 1609-1621

Sugimoto-Shirasu K, Roberts K (2003) "Big it up": endoreduplication and cell-size control in plants. Current Opinion in Plant Biology **6:** 544-553

Sun CW, Chen LJ, Lin LC, Li HM (2001) Leaf-specific upregulation of chloroplast translocon genes by a CCT motif-containing protein, CIA2. Plant Cell **13:** 2053-2061

Sun J, Zhang CL, Deng SR, Lu CF, Shen X, Zhou XY, Zheng XJ, Hu ZM, Chen SL (2012) An ATP signalling pathway in plant cells: extracellular ATP triggers programmed cell death in *Populus euphratica*. Plant Cell and Environment **35:** 893-916

Sundberg E, Slagter JG, Fridborg I, Cleary SP, Robinson C, Coupland G (1997) *ALBINO3*, an *Arabidopsis* nuclear gene essential for chloroplast differentiation, encodes a chloroplast protein that shows homology to proteins present in bacterial membranes and yeast mitochondria. Plant Cell **9:** 717-730

Takechi K, Sodmergen, Murata M, Motoyoshi F, Sakamoto W (2000) The *YELLOW VARIEGATED* (*VAR2*) locus encodes a homologue of FtsH, an ATP-dependent protease in *Arabidopsis*. Plant and Cell Physiology **41:** 1334-1346

Tamagnone L, Merida A, Parr A, Mackay S, Culianez-Macia FA, Roberts K, Martin C (1998) The AmMYB308 and AmMYB330 transcription factors from *Antirrhinum* regulate phenylpropanoid and lignin biosynthesis in transgenic tobacco. Plant Cell **10:** 135-154

Tamagnone L, Merida A, Stacey N, Plaskitt K, Parr A, Chang CF, Lynn D, Dow JM, Roberts K, Martin C (1998) Inhibition of phenolic acid metabolism results in precocious cell death and altered cell morphology in leaves of transgenic tobacco plants. Plant Cell **10:** 1801-1816

Tanaka R, Kobayashi K, Masuda T (2011) Tetrapyrrole Metabolism in *Arabidopsis thaliana*. The Arabidopsis book / American Society of Plant Biologists **9:** e0145-e0145

Tao Y, Ferrer J-L, Ljung K, Pojer F, Hong F, Long JA, Li L, Moreno JE, Bowman ME, Ivans LJ, Cheng Y, Lim J, Zhao Y, Ballaré CL, Sandberg G, Noel JP, Chory J (2008) Rapid synthesis of auxin via a new tryptophan-dependent pathway is required for shade avoidance in plants. Cell **133:** 164-176

Tiller N, Weingartner M, Thiele W, Maximova E, Schöttler MA, Bock R (2012) The plastid-specific ribosomal proteins of *Arabidopsis thaliana* can be divided into non-essential proteins and genuine ribosomal proteins. The Plant Journal **69:** 302-316

Tilney-Bassett RAE (1975) Genetics of variegated plants. *In* CW Birky, PS Perlman, TJ Byers, eds, Genetics and biogenesis of mitochondria and chloroplasts. Ohio State University Press, Columbus, Ohio, pp 268-308

Tirlapur UK, Dahse I, Reiss B, Meurer J, Oelmüller R (1999) Characterization of the activity of a plastid-targeted green fluorescent protein in *Arabidopsis*. European Journal of Cell Biology **78:** 233-240

Tsiantis M, Hay A (2003) Comparative plant development: The time of the leaf? Nature Reviews Genetics **4:** 169-180

Tsukaya H (2006) Mechanism of leaf-shape determination. *In* Annual Review of Plant Biology, Vol 57, pp 477-496

Tsukaya H (2008) Leaf Development. *In* The Arabidopsis Book, Vol null. The American Society of Plant Biologists, pp 1-23

Tsukaya H, Okada H, Mohamed M (2004) A novel feature of structural variegation in leaves of the tropical plant *Schismatoglottis calyptrata*. Journal of Plant Research **117:** 477-480

Turgeon R (2010) The role of phloem loading reconsidered. Plant Physiology **152:** 1817-1823

Turner JG, Mitchell RE (1985) Association between symptom development and inhibition of ornithine carbamoyltransferase in bean leaves treated with phaseolotoxin. Plant Physiology **79:** 468-473

Tzin V, Galili G (2010) New insights into the shikimate and aromatic amino acids biosynthesis pathways in plants. Molecular Plant **3:** 956-972

Ueno O (1998) Induction of Kranz anatomy and C_4-like biochemical characteristics in a submerged amphibious plant by abscisic acid. Plant Cell **10:** 571-583

Van der Graaff E, Hooykaas P, Lein W, Lerchl J, Kunze G, Sonnwald U, Boldt R (2004) Molecular analysis of “de novo” purine biosynthesis in solanaceous species and in *Arabidopsis thaliana*. Frontiers in Bioscience **9:** 1803-1816

Vanlerberghe GC, McIntosh L (1997) Alternative oxidase: From gene to function. Annual Review of Plant Physiology and Plant Molecular Biology **48:** 703-734

Van Lijsebettens M, Vanderhaeghen R, Deblock M, Bauw G, Villarroel R, Van Montagu M (1994) An S18 ribosomal protein gene copy at the *Arabidopsis PFL* locus affects plant development by its specific expression in meristems. Embo Journal **13:** 3378-3388

Velez-Ramirez AI, van Ieperen W, Vreugdenhil D, Millenaar FF (2011) Plants under continuous light. Trends in Plant Science **16:** 310-318

Vogt T (2010) Phenylpropanoid biosynthesis. Molecular Plant **3:** 2-20

Voll L, Häusler RE, Hecker R, Weber A, Weissenböck G, Fiene G, Waffenschmidt S, Flügge UI (2003) The phenotype of the *Arabidopsis cue1* mutant is not simply caused by a general restriction of the shikimate pathway. Plant Journal **36:** 301-317

Voll LM, Allaire EE, Fiene G, Weber APM (2004) The *Arabidopsis phenylalanine insensitive growth* mutant exhibits a deregulated amino acid metabolism. Plant Physiology **136:** 3058-3069

Von Wirén N, Mori S, Marschner H, Römheld V (1994) iron inefficiency in maize mutant ys1 (*Zea mays* L. cv yellow-stripe) is caused by a defect in uptake of iron phytosiderophores. Plant Physiology **106:** 71-77

Wang Q, Sullivan RW, Kight A, Henry RL, Huang JR, Jones AM, Korth KL (2004) Deletion of the chloroplast-localized *Thylakoid formation1* gene product in *Arabidopsis* leads to deficient thylakoid formation and variegated leaves. Plant Physiology **136:** 3594-3604

Wang YC, Duby G, Purnelle B, Boutry M (2000) Tobacco *VDL* gene encodes a plastid DEAD box RNA helicase and is involved in chloroplast differentiation and plant morphogenesis. Plant Cell **12:** 2129-2142

Westphal S, Heins L, Soll J, Vothknecht UC (2001) Vipp1 deletion mutant of *Synechocystis*: A connection between bacterial phage shock and thylakoid biogenesis? Proceedings of the National Academy of Sciences **98:** 4243-4248

Westphal S, Soll J, Vothknecht UC (2001) A vesicle transport system inside chloroplasts. Febs Letters **506:** 257-261

Wetzel CM, Jiang CZ, Meehan LJ, Voytas DF, Rodermel SR (1994) Nuclear-organelle interactions: the *immutans* variegation mutant of *Arabidopsis* is plastid autonomous and impaired in carotenoid biosynthesis. Plant Journal **6:** 161-175

Williams ML, Farrar JF, Pollock CJ (1989) Cell specialization within the parenchymatous bundle sheath of barley. Plant, Cell and Environment **12:** 909-918

Winter H, Lohaus G, Heldt HW (1992) Phloem transport of amino-acids in relation to their cytosolic levels in barley leaves. Plant Physiology **99:** 996-1004

Witz S, Jung B, Fürst S, Möhlmann T (2012) *De novo* pyrimidine nucleotide synthesis mainly occurs outside of plastids, but a previously undiscovered nucleobase importer provides substrates for the essential salvage pathway in *Arabidopsis*. The Plant Cell Online **24:** 1549-1559

Woo NS, Gordon MJ, Graham SR, Rossel JB, Badger MR, Pogson BJ (2011) A mutation in the purine biosynthetic enzyme ATASE2 impacts high light signalling and acclimation responses in green and chlorotic sectors of *Arabidopsis* leaves. Functional Plant Biology **38:** 401-419

Woodson JD, Chory J (2008) Coordination of gene expression between organellar and nuclear genomes. Nat Rev Genet **9:** 383-395

Wu DY, Wright DA, Wetzel C, Voytas DF, Rodermel S (1999) The *IMMUTANS* variegation locus of *Arabidopsis* defines a mitochondrial alternative oxidase homolog that functions during early chloroplast biogenesis. Plant Cell **11:** 43-55

Wu G-Z, Xue H-W (2010) *Arabidopsis* ß-Ketoacyl-[Acyl Carrier Protein] Synthase I Is Crucial for Fatty Acid Synthesis and Plays a Role in Chloroplast Division and Embryo Development. Plant Cell **22:** 3726-3744

Wuest SE, Vijverberg K, Schmidt A, Weiss M, Gheyselinck J, Lohr M, Wellmer F, Rahnenfuehrer J, von Mering C, Grossniklaus U (2010) Arabidopsis Female Gametophyte Gene Expression Map Reveals Similarities between Plant and Animal Gametes. Current Biology **20:** 506-512

Wycliffe P, Sitbon F, Wernersson J, Ezcurra I, Ellerström M, Rask L (2005) Continuous expression in tobacco leaves of a *Brassica napus* PEND homologue blocks differentiation of plastids and development of palisade cells. Plant Journal **44:** 1-15

Yamaguchi M, Takechi K, Myouga F, Imura S, Sato H, Takio S, Shinozaki K, Takano H (2012) Loss of the plastid envelope protein AtLrgB causes spontaneous chlorotic cell death in *Arabidopsis thaliana*. Plant and Cell Physiology **53:** 125-134

Yamamoto YY, Puente P, Deng X-W (2000) An *Arabidopsis* cotyledon-specific albino locus: a possible role in 16S rRNA maturation. Plant and Cell Physiology **41:** 68-76

Yamasaki H, Sakihama Y, Ikehara N (1997) Flavonoid-peroxidase reaction as a detoxification mechanism of plant cells against H2O2. Plant Physiology **115:** 1405-1412

Yanai O, Shani E, Dolezal K, Tarkowski P, Sablowski R, Sandberg G, Samach A, Ori N (2005) Arabidopsis KNOXI proteins activate cytokinin biosynthesis. Current Biology **15:** 1566-1571

Yang Y, Jin H, Chen Y, Lin W, Wang C, Chen Z, Han N, Bian H, Zhu M, Wang J (2012) A chloroplast envelope membrane protein containing a putative LrgB domain related to the control of bacterial death and lysis is required for chloroplast development in *Arabidopsis thaliana*. New Phytologist **193:** 81-95

Yaronskaya E, Ziemann V, Walter G, Averina N, Börner T, Grimm B (2003) Metabolic control of the tetrapyrrole biosynthetic pathway for porphyrin distribution in the barley mutant *albostrians*. Plant Journal **35:** 512-522

Yasuno R, Wada H (2002) The biosynthetic pathway for lipoic acid is present in plastids and mitochondria in *Arabidopsis thaliana*. Febs Letters **517:** 110-114

Yoshida S, Mandel T, Kuhlemeier C (2011) Stem cell activation by light guides plant organogenesis. Genes & Development **25:** 1439-1450

Yu F, Fu AG, Aluru M, Park S, Xu Y, Liu HY, Liu XY, Foudree A, Nambogga M, Rodermel S (2007) Variegation mutants and mechanisms of chloroplast biogenesis. Plant Cell and Environment **30:** 350-365

Yu F, Park S, Rodermel SR (2004) The *Arabidopsis* FtsH metalloprotease gene family: interchangeability of subunits in chloroplast oligomeric complexes. Plant Journal **37:** 864-876

Yu F, Park S, Rodermel SR (2005) Functional redundancy of AtFtsH metalloproteases in thylakoid membrane complexes. Plant Physiology **138:** 1957-1966

Zaegel V, Guermann B, Le Ret M, Andrés C, Meyer D, Erhardt M, Canaday J, Gualberto JM, Imbault P (2006) The plant-specific ssDNA binding protein OSB1 is involved in the stoichiometric transmission of mitochondrial DNA in *Arabidopsis*. Plant Cell **18:** 3548-3563

Zaltsman A, Feder A, Adam Z (2005) Developmental and light effects on the accumulation of FtsH protease in *Arabidopsis* chloroplasts - implications for thylakoid formation and photosystem II maintenance. Plant Journal **42:** 609-617

Zaltsman A, Ori N, Adam Z (2005) Two types of FtsH protease subunits are required for chloroplast biogenesis and photosystem II repair in *Arabidopsis*. Plant Cell **17:** 2782-2790

Zelisko A, García-Lorenzo M, Jackowski G, Jansson S, Funk C (2005) AtFtsH6 is involved in the degradation of the light-harvesting complex II during high-light acclimation and senescence. Proceedings of the National Academy of Sciences of the United States of America **102:** 13699-13704

Zhang K, Letham DS, John PCL (1996) Cytokinin controls the cell cycle at mitosis by stimulating the tyrosine dephosphorylation and activation of $p34^{cdc2}$-like H1 histone kinase. Planta **200:** 2-12

Zhang R, Wang B, Jian O, Li J, Wang Y (2008) *Arabidopsis* indole synthase, a homolog of tryptophan synthase alpha, is an enzyme involved in the Trp-independent indole-containing metabolite biosynthesis. Journal of Integrative Plant Biology **50:** 1070-1077

Zhao YD, Christensen SK, Fankhauser C, Cashman JR, Cohen JD, Weigel D, Chory J (2001) A role for flavin monooxygenase-like enzymes in auxin biosynthesis. Science **291:** 306-309

Zhao YD, Hull AK, Gupta NR, Goss KA, Alonso J, Ecker JR, Normanly J, Chory J, Celenza JL (2002) Trp-dependent auxin biosynthesis in *Arabidopsis*: involvement of cytochrome P450s CYP79B2 and CYP79B3. Genes and Development **16:** 3100-3112

Zhao Z, Andersen SU, Ljung K, Dolezal K, Miotk A, Schultheiss SJ, Lohmann JU (2010) Hormonal control of the shoot stem-cell niche. Nature **465:** 1089-U1154

Zhao Z, Assmann SM (2011) The glycolytic enzyme, phosphoglycerate mutase, has critical roles in stomatal movement, vegetative growth, and pollen production in *Arabidopsis thaliana*. Journal of Experimental Botany **62:** 5179-5189

Zrenner R, Riegler H, Marquard CR, Lange PR, Geserick C, Bartosz CE, Chen CT, Slocum RD (2009) A functional analysis of the pyrimidine catabolic pathway in *Arabidopsis*. New Phytologist **183:** 117-132

Zrenner R, Stitt M, Sonnewald U, Boldt R (2006) Pyrimidine and purine biosynthesis and degradation in plants. Annual Review of Plant Biology **57:** 805-836

Zybailov B, Rutschow H, Friso G, Rudella A, Emanuelsson O, Sun Q, van Wijk KJ (2008) Sorting signals, N-terminal modifications and abundance of the chloroplast proteome. Plos One **3:** e1994

The authors` contributions to Manuscript 1

C.R. wrote the manuscript.

A.B. and **A.P.M.W.** participated in drafting of the manuscript.

V.
Manuscript 2

The leaf reticulate mutant *dov1*
is impaired in the
first step of purine metabolism

Molecular Plant • Pages 1–15, 2012 RESEARCH ARTICLE

The Leaf Reticulate Mutant *dov1* Is Impaired in the First Step of Purine Metabolism

Christian Rosar[a], Kerstin Kanonenberg[a], Arun M. Nanda[a,b], Michael Mielewczik[c,d], Andrea Bräutigam[a], Ondřej Novák[e], Miroslav Strnad[e], Achim Walter[c,d] and Andreas P.M. Weber[a,e,1]

a Institute for Plant Biochemistry, Heinrich-Heine-Universität, Universitätsstrasse 1, D-40225 Düsseldorf, Germany
b Present address: Institute of Bio- and Geosciences, IBG-1: Biotechnology, Forschungszentrum Jülich, D-52425 Jülich, Germany
c Institute of Bio- and Geosciences, IBG-2: Plant Sciences, Forschungszentrum Jülich, D-52425 Jülich, Germany
d Present address: Institute of Agricultural Sciences, Universitätstrasse 2, ETH Zürich, CH-8092 Zürich, Switzerland
e Laboratory of Growth Regulators, Palacky University & Institute of Experimental Botany AS CR, Slechtitelu 11, CZ-78371 Olomouc, Czech Republic

ABSTRACT A series of reticulated *Arabidopsis thaliana* mutants were previously described. All mutants show a reticulate leaf pattern, namely green veins on a pale leaf lamina. They have an aberrant mesophyll structure but an intact layer of bundle sheath cells around the veins. Here, we unravel the function of the previously described reticulated EMS-mutant *dov1* (differential development of vascular associated cells 1). By positional cloning, we identified the mutated gene, which encodes glutamine phosphoribosyl pyrophosphate aminotransferase 2 (ATase2), an enzyme catalyzing the first step of purine nucleotide biosynthesis. *dov1* is allelic to the previously characterized *cia1-2* mutant that was isolated in a screen for mutants with impaired chloroplast protein import. We show that purine-derived total cytokinins are lowered in *dov1* and crosses with phytohormone reporter lines revealed differential reporter activity patterns in *dov1*. Metabolite profiling unraveled that amino acids that are involved in purine biosynthesis are increased in *dov1*. This study identified the molecular basis of an established mutant line, which has the potential for further investigation of the interaction between metabolism and leaf development.

Key words: leaf development; reticulated mutants; cytokinin; growth kinetics; purine metabolism.

INTRODUCTION

Two different processes in leaf development can be distinguished: (1) the developmental program that governs leaf overall shape and size, and (2) the processes controlling internal leaf architecture. Schematically, all internal leaf tissues are wedged between two epidermal cell layers. In between, the mesophyll tissue harbors the photosynthetic activity. The mesophyll surrounds the vasculature that transfers solutes and water. During leaf development, at least in *Arabidopsis thaliana* (thale cress), the veins differentiate prior to the mesophyll because mesophyll differentiation precludes additional minor vein development (Pyke et al., 1991; Candela et al., 1999; Hoffmann and Poorter, 2002). In some species with prominent veins, it has been shown that potential quantum yield of photosystem II (F_v/F_m) reaches a maximum before maximal leaf expansion is reached and that, in general, differentiation processes of major veins precede mesophyll growth and differentiation (Walter et al., 2004). Vein development and differentiation have been well characterized, and depend on an intricate interplay of various phytohormones, including auxin gradients (Mattsson et al., 2003; Rolland-Lagan, 2008). However, the cues for mesophyll differentiation remain unknown. On the basis of mutant analyses in *Arabidopsis*, the bundle sheath, a chlorenchymatic cell layer tightly surrounding the vasculature, has been hypothesized to play an important role in mesophyll differentiation (Kinsman and Pyke, 1998; Streatfield et al., 1999; González-Bayón et al., 2006). A class of mutants displaying a reticulated leaf phenotype was reported that is characterized by a well-differentiated bundle sheath with intact chloroplasts and a mesophyll tissue that is pale to white with fewer cells and/or disrupted chloroplasts (Kinsman and Pyke, 1998).

George Rédei described the first reticulated mutant *reticulata* (*re*) and used it as a visible marker in genetic crosses (Rédei and Hironyo, 1964). Several additional reticulated mutants have been implicated in leaf differentiation since *cab*

[1] To whom correspondence should be addressed. E-mail aweber@uni-duesseldorf.de, fax +49-211-8113706, tel. +49-211-8112347.

doi: 10.1093/mp/sss045
Received 4 September 2011; accepted 22 March 2012

underexpressed 1 (*cue1*) (Li et al., 1995), *venosa 1–6* (*ven1-6*) (Berná et al., 1999), and *differential development of vascular associated cells 1* (*dov1*) (Kinsman and Pyke, 1998).

Ven2 is allelic to *re* (Berná et al., 1999). The gene affected in *re* was positionally cloned and shown to encode a chloroplast-localized membrane protein (González-Bayón et al., 2006). The function of the gene product remains unknown to date. *Re* mutants have a reticulated leaf phenotype with fewer mesophyll cells compared to wild-type (González-Bayón et al., 2006).

Cue1 is defective in the phospho*enol*pyruvate–phosphate translocator (PPT) of the chloroplast envelope membrane (Streatfield et al., 1999). Initially, it was hypothesized to be 'a cell-specific positive regulator linking light and intrinsic developmental programs in *Arabidopsis* leaf mesophyll cells' (Li et al., 1995). Similarly to *re*, *cue1* mutants have fewer mesophyll cells that contain a lower number of chloroplasts (Li et al., 1995). PPT imports phospho*enol*pyruvate (PEP) into the chloroplasts, where it is used as the major precursor of the shikimic acid pathway (Schmid and Amrhein, 1995; Fischer et al., 1997; Knappe et al., 2003; Voll et al., 2003; Tzin and Galili, 2010). The *cue1* mutant contains lower amounts of aromatic amino acids, has a deregulated amino acid metabolism, and contains reduced levels of shikimate-derived secondary metabolites (Streatfield et al., 1999; Voll et al., 2003). The *cue1* phenotype could be rescued by supplementation with all three aromatic amino acids tryptophan, tyrosine, and phenylalanine. It was concluded that the *cue1* phenotype is caused by either decreased supply of aromatic amino acids or by a lack of aromatic amino acid-derived metabolites (Streatfield et al., 1999; Voll et al., 2003). On the basis of these results, it was hypothesized that a chloroplast-derived signal, that is dependent on either PEP or its metabolic products, causes the reticulated *cue1* leaf phenotype (Streatfield et al., 1999).

A different genetic screen for altered leaf phenotypes yielded the reticulated *venosa 1* to *6* (*ven1-6*) mutant series (Berná et al., 1999). In addition to *ven2*, which is allelic to *re*, *ven3* and *ven6* were recently identified at the molecular level (Mollá-Morales et al., 2011). Much like *cue1*, the *ven3* and *ven6* gene products are involved in amino acid metabolism. *Ven3* and *ven6* encode subunits of the carbamoyl phosphate synthase required for ornithine to citrulline conversion during arginine biosynthesis (Mollá-Morales et al., 2011). *Ven3* and *ven6* are single-copy genes in *A.*. Although arginine synthesis is essential in *A. thaliana*, *ven3* and *ven6* are not fully penetrant, leading to basal levels of arginine synthesis and survival of the plant (Mollá-Morales et al., 2011). The pale to white mesophyll tissue with fewer mesophyll cells and chloroplasts is credited to disturbed protein biosynthesis. It was concluded that arginine is vital for correct leaf development (Mollá-Morales et al., 2011). In line with these findings, mutants that are defective in ribosomal protein subunits and are consequently disturbed in protein biosynthesis also show reticulated leaves (Horiguchi et al., 2011).

Dov1, another reticulated mutant, was discovered in a screen to identify genes that are involved in the differential development of vasculature associated tissues (Kinsman and Pyke, 1998). All mutants identified in this screen possessed a reticulate leaf structure (Kinsman and Pyke, 1998). The phenotype is specific to leaves, and not seen in cotyledons and other aerial tissues. The *dov1* mutation is nuclear recessive and is allelic neither to *cue1* nor to *re* (Kinsman and Pyke, 1998). *Dov1*, which is in the Enkheim-2 (En-2) background, was not positionally cloned to date (Kinsman and Pyke, 1998).

Recently, interest in the bundle sheath has been renewed, since it is a key tissue in C_4 photosynthesis but little understood in C_3 plants (Kobayashi et al., 2009; Aubry et al., 2011). In this study, to gain insight into the role of the bundle sheath during mesophyll differentiation in C_3 plants, *dov1* mutant plants were analyzed with regard to their growth patterns, metabolism, hormone levels, and hormone responses. The affected gene was positionally cloned and identified as ATase2, one of three isoenzymes that catalyze the first step of purine biosynthesis. Since *re*, *cue1*, *ven2*, *ven3*, *ven6*, and *dov1* are now positionally cloned, the *signaling hypothesis* and the *limited supply hypothesis* are critically discussed.

RESULTS

Plant Growth Rates and Photosynthetic Capacity

Dov1 plants were smaller than wild-type controls (Kinsman and Pyke, 1998). *Dov1* was also variable in its penetrance, depending on environmental conditions and plant age (Kinsman and Pyke, 1998; our own observations). We investigated this phenotype in detail by simultaneous growth and photosynthetic performance measurements under controlled conditions.

Growth was determined by means of non-destructive image analysis estimating the rosette size from consecutive images taken at the same time each day. The relative growth rate (RGR) was calculated to assess the relative increase of projected leaf area from observation point to observation point (Hoffmann and Poorter, 2002; Jansen et al., 2009). Simultaneously, the ratio of variable fluorescence to maximum fluorescence (F_v/F_m) of dark-adapted leaves was measured to investigate changes in photosynthetic capacity with regard to energy transfer in intact photosystem II reaction centers.

At the beginning of the monitoring period, the plants were 21 day old (21 d post germination, dpg) (Figure 1A and Supplemental Table 1). At this time, the leaf area of the En-2 plants was 2.5 times larger than the area of the mutants, with 0.91 cm^2 (S.E. 0.07 cm^2) compared to 0.36 cm^2 (S.E. 0.03 cm^2). The reticulated pale phenotype was fully apparent at this point. After 9 d of constant monitoring, the difference in size increased to about 4.3-fold, comparing *dov1* to En-2 (1.73 cm^2; S.E. 0.11 and 7.40 cm^2; S.E. 0.46 cm^2, respectively).

The RGR of En-2 significantly exceeded that of *dov1* at three observation points, namely from 21 to 22, 23 to 24, and 25 to 27 dpg. Both RGR changes of mutants and wild-type changed simultaneously (Figure 1B and Supplemental Table 2).

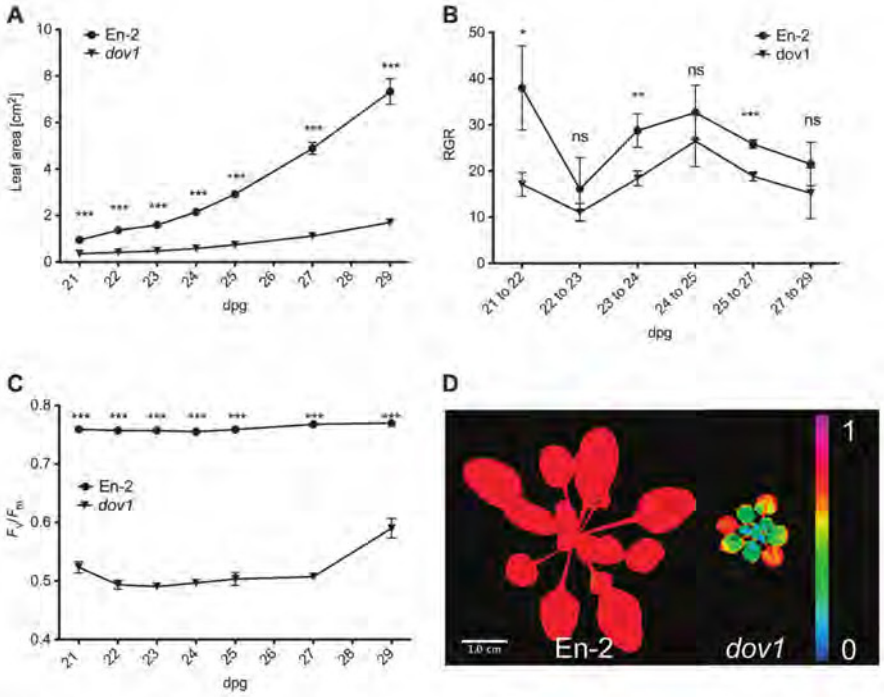

Figure 1. Growth Kinetics and Photosynthetic Activity of En-2 and *dov1* Plants.
(A) Total leaf area of En-2 and *dov1* from 21 to 29 d post germination (dpg) ($n > 15$).
(B) Relative growth rate (RGR) along 9 d of observation. RGR refers to two subsequent monitoring points.
(C) Photosynthetic capacity as indicated by F_v/F_m from 21 to 29 dpg.
(D) False color image of En-2 and *dov1* plants displaying F_v/F_m ratios. Plants shown are representative for plants of 29 dpg ($n > 15$). Error bars represent S.E. Asterisks indicate significance levels.

The photosynthetic performance as characterized by F_v/F_m of En-2 plants at all detected growth stages stayed at a constant level of about 0.78 (Figure 1C and Supplemental Table 1). Compared to wild-type, the *dov1* plants had significantly decreased F_v/F_m values of about 0.50 during the first seven observation days, indicating lower photosynthetic performance. During the time of observation, the overall F_v/F_m of *dov1* plants increased significantly from 0.50 at 25 dpg to 0.59 at 29 dpg by 18% ($p = 0.0001$).

The photosynthetic performance of *dov1* varied not only over time, but also with leaf age (Figure 1D). Within a rosette, the oldest leaves (the outermost whirl of the rosette) had a potential photosynthetic performance almost comparable to wild-type as indicated by the close to red color of the F_v/F_m false color image. Intermediately aged leaves appeared mostly green in the pseudo-fluorescence images, while the youngest leaves are green to blue in color. In younger *dov1* leaves, the photosynthetic performance was highest at the leaf tip. In En-2, the F_v/F_m ratio was constant across different leaf ages of the plant rosette (Figure 1D), which also appeared uniformly green to the eye (Figure 2D). The *dov1* parameters were consistent with the visible phenotype: the youngest leaves (with the exception of cotyledons) displayed the most severe visible phenotype, while older leaves turned green (Figures 2D, 3B, and 3D). The decreased photosynthetic capacity is also reflected by the lowered chlorophyll contents of *dov1* compared to En-2 (Supplemental Figure 1A).

Map-Based Cloning of *dov1* and Testing for Allelism

The key to interpreting these and previous results (Kinsman and Pyke, 1998) was to identify the affected gene in *dov1*. *Dov1* is an EMS-mutant in the En-2 background. To map the *dov1* mutation, it was crossed into the Col-0 background. Thirty-five PCR markers were inferred from known polymorphisms between Landsberg *erecta* (*Ler*) and Col-0 accessions that were extracted from the TAIR database (Swarbreck et al., 2008), and tested for applicability to an En-2/Col-0 cross. 15 suitable markers covering all chromosomes were used for rough mapping of the mutation. Eighty-eight plants with the *dov1* phenotype were selected from the F2-progeny of the mapping cross. They were analyzed using the above-mentioned PCR markers. The mutation was linked to both markers 12 and 19 on the lower arm of chromosome four (Figure 2A). The two additional markers M45 and M47 were established on the lower arm of chromosome four (see Supplemental Table 3 for markers used). The mapping population

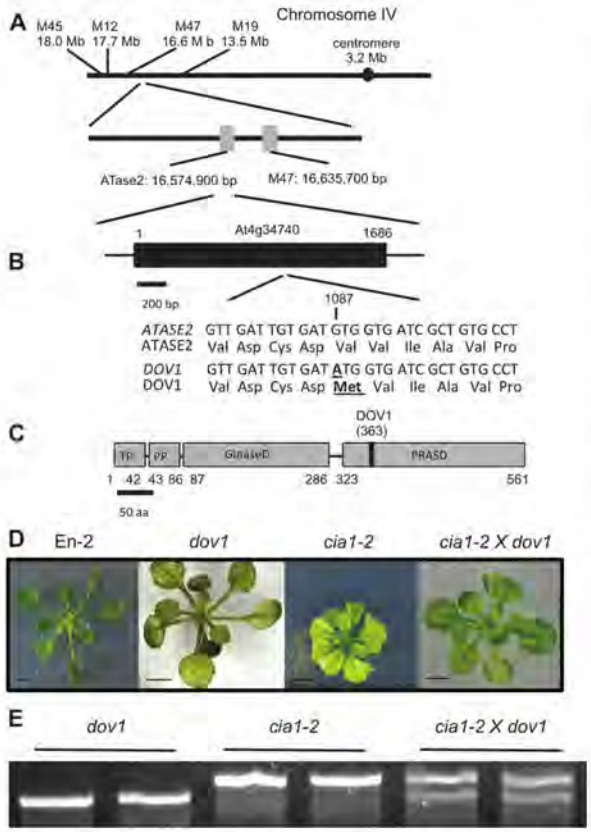

Figure 2. Mapping of *DOV1* and Allelism Test.

(A) Map-based cloning of *dov1* and markers used.

(B) The single exon gene is mutated at position 1087, giving rise to a valine-to-methionine exchange.

(C) Schematic domain structure of ATase2. cTP, predicted chlorplast transit peptide; PP, pro-peptide; GlnaseD, glutaminase domain; PRASD, PRA synthase domain.

(D) Four-week-old plants of En-2, *dov1*, *cia1-2*, and F1-offspring of *cia1-2* x *dov1*. The F1-cross showed the reticulated pattern of both *cia1* and *dov1* parent plants.

(E) Gel electrophoresis of PCR products on genomic DNA with marker 12. The homozygous state of *dov1* and *cia1-2* is indicated by smaller and larger band sizes, respectively. The heterozygous state of F1 plants of a cross between *cia1-2* and *dov1* (*cia1-2* x *dov1*) is indicated by two bands.

was extended to 556 F_2-plants, resulting in recombination frequencies of 8.80% for marker 19, 6.94% for marker 12, 9.84% for marker 45, and 0.27% for marker 47.

This mapping population yielded an interval with 60 genes (data not shown), which was screened for candidate genes. The interval included the gene At4g34740, which encodes for ATase2. The ATase2 mutants *cia1-1*, *cia1-2*, and *atd2*, which are all in the Col-0 background, show phenotypes similar to *dov1* (Hung et al., 2004; van der Graaff et al., 2004). Hence, we hypothesized that *dov1* might be defective in ATase2 function.

To test whether the At4g34740 gene was indeed mutated, the coding sequence including the 5′-UTR and 3′-UTR of At4g34740 was isolated from *dov1* and wild-type by PCR and sequenced. A comparison of the sequences from the En-2 wild-type and *dov1* revealed a substitution of a single nucleotide from guanine to adenine. This mutation causes an amino acid exchange from valine to methionine at position 363 (Val363Met) relative to the start codon of the ATase2 protein (Figure 2B and 2C). Val363 was either conserved or changed conservatively in all organism tested (Supplemental Figure 2). The mutation in *dov1* was located in the PRA synthase domain (PRSAD) of the ATase2 protein (Figure 2C).

The genetic mapping results were confirmed by testing *dov1* and *cia1-2* for allelism. *Cia1-2* in the Col-0 background was crossed with *dov1* in the En-2 background. The resulting F_1-generation showed the same phenotype as *dov1* and *cia1-2* (Figure 2D). The F_1-offspring was heterozygous with regard to En-2 and Col-0, as indicated by the simple sequence length polymorphism marker (SSLP-marker) 12 (Figure 2E). The test confirmed that *dov1* is an allele of *cia1-2*, and thereby a new allele of all known ATase2 mutant lines.

Mutant *dov1* ATase2 Has No Activity *In Vitro*

ATases are ubiquitous enzymes that catalyze the first step in the *de novo* purine biosynthesis. ATases convert glutamine into glutamate by amination of 5-phosphoribosyl-1-pyrophosphate (PRPP) to 5-phospho-ribosylamine (PRA) (Zrenner et al., 2006). PRA is used to produce purine nucleotides in a series of downstream enzymatic reactions (Zrenner et al., 2006) (Figure 4). To test whether the *dov1* mutation in a conserved residue of the PRSAD (Figure 2C and Supplemental Figure 2) affected the function of ATase2, the ATase2 and the mutated DOV1 protein were heterologously expressed in *E. coli*. The ATases of all eukaryotic and many prokaryotic organisms are N-terminally flanked by a pro-peptide (PP) that is auto-catalytically cleaved to give rise to a cysteine residue. The SH-group of the cysteine acts in the catalytic site of the glutaminase domain (Walsh et al., 2007). Additionally, the *Arabidopsis* ATase2 carries a chloroplast-targeting transit peptide (cTP) at its N-terminal end (Emanuelsson et al., 2000; Hung et al., 2004; Walsh et al., 2007). To express both the mutated DOV1 and the wild-type ATase2 enzymes in *E. coli*, the predicted cTP was eliminated and the 11 amino acids of the PP were kept in order not to interfere with the enzyme's function (Walsh et al., 2007). Both proteins were expressed with and without hexahistidine tags for detection and purification. The tagged wild-type enzyme showed no activity (data not shown). We hence chose the untagged, recombinantly expressed ATases from wild-type and *dov1* for further analyses. Total protein was isolated, and the enzyme activity was tested in a two-step assay (Walsh et al., 2007). A reaction lacking the substrate PRPP was used as a negative control. Unlike the wild-type enzyme, the DOV1 enzyme showed no activity above background level in all experiments (Figure 5A).

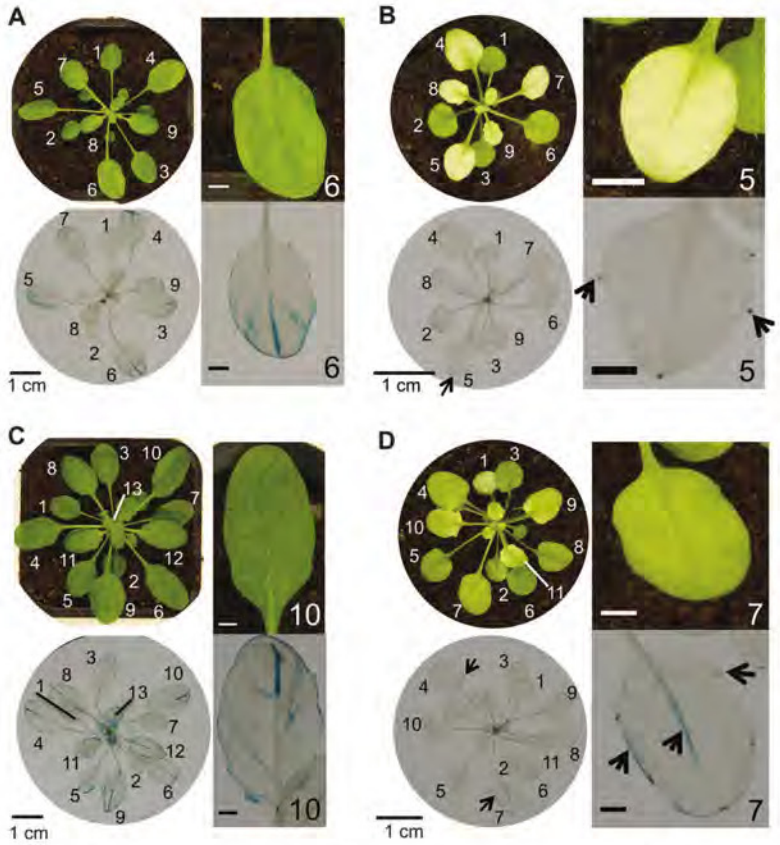

Figure 3. Cytokinin (ARR5–GUS) **(A, B)** and Auxin (DR5–GUS) **(C, D)** reporter Assays in Wild-Type and *dov1* Background of 8-Week-Old Plants, Respectively.

Pictures were taken before and immediately after GUS staining. The number of leaves are arranged from oldest to youngest leaves beginning with 1. The scale-up of single representative leaves is shown right to the whole rosettes. The scale bar in the magnification corresponds to 0.2 cm.

ATASE Activity Is Reduced in *dov1* Plants

Three different ATase isoforms are present in *A. thaliana* of which all three are expressed to different degrees in leaf tissue (Hung et al., 2004; Supplemental Figures 2 and 3). To assess whether total ATase activity was lowered in *dov1* or whether the two other isoforms ATase1 and ATase3 were able to compensate for ATase2, ATase activity was determined *in planta*. En-2 plants had a significantly 1.8-fold higher total ATase activity than *dov1* (Figure 5B).

Metabolite Profiling of *dov1*

Purine levels were decreased in the *dov1* allele *cia1* (Hung et al., 2004). To assess whether the defect in ATase2 also had a direct influence on the amino acids involved in purine biosynthesis, we profiled amino acids and organic acids by gas chromatography coupled to mass spectrometry (GC–MS).

The steady-state levels of seven amino acids were significantly increased in the *dov1* mutant: α-alanine (2.5-fold), asparagine (21.3-fold), aspartate (4.1-fold), glycine (2.3-fold), proline (11.5-fold), lysine (6.6-fold), and ornithine (15.8-fold) (Figure 6). Inorganic phosphate was also increased (12.9-fold). The biological variation in metabolite contents was higher in *dov1* compared to wild-type (Figure 6 and Supplemental Table 4). All other tested metabolites, including all carbohydrates, were not significantly changed in their relative amounts between wild-type and *dov1* (Supplemental Table 4).

Quantitation of Cytokinin Levels and Complementation with Cytokinin

Because cytokinins are purine-derived (Mok and Mok, 2001; Smith and Atkins, 2002) and play crucial roles in leaf development (DeMason, 2005; Efroni et al., 2010), cytokinin levels were profiled in *dov1*.

The total content of all determined cytokinins, namely free cytokinin bases and conjugated forms, were significantly decreased by 22% ($p = 0.0363$) in *dov1* compared to the wild-type (Figure 7B and Supplemental Table 5).

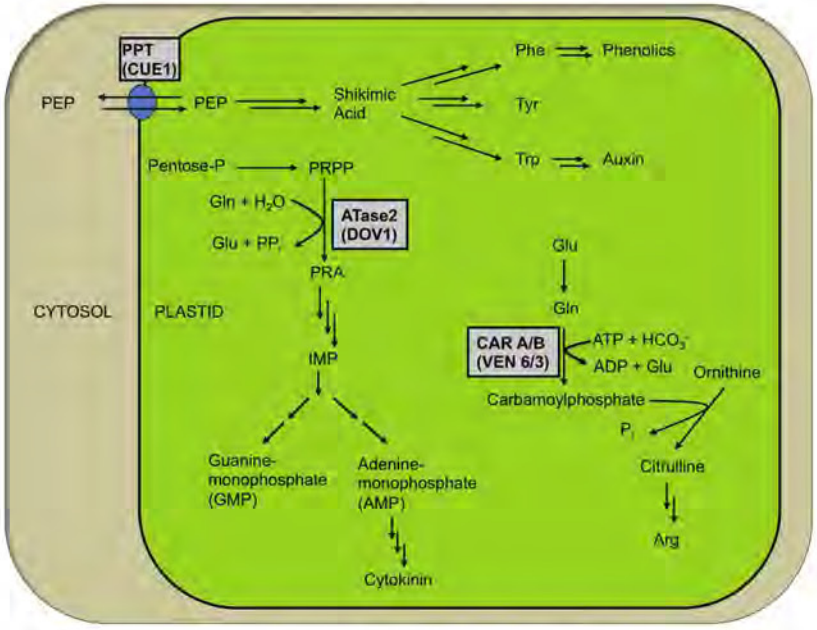

Figure 4. Schematic Overview of the Metabolic Pathways of the Reticulated Mutants *dov1*, *ven3/6*, and *cue1*.

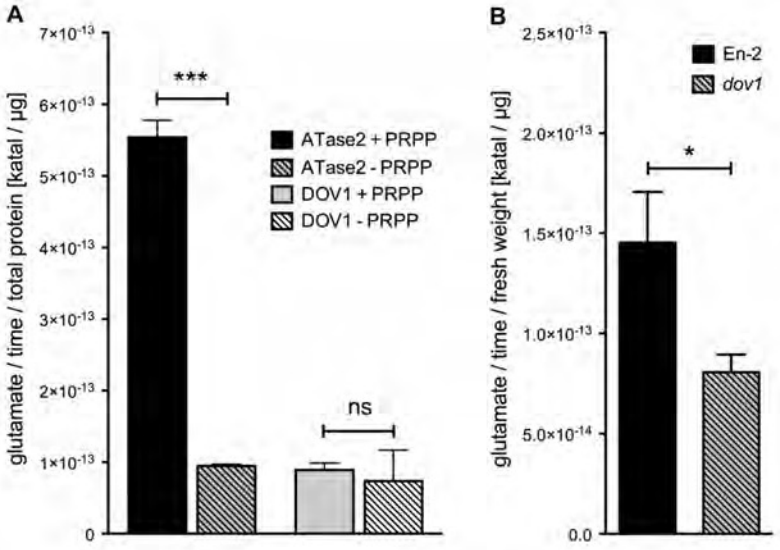

Figure 5. Enzymatic Activity of ATase and the Mutated DOV1-Protein.
(A) Enzymatic activity of heterologously expressed ATase2 and DOV1 in *E. coli* ($n = 4$).
(B) *In planta* total ATase activity in En-2 and *dov1* ($n = 5$).

While total iP-cytokinins and *cis*-zeatin cytokinins were at the same level in wild-type and *dov1*, total *trans*-zeatin cytokinins were significantly decreased by 34% in the mutant compared to the wild-type ($p = 0.0035$). The *trans*-zeatin cytokinins represented the vast majority of cytokinins in both wild-type and *dov1* (Figure 7B and Supplemental Table 5). Some conjugated *trans*-zeatin cytokinins were higher in the wild-type than in *dov1*, and vice versa (Supplemental Table 5). The conjugated derivates are considered deactivated (Mok and Mok, 2001; Bajguz and Piotrowska, 2009).

Despite overall lowered cytokinin contents in *dov1*, the free active cytokinin base *trans*-zeatin (tZ) was increased in *dov1* (2.9-fold). *Cis*-zeatin (cZ) and N^6-(Δ^2-isopentyl)adenine (iP) levels were indistinguishable between *dov1* and wild-type

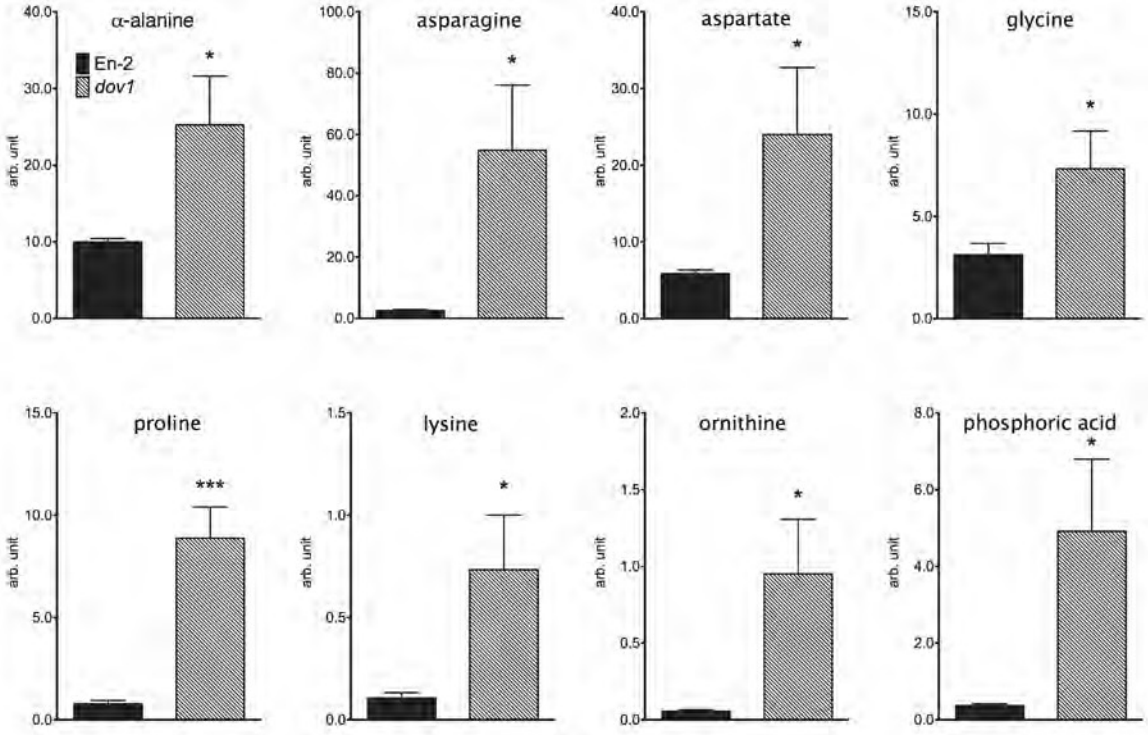

Figure 6. Significantly Changed Steady-State Metabolite Levels in 7-Week-Old En-2 and *dov1* Rosettes before Transition to Budding and Flowering.

Plants were grown under 12-h/12-h light/dark cycle at 100 μE m^{-2} s^{-1}. Samples were taken in the middle of the light period. Arbitrary units (arb. units) are shown. The error bars represent S.E. Asterisks indicate significance levels. n(En-2) = 8, n(*dov1*) = 7.

(Figure 7C and Supplemental Table 5). The latter three cytokinin bases are considered as the physiological active forms, with cZ having the weakest activity (Leonard et al., 1969; Schmitz et al., 1972a, 1972b; Matsubara, 1980; Mok and Mok, 2001). tZ and iP are the major forms in *Arabidopsis* (Sakakibara, 2006).

To test whether the *dov1* phenotype could be restored by exogenous application of cytokinin, plants were biochemically supplemented with the cytokinin derivate 6-benzylaminopurine (BA) (Figure 7A). However, the BA feeding had an effect on neither the En-2 nor the *dov1* plants at very low concentrations (0.001 and 0.01 nM). With increasing concentrations of BA (0.1 and 1.0 nM), the wild-type plants showed stunted growth with pale leaves, and the *dov1* plants did not re-green. Thus, above a threshold level of external BA application, the phenotypes of wild-type and *dov1* resembled each other. Both mutant line and wild-type showed toxic syndromes with increasing BA concentration. Similar results were found when growing *cia1-2* on cytokinin plates (Hung et al., 2004).

A Cytokinin Reporter but Not an Auxin Reporter Responds Differentially in *dov1*

Cytokinins and auxin play crucial roles in leaf development (DeMason, 2005; Rolland-Lagan, 2008; Efroni et al., 2010). To investigate whether these phytohormones displayed distinct physiological patterns in *dov1*, we crossed the mutant into ARR5–GUS (D'Agostino et al., 2000) and DR5–GUS reporter lines (Ulmasov et al., 1997; Robles et al., 2010), respectively. Eight-week-old rosettes with wild-type and *dov1* morphology were selected for GUS staining. Plants were documented immediately before and after GUS staining (Figure 3).

Leaves of every developmental stage from wild-type plants harboring the ARR5–GUS construct showed GUS activity (Figure 3A). Both younger (e.g. leaf 8) and older leaves showed less activity than intermediately aged leaves (leaves 3, 4, 5, 6, and 7). The latter showed a higher GUS activity around the major veins, on the leaf lamina with emphasis at the distal tip part, at the leaf margins, and at the hydathodes (Figure 3A). The GUS staining in *dov1* background at all leaf developmental stages was restricted to the hydathodes of the leaf teeth, as indicated by the arrows (Figure 3B). These GUS staining patterns coincided with neither pale nor green areas of the leaves (Figure 3B).

The DR5–GUS reporter in the wild-type background displayed activity in all rosette leaves (Figure 3C). Older leaves showed less activity than younger and intermediately aged

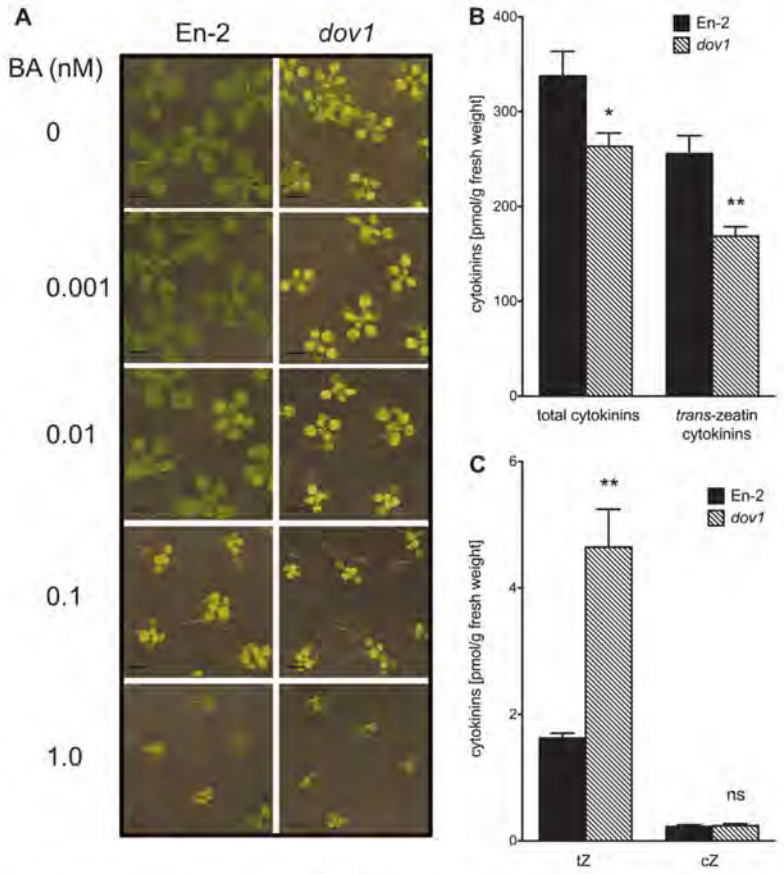

Figure 7. Exogenous Application of Cytokinin to En-2 and *dov1* Plants and Cytokinin Concentrations of En-2 and *dov1*.

(A) Three-week-old En-2 and *dov1* plants exogenously supplemented with increasing concentrations of 6-benzylaminopurine (BA) in 1 MS medium. The scale bar corresponds to 0.5 cm.

(B) Levels of total cytokinins and total *trans*-zeatin cytokinin derivates of 7-week-old En-2 and *dov1* plants.

(C) Levels of the active cytokinins *trans*-zeatin (tZ) and *cis*-zeatin (cZ) of 7-week-old En-2 and *dov1* plants. Error bars represent S.E. Stars indicate significance levels ($n = 5$). Plants for (A), (B), and (C) were grown under 12-h/12-h light/dark cycle at 100 $\mu E\ m^{-2}\ s^{-1}$.

leaves, with restriction of the GUS staining to the leaf margin (e.g. leaf 2). In intermediately aged leaves (leaves 5–12), the GUS staining is primarily found around the major veins, the leaf margins, and the hydathodes of the leaf teeth (Figure 3C). Younger, emerging leaves showed GUS staining at the leaf basis and around the margins. GUS activity in the *dov1* background was generally less pronounced than in the wild-type control (Figure 3D). Whereas the oldest leaves (e.g. leaf 1) only showed staining at the hydathodes, intermediately aged leaves (e.g. leaves 4, 7, and 9) displayed GUS staining along the leaf margin, the hydathodes, and the major veins as indicated by the arrows (Figure 3D). The staining in the youngest emerging leaves was restricted to the leaf tip. In comparison to the cytokinin reporter ARR5–GUS in the *dov1* background, the DR5–GUS reporter showed a generally more intense staining and had an intermediate phenotype when compared to the wild-type.

DISCUSSION

To understand the role of *dov1* in leaf development and organization, the mutant was phenotypically and metabolically characterized, and the defective gene identified.

Dov1 Is Defect in the ATase2 Gene Product

The defective gene in the *dov1* mutant was unknown, although it is one of the hallmark mutants used in analyzing internal leaf development (Kinsman and Pyke, 1998). The reason for this was probably its genetic background in En-2.

We mapped *dov1* to the gene locus At4g34740, which encodes ATase2, the enzyme catalyzing the first step of purine biosynthesis. In the mutant enzyme, valine at position 363 was exchanged to methionine (Figure 2B and 2C). *In vitro*, no enzyme activity was measured. Hence, Val363 is essential for the enzyme function (Figure 5A). The valine residue is conserved in

ATase2 proteins from bacteria to plants (Supplemental Figure 2). *A. thaliana* harbors three loci for ATases: ATase1, 2, and 3. Since the purine biosynthesis is essential, viability of *dov1* depends on the activities of ATases 1 and 3 (Supplemental Figures 3 and 4). Therefore, we tested to what degree total ATase activity is lowered in *dov1*. *Dov1* showed a 1.8-fold decrease in total ATase activity in its aerial tissues (Figure 5B). This decrease was due to the defect of the mutated ATase2 enzyme because the mutated recombinant protein DOV was not functional *in vitro* (Figure 5A).

The previously reported ATase2 mutants *cia1-1*, *cia1-2*, and *atd2* showed phenotypes similar to *dov1* with pale and reticulated leaves (Hung et al., 2004; van der Graaff et al., 2004). Crosses of *dov1* with *cia1-2* confirmed allelism. This indicates that the two domains of ATase2 (Figure 2C, 2D and 2E) might act in *cis*, not in *trans*, although this hypothesis awaits testing in the future. The mutation in *dov1* was localized to the PRA domain while the mutations in the *cia* mutants were localized to the glutaminase domain (Hung et al., 2004). These tests confirmed that *dov1* is a new allele of ATase2.

Consequences of Limited Purine Availability for Primary Leaf Metabolism

Mutants in ATase2 had lower purine levels in leaves compared to wild-type (Hung et al., 2004; van der Graaff et al., 2004). The mutants could be complemented with externally applied purines (Hung et al., 2004), which showed that a functional salvage pathway was capable of supplying almost enough purines to the leaf. Despite the fact that the ATase2 mutants *cia1* (Hung et al., 2004), *atd2* (van der Graaff et al., 2004), and *dov1* (Kinsman and Pyke, 1998) grew much more slowly compared to wild-type (Figure 1A and 1B), the growth reduction was not strong enough to permit the formation of small, but green leaves with intact chloroplasts.

Within the leaf, not only purine levels were changed (Hung et al., 2004), but also several proteinogenic amino acids and inorganic phosphate had altered steady-state levels (Figure 6 and Supplemental Table 4). The increased levels of the purine building blocks aspartate and glycine (Zrenner et al., 2006) might result from the decreased purine production in *dov1* (Figures 4 and 6). The increased amounts of N-rich amino acids asparagine, lysine, and the asparagine precursor ornithine, as well as the increasein f alanine, aspartate, and glycine, and the overall stable level of carbohydrates might be a consequence of an altered C/N-homeostasis. Purines bind considerable amounts of nitrogen (Reinbothe and Mothes, 1962; Smith and Atkins, 2002). Lowered leaf purine levels may lead to an increased flux of N into the biosynthesis of N-rich amino acids as a compensatory effect. The increase in proline may indicate that the plants perceive the lack of purines as a stress that activates a generic stress response, such as the accumulation of proline (Delauney and Verma, 1993; Parry et al., 2005; Verdoy et al., 2006; Lea et al., 2007; Nicotra et al., 2011). Since the metabolites determined were either at the same level or higher in *dov1* compared to the wild-type, these metabolites were not causal for the phenotype.

Cytokinins and Altered Growth Patterns of *dov1* Leaves

We and others observed that *dov1* mutants, depending on their growth density on MS-plates, the day/night-cycle length as well as their age, varied considerably for the extent of reticulation and paleness of their leaves (data not shown; Kinsman and Pyke, 1998). The growth screens revealed a constant growth rate of both *dov1* and wild-type plants, with a generally lower rate of *dov1* (Figure 1A and 1B).

Photosynthetic performance and the visible phenotype of *dov1* not only varied with plant age, but also showed an age-related pattern. Older *dov1* leaves displayed almost normal photosynthetic performance, while younger leaves had their highest performance at the leaf tip. In wild-type, the photosynthetic performance was independent of leaf age (Figures 1D).

The age-related differences did not correlate with the expression patterns of the ATases because they did not vary in expression during leaf development (public data from the *Arabidopsis* efp browser; Supplemental Figure 3; Winter et al., 2007).

Purines are precursors of cytokinins (Mok and Mok, 2001), which are known to drive the mitotic events in plants (Redig et al., 1996), and are abundant in meristematic tissues (Nishinari and Syono, 1980; Ascough et al., 2009). It was shown that purine biosynthesis genes have a stronger expression in mitotically active tissues, and are thus involved in cell division (Zhang et al., 1996; van der Graaff et al., 2004; Zrenner et al., 2009).

To assess the role of cytokinins in *dov1* leaf development, cytokinin levels in leaves were determined and the response to active cytokinins (Shtratnikova and Kulaeva, 2008) was assessed by the ARR5–GUS-promoter activity in the *dov1* background. Total cytokinin levels were decreased in *dov1* compared to wild-type (Figure 7B), reflecting the decreased total ATase activity (Figure 5B). ATase1 and 3 apparently did not fully compensate the cytokinin biosynthesis. The active tZ, however, was increased in *dov1*. tZ is reported to be the most active cytokinin, while the conjugated derivates are assumed to be non-active (Mok and Mok, 2001; Bajguz and Piotrowska, 2009). While the cytokinin response, as indicated by the ARR5–GUS reporter, was found on the leaf lamina, around the midvein, the margins, and the hydathodes of younger wild-type leaves, the cytokinin response in *dov1* was restricted to the hydathodes of each rosette leaf. The cause of this restriction is likely due to the lack of supply with purines caused by the inactivity of ATase2. The activity in hydathodes as a site of high transpiration might reflect an accumulation of cytokinins from the transpiration stream (Aloni et al., 2005). At the hydathodes, the active cytokinins do not contribute to leaf growth. Furthermore, exogeneous cytokinin application reverted neither the *dov1* nor the *cia1-2* phenotype (Hung et al.,

2004). The cytokinin even had toxic effects to both wild-type and mutant plants (Figure 7A).

Auxin responsiveness in the *dov1* background is not as restricted as the cytokinin response (Figure 3B and 3D). In some leaves, there was still a response to auxin at the leaf margins and in the major veins (Figure 3D). Thus, the responsiveness seemed to be intermediary. The responsiveness, even if limited compared to the wild-type, is likely to be explained by the fact that auxin biosynthesis is not directly dependent upon purines (Zhao, 2010) (Figure 4). However, it is tempting to speculate that the lowered auxin activity in the *dov1* background compared to the wild-type is an indirect consequence of altered cytokinin levels, particularly since it is known that there is an extensive crosstalk between auxin and cytokinin action (Moubayidin et al., 2009).

Taken together, limited supply provided a likely explanation for the large phenotypic plasticity in the *dov1* mutant (this publication; Kinsman and Pyke, 1998; Hung et al., 2004; van der Graaff et al., 2004). The plasticity was not due to inherent variability of the genotype because the standard errors for all parameters measured under controlled conditions were small (Figures 1A–1C, 5, 6, and 7, and Supplemental Tables 1, 2, 4, and 5). Phenotypic variability may result from conditions that decrease purine demand. Mature leaves with only few dividing cells possibly require less *de novo* purine biosynthesis. Thus, decreased supply of purines, such as in old mature leaves as compared to young leaves, permitted old leaves to turn green.

The Basis of Reticulated Leaf Patterning

The basis of the reticulated leaf pattern in *dov1*, *re*, *cue1*, *ven3*, and *ven6* has not been addressed conclusively to date. Strikingly, all functionally characterized reticulated mutants are affected in primary metabolic genes and consequently in primary metabolism (Streatfield et al., 1999; Mollá-Morales et al., 2011; this work), although all were initially hypothesized in a *signaling hypothesis* to encode regulatory components important for mesophyll differentiation.

In none of the reticulated mutants reported to date has the effect on plant hormones been investigated. Since cytokinin is involved in cell division and auxin in overall leaf differentiation (DeMason, 2005; Rolland-Lagan, 2008; Efroni et al., 2010), the response to these hormones were tested in this study, using reporter constructs.

Cue1 is involved in shikimic acid and thus aromatic amino acid biosynthesis, *ven3* and *ven6* are involved in arginine synthesis, and *dov1* contributes to *de novo* purine synthesis. All of the affected pathways localize to the plastid (Figure 4). Despite their co-localization, the pathways are not directly connected, because, apart from the fact that the purine-based metabolite ATP is the general energy currency of the cell, they do not share substrates or products (Figure 4). Moreover, metabolites, which would require products of all three pathways for their synthesis, have not been described to date. While this does not exclude the hypothesis of a signaling molecule as the cause of the phenotype (Kinsman and Pyke, 1998; Streatfield et al., 1999), it makes it at least unlikely.

Analysis of the *ven3* and *ven6* mutants and experiments using arginine biosynthesis inhibitors in pea leaves conclusively demonstrated that leaves turn white in the absence of arginine (Turner and Mitchell, 1985). *Ven3* and *ven6* mutants have decreased levels of arginine and/or citrulline (Mollá-Morales et al., 2011). Unlike *re* and *cue1*, *ven3* and *ven6* have already been considered metabolic rather than signaling mutants (Mollá-Morales et al., 2011).

Cue1 is a full knockout of one of two plastidial phospho*enol*pyruvate–phosphate translocators (PPTs), which feed the plastid-localized shikimic acid pathway with phospho*enol*pyruvate and all reactions depending on it. The steady-state amino acid levels reflect an imbalance of non-aromatic to aromatic amino acids, a decrease in phenylalanine, and a reduced flux into phenylalanine-derived secondary metabolites (Streatfield et al., 1999; Voll et al., 2003). However, transgenic wild-type-like plants in the *cue1* background harboring an overexpressed plastidic enzyme, which produces PEP, had overall diminished aromatic amino acids (Voll et al., 2003; Weber et al., 2004). Thus, it has been argued that the affected aromatic amino acids biosynthesis is not simply the cause of the *cue1* phenotype (Voll et al., 2003). Rather, a metabolic signal involved in leaf development was postulated.

Unlike the *ven3* and *ven6* mutations, which are leaky, *cue1* is a complete knockout of PPT1. Survival of the plants is likely dependent on a second transporter with identical transport function but different expression domains (Knappe et al., 2003). Taking the plant's response to a *cue1* knockout (Streatfield et al., 1999; Voll et al., 2003) into account, the limited phenylalanine and its derived secondary metabolites availability may well be the primary cause of the reduced cell number and paleness in *cue1*. This is supported by the fact that ribosomal protein mutants with limited protein biosynthesis also show reduced cell number (Horiguchi et al., 2011).

Similarly to *ven3*, *ven6*, and *cue1*, the *dov1* gene product ATase2 also provides a metabolite that is essential to the cell, purine. Similarly to *cue1*, the absence of *dov1* can be partially compensated by additional isoforms. Hence, purines can still be produced *in planta* by ATase1 and 3, albeit they are not highly expressed in leaf tissue (Supplemental Figure 3). The decreased total cytokinin levels and the restricted cytokinin response pattern in *dov1* are likely to be seen as a lack of supply with purines.

The joint interpretation of the three mutants *ven3/6*, *cue1*, and *dov1* with apparent defects in mesophyll but healthy bundle sheaths points to limited supply of essential metabolites as the main reason for the reticulate phenotypes observed. Why, then, are the bundle sheaths and the leaf margins green or at least greener than the remainder of the leaf? Vein and therefore bundle sheath differentiation predates mesophyll differentiation (Kinsman and Pyke, 1998). Hence, if a limited supply of metabolites is given, either in the leaf itself or from other organs, the early differentiating tissues can properly form,

while tissues differentiating later are more likely to be limited. In true leaves, only the early differentiating bundle sheaths and nearby tissues are green, while mesophyll is bleached (Li et al., 1995; Kinsman and Pyke, 1998; González-Bayón et al., 2006; Mollá-Morales et al., 2011). The transport of primary metabolites via the vasculature is likely sufficient to deliver enough metabolites to allow greening of the tissue. Vascular-located transporters for amino acids (Frommer et al., 1995) and putative vascular purine transporters (Maurino et al., 2006) have been identified.

The detailed analysis of photosynthetic performance in *dov1* supports this hypothesis. Once cell division stops and leaves mature, the supply of purines from other sources may again be sufficient to allow re-greening of the older leaves (Figure 2D, 3B and 3D) and recovery of photosynthetic performance (Figure 1C and 1D). This indicates that mesophyll cell aberrations are not permanent. The nature of the *dov1* mutant supports a *limited supply* rather than a *signaling hypothesis* as the reason for reticulation. The mapping of the remaining reticulated mutants and the elucidation of *re* function will be instrumental in distinguishing between these two hypotheses.

METHODS

Plant Material, General Growth Conditions, and Plant Lines

Arabidopsis thaliana plants were grown under controlled conditions in climate chambers. The day/night cycle was chosen as 12 h light and 12 h with a photosynthetically active radiation of 100 $\mu E\ m^{-2}\ s^{-1}$. Temperature was set to 22°C during light, and 18°C during the dark period. In special experiments, the deviant growth conditions are indicated.

Seeds were surface-sterilized with chlorine gas in a desiccator as previously described (Desfeux et al., 2000), spotted on solid 1 Murashige and Skoog (MS)-medium with vitamins containing 0.8% (*w/w*) plant agar (Murashige and Skoog, 1962), and stratified at 4°C for 4 d. All plant material was germinated and grown in 1 MS medium.

The *dov1*-seeds were obtained from our laboratory stock, whereas the EMS-mutant *cia1-2* was obtained from the European Arabidopsis Stock Centre. DR5–GUS- and ARR5–GUS-plants were kindly provided by Rüdiger Simon and Nicole Stahl (Institute of Developmental Genetics, Heinrich-Heine-University, Düsseldorf). DR5 is an artificial promoter that reacts to changed auxin perception (Ulmasov et al., 1997; Robles et al., 2010). ARR5–GUS indicates changing cytokinin patterns (D'Agostino et al., 2000).

DR5–GUS and ARR5-GUS-reporter lines were crossed into *dov1*. The F_2-generation of both the DR-5–GUS and the ARR5–GUS-crosses with *dov1* was visually selected for the *dov1* and En-2 phenotype. *Dov1* and En-2 phenotypic plants of the F_2 generation were screened via GUS staining for changing GUS-patterns.

Mapping of *dov1*

Dov1, which is an EMS-mutant in the En-2 background, was crossed into the Col-0 background in order to map the mutant. Map-based cloning was adapted and performed as previously described (Jander et al., 2002). Thirty-five PCR markers were inferred from known polymorphisms between Ler and Col-0, and tested for applicability to an En-2/Col-0 cross. Four markers did not yield PCR products under the conditions used and 16 markers were not different between Col-0 und En-2. 15 suitable markers covering all chromosomes were used for rough mapping of the mutation (see Supplemental Table 5 for all markers used). Eighty-eight plants with the *dov1* phenotype were selected from the F_2-progeny of the mapping cross. They were analyzed using the 15 PCR markers. The mutation was linked to both markers 12 and 19 on the lower arm of chromosome four. The additional markers M45 and M47 were established on the lower arm of chromosome four. Recombination was calculated to test for the linkage of loci. The mapping population was extended to 556 F_2-plants resulting in recombination frequencies of 8.80% for marker 19, 6.94% for marker 12, 9.84% for marker 45, and 0.27% for marker 47. This mapping population yielded an interval with 60 candidate genes, which was screened for candidate genes. The interval included the gene At4g34740.

The candidate Atase2 was isolated by PCR-based means with the forward primer 5'-aaccgaatcaaattttagtaaatagag-3' binding in the 5'-UTR, and the reverse primer 5'-aaattgaccccaaaaccaaa-3' binding in the 3'-UTR. After cloning into the blunt end vector pJET1.2 (Fermentas, Thermo Scientific, Germany), the PCR product was sequenced. The described base pair exchange at position 1087 in *dov1* was detected.

The recombination frequency (RF) in percentage represents the ratio of recombinant gametes with regard to the *dov1* locus to the total number of gametes. The RF was calculated by the equation RF = ((2*n(Col-0) + 1*n(het) + 0*n(En-2))/2n, where n(Col-0) is the number of plants homozygous for the Col-0 allele, n(het) is the number of plants for the heterozygous plants, n(En-2) is the number of plants for the En-2 allele, and n is the total number of plants analyzed. A RF $\geq$ 50% was regarded as free recombination, namely as unlinked loci, whereas a RF $<$ 50% was considered as coupled recombination, namely linked loci.

GUS Staining

GUS-staining was performed as previously described (Mattsson et al., 2003). Whole rosettes of 6-week-old *dov1* and En-2 plants were vacuum infiltrated with the GUS staining solution (0.1 M NaH_2PO_4, pH 7.0; 10 mM Na_2EDTA; 0.5 M Sodium-Ferricyanide $K_3[Fe(CN)_6]$; 0.5 M Sodium-Ferrocyanide $K_4[Fe(CN)_6] \times 3H_2O$, 0.1% Triton X-100, and 1 mM 5-bromo-4-chloro-3-indoyl-beta-GlcUA (Inalco Spa)). The samples were incubated at 37°C for 24 h. Hereafter, the staining solution was removed, and fixation solution was added (50% (m/m) Ethanol, 5% (m/m) Glacial acetic acid, and 3.7% (m/m)

Formaldehyde). The samples stored in the staining solution were incubated for 10 min at 65°C. The leaf tissue was destained three times after removal of the fixation solution with 80% (m/m) Ethanol. Pictures were taken with a digital camera (Canon D40).

Biochemical Complementation with Cytokinin

After 7 d of growth on MS-plates, seedlings were transferred onto MS-plates containing different concentrations of 6-benzylaminopurine (0.001, 0.01, 0.1, and 1 nM BA). Plants were monitored for an additional 2 weeks. Pictures were taken with a digital camera (Canon D40).

Metabolite Profiling

Dov1 and En-2-plants were grown under controlled conditions in a light chamber in a 12-h/12-h light/dark cycle (100 μE m^{-2} s^{-1}) on 1 MS medium (Murashige and Skoog, 1962), and transferred on soil after 2 weeks. Whole rosettes from 7-week-old *dov1* and En-2 plants were harvested before flowering, and snap-frozen in liquid nitrogen. Polar metabolites from homogenized rosette material samples (~50 mg) were extracted using a chloroform–methanol extraction protocol (Fiehn, 2006). The extraction mix was vortexed for 20 s, shaken in a rotating device for 6 min at 4°C, then centrifuged for 2 min at 20 000 *g*. 1 ml of the supernatant was vortexed for 10 s. 100 μl of this extract was lyophilized and derivatized using methoxyamine hydrochloride in pyridine followed by N-methyl-N-(trimethylsilyl-)fluoroacetamide (MSFTA) treatment (Fiehn, 2006).

The relative amounts of 15 amino acids, 12 carbohydrates, eight carboxylic acids, shikimate, and phosphate were determined as described previously (Gowik et al., 2011).

Cytokinin Quantification

Plants were grown as described for metabolite profiling. Five rosettes of each En-2 and *dov1* rosettes were pooled. Five replicates of each pooled sample were used for cytokinin quantification. For endogenous cytokinins analysis, extraction and purification were performed according to the method previously described (Novák et al., 2003). Levels of cytokinins were quantified by ultra-performance liquid chromatography–electrospray tandem mass spectrometry (UPLC_MS/MS) (Novák et al., 2008).

Chlorophyll Determination

Plants were grown for 5 weeks under 16-h/8-h light/dark at 100 μE m^{-2} s^{-1} at 22°C/18°C. Plant material was harvested in the middle of the light period, snap-frozen in liquid nitrogen, and homogenized by grinding in a mortar. The fresh weight was determined and the chlorophyll concentration was determined as described previously (Porra et al., 1989).

Enzymatic Assays

The enzyme activity assay was conducted as previously reported (Kim et al., 1996; van der Graaff et al., 2004) and adapted to *Arabidopsis thaliana*. Aerial parts of 6-week-old plants, grown on MS-plates, were harvested before budding and flowering, processed, and used for measuring ATase activity. 0.8 g of *Arabidopsis* plant material were homogenized in 1 ml of plant extraction buffer (pH 6.8, 1 mM EDTA, 1 mM $MgCl_2$, 5 mM glutathione, 20 mM DTT, 0.1 mM phenylmethanesulfonyl fluoride (PMSF), 0.1 mM 4-(2-Aminoethyl) benzenesulfonyl fluoride hydrochloride (AEBSF), 2 μM Pepstatin A). The homogenate was centrifuged for 1 min at 20 000 *g*. The supernatant was desalted using Zeba™Spin Desalting Columns (Thermo Scientific). The flow-through was used for the activity assay.

ATase activity was determined by measuring the PRPP-dependent formation of glutamate from glutamine. 50 μl aliquots of plant extract were assayed in 100 μl of assay I reaction mix, which contained in final concentrations: 5 mM $MgCl_2$, 3 mM PRPP, 20 mM NaF, 5 mM glutamine. Control assays were performed by adding glutamine but no PRPP. The reactions were stopped at 100°C for 3 min in a water bath. Glutamate concentration was measured using the glutamate dehydrogenase method (Messenger and Zalkin, 1979). The assay contained 50 mM Tris-HCl, pH 8.0, 267 μl ml^{-1} H_2O, 3 mM 3-Acetylpyridine adenine dinucleotide (APAD), 133 μl ml^{-1} assay I reaction mix, 4 U ml^{-1} glutamate dehydrogenase. The formation of $APADH^+$ was monitored in a plate reader at 363 nm (Biotek plate reader KC4 with supplied software). PRPP-dependent activity was calculated by subtracting the PRPP-independent activity.

GROWSCREEN FLUORO Analysis of Growth, Fluorescence, and Phenotypic Properties

Batches of plants grown on soil were analyzed for growth and phenotypic properties by using the GROWSCREEN FLUORO phenotyping platform as described previously (Jansen et al., 2009). 15 or more biological replicates were used for each of the En-2 plants and the *dov1* mutants. The phenotyping set-up uses a fluorescence-imaging camera together with an illumination head to automatically acquire images of every plant inside the batches placed in the set-up (Jansen et al., 2009). Plants were imaged non-invasively for a period of 9 d at the same time every day. For calculation of F_v/F_m, plants were dark-adapted for 30 min. Based on the acquired images, image analysis provided several datasets for each mutant and wild-type plants, including the RGR, and efficiency of photosystem II (Walter et al., 2007; Jansen et al., 2009). The RGR was calculated using the equation RGR = (mean of $\ln(A_2)$ – mean of $\ln(A_1))/t_2 - t_1$) (Hoffmann and Poorter, 2002; Jansen et al., 2009).

Statistical Analysis

Statistical significance was assessed by the Student's *t*-test. Probability values (p) <0.05 were considered being significant. One star indicates $p < 0.05$, two stars indicate $p < 0.01$, and three stars indicate $p < 0.0001$. The standard error of the mean (S.E.) is indicated in all plots, if not indicated otherwise.

Alignment of Protein Sequences

Protein Atase2 sequences of different organisms were inferred from publicly available databases. Alignment of the sequences was performed with CLC Genomic Workbench (www.clcbio.com). The settings were chosen as follows: default alignment, gap open cost 10, gap extension 1, and end gap cost as any other.

SUPPLEMENTARY DATA

Supplementary Data are available at *Molecular Plant Online.*

FUNDING

This work was funded by grants of the Deutsche Forschungsgemeinschaft (DFG CRC 590 to A.P.M.W. and iRTG 1525 to A.P.M.W. and A.W.) and by Grant No. KAN200380801 to M.S.

ACKNOWLEDGMENTS

We thank Prof. Dr. Rüdiger Simon and Dr. Yvonne Stahl for providing us with the ARR5–GUS and DR5-GUS reporter lines. We appreciate technical assistance by Katrin L. Weber and Elisabeth Klemp with GC/MS-analysis of metabolites and by Manuel Wagner with plate growth assays. We thank Steffen köhler for assistance with photographic documentation of the reporter lines and the cytokinin plate assays. No conflict of interest declared.

REFERENCES

Aloni, R., Langhans, M., Aloni, E., Dreieicher, E., and Ullrich, C.I. (2005). Root-synthesized cytokinin in *Arabidopsis* is distributed in the shoot by the transpiration stream. J. Exp. Bot. **56,** 1535–1544.

Ascough, G.D., et al. (2009). Hormonal and cell division analyses in *Watsonia lepida* seedlings. J. Plant Physiol. **166,** 1497–1507.

Aubry, S., Brown, N.J., and Hibberd, J.M. (2011). The role of proteins in C_3 plants prior to their recruitment into the C_4 pathway. J. Exp. Bot. **62,** 3049–3059.

Bajguz, A., and Piotrowska, A. (2009). Conjugates of auxin and cytokinin. Phytochem. **70,** 957–969.

Berná, G., Robles, P., and Micol, J.L. (1999). A mutational analysis of leaf morphogenesis in *Arabidopsis thaliana*. Genetics. **152,** 729–742.

Candela, H., Martinez-Laborda, A., and Micol, J.L. (1999). Venation pattern formation in *Arabidopsis thaliana* vegetative leaves. Dev. Biol. **205,** 205–216.

D'Agostino, I.B., Deruère, J., and Kieber, J.J. (2000). Characterization of the response of the *Arabidopsis* response regulator gene family to cytokinin. Plant Physiol. **124,** 1706–1717.

Delauney, A.J., and Verma, D.P.S. (1993). Proline biosynthesis and osmoregulation in plants. Plant J. **4,** 215–223.

DeMason, D.A. (2005). Auxin–cytokinin and auxin–gibberellin interactions during morphogenesis of the compound leaves of pea (*Pisum sativum*). Planta. **222,** 151–166.

Desfeux, C., Clough, S.J., and Bent, A.F. (2000). Female reproductive tissues are the primary target of *Agrobacterium*-mediated transformation by the *Arabidopsis* floral-dip method. Plant Physiol. **123,** 895–904.

Efroni, I., Eshed, Y., and Lifschitz, E. (2010). Morphogenesis of simple and compound leaves: a critical review. Plant Cell. **22,** 1019–1032.

Emanuelsson, O., Nielsen, H., Brunak, S., and von Heijne, G. (2000). Predicting subcellular localization of proteins based on their N-terminal amino acid sequence. J. Mol. Biol. **300,** 1005–1016.

Fiehn, O. (2006). Metabolite profiling in *Arabidopsis*. In *Arabidopsis* Protocols, 2nd edn, Salinas, J., and Sanchez-Serrano, J.J., eds. Methods in Molecular Biology ser. (Totowa, NJ: Humana Press), pp. 439–447.

Fischer, K., et al. (1997). A new class of plastidic phosphate translocators: a putative link between primary and secondary metabolism by the *phosphoenolpyruvate/phosphate* antiporter. Plant Cell. **9,** 453–462.

Frommer, W.B., Hummel, S., Unseld, M., and Ninnemann, O. (1995). Seed and vascular expression of a high-affinity transporter for cationic amino acids in *Arabidopsis*. Proc. Natl Acad. Sci. U S A. **92,** 12036–12040.

González-Bayón, R., et al. (2006). Mutations in the *RETICULATA* gene dramatically alter internal architecture but have little effect on overall organ shape in *Arabidopsis* leaves. J. Exp. Bot. **57,** 3019–3031.

Gowik, U., Brautigam, A., Weber, K.L., Weber, A.P.M., and Westhoff, P. (2011). Evolution of C_4 photosynthesis in the genus *Flaveria*: how many and which genes does it take to make C_4? Plant Cell. **23,** 2087–2105.

Hoffmann, W.A., and Poorter, H. (2002). Avoiding bias in calculations of relative growth rate. Ann. Bot. **90,** 37–42.

Horiguchi, G., et al. (2011). Differential contributions of ribosomal protein genes to *Arabidopsis thaliana* leaf development. Plant J. **65,** 724–736.

Hung, W.F., Chen, L.J., Boldt, R., Sun, C.W., and Li, H.M. (2004). Characterization of *Arabidopsis* glutamine phosphoribosyl pyrophosphate amidotransferase-deficient mutants. Plant Physiol. **135,** 1314–1323.

Jander, G., Norris, S.R., Rounsley, S.D., Bush, D.F., Levin, I.M., and Last, R.L. (2002). *Arabidopsis* map-based cloning in the post-genome era. Plant Physiol. **129,** 440–450.

Jansen, M., et al. (2009). Simultaneous phenotyping of leaf growth and chlorophyll fluorescence via GROWSCREEN FLUORO allows detection of stress tolerance in *Arabidopsis thaliana* and other rosette plants. Funct. Plant Biol. **36,** 902–914.

Kim, J.H., Krahn, J.M., Tomchick, D.R., Smith, J.L., and Zalkin, H. (1996). Structure and function of the glutamine phosphoribosylpyrophosphate amidotransferase glutamine site and communication with the phosphoribosylpyrophosphate site. J. Biol. Chem. **271,** 15549–15557.

Kinsman, E.A., and Pyke, K.A. (1998). Bundle sheath cells and cell-specific plastid development in *Arabidopsis* leaves. Development. **125,** 1815–1822.

Knappe, S., Löttgert, T., Schneider, A., Voll, L., Flügge, U.I., and Fischer, K. (2003). Characterization of two functional *phosphoenolpyruvate/phosphate translocator (PPT)* genes in *Arabidopsis-*

AtPPT1 may be involved in the provision of signals for correct mesophyll development. Plant J. **36,** 411–420.

Kobayashi, H., Yamada, M., Taniguchi, M., Kawasaki, M., Sugiyama, T., and Miyake, H. (2009). Differential positioning of C_4 mesophyll and bundle sheath chloroplasts: recovery of chloroplast positioning requires the actomyosin system. Plant Cell Physiol. **50,** 129–140.

Lea, P.J., Sodek, L., Parry, M.A.J., Shewry, R., and Halford, N.G. (2007). Asparagine in plants. Ann. Appl. Biol. **150,** 1–26.

Leonard, N.J., Hecht, S.M., Skoog, F., and Schmitz, R.Y. (1969). Cytokinins: synthesis, mass spectra, and biological activity of compounds related to zeatin. Proc. Natl Acad. Sci. U S A. **63,** 175–182.

Li, H.M., Culligan, K., Dixon, R.A., and Chory, J. (1995). *CUE1*: a mesophyll cell-specific positive regulator of light-controlled gene expression in *Arabidopsis*. Plant Cell. **7,** 1599–1610.

Matsubara, S. (1980). Structure-activity-relationships of cytokinins. Phytochem. **19,** 2239–2253.

Mattsson, J., Ckurshumova, W., and Berleth, T. (2003). Auxin signaling in *Arabidopsis* leaf vascular development. Plant Physiol. **131,** 1327–1339.

Maurino, V.G., Grube, E., Zielinski, J., Schild, A., Fischer, K., and Flügge, U.I. (2006). Identification and expression analysis of twelve members of the nucleobase-ascorbate transporter (NAT) gene family in *Arabidopsis thaliana*. Plant Cell Physiol. **47,** 1381–1393.

Messenger, L.J., and Zalkin, H. (1979). Glutamine phosphoribosylpyrophosphate amidotransferase from *Escherichia coli*: purification and properties. J. Biol. Chem. **254,** 3382–3392.

Mok, D.W.S., and Mok, M.C. (2001). Cytokinin metabolism and action. Ann. Rev. Plant Physiol. Plant Mol. Biol. **52,** 89–118.

Mollá-Morales, A., et al. (2011). Analysis of *ven3* and *ven6* reticulate mutants reveals the importance of arginine biosynthesis in *Arabidopsis* leaf development. Plant J. **65,** 335–345.

Moubayidin, L., Di Mambro, R., and Sabatini, S. (2009). Cytokinin–auxin crosstalk. Trends Plant Sci. **14,** 557–562.

Murashige, T., and Skoog, F. (1962). A revised medium for rapid growth and bio assays with tobacco tissue cultures. Physiol. Plant. **15,** 473–497.

Mustroph, A., et al. (2009). Profiling translatomes of discrete cell populations resolves altered cellular priorities during hypoxia in *Arabidopsis*. Proc. Natl Acad. Sci. U S A. **106,** 18843–18848.

Nicotra, A.B., et al. (2011). The evolution and functional significance of leaf shape in the angiosperms. Func. Plant Biol. **38,** 535–552.

Nishinari, N., and Syono, K. (1980). Identification of cytokinins associated with mitosis in synchronously cultured tobacco cells. Plant Cell Physiol. **21,** 383–393.

Novák, O., Hauserová, E., Amakorová, P., Doležal, K., and Strnad, M. (2008). Cytokinin profiling in plant tissues using ultra-performance liquid chromatography–electrospray tandem mass spectrometry. Phytochem. **69,** 2214–2224.

Novák, O., Tarkowski, P., Tarkowska, D., Doležal, K., Lenobel, R., and Strnad, M. (2003). Quantitative analysis of cytokinins in plants by liquid chromatography-single-quadrupole mass spectrometry. Anal. Chim. Acta. **480,** 207–218.

Parry, M.A.J., Flexas, J., and Medrano, H. (2005). Prospects for crop production under drought: research priorities and future directions. Ann. Appl. Biol. **147,** 211–226.

Porra, R.J., Thompson, W.A., and Kriedemann, P.E. (1989). Determination of accurate extinction coefficients and simultaneous-equations for assaying chlorophyll a and chlorophyll b extracted with four different solvents: verification of the concentration of chlorophyll standards by atomic absorption spectroscopy. Biochim. Biophys. Acta. **975,** 384–394.

Pyke, K.A., Marrison, J.L., and Leech, R.M. (1991). Temporal and spatial development of the cells of the expanding first leaf of *Arabidopsis thaliana* (L.) heynh. J. Exp. Bot. **42,** 1407–1416.

Rédei, G.P., and Hironyo, Y. (1964). Linkage studies. Arabidopsis Information Service. **1,** 9–10.

Redig, P., Shaul, O., Inzé, D., Van Montagu, M., and Van Onckelen, H. (1996). Levels of endogenous cytokinins, indole-3-acetic acid and abscisic acid during the cell cycle of synchronized tobacco BY-2 cells. FBS Lett. **391,** 175–180.

Reinbothe, H., and Mothes, K. (1962). Urea, ureides, and guanidines in plants. Annu. Rev. Plant Biol. **13,** 129–150.

Robles, P., et al. (2010). The *RON1/FRY1/SAL1* gene is required for leaf morphogenesis and venation patterning in *Arabidopsis*. Plant Physiol. **152,** 1357–1372.

Rolland-Lagan, A.-G. (2008). Vein patterning in growing leaves: axes and polarities. Curr. Opin. Genet. Dev. **18,** 348–353.

Sakakibara, H. (2006). Cytokinins: activity, biosynthesis, and translocation. Ann. Rev. Plant Biol. **57,** 431–449.

Schmid, J., and Amrhein, N. (1995). Molecular organization of the shikimate pathway in higher plants. Phytochem. **39,** 737–749.

Schmitz, R.Y., Skoog, F., Bock, R.M., Leonard, N.J., and Hecht, S.M. (1972a). Comparison of cytokinin activities of naturally occurring ribonuclease. Phytochem. **11,** 1603–1610.

Schmitz, R.Y., Skoog, F., Playtis, A.J., and Leonard, N.J. (1972b). Cytokinins: synthesis and biological activity of geometric and position isomers of zeatin. Plant Physiol. **50,** 702–705.

Shtratnikova, V.Y., and Kulaeva, O.N. (2008). Cytokinin-Dependent Expression of the ARR5::GUS Construct during Transgenic Arabidopsis Growth. Russian Journal of Plant Physiology **55,** 756–764.

Smith, P.M.C., and Atkins, C.A. (2002). Purine biosynthesis: big in cell division, even bigger in nitrogen assimilation. Plant Physiol. **128,** 793–802.

Streatfield, S.J., et al. (1999). The *phosphoenolpyruvate/phosphate translocator* is required for phenolic metabolism, palisade cell development, and plastid-dependent nuclear gene expression. Plant Cell. **11,** 1609–1621.

Swarbreck, D., et al. (2008). The Arabidopsis Information Resource (TAIR): gene structure and function annotation. Nucl. Acids Res. **36,** D1009–D1014.

Turner, J.G., and Mitchell, R.E. (1985). Association between symptom development and inhibition of ornithine carbamoyltransferase in bean leaves treated with phaseolotoxin. Plant Physiol. **79,** 468–473.

Tzin, V., and Galili, G. (2010). New insights into the shikimate and aromatic amino acids biosynthesis pathways in plants. Mol. Plant. **3,** 956–972.

Ulmasov, T., Murfett, J., Hagen, G., and Guilfoyle, T.J. (1997). Aux/IAA proteins repress expression of reporter genes containing natural and highly active synthetic auxin response elements. Plant Cell. **9,** 1963–1971.

van der Graaff, E., et al. (2004). Molecular analysis of '*de novo*' purine biosynthesis in solanaceous species and in *Arabidopsis thaliana*. Front. Biosci. **9,** 1803–1816.

Verdoy, D., De la Peña, T.C., Redondo, F.J., Lucas, M.M., and Pueyo, J.J. (2006). Transgenic *Medicago truncatula* plants that accumulate proline display nitrogen-fixing activity with enhanced tolerance to osmotic stress. Plant Cell Environ. **29,** 1913–1923.

Voll, L.M., et al. (2003). The phenotype of the *Arabidopsis cue1* mutant is not simply caused by a general restriction of the shikimate pathway. Plant J. **36,** 301–317.

Walsh, T.A., et al. (2007). Chemical genetic identification of glutamine phosphoribosylpyrophosphate amidotransferase as the target for a novel bleaching herbicide in *Arabidopsis*. Plant Physiol. **144,** 1292–1304.

Walter, A., et al. (2007). Dynamics of seedling growth acclimation towards altered light conditions can be quantified via GROWSCREEN: a setup and procedure designed for rapid optical phenotyping of different plant species. New Phytol. **174,** 447–455.

Walter, A., Rascher, U., and Osmond, B. (2004). Transitions in photosynthetic parameters of midvein and interveinal regions of leaves and their importance during leaf growth and development. Plant Biol. **6,** 184–191.

Weber, A.P.M., Schneidereit, J., and Voll, L.M. (2004). Using mutants to probe the *in vivo* function of plastid envelope membrane metabolite transporters. J. Exp. Bot. **55,** 1231–1244.

Winter, D., Vinegar, B., Nahal, H., Ammar, R., Wilson, G.V., and Provart, N.J. (2007). An 'Electronic Fluorescent Pictograph' browser for exploring and analyzing large-scale biological data sets. PloS One. **2,** 1–12.

Zhang, K., Letham, D.S., and John, P.C.L. (1996). Cytokinin controls the cell cycle at mitosis by stimulating the tyrosine dephosphorylation and activation of $p34^{cdc2}$-like H1 histone kinase. Planta. **200,** 2–12.

Zhao, Y.D. (2010). Auxin biosynthesis and its role in plant development. In Annual Review of Plant Biology, Vol. 61, Merchant S. Briggs W.R. and Ort D., eds. (Palo Alto, California: Town), pp. 49–64.

Zrenner, R., et al. (2009). A functional analysis of the pyrimidine catabolic pathway in *Arabidopsis*. New Phytol. **183,** 117–132.

Zrenner, R., Stitt, M., Sonnewald, U., and Boldt, R. (2006). Pyrimidine and purine biosynthesis and degradation in plants. Annu. Rev. Plant Biol. **57,** 805–836.

Supplemental Data

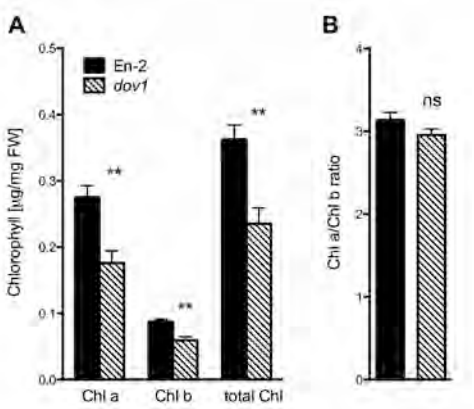

Supplemental Figure 1: Chlorophyll content of En-2 and *dov1*. n = 4. (A) Chlorophyll a and Chlorophyll b concentration (B) Chlorophyll a/b-ratio.

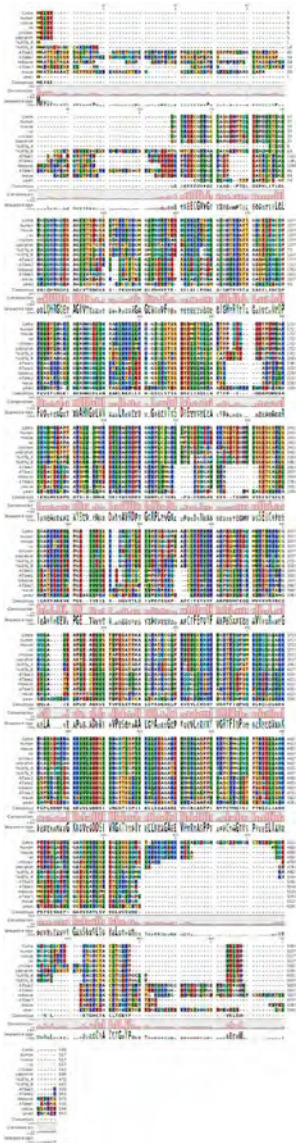

Supplemental Figure 2: Cross-taxa alignment of Atases. The last row represents to consensus sequence.

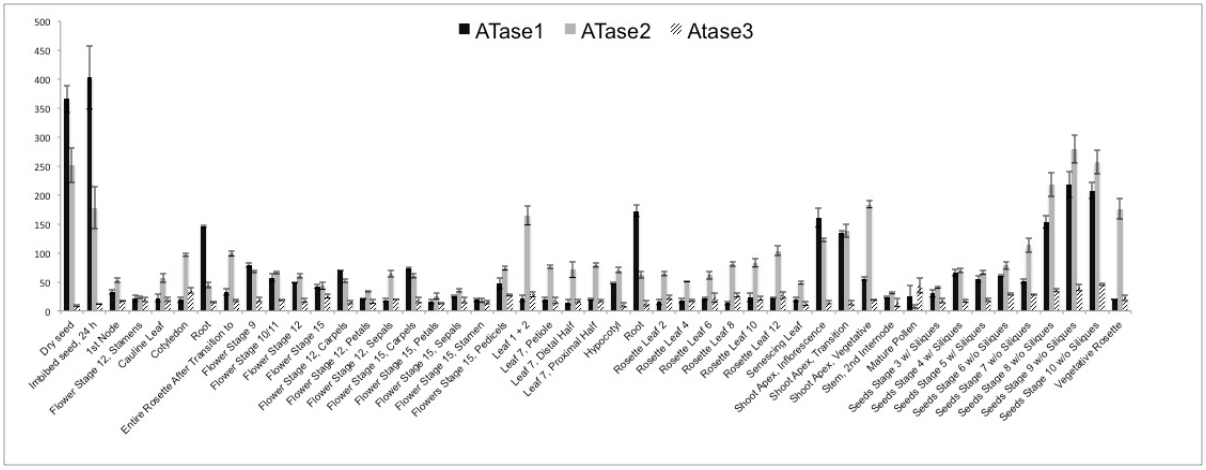

Supplemental Figure 3: Absolute values of tissue specific expression patterns of ATase1, ATase2, and ATase3. Data taken from the Arabidopsis eFP browser (Winter et al., 2007). The error bars represent S.D.

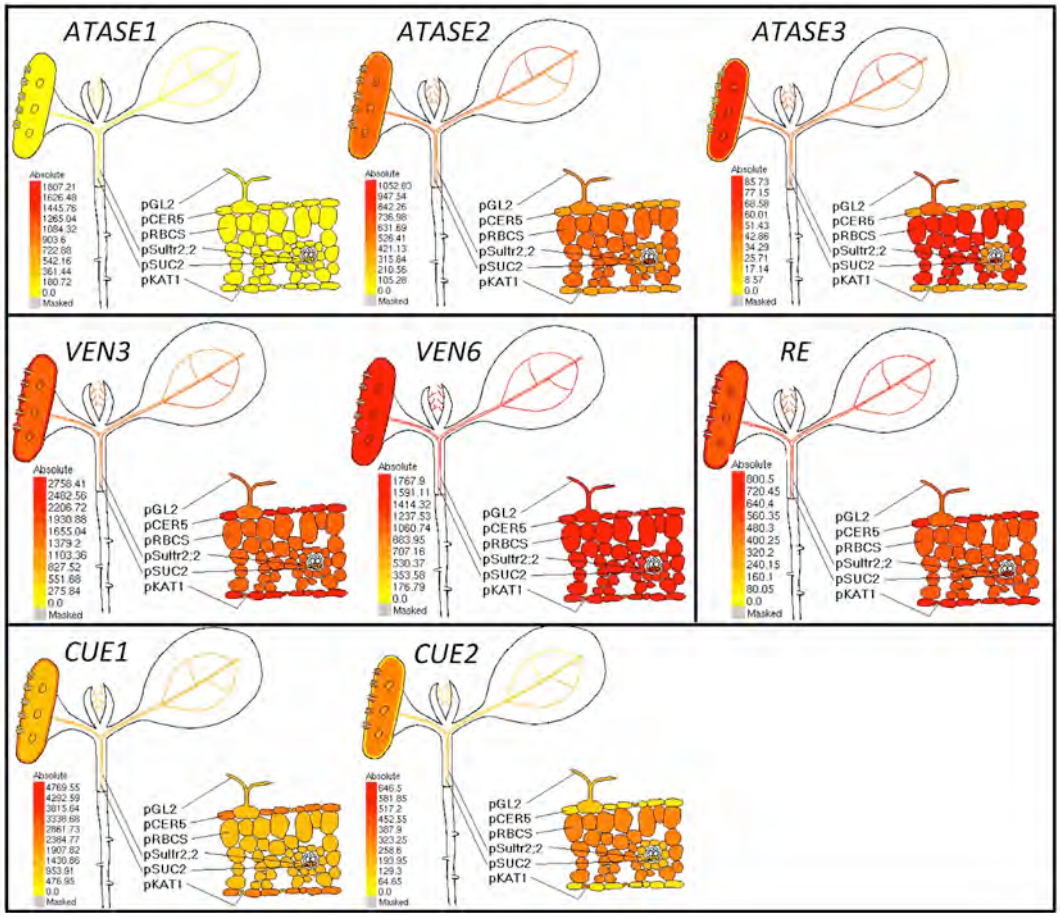

Supplemental Figure 4: Absolute values of cell type specific expression patterns of ATase1 (At2g16570), ATase2 (At4g34740), ATase3 (At4g38880), VEN3 (At1g29900), VEN6 (At3g27740), RE (At2g37860), CUE1 (At5g33320), and CUE2 (At3g01550). Data taken from the cell type specific Arabidopsis eFP browser (Mustroph et al., 2009).

Supplemental Table 1: Total leaf area and simultaneously measured F_v/F_m of En-2 and *dov1* plants. Plants were monitored for 9 days, beginning at 21 days post germination (21 d.p.g.). Errors are indicated as S.E.; n ≥ 15; N.D.: data points were not determined. p-values are shown.

	Leaf area					F_v/F_m				
	En-2		*dov1*			En-2		*dov1*		
d.p.g.	Average	± S.E	Average	± S.E	p-value	Average	± S.E	Average	± S.E	p-value
21	0.91	0.07	0.36	0.03	<0.0001	0.76	0.00	0.52	0.01	<0.0001
22	1.23	0.03	0.41	0.10	<0.0001	0.76	0.00	0.49	0.03	<0.0001
23	1.51	0.11	0.48	0.04	<0.0001	0.76	0.00	0.49	0.01	<0.0001
24	2.15	0.13	0.58	0.05	<0.0001	0.76	0.00	0.50	0.01	<0.0001
25	2.73	0.18	0.74	0.06	<0.0001	0.76	0.00	0.50	0.01	<0.0001
26	N.D.	N.D.	N.D	N.D.	N.D.	N.D.	N.D.	N.D	N.D.	N.D.
27	4.6	0.29	1.12	0.07	<0.0001	0.77	0.00	0.51	0.01	<0.0001
28	N.D.	N.D.	N.D.	N.D.	N.D.	N.D.	N.D.	N.D.	N.D.	N.D.
29	7.4	0.46	1.73	0.11	<0.0001	0.77	0.00	0.59	0.02	<0.0001

Supplemental Table 2: Relative growth rate (RGR) of plants. RGRs were calculated between two subsequent observation points. p-values are shown.

	Relative Growth Rate (RGR)				
	En-2		*dov1*		
d.p.g.	Average	± S.E.	Average	± S.E	p-value
21 to 22	38.04	9.16	17.14	2.60	0.0150
22 to 23	16.13	6.80	11.02	1.91	0.04105
23 to 24	28.80	3.64	18.44	1.59	0.0075
24 to 25	32.70	5.89	26.54	5.57	0.4632
25 to 27	25.86	0.93	18.89	0.97	< 0.0001
27 to 29	21.54	4.73	15.21	5.53	0.3948

Supplemental Table 3: Markers used for mapping of *dov1*. L.A.: Lower Arm; U.A.: Upper Arm; Chr.: Chromosome, M: Marker

Quality of PCR-products	Name of marker	Sequence of primers (5´- primer - 3´)	location	Product size [bp]	
				Col-0	En-2
no amplification of products	M1 – LUGSSLP647	CCTTTGAGAGTGAAAACTGAAACG	Chr. 1 – L.A.	128	-
		CAATTTGACCAAACTATTTATTTACACAATTA			
	M11 – CIW11	CCCCGAGTTGAGGTATT	Chr. 3 – U.A.	-	-
		GAAGAAATTCCTAAAGCATTC			
	M14 – CIW5	AGATTTACGTGGAAGCAAT	Chr. 4 – U.A.	-	-
		CACCGCCACCATACGAGCAT			
	M18 – F5O24(A)	CGCCGTTTCCGTAACAAGC	Chr.5 – U.A.	-	-
		TGACCGCCACCAGTATCGC			
suitable markers	M6 – LUGSSLP712	TTTTCAATGTTGTCTAAGGACGCT	Chr.2 – L.A.	160	160
		CAGGAACGTATAACCTGAGTATAATAAAACT			
	M7 – LUGSSLP41	TGCATCAGTTTTGGTTGTGTGATCT	Chr. 2 – U.A.	210	210
		GCTGTATTTTCCATAGGGGGCA			
	M13 – TGSSLP2	GGGAGATTAAAGAAGCCTTTGC	Chr. 4 – L.A.	1300	1300
		GTGCGGTTAACTGTTCGGTTACC			
	M15 – CER456385	CACCGCCACCATACGAGCAT	Chr. 5 – L.A.	210	210
		TTCTGGCGGAGGATACTTCTTGAA			
	M16 – LUGSSLP861	TGGTAAGCACATGCGGCGTGAT	Chr. 5 – L.A	210	210
		AGCTTTGGGTTTCTCTTAGATTTACT			
	M20 – NPR1	GTTGATGTACATAAATATATATTACAAATC	Chr. 20 – L.A.	600	600
		CCGGGTGTAAAGATAGCACCTT			
	M21 – on BAC F4C21	TGACGATGGAGATTGCTCTG	Chr. 4 – U.A.	379	379
		AGTGGCTCATCGTTCGAGAT			
	M22 – on BAC F7D11	TTGGAGAACTATACCGCATCG	Chr. 2 – U.A.	393	393
		GCACAAAATAGTTTTATTCTGATTGG			
	M23 – on BAC F4C21	TGACGATGGAGATTGCTCTG	Chr. 4 – U.A.	379	379
		AGTGGCTCATCGTTCGAGAT			
	M24 – on BAC T5L23	CGTCACAAAGCTGCCTACAA	Chr. 4 – U.A:	396	396
		CATCGGGTTTAATTGGTTGG			
	M25 – on BAC F24B18	TTCAGGATTTCGAGGTAGCC	Chr. 5 – L.A.	215	215
		AGCAGACAGCTGCAATTTCC			
	M26 – on BAC MYN8	GGATTTTCCTTGCAAGTCGT	Chr. 5 – L.A.	240	240
		TGAAATTTGCAAGGTGTTTCT			
	M27 – on BAC F15A18	CGAAACTGGTTCGGTCTTTC	Chr. 5 – U.A.	184	184
		CGCTTGAAGGTGAGGAAGAA			
	M30 – CIW5	GGTTAAAAATTAGGGTTACGA	Chr. 4 – U.A.	164	-
		AGATTTACGTGGAAGCAAT			
	M31 – JV30/31	CATTAAAATCACCGCCAAAAA	Chr. 4 – U.A.	194	-
		TTTTGTTACATCGAACCACACA			
	M35 – CIW15	TCCAAAGCTAAATCGCTAT	Chr. 5 – U.A.	177	177
		CTCCGTCTATTCAAGATGC			
	M2 – NGA280	GGCTCCATAAAAAGTGCACC	Chr. 1 – L.A.	110	90
		CTGATCTCACGGACAATAGTGC			
	M3 – F22O13A	GCCGGCCGCTCCTCCAT	Chr.1 – U.A.	>300	210
		GCGTTCCCAAATTGTTATCTCCAT			
	M4 – LUGSSLP809	TGTGTCGTCCATGCTTCACTCT	Chr.1 – U.A.	130	135
		CCGAGGAATGAATTTATTTATGGTACTT			
	M5 – NGA168	GAGGACATGTATAGGAGCCTCG	Chr.2 – L.A.	160	140
		TCGTCTACTGCACTGCCG			
	M8- CIW21	TGATTTTGAAGAGTTGAAACC	Chr.3 – L.A.	220	>300
		TTGAGCAAAGACACTACTGAA			
	M9- T16K5-TGF	TTGTCGAAATAAAAATTGACCGTTA	Chr.3 – L.A.	190	150
		TGGATGTGGATTCTATTGTTTCTCA			
	M10 – NGA162	CTCTGTCACTCTTTTCCTCTGG	Chr.3 – U.A.	110	90
		CATGCAATTTGCATCTGAGG			
	M12 – LUGSSLP841	TGATTAAGGATTCTAACTACATTGGGA	Chr. 4 – L.A.	210	160
		GGCTCATCTTGATTATATCTACACACATAAG			
	M17 – CIW14	CATGATCCATCGTCTTAGT	Chr. 5 – U.A.	190	180
		AATATCGCTTGTTTTTGC			
	M19 – LT5	AGATGCAACAATAAGATGTTGAGG	Chr. 4 – L.A.	550	500
		GAGATCTGCGATGGTGAAATTG			
	M28 – CIW2	CCCAAAAGTTAATTATACTGT	Chr. 2 – U.A.	105	90
		CCGGGTTAATAATAAATGT			
	M29	GCACATACCCACAACCAGAA	Chr. 2 – U.A.	213	smaller
		CCTTCACATCCAAAACCCAC			
	M32 – CIW9	CAGACGTATCAAATGACAAATG	Chr. 5 – L.A.	165	145
		GACTACTGCTCAAACTATTCGG			
	M33 – CIW10	CCACATTTTCCTTCTTTCATA	Chr. 5 – L.A.	140	larger
		CAACATTTAGCAAATCAACTT			
	M34 – U.A.	CAGTCTAAAAGCGAGAGTATGATG	Chr. 5 – U.A.	150	120
		GTTTTGGGAAGTTTTGCTGG			
	M45	CGACGAATCGACAGAATTAGG		150	140
		GCGAAAAAACAAAAAAATCCA			
	M47	TTAAAAGACAAACACTGCACGA			
		CCGGTCGATCTGGTTAGAG			

Supplemental Table 4: Relative steady state metabolite levels of seven week old rosettes of En-2 and *dov1* before budding and flowering. Plants were grown under 12h/12h light/dark cycle at 100 $\mu E/m^2/s$. Samples were taken in the middle of the light period. S.E. is shown. n (En-2) = 8, n (*dov1*) = 7. p-values are shown. Asterisks (*) indicate the significance level.

Metabolite	En-2		*dov1*		p-value	Significance level
	Average	± S.E.	Average	± S.E.		
α-Alanine	9.977	0.448	25.234	6.392	0.0239	*
Leucine	0.398	0.082	0.849	0.416	0.2764	ns
Valine	1.022	0.159	1.890	0.572	0.1225	ns
Glutamate	13.753	2.980	34.508	11.820	0.0930	ns
Proline	0.775	0.175	8.885	1.515	<0.0001	***
Aspartate	5.861	0.479	24.010	8.747	0.0443	*
Asparagine	2.568	0.362	54.813	21.260	0.0203	*
Isoleucine	0.505	0.127	0.865	0.333	0.3066	ns
Lysine	0.107	0.026	0.735	0.266	0.0256	*
Methionine	0.154	0.066	0.486	0.208	0.1319	ns
Phenylalanine	0.465	0.085	0.901	0.381	0.2861	ns
Glycine	3.128	0.546	7.323	1.840	0.0373	*
Serine	12.835	1.909	34.560	11.45	0.0666	ns
β-Alanine	0.049	0.017	0.076	0.018	0.3104	ns
Ornithine	0.055	0.011	0.951	0.355	0.0179	*
(Iso)-Citric Acid	14.164	1.539	42.364	16.120	0.0843	ns
Shikimate	0.941	0.300	1.080	0.310	0.7535	ns
Glucose	3.993	0.715	9.379	2.808	0.0695	ns
Fructose	1.230	0.260	3.247	1.545	0.1915	ns
Mannose	0.068	0.044	0.025	0.013	0.3847	ns
Xylose	0.108	0.041	0.063	0.039	0.4410	ns
Sorbitole	0.447	0.196	0.597	0.478	0.7543	ns
Myoinositol	12.448	0.733	12.790	4.063	0.9315	ns
Maltose	0.584	0.161	0.376	0.107	0.3167	ns
Sucrose	76.534	1.923	159.660	43.530	0.0611	ns
Raffinose	0.484	0.126	1.706	0.865	0.1582	ns
Lactate	2.903	0.6397	8.564	3.675	0.1285	ns
Succinic Acid	0.724	0.074	0.724	0.232	0.9973	ns
Fumaric Acid	26.672	3.566	24.753	10.470	0.8574	ns
Glycerole	1.978	0.318	4.167	1.180	0.0788	ns
Glyceric Acid	1.375	0.189	2.228	0.666	0.2134	ns
Glycolic acid	1.050	0.286	1.437	0.433	0.4606	ns
Maleic Acid	0.473	0.039	0.857	0.2496	0.1478	ns
Malic Acid	12.085	0.435	28.997	8.834	0.0606	ns
Malonic acid	0.004	0.002	0.004	0.002	0.9738	ns
Gluconic Acid	0.113	0.037	0.098	0.044	0.7963	ns
Oxalate	3.923	0.627	9.662	3.926	0.1463	ns
GABA	0.075	0.024	0.033	0.009	0.1390	ns
Hydroxybutyric Acid	0.255	0.139	0.131	0.04399	0.4382	ns
Phosphoric Acid	0.376	0.041	4.915	1.880	0.0222	*

Supplemental Table 5: Steady state cytokinin contents of seven week old rosettes of En-2 and *dov1* before flowering. Plants were grown under 12h/12h light/dark cycle at 100 µE/m^2/s. Samples were taken in the middle of the light period. S.E. is shown. n (En-2) = 5, n (*dov1*) = 5. Abbreviations used can be found in (Novak et al., 2008). tZ = *trans*-zeatin; cZ: *cis*-zeatin; iP: N_6-(Δ^2-isopently)adenine; DHZ: dihydrozeatin; R: riboside; OG: *O*-glucoside; 7G: 7-glucoside; 9G: 9-glucoside; 5`MP: 5`-monophosphate

Cytokinin	En-2 [pmol/g]		*dov1* [pmol/g]		p-value	Significance level
	Average	± S.E.	Average	± S.E.		
tZ	1.62	0.08	4.65	0.60	0.001	**
tZOG	1.07	0.08	0.98	0.01	0.52	ns
tZR	0.72	0.08	1.22	0.09	0.0033	**
tZROG	0.90	0.12	1.27	0.07	0.0308	*
tZ7G	221.53	18.62	143.32	8.88	0.0053	**
tZ9G	25.20	0.47	15.38	0.94	<0.0001	ns
tZR5`MP	4.63	0.70	1.99	0.25	0.0066	**
Total *trans* cytokinins	255.67	18.90	168.81	9.82	0.0035	**
cZ	0.23	0.03	0.24	0.03	0.8122	ns
cZOG	0.27	0.02	0.26	0.02	0.7215	ns
cZR	0.05	0.01	0.06	0.01	0.2687	ns
cZROG	0.88	0.07	1.56	0.07	0.0001	*
cZ9G	0.13	0.01	0.12	0.02	0.7983	ns
cZR5`MP	0.86	0.06	0.52	0.05	0.0027	**
Total *cis* cytokinins	2.42	0.08	2.76	0.14	0.0759	*
DHZ7G	15.80	2.48	14.11	1.48	0.5752	ns
DHZ9G	0.13	0.02	0.19	0.03	0.1148	ns
Total dehydro cytokinins	15.93	2.48	14.30	1.50	0.5914	ns
iP	0.11	0.01	0.08	0.08	0.0841	ns
iPR	0.11	0.02	0.21	0.03	0.0182	*
iP7G	57.42	6.53	71.02	4.47	0.1237	ns
iP9G	0.92	0.05	1.30	0.07	0.0026	**
iPR5`MP	5.05	0.16	4.96	0.40	0.8380	ns
Total isopentyl cytokinins	63.61	6.52	77.57	4.70	0.1213	ns
Total cytokinins	337.63	26.01	263.44	14.00	0.0363	*

The authors`contributions to Manuscript 2

C.R. wrote the manuscript, established plant growth rates and photosynthetic capacity (Figure 1) in cooperation with **M.M**. **C.R.** performed auxin- and cytokinin-response assays (Figure 3). Polar metabolite analysis was done in cooperation with **K.K.** (Figure 6). Cytokinin determination was done by **C.R.** in cooperation with **O.N.** and **M.S.** (Figure 7). Cytokinin plate assays (Figure 7) and chlorophyll determination was done by **C.R.** Bioinformatical studies (Supplemental Figure 2, 3, and 4) was accomplished by **C.R**, for Supplemental Figure 2 together with **Simon Schliesky**.

K.K. performed map-based cloning together with **A.M.N.** (Figure 2) and enzyme activity tests in cooperation with **A.B.** (Figure 5).

A.M.N. performed map-based cloning together with **K.K.** (Figure 2)

M.M. determined plant growth rates and photosynthetic capacity (Figure 1) in cooperation with **C.R.**

A.B. performed enzyme activity tests in cooperation with **K.K.** (Figure 5)

O.N. performed cytokinin determination in cooperation with **C.R.** (Figure 7)

A.B. and **A.P.M.W.** participated in drafting of the manuscript.

Manuscript 2 was published in *Molecular Plant* (impact factor 5.546).

VI.
Manuscript 3

Reticulata, a supply mutant
affected in
amino acid homeostasis

Reticulata, a supply mutant affected in amino acid homeostasis

Christian Rosar[a], Pia Stähr[b], Jessica Schmitz[b], Michael Mielewczik[c], Andrea Bräutigam[a], Ondřej Novák[d], Miroslav Strnad[d], Achim Walter[c], Rainer Häusler[c], Ulf-Ingo Flügge[b], Andreas P. M. Weber [a,e]

a Institute for Plant Biochemistry and Cluster of Excellence on Plant Sciences (CEPLAS), Heinrich-Heine-Universität, Universitätsstraße 1, D-40225 Düsseldorf

b Botanical Institute, Biocenter Cologne, University of Cologne, Zülpicher Straße 47b, D-50674 Köln

c Institute of Agricultural Sciences, Universitätstrasse 2, ETH Zürich, CH-8092 Zürich

d Laboratory of Growth Regulators, Palacky University and Institute of Experimental Botany AS CR, Slechtitelu 11, CZ-78371 Olomouc

e to whom the correspondence should be addressed. Email: aweber@uni-duesseldorf.de; fax: +49-211-8113706; phone: +49-211-8112347

Abstract

A series of reticulated mutants with green veins on a pale leaf lamina has been described. These mutants are disturbed in mesophyll (M) architecture and are models for investigating leaf development. All but one of these mutants is deregulated in amino acid metabolism and two mutants showed altered phytohormone patterns. The hallmark mutant *cue1* is defective in the plastidic import of phospho*enol*pyruvate (PEP), a substrate for aromatic amino acids. *Cue1* is discussed as being defective either in the supply with aromatic amino acids or metabolic signals that mediate M development. These alternatives gave rise to the *supply* and the *signaling hypotheses*, respectively. A second mutant, *re*, has been known for more than fifty years but the function of it`s gene products remains elusive. In this study, we compare *re* and *cue1* with regard to both hypotheses. Transcriptional profiling, phytohormone determination and activity tests reinforced the hypothesis that *cue1* is more likely defective in signaling events because phytohormone genes and levels are deregulated. *Re*, however, shows a balanced homeostasis on the transcriptional level and on the phytohormone level. Metabolite analysis revealed that *re* is severely affected in amino acid homeostasis and lysine (lys) feeding reverted the phenotype. This indicates, that *re* is probably not due to signaling events, rendering a supply phenotype at least more likely. A role of amino acids as being essential in M development is discussed.

Key words

leaf development, reticulated mutants, phytohormones, growth kinetics and patterns, amino acid, and purine metabolism

Introduction

The development and growth of the leaf is dependent upon a complex interplay of various metabolic and signaling processes integrating external and internal stimuli (Byrne, 2005; Tsukaya, 2006; Tsukaya, 2008; Byrne, 2012). Amino acids, plant hormones and other molecules are involved in determining leaf size, shape and architecture (Bartlem et al., 2000; Mattsson et al., 2003; Ruuhola et al., 2003; Dimitrov and Zucker, 2006; De Smet and Jürgens, 2007; Muralla et al., 2007; Jing et al., 2009). Leaf development depends on processes governing overall leaf shape and processes establishing the inner leaf architecture (Rosar et al., 2012). Leaf reticulate mutants belong to the latter group, because they have less and/or smaller mesophyll (M) cells but an intact vasculature and bundle sheath (BS) (Kinsman and Pyke, 1998; Streatfield et al., 1999; González-Bayón et al., 2006; Jing et al., 2009; Rosar et al., 2012).

Various reticulated mutants have been described: *reticulata* (*re*) (Rédei and Hironyo, 1964; González-Bayón et al., 2006), *chlorophyll a/b binding protein (CAB) gene underexpressed1* (*cue1*) (Li et al., 1995; Streatfield et al., 1999; Voll et al., 2003)*, venosa 3* and *6* (Mollá-Morales et al., 2011), *tryptophan2* (*trp2*) (Last et al., 1991; Barczak et al., 1995; Jing et al., 2009), *NADPH-thioredoxin reductase* (*ntrc*) (Lepistö et al., 2009)*, and differential development of vasculature associated cells1* (*dov1*) (Kinsman and Pyke, 1998).

While *cue1*, *ven3*, *ven6, trp2* are defective in plastid amino acid biosynthesis, *dov1* (*differential development of vasculature associated cells1*) is disturbed in the *de novo* purine biosynthesis and is affected in phytohormone levels and responses (Rosar et al., 2012). *Cue1* is deficient in the plastidic import of phosphoenolpyruvate (PEP) (Streatfield et al., 1999), a precursor of aromatic amino acid biosynthesis in the shikimic acid pathway (Schmid and Amrhein, 1995; Fischer et al., 1997; Knappe et al., 2003; Voll et al., 2003; Tzin and Galili, 2010). *Cue1*, with high aromatic amino acid level on a relative scale (Streatfield et al., 1999), has a massively decreased phenylalanine concentration (Voll et al., 2003). Secondary phenylpropanoid compounds such as flavonoids, anthocyanins, hydroxycinnamic acids and simple phenolics are decreased (Streatfield et al., 1999; Voll et al., 2003). The *cue1* phenotype was reverted by application of all three aromatic amino acids at once (Streatfield et al., 1999). The authors concluded that the *cue1* phenotype is due to a limited supply with aromatic amino acids or thereof derived metabolites (Streatfield et al., 1999; Voll et al., 2003). They further hypothesized, that a chloroplast-derived signal, that is dependent on

PEP or it`s derived products, causes M differentiation and, if disrupted, leads to the reticulated phenotype (Streatfield et al., 1999). The signal could be generated in the BS/vein, since this tissue is well differentiated, and CUE1 likely exerts it`s function along the veins (Streatfield et al., 1999; Knappe et al., 2003; Rosar et al., 2012). This interpretation represents the *signaling hypothesis* of reticulation. *Ven3* and *ven6*, defective in the small and large carbamoylphosphate synthase subunit, respectively, are hampered in arginine (arg) biosynthesis (Mollá-Morales et al., 2011). Feeding of citrulline and arg reverted the phenotype (Mollá-Morales et al., 2011). The authors concluded that the supply of amino acids limits M development, and causes a growth retardation and leaf reticulation. This interpretation represents the *supply hypothesis*. *Trp2*, deficient in plastidic tryptophan (trp) synthesis, has reduced trp levels (Barczak et al., 1995; Radwanski et al., 1996; Ouyang et al., 2000; Jing et al., 2009). Trp supplementation rescued the phenotype resulting in normal M development, making the authors argue that the lack of trp is responsible for the phenotype (Jing et al., 2009). Much like *cue1*, *trp2*, *ven3* and *ven6*, *ntrc* is debalanced in amino acid metabolism. *Ntrc* is defective in the plastidic NADPH-thioredoxin reductase, a redox-active thioredoxin, regulating amongst others the shikimate pathway, enzymes of the aromatic amino acid biosynthesis and the trp synthase (Serrato et al., 2004; Lepistö et al., 2009). In *ntrc* plants the aromatic amino acid pool is increased and feeding of aromatic amino acids restores the phenotype (Lepistö et al., 2009). Auxin and cytokinin levels are decreased in *ntrc* (Lepistö et al., 2009), while auxin levels are increased in *trp2* (Jing et al., 2009).

Re, first described more than fifty years ago (Rédei and Hironyo, 1964), has been used as a morphological marker (González-Bayón et al., 2006). Nine alleles of *re* are known: *re-1* to *re-7* (González-Bayón et al., 2006), *re-8* (Overmyer et al., 2008) and *lower cell density1-1* (*lcd1-1*) (Barth and Conklin, 2003; González-Bayón et al., 2006). Although molecularly cloned (González-Bayón et al., 2006), the function of the protein has not been established. *Re* mutants were studied with regard to their morphology, photosynthetic performance and ROS-signaling (Barth and Conklin, 2003; González-Bayón et al., 2006; Overmyer et al., 2008). While the number of spongy and particularly palisade M cells is reduced without significant loss of cell size, vasculature and the BS is fully developed (González-Bayón et al., 2006). The number of chloroplasts per M cell and plastid morphology is not affected (Barth and Conklin, 2003; González-Bayón et al., 2006). The phenotype is restricted to cotyledons and leaves (Barth and Conklin, 2003; González-Bayón et al., 2006).

Taken together, *cue1*, *trp2*, *ven3*, *ven6*, and *ntrc* show a deregulated amino acid metabolism. Furthermore, *dov1*, *ntrc* and *trp2* are affected in phytohormone levels (Jing et al., 2009; Lepistö et al., 2009; Rosar et al., 2012). In this study, we compare *re* and *cue1* in order to shed light on the *supply* and *signaling hypothesis*.

Results

Genetic complementation of *re*, phylogeny, and plastid localization of RE

Although the defective gene was cloned (González-Bayón et al., 2006), *re* has not been genetically complemented with the wild-type gene. Complementation is important because the gene is present in two splice isoforms (Swarbreck et al. 2009; Supplemental Figure 1). The fifth exon contains a facultative STOP codon at it`s end, giving rise to two alternative proteins: RE_{long} (423 amino acids (AAs)) and RE_{short} (347 AAs) including the chloroplast transit peptide (cTP). RE_{long} is predicted to have two to six, and RE_{short} two to four transmembrane (TM) helices, depending on the algorithms (http://aramemnon.uni-koeln.de; Schwacke et al., 2003). The cTP is predicted to consist of 47 AAs (Chloro P1.1; (Emanuelsson et al., 2000).

PCR analysis showed that both splice isoforms are found *in planta* (Supplemental Figure 1 B, C). Thus, to assess which of the these is of functional relevance, *re-6* was transformed by stably introducing RE-gDNA (35S::RE), and the cDNA based constructs 35S::RE_{long} and 35S::RE_{short}, each under the control of the 35S promoter. While 35S::RE and 35S::RE_{long} complemented the mutant to be visually indistinguishable from wild-type, *re-6* was transformed with 35S::RE_{short} remained reticulated (Figure 1). Expressing RE_{long} without the predicted cTP (35S::$RE_{long, \Delta cTP}$) in *re-6* did not revert the phenotype (data not shown), indicating that the cTP is essential for RE`s function. RE overexpressor lines in the col-0 background (35S::RE; OX) showed wild-type like appearance (Figure 1) and contained higher transcript levels than wild-type (Supplemental Figure 2).

RE is specific to the green lineage of plants (González-Bayón et al., 2006) and belongs to a family in *Arabidopsis* with seven additional members (Supplemental Figure 3, Supplemental Table 1), all containing the domain of unknown function (DUF) 3411. Phylogenetic analysis demonstrates that the RE family of proteins is divided into three branches. Dicots, monocots and one green alga have family members on all three branches, while moss and fern species have members on only two branches.

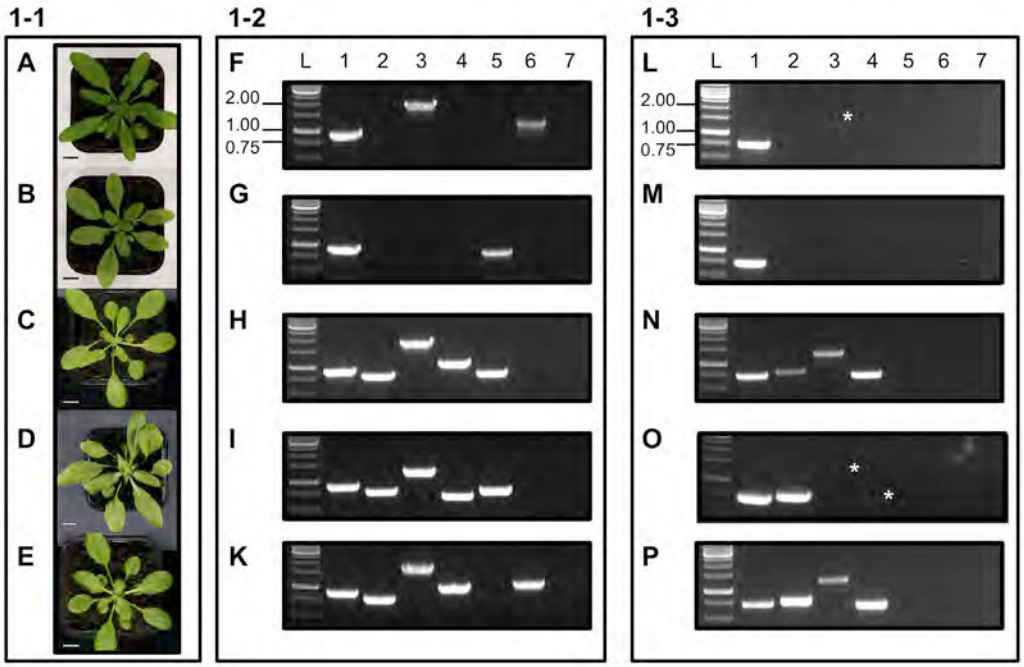

Figure 1: Wild-type, *re-6,* transformed plants and genotyping. **Figure 1-1 (A-E)**. Rosettes of col-0*, re-6*, transformed *re-6* and OX-plants. Plants are eight weeks old. Scale bar indicates 1.0 cm. **(A)** col-0. **(B)** *re-6.* **(C)** *re-6* with 35S::RE. **(D)** *re-6* with 35S::RE_{long}. **(E)** col-0 with 35S::RE (OX). **Figure 1-2 (G-M)**. PCR-confirmation of complemented *re-6* and overexpressor col-0 pants. PCRs were performed on gDNA. **(F)** col-0. **(G)** *re-6*. **(H)** *re-6* with 35S::RE. **(I)** *re-6* with 35S::RE_{long}. **(K)** col-0 with 35S::RE (OX). **Figure 1-3 (L-P)**. PCR-confirmation of genetically complemented *re-6* and overexpressor col-0 pants. PCRs were performed on cDNA. **(L)** col-0. **(M)** *re-6*. **(N)** *re-6* with 35S::RE. **(O)** *re-6* with 35S::RE_{long}. **(P)** col-0 with 35S::RE (OX). Asterisks indicate band. L: DNA ladder in kbp; 1: Actin control (CR39/CR40). 2: Hygromycin control (CR 43/CR37). 3: RE (Start to STOP, CR 161/162). 4: 5^{th} exon to NOS-terminator in pmDC32 vector (CR48/CR49). 5: T-DNA insertion of *re-6* (CR53/CR52). 6: col-0 background (CR51/CR52). 7: non binding primers (CR51/CR53).

RE was proposed to be plastid localized as it`s sequence contains a putative cTP (González-Bayón et al., 2006). RE was found in the plastid envelope fraction in proteomic analyses (Zybailov et al., 2008; Bräutigam and Weber, 2009; Ferro et al., 2010), but this to date has not been verified *in planta*. Hence, we transiently expressed *RE* (35S::*RE*::GFP) and RE_{long} (35S::RE_{long}::GFP), each C-terminally fused to GFP, in tobacco, confirming localization to the plastid envelope (Figure 2). The cTP fused to a GFP under control of the 35S-promoter (35S::TP_{RE}::GFP), localized to the plastid envelope. When the cTP was omitted, the GFP-tagged protein (ub10:: Δ cTP::RE) showed a cytosolic and the empty vector control (ub10::GFP) an accumulation of the GFP-protein within the epidermal cytoplasma (Figure 2).

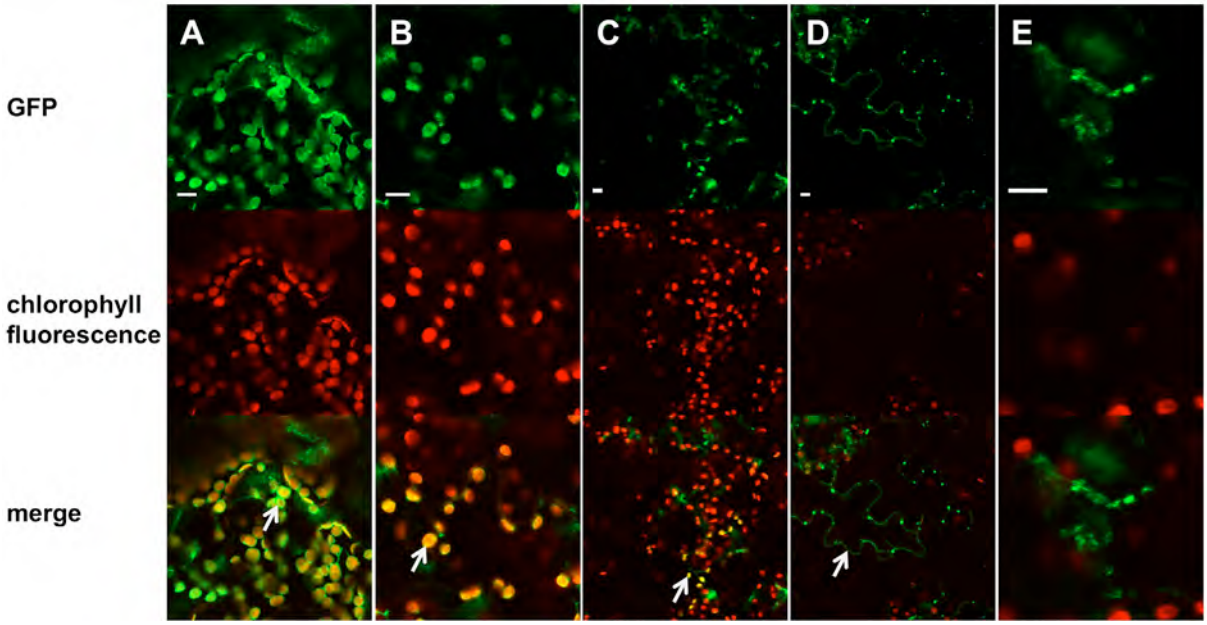

Figure 2. Transiently expressed RE-protein in tobacco localized to the chloroplast envelope of M cells. GFP-fluorescence, chlorophyll autofluorescence, and the merge is shown in the upper, middle and lower panels, respectively. **(A)** UB10::RE::GFP, **(B)** UB10::RE_{long}::GFP, and **(C)** 35S::cTP::GFP localize to the chloroplast envelope. **(D)** UB10::$RE_{\Delta cTP}$::GFP localizes to the cytosol. **(E)** The empty vector control (UB10::GFP) shows clumpy GFP accumulation. Scale bar: 10 µm. Arrow heads indicate plastidic **(A-D)** and cytosolic localization **(E)**.

Plant growth rates and photosynthetic performance

Leaves of *cue1* and *re* are decreased in leaf area compared to wild-type, with *re* being slightly (González-Bayón et al., 2006) and *cue1* being much smaller (Li et al., 1995). The penetrance of the *cue1* and *re* leaf phenotype is dependent on growth and light conditions (Streatfield et al., 1999; González-Bayón et al., 2006). While *lcd1* was not affected in photosynthetic performance (Barth and Conklin, 2003), *cue1*, was severely lowered in photosystem II (PSII) capacity (Streatfield et al., 1999; this study). To investigate the growth dynamics and photosynthetic performance, plant rosettes were investigated by simultaneous non-destructive growth and photosynthetic performance measurements under controlled conditions for ten days. Photosynthetic capacity was determined as the ratio of variable fluorescence to maximum fluorescence (F_v/F_m), reflecting PSII activity. To assess whether a change was obtained from data point to data point, the relative growth rate (RGR) was determined (Hoffmann and Poorter, 2002; Jansen et al., 2009). We started at the earliest day possible, i.e. 21 days post germination (dpg), due to resolution constraints regarding the very small size of *cue1* plants (Figure 3A, Supplemental Table 2). Along the observation period, col-0 increased most in total leaf area, followed by *re-6*, which was significantly smaller than col-0, except to 21 dpg. *Cue1* was already smaller than col-0 at 21 dpg and stayed much smaller than col-0 and *re-6* over the whole observation period. The *cue1* leaf area increased by the factor 2.9 from 21 dpg to 30 dpg. In the same time period the col-0 and *re-6* leaf area

increased 13.07 and 11.89 times, respectively (Figure 3A, Supplemental Table 2). At the first observation points the difference in leaf area of *re-6* and col-0 was not as big as at the end of the monitoring period. While the RGR of *re-6* significantly exceeded that of col-0 at three observation points, i.e. from 22 to 23 dpg, from 24 to 25 dpg, and from 27 to 28 dpg the RGR of *cue1* was at wild-type level at all time points (Figure 3B, Supplemental Table 3).

F_v/F_m of col-0 and *re-6* stayed at a constant level of about 0.78 over the whole observation period (Figure 3C, Supplemental Table 4), with *re-6* slightly exceeding col-0 at the first four time points. The photosynthetic capacity of *cue1* was decreased during the recording period and stayed at a fairly constant level around 0.65, thus was decreased by ca. 17% compared to wild-type.

Neither did the photosynthetic performance of *re-6* nor *cue1* vary over time nor with plant age. Within a rosette, all *re-6* leaves had a potential photosynthetic performance across different leaf ages of the plant rosette comparable to wild-type as indicated by the close to red color of the F_v/F_m false color image (Figure 3D). All leaves were reticulated at approximately the same level. The lowered chlorophyll amounts in *re-6* were not reflected in the photosynthetic capacity (Figure 10). The ratios of Chl a to Chl b in *re-6* and *cue1* were at wild-type level (Supplemental Figure 4), indicating that the stoichiometry of PSII to PSI was not altered (Ort, 1986).

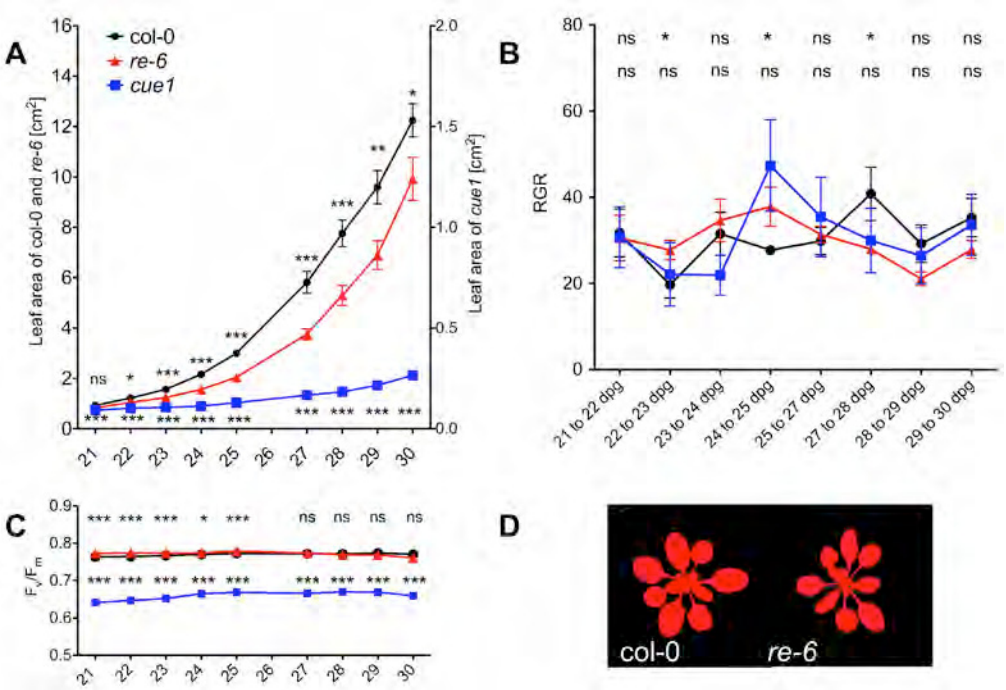

Figure 3: Growth kinetics and photosynthetic activity of col-0, *re-6* and *cue1* plants. **(A)** Total leaf area of col-0, *re-6* and *cue1* plants from 21 to 30 days post germination (dpg). **(B)** Relative growth rate (RGR) along 10 days of observation. RGR refers to two subsequent monitoring points. Upper row shows significance levels between col-0 and *re-6*, lower row between col-0 and *cue1*. **(C)** Photosynthetic capacity indicated by F_v/F_m from 21 to 30 dpg. **(D)** False color image of col-0, and *re-6* rosettes displaying F_v/F_m ratios. Plants shown are representative for plants of 30 dpg. (n > 15). Error bars represent S.E. Asterisks indicate significance levels.

DISP analysis – diel growth patterns in *re-6* are wild-type like

The penetrance of the *re* phenotype is dependent on the photoperiod and light-intensity (Overmyer et al., 2008; own observation). While the *re-8* allele was reticulated under standard conditions (12-h light/12-h dark), it was indistinguishable from wild-type under 8-h light/16-h dark cycle (Overmyer et al., 2008). To test if (i) the photoperiod influences the leaf growth pattern of *re-6* and if (ii) the observed delay in the growth of *re-6* was caused at certain time points within the photoperiod, diel growth patterns for *re-6* were determined under two different light regimes. The *cue1* mutant was too small to attach threads on the leaf surface, which is necessary to perform DISP analysis (Wiese et al., 2007). We used white light and red light since light qualities were linked to signaling processes for example in the reticulated mutant *ntrc* (Lepistö et al., 2009; Lepistö and Rintamäki, 2012). No difference between the diel growth pattern of col-0 and *re-6* was detected (Figure 4), indicating that the photoperiod and light quality does affect the growth pattern of *re-6*.

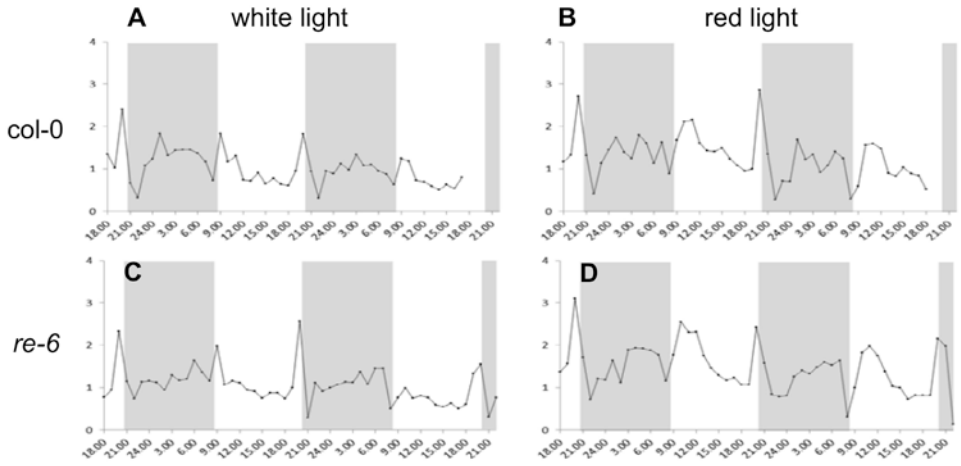

Figure 4. Relative diel growth patterns of col-0 **(A, B)** and *re-6* **(C, D)** during 12-h light/12-h dark cycle. Plants were grown in white **(A, C)** and red light **(B, D)**. Grey areas indicate night, white areas day.

Comparative transcript profiling of *re* and *cue1*

Reticulated mutants are discussed in the context of supply or signaling events (Streatfield et al., 1999; Rosar et al., 2012). Signaling in plants is attributed to phytohormones (Rubio et al., 2009; Santner and Estelle, 2009), nucleotides (Jeter et al., 2004; Chivasa and Slabas, 2012; Sun et al., 2012), carbohydrates (Eveland and Jackson, 2012), ROS (Streatfield et al., 1999; Overmyer et al., 2008; Kangasjärvi et al., 2009; Lepistö et al., 2009) and other molecules (Rubio et al., 2009). Reticulated mutants are deregulated in amino acid biosynthesis (Streatfield et al., 1999; Jing et al., 2009; Lepistö et al., 2009; Mollá-Morales et al., 2011). Thus, to decipher potential players of signaling or supply events, we carried out comparative transcript profiling of *lcd1*, *cue1* and col-0 of four-week old aerial parts.

Cue1 deviated in nine metabolic categories from wild-type, while *lcd1* was different in three groups (Figure 5A, 5C, Supplemental Data 1). Three cellular processes in *cue1* are overrepresented in upregulated genes: (i) cellular processes/RNA, (ii) nucleotide synthesis, and (iii) cytosolic ribosomes (Figure 5A, 5C). Category (i) includes all metabolic processes that are needed to synthesize RNAs of all kinds. Four processes are overrepresented in downregulated genes: (i) cell wall/cell wall proteins and the three photosynthetic categories (ii) photosynthesis/PSII, (iii) photosynthesis/cyclic electron flow and (iv) central carbon metabolism/Calvin Cycle. While one category, heat shock/protein folding was overrepresented in upregulated genes, the category protein degradation/ubiquitin was underrepresented in down-regulated genes (Figure 5A).

While genes regulated by zeatin and ethylene (ACC is an ethylene precursor) did not show a response in *cue1*, genes regulated by auxin, methyljasmonate and abscisic acid (ABA) displayed deviating response patterns in *cue1* compared to wild-type (Figure 5B). Genes controlled by auxin were massively downregulated in *cue1* plants.

In *lcd1*, two groups of overrepresented, upregulated genes were detected: (i) regulation/calcium and (ii) regulation kinase/phosphatase (Figure 5C). The category (iii) cellular processes/RNA was underrepresented in upregulated genes. All other remaining groups stayed at the wild-type levels, indicating that *lcd1* keeps the homeostasis at a stable level. While auxin responsive genes were overrepresented by up- and downregulation in *lcd1*, zeatin responsive genes were not changed in the transcriptional level (Figure 5D). Like in *cue1*, genes affected by methlyjasmonate and ABA were deregulated in *lcd1* (Figure 5D). *Re-8* is depressed in jasmonate-responsive gene expression (Overmyer et al., 2008).

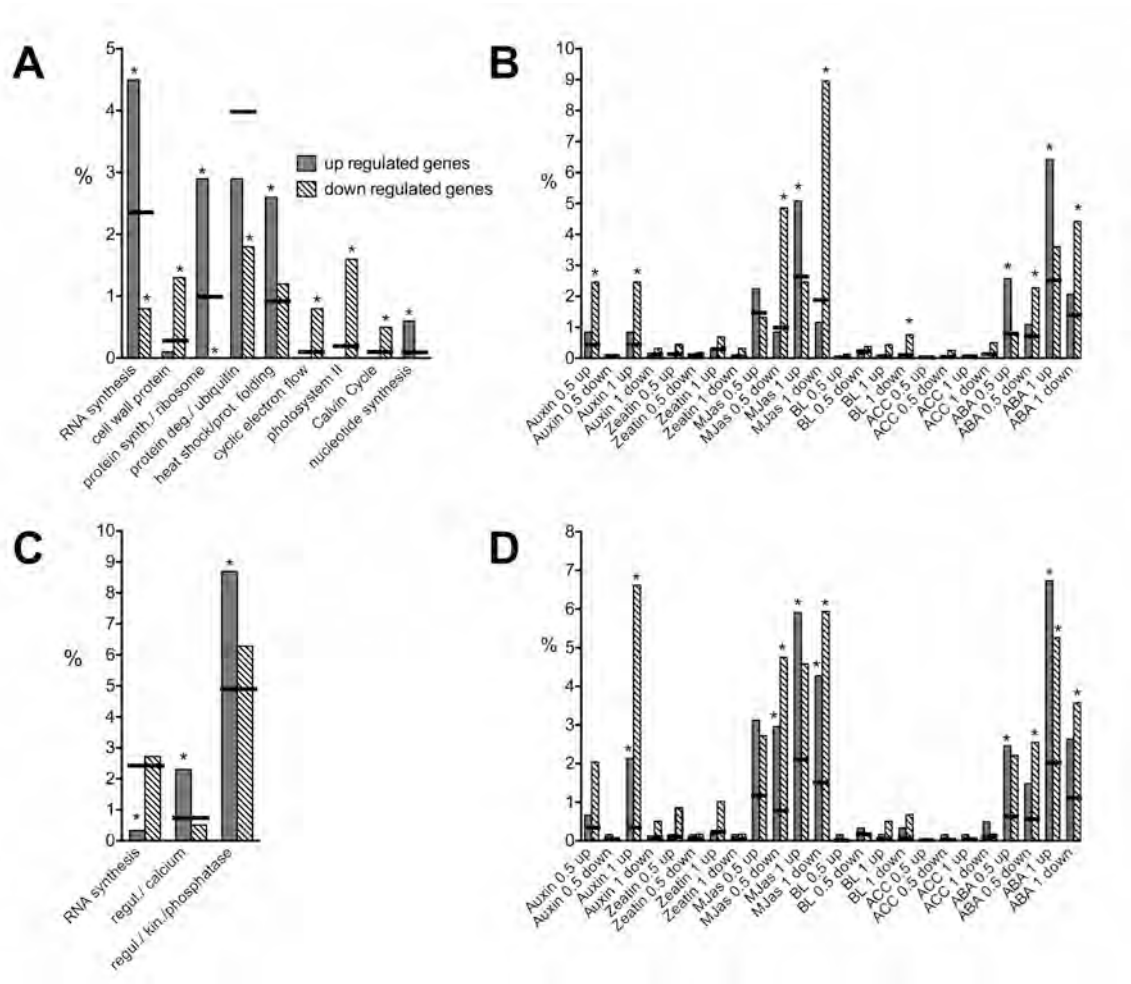

Figure 5: Genes representing functional categories are significantly altered in *cue1* **(A, B)** and *lcd1* **(C, D)** compared to col-0. **(A, B)** Cellular processes that are significantly altered are presented. **(C, D)** Responses to hormone treatments are shown. 0.5 and 1.0 indicate 0.5 and 1.0 hours of hormone treatment, respectively. Black lines represent percentage of category in genome. Stars indicate statistically significant difference ($p<0.01$; Bonferroni multiple testing correction for 190 categories). Protein synth: protein synthesis; protein deg.: protein degradation; regul.: regulation; kin.: kinase; MJas: methyl jasmonate; BL: brassinolide; ACC: 1-aminocyclopropane-1-carboxylic acid (ethylene precursor).

Cytokinin and auxin levels are mostly deregulated in *cue1* and not in *re*

Plant growth is dependent upon cytokinins and auxins (DeMason, 2005; Efroni et al., 2010; Mok and Mok, 2001). Both *cue1* and *lcd1* were affected on the transcripts level of auxin responsive genes (Figure 5B, 5D). To test if these observations were detectable on the metabolite levels, the steady state concentrations of cytokinins and auxins were determined (Figure 6, Supplemental Tables 5 and 6).

In *cue1* total cytokinins were increased by 16.9 % ($p= 0.0058$), cZ by 51.5% ($p= 0.0008$), and tZ was decreased by 51.5% ($p= 0.0008$), each compared to wild -type. One cytokinin derivate, namely tz9G, was not changed in *cue1*. All other derivates were either increased or decreased (Supplemental Table 5).

In *re-6* total cytokinins, tZ and cZ were not changed (Figure 6). Six out of 25 determined cytokinin derivates were significantly elevated, found in each cytokinin class (Supplemental Table 5). The *trans* zeatins represented the majority of cytokinins in wild-type, *re-6* and *cue1* (Supplemental Table 5). The *cis* cyctokinins, however, were overrepresented in the *cue1* plants with an increase of 72.3%, while these cytokinins were not changed in *re-6* (Supplemental Table 5).

All determined auxin derivates were increased in *re-6* and *cue1* rosettes compared to wild-type, with a pronounciation on *cue1* (Figure 6, Supplemental Figure 5). While total auxins, i.e. the sum of IAA, IAAasp, and IAAGlu, were increased by 20.1% (p= 0.0238) in *re-6*, they were increased by 117.4% (p< 0.0001) in *cue1*. *Re-6* rosettes displayed an increase of 29.2% (p= 0.0315), 37.6% (p= 0.0230), and 80.0% (p= 0.0073) for IAA, IAAasp, and IAAGlu, respectively. The same derivates were increased in *cue1* by 86.2% (0.0005), 429.3% (<0.0001), and 736.4% (<0.0001), respectively.

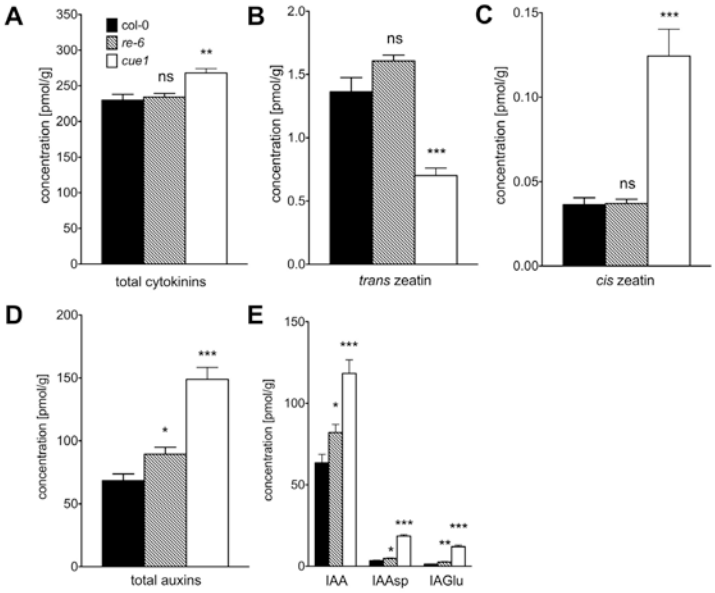

Figure 6. Phytohormone levels of col-0, *re-6* and *cue1* rosettes. **(A)** Total cytokinin levels. **(B)** *trans*-zeatin. **(C)** *cis*-zeatin. **(D)** Total auxin levels. **(E)** Indole-3-acetic acid (IAA), IAAsp, and IAA-Glu concentrations. IAAsp: indole-3-acetyl-aspartate. IAAGlu: indole-3-acetyl-glutamate. Error bars represent S.E. Asterisks indicate significance levels. n ≥ 5.

Auxin responses are more pronounced in the *re-6* background

To unravel the impact of phytohormone responses on leaf growth of *re-6* plants over a developmental time course, *re-6* was crossed into DR5-GUS and ARR5-GUS reporter lines (Figure 7). The DR-5-GUS reporter displays physiological response patterns of auxin (Robles et al., 2010; Ulmasov et al., 1997) and the ARR5-GUS-reporter of cytokinin (D'Agostino et al., 2000). Additionally, cell cycle activity was investigated by crossing the *re-6* into a

cycB1;1-GUS reporter line (Colon-Carmona et al., 1999; Sanchez-Calderon et al., 2005) (Supplemental Figure 5). Eight-week old rosettes with wild-type and *re-6* morphology were selected for GUS-activity and investigated by taking pictures immediately before and after staining. The ARR5-GUS reporter activity was not different between wild-type and *re-6* plants at all leaf ages. Leaves of every developmental stage of wild-type and *re-6* plants showed GUS activity (Figure 7A, 7B). The highest activity was detected in middle aged and old leaves in wild-type and *re-6* plants (e.g. leaf 4, Figure 7A and leaf 7, Figure 7B, lower panels). The staining patterns were patchy over the leaf lamina, but more pronounced around the veins, the margins, the distal part of the leaf lamina, and the hydathodes. A high staining intensity was detected at the petioles in the wild-type and *re-6* background. A high GUS activity was detected around the SAM and the leaf bases of young leaves in wild-type and *re-6* plants (Figure 7A, 7B). Wild-type and *re-6* plants have a restriction of the auxin activity to the leaf margins and the hydathodes (eg. leaf 5, Figure 7C and leaf 7, Figure 7B) with a generally higher activity in younger *re-6* leaves. No activity was detected around the SAM in neither wild-type nor *re-6*. The activity of the DR5-GUS reporter is higher in the *re-6* background, in line with increased auxin levels in *re-6* (Figure 6D and 6E).

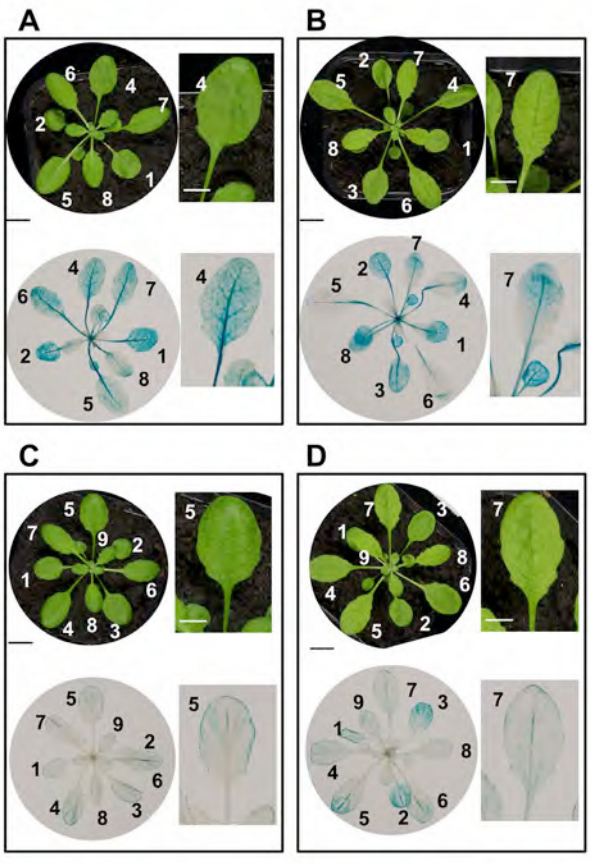

Figure 7. Cytokinin (ARR5-GUS) **(A,B)** and Auxin (DR5-GUS) **(C,D)** reporter assays in col-0 and *re-6* genetic background of seeven-week old plants. Pictures were taken immediately before and after GUS-staining. The leaves are numbered from oldest to youngest leaves starting with 1. The magnification of single representative leaves is shown right to the whole rosettes. The scale bars belonging to the rosette pictures and magnifications correspond to 1 cm and 0.5 cm, respectively.

The cycB1;1-GUS reporter in wild-type and *re-6* plants did not display distinguishable response patterns. Cell cycle activity was restricted to the SAM and the basis of developing young leaves. Activity was completely absent form middle aged and older rosette leaves (Supplemental Figure 5).

Amino acid and purine levels are deregulated

Despite transcriptional changes of genes involved in amino acid and purine metabolism were not detected, comparison to the molecularly identified reticulated mutants suggested a deregulation of amino acid and/or purine metabolism. These mutants, including *cue1*, are disturbed in primary metabolism, and restored by application of the appropriate metabolite (Streatfield et al., 1999; Hung et al., 2004; Jing et al., 2009; Lepistö et al., 2009; Mollá-Morales et al., 2011). Additionally, *cue1* is epistatic to *re*, suggesting the involvement in the same pathway (González-Bayón et al., 2006)

Thus, we hypothesized that *re* is affected in primary metabolism. To test if amino acid levels are altered in *re-6*, polar metabolites were extracted (Fiehn, 2006) of eight-week old rosette leaves grown under short day (SD, 12-h light/12-h dark cycle) and long day conditions (LD, 16-h light/8-h dark cycle). Two photoperiodic conditions were used because the extent of reticulation is dependent upon light conditions (Overmyer et al., 2008) and is stronger under LD (own observation, data not shown).

While almost all determined metabolites, either carbohydrates, amino acids or dicarboxylic acids, were upregulated in their amount under LD conditions, only little changes were observed for these metabolites under SD conditions (Supplemental Table 7, Supplemental Figure 6). Total amino acid contents, i.e. the sum of all amino acids determined, was significantly increased under LD but not under SD conditions (Figure 8 A, B, C, D). The only metabolite that was decreased under LD and SD conditions, both on a fresh weight and leaf area basis, was the amino acid lysine (lys) (Figure 8). Lys contents in *re-6* were decreased to the following levels compared to wild-type: 77.8 % for SD on FW basis, 69.4% for SD on leaf area basis, 59.4 % for LD on FW basis, and 56.3% for SD on leaf area basis (Figure 8E, 8F, 8G, 8H).

To investigate if metabolite accumulation patterns were differently regulated during day/night cycles, metabolite levels were determined at four sample points (Figure 8, Supplemental Figure 7): in the middle of the light period (14:00), one hour before darkness (21:00), in the middle of the night period (2:00), and one hour before transition to light (5:00). Generally, only minor differences in the metabolite contents of wild-type and *re-6* were observed. While some metabolites did not change with light and darkness, others responded to illumination. The amino acids phenylalanine, glycine, and serine changed in their relative

amount during the day/night cycle, with a general decrease during night and increase during day (Supplemental Figure 7, Supplemental Table 7). A similar behavior was observed for the carbohydrates sucrose, maltose, and the carboxylic acids fumaric acid, malic acid and maleic acid and the triol glycerol (Supplemental Figure 7). As for SD and LD, the only metabolite decreased at all observations points was lys (Figure 8I). The lys levels of the wild-type and the mutant stayed fairly stable during the whole observation period.

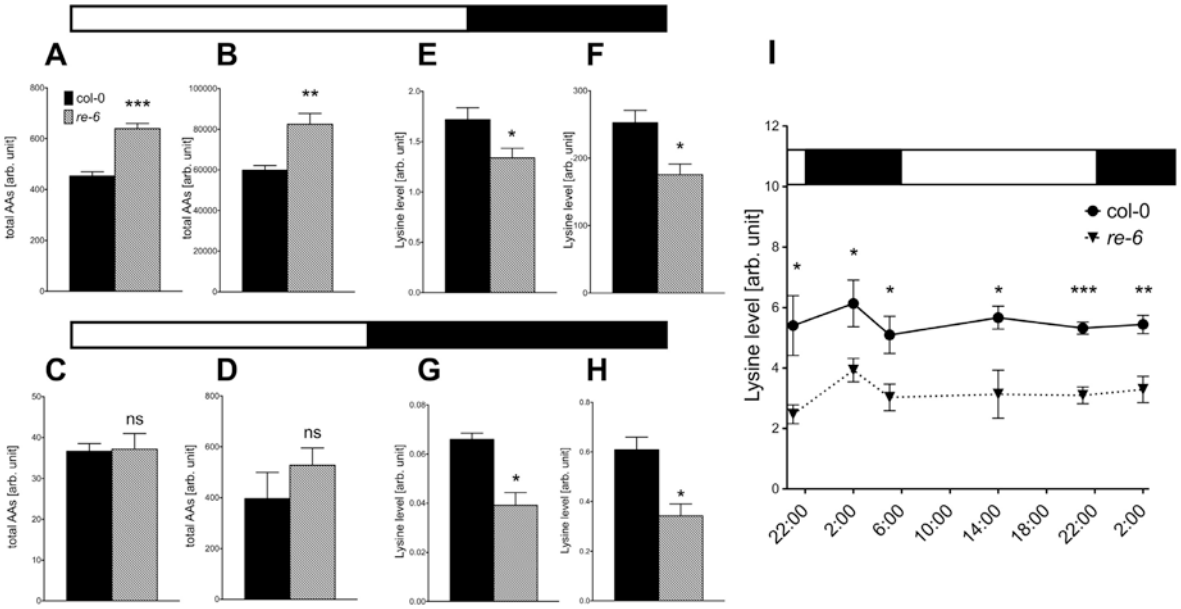

Figure 8. Relative steady state lysine contents of eight week old col-0 and *re-6* rosettes before transition to budding and flowering. Metabolite levels displayed in **(A)** – **(H)** were determined in the middle of the light period. All plants **(A)** - **(H)** were grown under 100µE m^{-2}-s^{-1} light intensity. **(A, B, E, F)** Plants grown under 16-h/8-h light-dark cycle (LD). **(B, D, G, H)** Plants grown under 12-h/12-h light-dark cycle (SD). **(A)** Total amino acids per FW; LD. **(B)** Total amino acids per area; LD. **(C)** Total amino acids per FW; SD. **(D)** Total amino acids per area; SD. **(E)** Lysine levels per FW; LD. **(F)** Lysine levels per area, LD. **(G)** Lysine levels per FW; SD. **(H)** Lysine levels per area; SD. **(I)** Time course metabolite profiling during 16-h/8-h light/dark cycle with sampling in the middle of the light period (14:00), one hour before dark (21:00), middle of the dark period (2:00), and one hour before the light period (5:00). Error bars represent S.E. Asterisks indicate significance levels. n ≥ 4. n (*re-6*, panel H) = 2. AA: amino acid

Since ATase2 mutants had lowered purine contents (Hung et al., 2004; Van der Graaff et al., 2004), we checked if purine levels were changed in *re-6*, *cue1*, and wild-type plants (Figure 9, Supplemental Table 10). All determined purine levels and the total amount were indistinguishable between *re-6* and wild-type, except for adenosine, which was increased in *re-6* by 40.8% (p= 0.0289). *Cue1*, however, displayed significantly increased total purine contents by 74.0% (p= 0.0003) (Figure 9). In contrast to *re-6*, all purines except of inosine were increased in *cue1* (Figure 9).

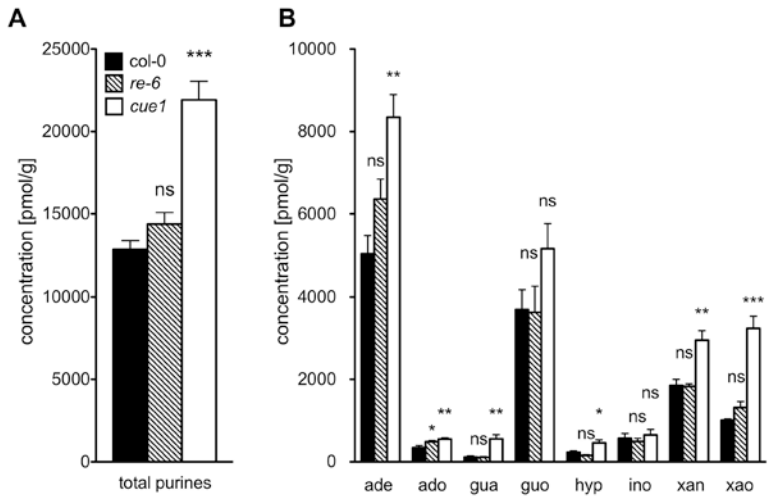

Figure 9. Steady state purine base and purine nucleoside levels of eight week old col-0, *re-6* and *cue1* rosettes before transition to budding and flowering. **(A)** Total purine concentrations. **(B)** Single Purine derivates. ade: adenine; ado: adenosine; gua: guanine; guo: guanosine; hyp: hypoxanthine; ino: inosine; xan: xanthine; xao: xanthosine. Error bars represent S.E. Asterisks indicate significance levels. n(col-0, *re-6*) ≥ 4.

Lysine and arginine reverted the *re-6* phenotype

Lys was the only amino acid lowered under all conditions tested and *RE* was co-regulated with a series of genes involved in amino acid metabolism, with a focus on lys metabolism. Both own co-expression analysis of publicly available data and data inferred from Atted-II provided this evidence (Supplemental Data 1 and 2). Thus, we investigated the behavior of *re-6* and the wild-type when supplemented with lys. Lys application visually reverted the phenotype at 0.2 and 0.4 mM (Figure 10). While total chlorophyll content was lowered to 86.0 % in *re-6* compared to wild-type, *re-6* chlorophyll levels increased to 0 mM lys wild-type levels when fed with 0.2 mM lys. The *re-6* mutant over-compensated the chlorophyll content at 0.2 mM lys feeding. At 0.4 mM lys, the chlorophyll levels were indistinguishable between wild-type and mutant. Leaf and plant size of supplemented *re-6* and col-0 plants, however, were smaller than the non-fed controls, likely due to toxic effects of amino acids (Voll et al., 2004). Similar results were observed when *re-6* and col-0 were fed with the basic amino acid arg (Supplemental Figure 8).

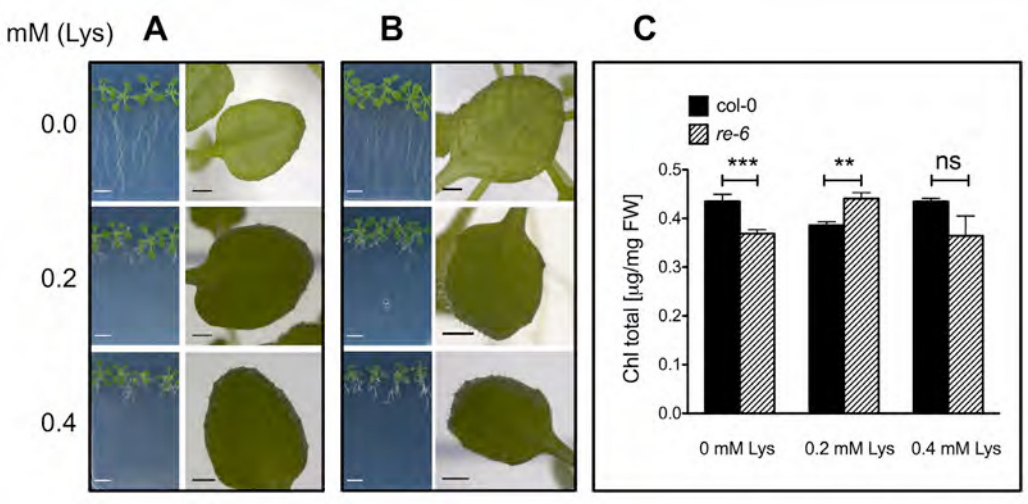

Figure 10. Biochemical complementation of *re-6* with lys. Plants were grown for seven days on MS-medium without amino acids, then transferred on lys containing media and grown for further two weeks. Plants were grown under 12-h/12-h light/dark cycle at 100 µE/m^2/s. **(A)** col-0 plants **(B)** *re-6* plants. **(C)** Total chlorophyll concentration of col-0 and *re-6* without and with lys. Error bars represent S.E. Asterisks indicate significance levels. Scale bars on the left panels of **(A)** and **(B)** correspond to 1 cm and on the right panels to 1 mm, respectively.

Discussion

Despite it`s gene locus is known (González-Bayón et al., 2006), RE´s function has not been established. However, all molecularly identified reticulated mutants are defective either directly or indirectly in primary metabolism (Jing et al., 2009; Lepistö et al., 2009; Mollá-Morales et al., 2011; Rosar et al., 2012). *Cue1* was discussed in the context of the *signaling* and the *supply hypothesis* (Streatfield et al., 1999; Rosar et al., 2012). We compared *cue1* and *re* mutants to investigate whether their nature favors one or the other hypothesis. For this purpose, we carried out growth analyses, transcriptional profiling, phytohormone determination, *in planta* hormone activity assays, metabolite profiling, and feeding studies.

RE_{long} is the functional splice variant

While the ectopic expression of RE_{long} reverted the reticulated phenotype, RE_{short} did not rescue the phenotype (Figure 1), indicating that only the long, and not the short splice isoform is functional. Either the resulting shortened mRNA stays stable or is subjected to degradation, which corresponds to lower transcript amounts of RE_{short} (Supplemental Figure 1). However, Barth and Conklin, 2003 found similar amounts of the truncated mRNA in col-0 and *lcd1*, making them speculate that protein targeting or folding may be negatively affected in the mutant. The allele *re-8* has a point mutation at the splice site of the fifth exon, resulting

in a predicted truncated protein (Overmyer et al., 2008). Alternative splicing is a mode of transcriptional regulation (Simpson et al., 2008; English et al., 2010; Syed et al., 2012). It mains to be elaborative if both splice variants exert different functions.

Transcriptional and metabolic responses in cue1 and *re*

While *cue1* is deregulated in nine, *re* is deregulated in three categories on the transcriptional level (Figure 5). *Cue1* is overrepresented in the categories RNA synthesis, nucleotide synthesis and cytosolic ribosomes (Figure 5). All theses groups converge in the process of protein biosynthesis. *Cue1* "underexpresses light-regulated nuclear genes encoding chloroplast localized proteins" (Streatfield et al., 1999). Total leaf protein is massively reduced in *cue1* (Voll et al., 2003). *Cue1* senses that there is not enough protein and tries to adjust via increased transcript levels of cytosolic ribosomes, RNA and thus nucleotide synthesis genes. Trying to compensate for lower protein levels on the transcriptional level may in turn provoke the transcriptional up-regulation of processes involved in heat shock/protein folding. Heat shock proteins are involved in the correct folding of functional proteins (Boston et al., 1996; Al-Whaibi, 2011; Horváth et al., 2012). Transcriptional deregulation of protein degradation and ubiquitin genes may be associated with an altered homeostasis of protein levels. Ubiquitination is involved in protein degradation via the proteasome (Kurepa and Smalle, 2008; Vierstra, 2009; Santner and Estelle, 2010) and was linked to signaling in plants (Santner and Estelle, 2010)

Four transcriptional categories are underrepresented in *cue1* (Figure 5): (i) cell wall proteins, (ii) PSII, (iii) cyclic electron flow, and (iv) central carbon metabolism/Calvin Cycle. The transcriptional reduction in cell wall protein synthesis could be due to the decrease of phenylpropanoid metabolism in *cue1* (Streatfield et al., 1999). Phenylpropanoids constitute to cell wall compounds like lignin or suberin (Holloway, 1983; Lewis and Yamamoto, 1990; Vogt, 2010). The down-regulation of PSII protein transcripts is in line with under-expressed nuclear encoded photosynthetic genes (Streatfield et al., 1999). *Cue1* was discovered in a screen for chlorophyll a/b under-expressed genes (Li et al., 1995).

In contrast to *cue1*, *lcd1* was overrepresented in two groups by up-regulated genes (Figure 5): (i) regulation/calcium and (iii) regulation kinase/phosphatase. These processes might be involved in signaling processes, such as calcium is involved in calmodulin signaling (Reddy, 2001; Kim et al., 2009). Phosphatases and kinases are associated with signaling processes, such as mitogen-activated kinases (Rodriguez et al., 2010). While *cue1* was overrepresented in up-regulated RNA synthesis genes, *lcd1* was underrepresented in this gene class (Figure 5A, 5C). A deregulated pattern of jasmonate responsive genes (Figure 5) was also observed and discussed in the context of *re*`s development (Overmyer et al., 2006).

The transcriptional changes in *cue1* are reflected on the physiological and metabolic level. *Re*, however, was changed in amino acid and carbohydrate homeostasis without observing altered patterns on the transcriptional level (Figure 8, Supplemental Figure 6, Supplemental Table 7). In *cue1*, the increased transcript levels of RNA and nucleotide synthesis genes (Figure 5) were reflected in a massively increased purine pool size (Figure 9). Also auxin levels were increased (Figure 6), along with changed transcriptional patterns in its synthesis genes (Figure 5). Auxin and *de novo* purine biosynthesis is dependent upon amino acids (Zrenner et al., 2006; Tao et al., 2008). Amino acid levels, except for reduced phenylalanine concentrations, are generally increased in *cue1*, particularly glutamine and asparagine (Streatfield et al., 1999). Glutamine is a key metabolite in the synthesis of purines (Hung et al., 2004; Zrenner et al., 2006; Rosar et al., 2012). The cytokinin metabolism, however, was not changed on the transcriptional but on the metabolite level in *cue1*. Total cytokinin levels were increased, with the tZ being lowered and cZ being increased (Figure 6, Supplemental Table 5). tZ, cZ and iP are considered to be the physiologically active forms, with cZ having the weakest activity (Leonard et al., 1969; Schmitz et al., 1972; Matsubara, 1980; Mok and Mok, 2001), and tZ and iP the major forms in *Arabidopsis* (Sakakibara, 2006). The conjugated forms are considered deactivated (Mok and Mok, 2001; Bajguz and Piotrowska, 2009). Furthermore, the changed transcriptional profile of PSII and Calvin Cycle genes parallels the massively decreased PSII-capacity, indicated by lowered F_v/F_m values (Figure 3C, Streatfield et al., 1999) and a limited Calvin Cycle activity (Streatfield et al., 1999). The transcriptional down-regulation of cyclic electron flow, which serves the production of the purine derivate ATP (Bukhov and Carpentier, 2004; Johnson, 2005), could be caused by the sensing of a high purine and thus high ATP-levels in the cell. Due to a decreased PSII activity and thus a likely decreased production of reduced reduction equivalents, such as NADPH, the Calvin Cycle transcripts are down-regulated.

Consequences of deregulated amino acid metabolism on leaf development

The reticulated mutants *cue1*, *trp2*, *ven3* and *ven6* and *ntrc* are disturbed in amino acid metabolism (Streatfield et al., 1999; Jing et al., 2009; Lepistö et al., 2009; Mollá-Morales et al., 2011). Amino acids are involved in leaf development (Jing et al., 2009).

Re-6 plants were deregulated in amino acid and carbohydrate metabolism (Figure 8, Supplemental Figure 6, Supplemental Table 7). Under LD conditions the deregulation was more pronounced than under SD. This parallels the penetrance of the phenotype, which is stronger reticulated under LD than under SD conditions (González-Bayón et al., 2006; own observation). Along day/night cycles, *re-6* behaved like wild-type with metabolite levels paralleling each other. The only decreased metabolite under all tested conditions was lys

(Figure 8). Similar observations with slightly decreased lys levels were made if a rate-limiting enzyme in lys biosynthesis was knocked out (Craciun et al., 2000). The lowered lys content could thus evoke the deregulation of amino acids contents, since their metabolic pathways are co-regulated. If histidine synthesis is inhibited, multiple amino acid synthesis genes and other metabolic pathways are activated, leading to an increase in at least ten amino acids (Guyer et al., 1995; Stepansky and Leustek, 2006). Plants affected in threonine biosynthesis show an over-accumulation of methionine (Bartlem et al., 2000) and plants down-regulated in lys biosynthesis have increased threonine levels (Craciun et al., 2000). The threonine level was increased in *re-6* under LD conditions (Supplemental Figure 6 and Supplemental Table 7). Much like *trp2*, *ven3 and 6*, *cue1* and *ntrc* were complemented by the appropriate amino acids (Streatfield et al., 1999; Jing et al., 2009; Lepistö et al., 2009; Mollá-Morales et al., 2011) lys and arg restored the *re-6* leaf phenotype (Figure 10, Supplemental Figure 8). Biochemical complementation with lys and arg made the involvement of basic amino acids in *re* likely. Amino acid supplementation led to shorter and highly branched roots, also observed when growing plants on glutamate containing medium (Walch-Liu et al., 2006). Increased root branching compensates for inhibition of primary root growth (Reed et al., 1998; Tsugeki and Fedoroff, 1999). There is evidence that auxins and/or cytokinins are involved in these processes (Casson and Lindsey, 2003). Plant hormones and amino acids share common pathways since the latter metabolites influence hormones by conjugation (Bajguz and Piotrowska, 2009; Westfall et al., 2010).

But how does the amino acid metabolism link to establishment of the leaf phenotype? Leaves of reticulated mutants are smaller and the M is decreased in cell number and/or size compared to wild-type controls (Kinsman and Pyke, 1998; Streatfield et al., 1999; González-Bayón et al., 2006; Jing et al., 2009). These characteristics are due to two successive processes: (i) cell proliferation and (ii) cell expansion, which are mainly controlled by cytokinins and auxins, respectively (Mizukami, 2001; Anastasiou and Lenhard, 2007; Tsukaya, 2008). Despite the epidermal dominance of leaf size control, M cells contribute to the final size of a leaf (Savaldi-Goldstein et al., 2007; Javelle et al., 2011; Pérez-Pérez et al., 2011; Powell and Lenhard, 2012). (Jing et al., 2009) linked the M structure to the growth kinetics of *trp2* mutants. *Trp2* leaves are at wild-type size during early development and growth decelerates at later stages. The authors argued that this implies an alteration in cell expansion rather than in cell proliferation. Conclusively, the M cell number in *trp2* was at wild-type level but the cell size was strongly reduced (Jing et al., 2009).

To address growth, we measured rosette growth kinetics over ten days (Figure 3). At the first observation point (21 dpg) *cue1* was smaller than wild-type. These results indicate that cell proliferation is slowed down in *cue1*, because growth by proliferation is predominant in younger plants. The growth of *cue1* in the later observation phase is likely due to cell

expansion rather than proliferation. The decreased tZ concentrations support a diminished cell cycle activity, while the increased auxin levels in *cue1* rosettes support the cell elongation process (Figure 6, Supplemental Tables 5 and 6). These results are in agreement with the observation that *cue1* has less, but not smaller M cells (Streatfield et al., 1999).

Total *re-6* leaf area was at wild-type level in young plants (21 dpg) and increased strongly over the observation period but remained smaller than the wild-type (Figure 3). The stark increase in *re-6* leaf size at the end of the observation period prompts at an occurring cell elongation. Indeed, *re* M cells are only slightly smaller but reduced in number compared to wild-type (González-Bayón et al., 2006). *Re* plants already contained less M cells in leaf primordia (González-Bayón et al., 2006). The almost wild-type cell size in *re* (González-Bayón et al., 2006) is likely achieved by cell elongation, which is in line with elevated auxin levels in *re* (Figure 6). The cytokinin levels, however, were not decreased in *re-6* (Figure 6). This might be due to the time point of phytohormone determination.

Carbohydrate (C)- and nitrogen (N)-metabolism is compartmentalized between vein-associated tissues (xylem, phloem, and/or BS) and M in C_3 plants (Leegood, 2008), similarly to C_4 plants. Cells within and around the vein of C_3 plants are important in the synthesis of metabolites associated with C-metabolism (Nolte and Koch, 1993; Schobert et al., 2004 Janacek et al., 2009). Three decarboxylases, which are also found in the C_4-BS, are highly active in vasculature-associated tissues (Hibberd and Quick, 2002). Pyruvate orthophosphate dikinase (PPDK) converts pyruvate into PEP (Hibberd and Quick, 2002), which is fed into the shikimate pathway for aromatic amino acid synthesis (Fischer et al., 1997; Knappe et al., 2003; Schmid and Amrhein, 1995; Tzin and Galili, 2010). The shikimate pathway is concentrated around the veins (Janacek et al., 2009). Some genes encoding amino acid synthesis enzymes (Craciun et al., 2000; Joshi et al., 2006) and amino acid transporters are expressed along the veins (Kwart et al., 1993; Fischer et al., 1995; Rentsch et al., 1996; Hirner et al., 1998; Ladwig et al., 2012), the latter preferentially in the BS. Further studies in various plant species gathered strong evidence that amino acid metabolism is vastly focused on vein associated tissues and compartmentalized between these and the M (Mitchell et al., 1992; Brugière et al., 2000; Schobert et al., 2004; Kichey et al., 2005; Turgeon, 2010).

Taken together, *cue1* is massively affected in auxin metabolism both on the transcriptional and metabolic level (Figure 5 and 6). Auxin, derived from tryptophan (Tao et al., 2008), was hypothesized to be involved in vascular differentiation (Kinsman and Pyke, 1998) and thus might be involved in signaling events triggering M differentiation. Additionally, cytokinin levels were increased in *cue1* but not *re-6* (Figure 6). Since these phytohormones are known to be signaling molecules in plants, *cue1* is at least likely defective in signaling events. However, a supply phenotype cannot be excluded for *cue1*. Metabolic changes on

the amino acid and purine levels in *re* were not observed on the transcriptional level. Thus, *re* keeps a stable homeostasis on the transcriptional level, but rather reacts to it`s impairment by posttranscriptional responses. This indicates, that re *is* likely not affected in a cytokinin or auxin derived signal that mediates M development. Since purine levels are unchanged, nucleotides less likely do not serve as signaling compounds (Thomas et al., 2000; Jeter et al., 2004; Chivasa and Slabas, 2012; Sun et al., 2012). However, signals, such as Ca^{2+} or kinase/phosphatase mediated signals, cannot be excluded. We suppose that a deregulated amino acid metabolism is associated with *re*`s phenotype. The localization of RE to the plastid, the photoperiod dependent metabolite levels, the fact that amino acid metabolism is linked to photosynthesis (Lam et al., 1995), and the comparison to other reticulated phenotypes provides strong support that *RE* is associated with amino acid metabolism. The molecular mechanism for lys deficiencies is currently under investigation.

Material and Methods

Chemicals

Chemicals were purchased from Sigma-Aldrich if not mentioned elsewhere. Chemicals and enzymes for recombinant DNA-techniques were purchased from Invitrogen, New England Biolabs, Fermentas, and Promega. All primers used in this study are listed in Supplemental Table 12.

Plant material, general growth conditions, and plant lines

Arabidopsis thaliana plants were grown under controlled conditions in climate chambers. The day/night cycle was chosen as 12-h light/12-hour or 16-h light/8-h dark with a photosynthetically active radiation of 100 μ E/m^2/s. The temperature was set to 22°C during the light, and 18°C during the dark period. *Arabidopsis thaliana* seeds were surface sterilized with chlorine gas in a desiccator as described (Desfeux et al., 2000), spotted on solid 1 Murashige and Skoog (MS)-medium with vitamins containing 0.8% (w/w) plant agar (Murashige and Skoog, 1962), and stratified at 4°C for 4 days. All plant material was germinated and grown in 1X MS medium and transferred on soil at the first true leaf stadium. *Re-6*-seeds (N 584529, SALK_084529) were obtained at NASC, the European Arabidopsis stock centre. *Cue1-6* (Streatfield et al., 1999) and *lcd1-1* seeds (Barth and Conklin, 2003) were taken from our laboratory stock. *Cue1-6* and *lcd1-1* are referred to as *cue1* and *lcd1* in this study, respectively. DR5-GUS-, ARR5-GUS- and cycB1;1-GUS-seeds were provided by Rüdiger Simon and Nicole Stahl (Institute of Developmental Genetics, Heinrich-Heine-

University, Düsseldorf). DR5 is an artificial promoter that reacts to changed auxin perception (Robles et al., 2010; Ulmasov et al., 1997). ARR5-GUS indicates changing cytokinin patterns (D'Agostino et al., 2000). The cycB1;1-GUS-reporter detects cell cycle activity (Colon-Carmona et al., 1999; Sanchez-Calderon et al., 2005). DR5-GUS-, ARR-5-GUS- and cycB1;1-GUS-reporter lines were crossed into *re-6*. The F2-generation of the DR-5-GUS and ARR5-GUS-crosses with *re-6* was visually selected for the *re-6* and col-0 phenotype. *Re-6* and col-0 phenotypic plants of the F2 generation were screened by GUS-staining for changing GUS-patterns. *Nicotiana benthamiana* was grown in a greenhouse for four to six weeks (Breuers et al., 2012).

Polymerase Chain Reaction and Agarose Gel Electrophoresis

Standard Polymerase Chain Reaction (PCR) was performed as previously described (Sambrook et al., 2001). Agarose gel electrophoresis was carried out in 1% and 2% Agarose-Gels in 1xTAE buffer (Sambrook et al., 2001). Size markers were used from Fermentas (Fermentas Gene Ruler™ 1kb DNA Ladder and Fermentas Gene Ruler™ Ultra Low Range DNA ladder).

Genomic DNA isolation and cDNA synthesis

For genomic DNA (gDNA) isolation a leaf was quick frozen in liquid nitrogen and ground to powder by adding 400 µl DNA extraction buffer (200 mM Tris/HCL pH 7.5, 200 mM NaCl, 25 mM EDTA, 0,5% (w/v) SDS). After homogenization, 150µl sodium-acetate was added and centrifuged for two minutes at full speed in a reaction vial. 450 µl isopropanol was added to 450 µl of the supernatant, incubated for two minutes at room temperature before centrifuging for five minutes at full speed. The pellet was washed with 700 µl 80% (m/m) ethanol, air dried and resuspended in 30 µl nuclease free water. All centrifugation steps were carried out at room temperature. For cDNA synthesis, RNA was extracted as described (Chomczynski and Sacchi, 1987; Chomczynski and Sacchi, 2006), DNase digested, and subjected to cDNA synthesis using either Superscript II or Superscript III (Invitrogen).

***Escherichia coli* transformation**

The *E.coli* strain One Shot® MACH1™ T1^R (Invitrogen) was heat-shock transformed with Gateway® destination vectors as described by the manufacturer (Invitrogen). Empty Gateway® destination vectors were propagated in One Shot® ccdb Survival™ 2T1R competent cells (Bernard and Couturier, 1992; Bahassi et al., 1995) as described by the manufacturer. Heat shock transformation was performed as described (Sambrook et al., 2001).

***Agrobacterium tumefaciens* and stable plant transformation**

The binary plant vectors were transformed into *Agrobacterium tumefaciens* GV3101 strain (Koncz and Schell, 1986) as previously described (Breuers et al., 2012). Either an electro-competent GV3101 strain was used for electroporation (Shen and Forde, 1989; Mersereau et al., 1990) or a heat shock competent GV3101 strain for heat shock transformation (Höfgen and Willmitzer, 1988). Transformed Agrobacteria were selected on appropriate YEB-antibiotic-media, containing rifampicin (50–150 μg/mL), gentamycin (25–50 μg/mL), and either kanamycin (25–50 μg/mL; pmDC32, pmDC83) or spectinomycin (100 μg/mL, pUBC-GFP), depending on the plasmid resistance. Positively transformed *Agrobacteria* were then used for transfection of *Arabidopsis thaliana*. Genetically stable *Arabidopsis* transformants by the floral dip method (Clough and Bent, 1998; Zhang et al., 2006) and for transient expression in tobacco.

Genetic complementation of *re-6* plants and overexpressor lines

Re-6 plants were transformed with RE_{long} and RE_{short} on the cDNA level, and with the RE on the gDNA level. Col-0 pants were transformed with and RE. The inserts were PCR-amplified either on cDNA or gDNA. The primers CR1/CR2 were used both for RE and RE_{long}, giving rise to 35S::RE and 35S::RE_{long}, respectively. RE_{short} was amplified with the primers CR1/CR19 on cDNA. The appropriate PCR-products were recombined via pDONR207 (Invitrogen) into the Gateway® destination vector pmDC32 (Curtis and Grossniklaus, 2003), driven by the ecoptically active 35S-overexpression promoter from the cauliflower mosaic virus. DNA sequences were verified by DNA-sequencing (GATC-biotech; www.gatc-biotech.com). The destination vector was transformed via the *Agrobacterium tumefaciens* strain GV3101 into *re-6*, using the floral dip method (Clough and Bent, 1998). The insertion of the constructs into the plant genome was tested by PCR. DNA integrity was tested by PCR with primers CR39/CR40 against Actin7 (At5g09810), giving a signal of 918 bp on gDNA and 734 bp on cDNA. The signal of the PCR-product by CR43/CR47 at a size of 794 bp indicated the presence of the hygromycin gene encoded by the vector pmDC32. The primer combination CR161/CR162 bound on *RE*, giving rise to PCR products of 1841 bp on gDNA-constructs and 1299 bp on cDNA-constructs. The combination CR48/CR49 gave a PCR-signal at 1060 bp in the presence of the fifth exon of the RE gene and the NOS-terminator of pmDC32. The primer combinations CR53/CR52, CR51/52, and CR51/53 were used to detect the T-DNA insertion of the *re-6* mutant (SALK_084529). The following PCR products were obtained: CR53/CR52 at ca. 700 bp a homozygous *re-6* plant, CR51/52 at ca. 900 bp indicated col-0 background and CR51/53 giving no signal due to the direction of the T-DNA insertion.

PCR based detection of splice forms

PCR was performed on cDNA of col-0 leaves with the primer combinations F/R1 and F7R2. F binds on the fifth exon of RE, R1 on the fifth intron and R2 on the sixth exon. On cDNA, the long slice variant RE_{long} gives rise to a fragment of 55bp and the short variant RE_{short} to 67 bp. R1 specifically binds on the 3`-UTR of RE_{short}.

Plasmid construction for transient expression in tobacco and localization of RE

For localization in a transient *Nicotiana* expression system, RE (CR1/CR4), RE_{long} (CR1/CR4), and the $RE_{long, \Delta cTP}$ (CR6/CR4) were cloned into the Gateway® compatible C-terminal eGFP-tagged vector pUB-GFP driven by the ubiquitin10 promoter (Grefen et al., 2010). The predicted cTP (CR1/CR116) was cloned in the plant expression pmDC83 vector for C-terminal protein expression (Curtis and Grossniklaus, 2003).

Transient expression of protein in *Nicotiana tabacum* for *in planta* studies

These studies were carried out as decribed (Breuers et al., 2012). 5mL liquid cultures of positively transformed *Agrobacterium* GV3101 (see above) were grown in LB medium with appropriate antibiotics (see above) at 30°C for 16 to 24 hours. Centrifugated cells were resuspended in infiltration buffer (IF, 2 mM Na_3PO_4, 50 mM MES/KOH (pH 7.6), 5 mg/mL glucose, 200 mM acetosyringone). A bacterial suspension (OD_{600} = 0.05) was used for infiltration of *N. tabacum* leaves as described elsewhere (Batoko et al., 2000). Infiltrated plants were grown under 16-h/8-h light/dark at 27°C/24°C, respectively, for ca. three to five days. Leaf discs were pressed between a microscope slide and a cover slip and observed under the Zeiss LSM 510 META microscope.

Confocal microscopic analysis

Whole leaf M cells of *N. tabacum* were analyzed with a Zeiss LSM 510 META confocal laser-scanning microscope as described by Breuers et al., 2012. GFP and chlorophyll were excited with an Argon-laser at 488 nm and emission was collected at 505-550 nm and >650 nm, respectively. Pictures were processed and merged using the freeware GIMP (www.gimp.org).

GROWSCREEN FLUORO analysis of growth, fluorescence and phenotypic properties

Batches of plants grown on soil were analyzed for growth and phenotypic properties by using the GROWSCREEN FLUORO phenotyping platform as described (Jansen et al., 2009). Fifteen or more biological replicates were used for each col-0, *re-6* and *cue1* mutants. The phenotyping setup uses a fluorescence-imaging camera together with an illumination head to automatically acquire images of every plant inside the batches placed in the setup

(Jansen et al., 2009). Plants were imaged non-invasively for a period of ten days at the same time every day. For calculation of F_v/F_m, plants were dark adapted for 30 minutes. Based on the acquired images, image analysis provided several datasets for each mutant and wild-type plants, including the relative growth rate (RGR) and efficiency of photosystem II (Walter et al., 2007; Jansen et al., 2009). RGR was calculated using the equation RGR= (mean of $\ln(A_2)$ - mean of $\ln(A_1)/t_2-t_1$) (Hoffmann and Poorter, 2002; Jansen et al., 2009).

Co-regulation analysis

Co-regulation analysis was performed using the Atted-II vers. 6.1 database (http://atted.jp/; Obayashi et al.; Obayashi et al., 2007). Co-regulated genes were searched by with the default settings, using At2g37860 as query.

Transcriptional profiling and data analysis

Plants were grown under 16-h light/8-h dark, RNA from leaves was isolated as described previously (Stähr, 2010). An Affimetrix GeneChip®-3`IVT-Express-Kit was used for expression profiling (Stähr, 2010). Two replicates of each *cue1*, *lcd1-1* and col-0 plants were hybridized with Affimetrix Chips. The resulting .cel files were read into Robina and analyzed with modified standard parameters (rma normalization, limma, pairwise tests of significant change with $p<0.01$, Benjamini Hochberg corrected, no log-fold change limits). The resulting tables are available in the Excel sheet as *DataTable* (Supplemental Data 1). For analysis, all non-matching AGIs and controls were deleted and the table renamed to *DataTable_AffysmatchingAGIs_only*. For the hormone treatments available from the AtGenExpress project (seedlings treated with the appropriate hormone or mock control for 0.5h, 1h and 3h) were downloaded, decoded, analyzed with robina and standard parameters (rma normalization, limma, pairwise tests of significance with $p<0.05$, Benjamini Hochberg corrected, no log fold change limits) and the results were added to the data table. For the enrichment analysis, the percentage of genes in a category (over all genes on the Affymetrix-chip) was calculated. The percentage of up-regulated genes in a category (over all up-regulated genes) and the percentage of down-regulated genes in a category (over all down-regulated genes) are also calculated. A Fishers Exact Test determines if the absolute numbers in the up- or down-regulated column, respectively, are different from the numbers in the category on the Affychip. For Fisher`s Exact Test, $p<0.05$ with Bonferroni correction for 190 categories was used.

Metabolite profiling of polar metabolites

Re-6 and col-0 plants were grown under controlled conditions in a light chamber in a 16-h/8-h (100 µE/m^2/s) and 12-h/12-h light/dark cycle (100 µE/m^2/s), respectively, on 1 MS-medium (Murashige and Skoog, 1962), and transferred on soil after two weeks. Whole

rosettes from seven-week-old *re-6* and col-0 plants were harvested before flowering, and snap-frozen in liquid nitrogen. Polar metabolites from homogenized rosette material samples (ca. 50 mg) were extracted using a chloroform-methanol extraction protocol (Fiehn, 2006). The extraction mix was vortexed for 20 seconds, shaken in a rotating device for six minutes at 4°C, centrifuged for two minutes at 20.000g. 1mL of the supernatant was vortexed for ten seconds, shaken in a rotating device for 6 minutes at 4°C, centrifuged for two min at 20.000g. 100µl of this extract was lyophilized, and derivatized using methoxyamine hydrochloride in pyridine followed by N-methyl-N-(trimethylsilyl-)fluoroacetamide (MSFTA) treatment (Fiehn, 2006). The relative amounts of seventeen amino acids, nine carbohydrates, ten carboxylic acids, and shikimate were determined as described previously (Gowik et al., 2011). For calculating the total amino acids levels, the following metabolites were taken: α-ala, leu, val, glu, Asp, ile, asn, met, cys, phe, tyr, gly, ser, and lys.

GUS-staining

GUS-staining was performed as described (Mattsson et al., 2003). Whole rosettes of seven-week old plants were vacuum infiltrated with the GUS staining solution (0.1 M NaH_2PO_4, pH 7.0; 10 mM Na_2EDTA; 0.5 M Sodium-Ferricyanide $K_3[Fe(CN)_6]$; 0.5 M Sodium-Ferrocyanide $K_4[Fe(CN)_6]$ x $3H_2O$, 0.1% Triton X-100, and 1 mM 5-bromo-4-chloro-3-indoyl-beta-GlcUA (Inalco Spa)). The samples were incubated at 37°C for 24 hours. Hereafter, the staining solution was removed, and fixation solution was added (50% (w/w) ethanol, 5% (w/w) glacial acetic acid, and 3.7 % (w/w) formaldehyde). The samples stored in the staining solution were incubated for ten minutes at 65°C. The leaf tissue was destained three times after removal of the fixation solution with 80% (w/w) ethanol. Pictures were taken with a digital camera (Canon D40).

Chlorophyll determination

Plants were grown in a 12-h/12-h light/dark cycle (100 µE/m^2/s) for four weeks under 12-h light/12-h dark on 1 MS-plates. Plant material was harvested in the middle of the light period, snap-frozen in liquid nitrogen, and homogenized by grinding in a mortar. The fresh weight was measured and the chlorophyll concentration determined as described (Porra et al., 1989).

Cytokinin and auxin quantitation

Plants were grown in a 12-h/12-h light/dark cycle (100 µE/m^2/s). Five rosettes of each col-0, *re-6* and *cue1* rosettes were pooled. Five replicates of each pooled sample were used for cytokinin and auxin quantitation. For endogenous cytokinins analysis, extraction and purification was performed according to the method previously described (Novák et al.,

2003). Levels of cytokinins were quantified by ultra performance liquid chromatography-electrospray tandem mass spectrometry (UPLC_MS/MS) (Novák et al., 2008). Endogenous auxin concentrations were determined as described previously (Ascough et al., 2009; Novák et al., 2012).

Biochemical complementation with amino acids

After seven days of growth on MS-plates (12-h light/12-h dark), seedlings were transferred onto MS-plates containing different concentrations of lys and arg. Plants were monitored for an additional two weeks. Pictures were taken with a digital camera (Canon D40).

Statistical Analysis

For metabolic determination, statistical significance was assessed by the Student`s *t*-test. Probability values (p) <0.05 were considered being significant. One star indicates $p<0.05$, two stars indicate $p<0.01$, and three stars indicate $p<0.0001$. The standard error of the mean (S.E.) is indicated in all plots, if not indicated elsewise. Analysis was performed and graphs generated with Prism (GraphPad). Statistical analysis for microarray analysis was performed as described above.

Phylogenetic analysis and tree construction

Sequences were extracted from public databases using the Blast Explorer followed by manual curation to remove partial sequences. Blast Hits in Blast Explorer were only present in the green lineage. Sequences were aligned with MUSCLE and default settings and cured with Gblocks (smaller final blocks, allow gap positions within final blocks and allow less strict flanking positions enabled). The phylogeny was established using PhyML using 100 bootstraps. The tree was rendered with TreeDyn. Branches with bootstraps support lower than 50% were collapsed.

Acknowledgement

We thank Prof. Dr. Rüdiger Simon and Dr. Yvonne Stahl providing us with the ARR5-GUS, DR-5-GUS, and cycB1;1-GUS reporter lines. We appreciate technical assistance by Katrin L. Weber and Elisabeth Klemp with GC/MS-analysis of metabolites. We thank Steffen Jäger for assistance with photographic documentation of plants and Frederique K.H. Breuers for support with confocal microscopy. CR thanks the “Studienstiftung des deutschen Volkes” for support.

Funding:

This work was funded by grants of the Deutsche Forschungsgemeinschaft (DFG CRC 590 to APMW and iRTG 1525 to APMW and AW) and by Grant No: KAN200380801 to MS.

Supplemental Figures

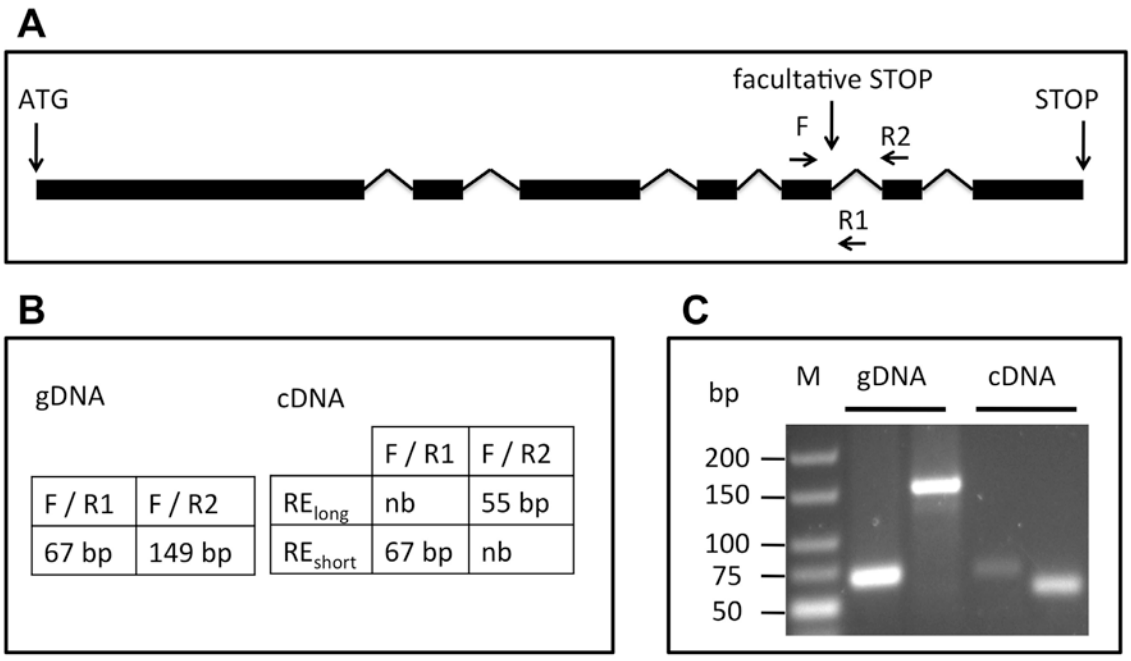

Supplemental Figure 1. RE has two splice variants: *RE*$_{long}$ and *RE*$_{short}$. **(A)** Screening strategy. Black bars indicate exons, thin bars introns. Forward primer F binds on fifth exon, reverse primer R1 on fifth intron, and reverse primer R2 on sixth exon. **(B)** Table shows expected band sizes of different primer combinations F/R1 and F/R2 when PCR is performed on gDNA and cDNA. nb: no band expected. **(C)** PCR performed with 28 cycles. The two bands of 67 bp and 55 bp indicate that two splice variants are existant: *RE*$_{long}$ and *RE*$_{short}$. Two-week old col-0 plants were used. M: size marker.

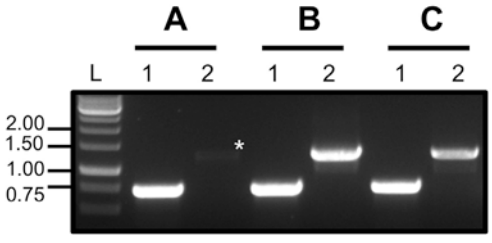

Supplemental Figure 2. Quantative PCR on cDNA of col-0, *re-6*-complementant and col-0-overexpressor plants. 1: Actin control (CR39/CR40). 2: RE (start to stop, CR 161/CR162). Asterisks indicates band. **(A)** col-0. **(B)** *re-6* with 35S::*RE*$_{long}$. **(C)** *col-0* with 35S::*RE*$_{long}$ (OX).

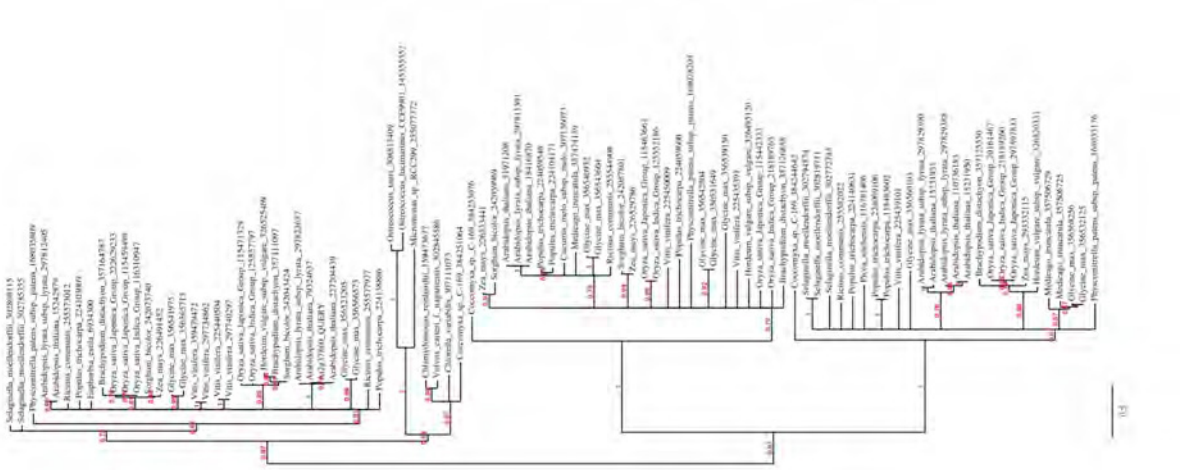

Supplemental Figure 3. Phylogenetic tree of plant specific proteins harboring DUF 3411.

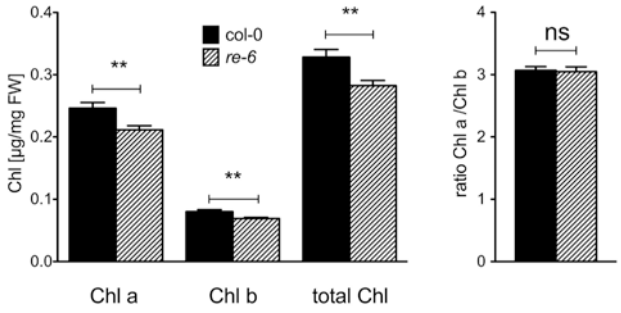

Supplemental Figure 4. Chlorophyll (chl) concentrations of col-0 and *re-6*. **(A)** chl a level. **(B)** chl b level. **(C)** Total chl, i.e. sum of chl a and chl b. **(D)** Chl a/ Chl b ratio.

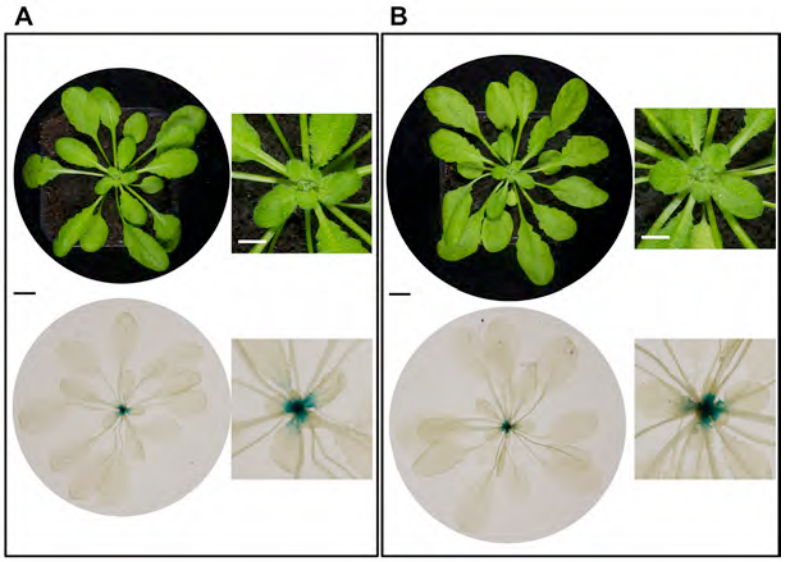

Supplemental Figure 5. Cell cycle (cycb1.1-GUS) reporter assays in col-0 **(A)** and *re-6* **(B)** genetic background of eight week old plants. Pictures were taken immediately before and after GUS-staining. The magnification of the shoot meristemtic tissue is shown right to the whole rosettes. The scale bars belonging to the rosette pictures and magnifications correspond to 1 cm and 0.5 cm, respectively.

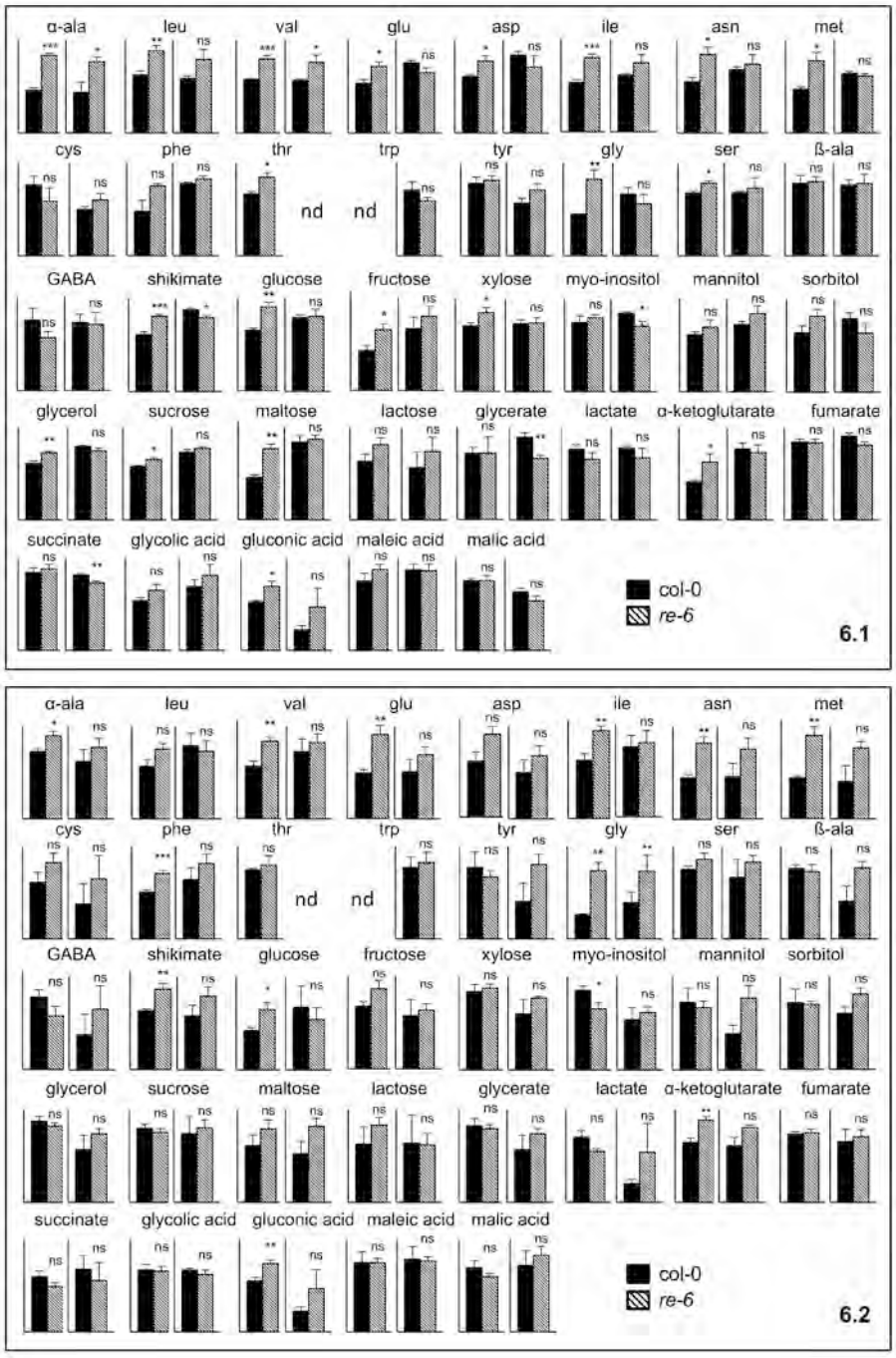

Supplemental Figure 6. Relative steady state polar metabolite contents of eight-week old col-0 and *re-6* rosettes before transition to budding and flowering. Metabolite levels were determined in the middle of the light period. **Figure 6.1:** Metabolites determined on FW basis. Left graph: LD conditions, right graph SD conditions. **Figure 6.2:** Metabolites determined on leaf area basis. Left graph: LD conditions, right graph SD conditions. All plants were grown under 100 µE m^{-2}-s^{-1} light intensity. Plants grown under 16-h/8-h light-dark cycle (LD). Plants grown under 12-h/12-h light-dark cycle (SD). Error bars represent S.E. Asterisks indicate significance levels. ns: not significant. n ≥ 4.

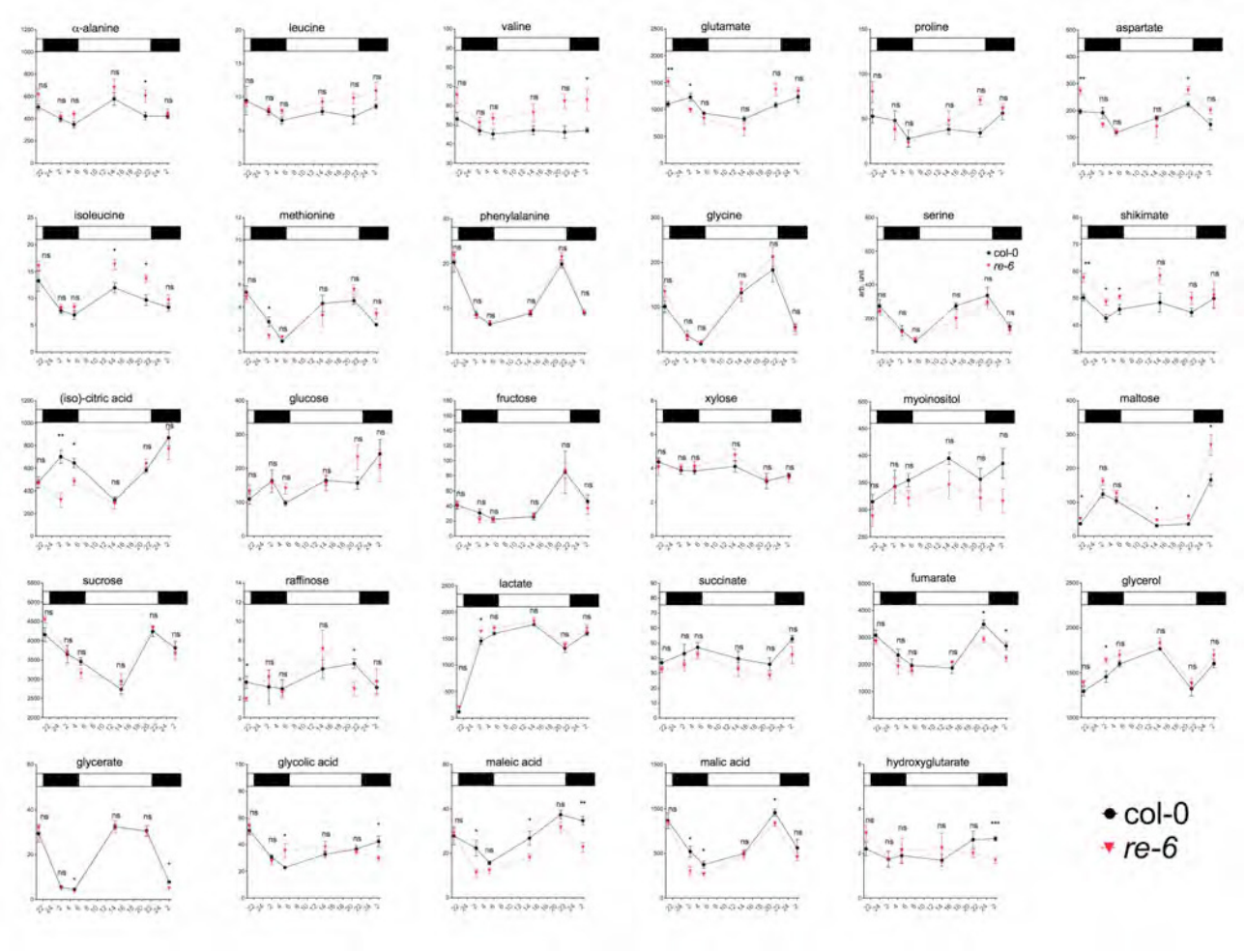

Supplemental Figure 7. Time course metabolite profiling during 16-h/8-h light/dark cycle with sampling in the middle of the light period (14:00), one hour before dark (21:00), middle of the dark period (2:00), and one hour before the light period (5:00). Error bars represent S.E. Asterisks indicate significance levels. ns: not significant. n ≥ 4.

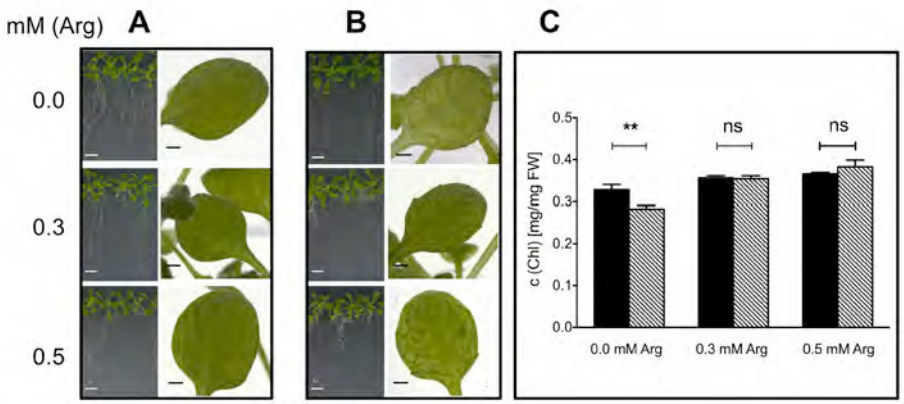

Supplemental Figure 8. Biochemical complementation of *re-6* with arginine. Plants were grown for seven days on MS-medium without amino acids and then transferred on arginine (arg) containing media and grown for further two weeks. Plants were grown under 12-h/12-h light/dark cycle at 100 µE/ m^2/s^{-1}. **(A)** col-0 plants **(B)** *re-6* plants. **(C)** Total chlorophyll concentrations of col-0 and *re-6* fed with arginine and controls. Error bars represent S.E. Asterisks indicate significance levels. Scale bars on the left panels of **(A)** and **(B)** correspond to 1 cm and on the right panels to 1 mm, respectively.

Supplemental Tables

Supplemental Table 1: *Arabidopsis thaliana* proteins with DUF3411 domain. Na: not assigned

Arabidopsis genome identifier	name
At2g37860	RE, LCD
At5g22790	RE-R1
At3g08630	na
At3g08640	na
At5g12470	na
At5g24690	na
At2g40400	na
At3g56140	na

Supplemental Table 2: Total leaf area of col-0, *re-6*, and *cue1* plants. Plants were monitored for ten days, beginning at 21 days post germination (21 dpg). Errors are indicated as S.E. n > 15. nd: data points were not determined.

	Leaf area							
	col-0		*re-6*		col-0/*re-6*	*cue1*		col-0/*cue1*
dpg	Average	± S.E.	Average	± S.E.	p-value	Average	± S.E.	p-value
21	0.937	0.039	0.835	0.040	0.0752	0.093	0.006	<0.0001
22	1.219	0.051	1.038	0.055	0.0225	0.102	0.008	<0.0001
23	1.564	0.065	1.239	0.056	0.0005	0.106	0.008	<0.0001
24	2.167	0.109	1.559	0.071	<0.0001	0.113	0.009	<0.0001
25	3.001	0.125	2.047	0.096	<0.0001	0.130	0.010	<0.0001
26	nd	nd	nd	nd	nd	nd	nd	nd
27	5.816	0.431	3.757	0.217	<0.0001	0.166	0.012	<0.0001
28	7.758	0.528	5.299	0.393	0.0005	0.184	0.013	<0.0001
29	9.595	0.665	6.893	0.571	0.0039	0.215	0.015	<0.0001
30	12.247	0.659	9.924	0.854	0.0417	0.266	0.021	<0.0001

Supplemental Table 3: Relative growth rate (RGR) of col-0, *re-6*, and *cue1* plants. RGRs were calculated between subsequent observation points.

	Relative Growth Rate (RGR)							
	col-0		*re-6*		col-0/*re-6*	*cue1*		col-0/*cue1*
d.p.g.	Average	± S.E.	Average	± S.E	p-value	Average	± S.E	p-value
21 to 22	31.74	5.57	30.55	5.28	0.8781	30.74	5.57	0.9265
22 to 23	19.69	3.06	27.77	2.24	0.0413	16.69	3.06	0.7797
23 to 24	31.54	4.99	34.63	4.93	0.6628	21.94	4.65	0.2104
24 to 25	27.73	1.15	37.83	4.52	0.0257	47.37	10.63	0.0888
25 to 27	29.85	3.13	31.38	3.75	0.6853	35.46	9.22	0.6282
27 to 28	40.80	6.18	27.99	0.98	0.0496	29.98	7.46	0.3228
28 to 29	29.22	4.36	21.08	1.60	0.1040	26.43	6.46	0.7492
29 to 30	35.30	4.43	27.86	2.05	0.1716	33.61	7.09	0.8446

Supplemental Table 4: F_v/F_m of col-0, *re-6*, and *cue1* plants. Plants were monitored for 10 days, beginning at 21 days post germination (21 dpg). Errors are indicated as S.E. n > 15. nd: data points were not determined.

	F_v/F_m							
	col-0		*re-6*			*cue1*		col-0/*cue1*
dpg	Average	± S.E.	Average	± SE	± S.E.	Average	± S.E.	p-value
21	0.76	0.00	0.77	0.00	<0.0001	0.64	0.00	<0.0001
22	0.76	0.00	0.77	0.00	<0.0001	0.65	0.00	<0.0001
23	0.77	0.00	0.77	0.00	<0.0001	0.65	0.00	<0.0001
24	0.77	0.00	0.77	0.00	0.0034	0.66	0.00	<0.0001
25	0.77	0.00	0.78	0.00	<0.0001	0.67	0.00	<0.0001
26	nd	nd	nd	nd	nd	nd	0.00	<0.0001
27	0.77	0.00	0.77	0.00	0.5637	0.67	0.00	<0.0001
28	0.77	0.00	0.77	0.00	0.5931	0.67	0.00	<0.0001
29	0.77	0.00	0.77	0.00	0.3821	0.67	0.00	<0.0001
30	0.77	0.00	0.76	0.00	0.0928	0.67	0.01	<0.0001

Supplemental Table 5: Steady state cytokinin contents of eight-week old rosettes of col-0, *re-6*, and *cue1* before flowering. Plants were grown under 12-h/12-h light/dark cycle at 100 μ E/m^2/s. Samples were taken in the middle of the light period. S.E. is shown. Asterisks (*) indicate the significance level. n = 5. Abbreviations according to (Novák et al., 2008). tZ = *trans*-zeatin; cZ: *cis*-zeatin; iP: N_6-(Δ^2-isopently)adenine; DHZ: dihydrozeatin; R: riboside; OG: *O*-glucoside; 7G: 7-glucoside; 9G: 9-glucoside; 5`MP: 5`-monophosphate.

Cytokinin	col-0 [pmol/g]		*re-6* [pmol/g]		p-value	Sig. Lev.	*cue1* [pmol/g]		p-value	Sig. Lev.
	Average	± S.E.	Average	± S.E.			Average	± S.E.		
tZ	1.363	0.111	1.607	0.046	0.0782	ns	0.702	0.059	0.0008	***
tZOG	11.544	0.686	10.533	0.917	0.4030	ns	7.407	0.388	0.0008	***
tZR	0.371	0.032	0.950	0.095	0.0004	***	0.216	0.014	0.0022	**
tZROG	1.783	0.117	2.283	0.125	0.0192	*	2.204	0.090	0.0212	*
tZ7G	129.250	5.399	126.270	2.354	0.6266	ns	156.360	2.967	0.0023	**
tZ9G	22.987	1.474	20.841	0.877	0.2462	ns	22.466	0.880	0.7692	ns
tZR5`MP	11.311	0.846	13.282	0.708	0.1118	ns	2.081	0.133	<0.0001	***
Total *trans* cytokinins	178.61	7.73	175.77	4.41	0.7575	ns	175.766	4.412	0.7575	ns
cZ	0.036	0.004	0.037	0.003	0.8864	ns	0.124	0.016	0.0007	***
cZOG	0.636	0.062	0.547	0.038	0.2582	ns	1.014	0.124	0.0259	*
cZR	0.154	0.017	0.193	0.016	0.1318	ns	0.610	0.053	<0.0001	***
cZROG	1.173	0.088	1.449	0.054	0.0284	*	2.822	0.079	<0.0001	***
cZ9G	0.110	0.009	0.133	0.005	0.0546	ns	0.774	0.037	<0.0001	***
cZR5`MP	1.828	0.089	1.880	0.094	0.6983	ns	1.437	0.093	<0.0162	*
Total *cis* cytokinins	3.937	0.214	4.238	0.085	0.2259	ns	6.782	0.160	<0.0001	***
DHZ	0.013	0.002	0.015	0.002	0.4615	ns	0.008	0.001	0.0237	*
DHZOG	0.159	0.012	0.173	0.024	0.6162	ns	0.103	0.011	0.0092	**
DHZR	0.040	0.003	0.112	0.011	0.0002	***	0.072	0.006	0.0012	**
DHZROG	0.037	0.005	0.120	0.008	0.0000	***	0.104	0.010	0.0003	***
DHZ7G	17.521	0.783	16.798	0.663	0.5008	ns	13.152	0.298	0.0008	***
DHZ9G	0.141	0.005	0.136	0.006	0.6124	ns	0.108	0.005	0.0026	**
DHZR5`MP	0.068	0.005	0.097	0.013	0.0755	ns	0.040	0.007	0.0132	*
Total dehydro cytokinins	17.979	0.789	17.452	0.693	0.6292	ns	13.238	0.133	0.0040	**
iP	0.276	0.021	0.237	0.030	0.3156	ns	0.195	0.018	0.0179	*
iPR	0.361	0.042	0.386	0.051	0.7140	ns	0.161	0.018	0.0023	**
iP7G	24.450	0.884	30.509	1.826	0.0174	*	64.734	1.478	<0.0001	***
iP9G	0.592	0.009	0.722	0.057	0.0548	ns	0.704	0.025	0.0032	**
iPR5`MP	3.470	0.238	4.992	0.175	0.0009	***	1.165	0.120	<0.0001	***
Total isopentyl cytokinins	29.150	0.755	36.846	1.884	**	0.053	66.958	1.461	<0.0001	***
Total cytokinins	229.674	8.214	234.301	5.000	0.6433	ns	267.856	6.141	0.0058	**

Supplemental Table 6: Steady state auxin contents of eight-week old rosettes of col-0, *re-6*, and *cue1* before flowering. Plants were grown under 12-h/12-h light/dark cycle at 100 µE/m^2/s. Samples were taken in the middle of the light period. S.E. is shown. Asterisks (*) indicate the significance level. n = 4. IAA: indole-3 acetic acid; IAAsp: indole-3-acetyl-aspartate; IAAGlu: indole-3-acetyl-glutamate.

Auxin	col-0 [pmol/g]		*re-6* [pmol/g]		p-value	Sig. Lev.	*cue1* [pmol/g]		p-value	Sig. Lev.
	Aver.	± S.E.	Aver.	± S.E.			Aver.	± S.E.		
IAA	63.541	5.173	82.115	4.919	0.0315	*	118.320	8.305	0.0005	***
IAAsp	3.499	0.325	4.814	0.338	0.0230	*	18.520	0.902	<0.0001	***
IAAGlu	1.436	0.095	2.580	0.306	0.0073	**	12.010	0.953	<0.0001	***
Total auxins	68.477	5.326	89.509	5.364	0.0238	*	148.845	9.468	<0.0001	***

Supplemental Table 7: Relative steady state metabolite levels of eight-week old rosettes of col-0, *re-6*, and *cue1* before budding and flowering. Plants were grown under 16-h/8-h and 12-h/12-h light/dark cycle at µE/m^2/s. Samples were taken in the middle of the light period. Error bars represent S.E. Asterisks indicate significance levels. n ≥ 4. Numbers in brackets indicate deviating replicate numbers. Values at each condition are not comparable among each other.

	16-h light/8-h dark FW basis						**12-h light/12-h dark FW basis**					
Metabolite	col-0		*re-6*		p-value	sig. lev.	col-0		*re-6*		p-value	sig. lev.
	Aver.	± S.E.	Aver.	± S.E.			Aver.	± S.E.	Aver.	± S.E.		
α-alanine	91.96	5.46	167.44	4.48	<0.0001	***	3.483	0.897	6.147	0.402	0.0266	*
leucine	1.88	0.14	2.67	0.16	0.0054	**	0.059	0.002	0.080	0.011	0.1100	ns
valine	11.50	0.28	15.96	0.81	0.0008	***	0.340	0.010	0.457	0.049	0.0467	*
glutamate	134.26	9.67	179.61	12.19	0.0195	*	11.321	0.428	9.766	0.768	0.1147	ns
aspartate	36.39	0.96	45.56	3.43	0.0212	*	8.408	0.369	7.109	1.214	0.3358	ns
asparagine	11.03	1.00	16.99	1.57	0.0125	*	0.272	0.014	0.296	0.042	0.6010	ns
isoleucine	2.66	0.14	4.00	0.21	0.00007	***	0.092	0.003	0.112	0.013	0.1798	ns
lysine	1.72	0.12	1.34	0.09	0.0364	*	0.066	0.003	0.039	0.005	0.0017	**
methionine	1.42	0.07	2.34	0.27	0.0106	*	0.096	0.003	0.092	0.004	0.4373	ns
cysteine	0.19	0.02	0.15	0.04	0.3396	ns	0.007	0.0008	0.009	0.001	0.1958	ns
phenylalanine	2.40	0.60	3.76	0.13	0.0585	ns	0.117	0.002	0.125	0.005	0.2537	ns
threonine	33.38	1.24	42.47	2.41	0.0100	*	nd	nd	nd	nd	nd	nd
tryptophan	nd	nd	nd	nd	nd	nd	0.071	0.010	0.059	0.004	0.2598	ns
tyrosine	0.20	0.02	0.21	0.01	0.7143	ns	0.023	0.002	0.028	0.003	0.1315	ns
glycine	22.46	0.07	41.28	4.91	0.0050	**	2.658	0.279	2.242	0.392	0.4125	ns
serine	135.23	5.41	156.74	4.96	0.0190	*	10.189	0.280	10.939	1.685	0.6723	ns
β-alanine	0.31	0.03	0.32	0.02	0.8655	ns	0.038	0.003	0.039	0.005	0.8642	ns
GABA	0.75	0.13	0.56	0.07	0.2383	ns	0.011	0.001	0.011	0.002	0.8920	ns
shikimate	12.23	0.64	16.16	0.42	0.0009	***	0.701	0.015	0.635	0.019	0.0230	*
glucose	12.93	0.54	18.00	0.99	0.0020	**	1.656	0.316	1.987	0.271	0.4506	ns
fructose	5.99	0.72	9.13	0.91	0.0263	*	0.473	0.018	0.481	0.046	0.8748	ns
xylose	1.06	0.05	1.27	0.08	0.0429	*	0.059	0.003	0.059	0.005	0.9369	ns
myo-inositol	111.29	10.84	118.97	5.15	0.5398	ns	8.394	0.169	7.018	0.534	0.0394	*
mannitol	4.87	0.25	5.53	0.61	0.3511	ns	0.216	0.011	0.251	0.026	0.2495	ns
sorbitol	0.13	0.02	0.16	0.02	0.1304	ns	0.078	0.006	0.063	0.010	0.2411	ns
glycerol	24.49	1.01	29.02	0.67	0.0058	**	1.955	0.020	1.870	0.075	0.1440	ns
sucrose	865.79	15.90	976.33	29.96	0.0115	*	44.051	1.514	46.373	1.371	0.2884	ns
maltose	4.30	0.25	7.22	0.48	0.0007	***	0.210	0.017	0.218	0.011	0.7196	ns
lactose	0.13	0.02	0.16	0.02	0.1304	ns	0.005	0.001	0.006	0.001	0.4792	ns
glycerate	10.70	1.01	10.74	2.62	0.9880	ns	0.535	0.031	0.399	0.021	0.0066	**
lactate	30.54	2.01	26.26	2.88	0.2583	ns	1.549	0.051	1.345	0.206	0.3692	ns
α-ketoglutarate	0.33	0.02	0.50	0.07	0.0483	*	0.031	0.003	0.029	0.003	0.7267	ns
fumarate	845.17	33.95	838.26	37.07	0.8942	ns	54.584	2.095	48.657	2.063	0.0786	ns
succinate	8.42	0.51	8.81	0.52	0.6055	ns	0.407	0.008	0.365	0.008	0.0050	**
glycolic acid	8.03	0.45	9.74	0.98	0.1514	ns	0.344	0.037	0.406	0.057	0.3935	ns
gluconic acid	0.79	0.03	1.03	0.08	0.0209	*	0.003	0.001	0.007	0.003	0.2719	ns
maleic acid	4.48	0.53	5.25	0.32	0.2487	ns	0.218	0.016	0.215	0.024	0.9150	ns
malic acid	225.32	6.79	226.01	17.16	0.9713	ns	9.509	0.559	8.007	0.816	0.1675	ns

	16-h light /8-h dark leaf area basis						**12-h light/12-h dark leaf area basis**					
Metabolite	col-0		*re-6*		p-value	sig. lev.	col-0		*re-6*		p-value	sig. lev.
	Aver.	± S.E.	Aver.	± S.E.			Aver.	± S.E.	Aver.	± S.E.		
α-alanine	28948.38	1373.21	35714.47	1986.42	0.0251	*	92.50	19.41	115.81	14.47	0.3685	ns
leucine	169.28	23.04	225.34	17.47	0.0797	ns	0.79	0.13	0.73	0.11	0.7390	ns
valine	1318.77	133.53	1960.21	105.31	0.0040	**	4.35	0.82	4.95	0.56	0.5576	ns
glutamate	6876.68	555.13	12772.77	1382.09	0.0052	**	75.98	20.76	103.93	13.07	0.2832	ns
aspartate	3389.82	564.17	5050.00	485.46	0.0515	ns	99.29	27.80	135.90	21.68	0.3378	ns
asparagine	448.46	37.15	826.13	66.20	0.0011	**	1.14	0.36	1.88	0.30	0.1714	ns
isoleucine	235.32	28.22	355.98	19.56	0.0056	**	1.13	0.19	1.20	0.19	0.8151	ns
lysine	252.72	18.10	175.50	15.88	0.0105	*	0.61 (2)	0.05	0.34	0.05	0.0279	*
methionine	102.43	5.80	210.59	21.73	0.0017	**	0.81	0.17	1.03	0.13	0.3605	ns
cysteine	15.26	2.66	20.52	2.57	0.1914	ns	0.06	0.01	0.09	0.01	0.1149	ns
phenylalanine	405.68	19.27	564.99	24.75	0.0008	***	1.28	0.26	1.62	0.21	0.3416	ns
threonine	4467.57	80.84	4777.71	605.93	0.6563	ns	nd	nd	nd	nd	nd	nd
tryptophan	nd	nd	nd	nd	nd	nd	0.62	0.09	0.66	0.09	0.7547	ns
tyrosine	30.89	6.71	26.79	2.71	0.5589	ns	0.10	0.05	0.20	0.03	0.1159	ns
glycine	2605.91	97.67	7345.80	895.67	0.0010	**	103.93	13.07	36.93	8.76	0.0051	**
serine	15016.28	684.81	17155.29	1376.33	0.2251	ns	99.49	29.24	124.08	10.94	0.4150	ns
β-alanine	76.13	3.78	72.69	7.68	0.7155	ns	0.32	0.13	0.61	0.06	0.0763	ns
GABA	181.61	18.30	134.29	24.11	0.1656	ns	0.04	0.02	0.07	0.03	0.4778	ns
shikimate	1765.01	61.77	2423.76	165.33	0.0073	**	5.75	1.13	7.87	1.02	0.2239	ns
glucose	3329.98	258.26	5142.66	572.45	0.0249	*	13.38	4.57	10.71	2.57	0.6085	ns
fructose	1329.92	99.61	1708.41	182.20	0.1203	ns	4.53	1.39	5.02	0.55	0.7312	ns
xylose	167.50	15.68	175.30	8.77	0.6601	ns	0.48	0.13	0.61	0.02	0.2522	ns
myo-inositol	16992.56	932.10	13083.37	1267.74	0.0405	*	80.08	19.93	91.61	9.03	0.5780	ns
mannitol	1444.29	311.69	1326.95	144.98	0.7254	ns	1.92	0.45	3.83	0.67	0.0814	ns
sorbitol	107.31	22.17	104.72	4.68	0.0903	ns	0.36	0.04	0.48	0.04	0.0874	ns
glycerol	4386.22	270.51	4130.74	171.42	0.4299	ns	20.26	4.67	27.71	5.92	0.3955	ns
sucrose	159309.7	9147.16	151523.0	8294.57	0.5437	ns	592.28	146.62	644.17	69.08	0.7392	ns
maltose	920.56	171.92	1190.07	225.68	0.2629	ns	1.31	0.34	2.05	0.21	0.1070	ns
lactose	18.90	5.49	24.93	2.47	0.3147	ns	0.06	0.03	0.06	0.01	0.9497	ns
glycerate	2065.22	197.52	1985.05	114.87	0.7226	ns	4.58	1.24	5.93	0.46	0.2977	ns
lactate	7044.67	699.58	5493.05	318.05	0.0604	ns	16.32	3.65	43.30	24.92	0.4045	ns
α-ketoglutarate	38.85	2.84	53.29	2.41	0.0036	**	0.31	0.05	0.41	0.01	0.0653	ns
fumarate	110262.7	4564.4	113050.3	5585.62	0.7160	ns	655.94	134.57	711.12	74.73	0.7158	ns
succinate	889.90	92.87	731.02	61.57	0.1753	ns	3.38	0.74	2.78	0.97	0.6627	ns
glycolic acid	1332.50	119.91	1309.15	158.63	0.8862	ns	9.99	0.30	9.28	0.73	0.3133	ns
gluconic acid	82.21	5.67	110.1	6.04	0.0091	**	0.003	0.001	0.007	0.003	0.2719	ns
maleic acid	746.66	119.57	746.87	46.76	0.9986	ns	3.13	0.54	3.05	0.18	0.8804	ns
malic acid	27470.10	3079.74	23732.19	1237.55	0.2584	ns	107.18	23.60	123.57	14.18	0.5548	ns

Supplemental Table 8: Total amino acid levels of eight-week old rosettes of col-0, *re-6*, and *cue1* before budding and flowering. Plants were grown under 16-h/8-h and 12-h/12-h light/dark cycle at 100 μ E/m^2/s. Samples were taken in the middle of the light period.. Error bars represent S.E. Asterisks indicate significance levels. n ≥ 4. Sample values at each condition are not comparable among each other.

Total amino acids at	Average (col-0)	± S.E.	Average *(re-6*)	± S.E.	p-value	Sig. lev.
16-h light/8-h dark FW basis	453.30	16.77	639.01	20.85	0.0001	***
12-hlight/12-h dark FW basis	36.03	1.90	37.17	3.87	0.9042	ns
16-h light/8-h dark leaf area basis	59815.89	2351.61	82404.39	5303.78	0.0056	**
12-h light/12-h dark leaf area basis	396.50	103.29	527.81	67.70	0.3158	ns

Supplemental Table 9: Relative steady state metabolite levels of eight week old rosettes of col-0, *re-6*, and *cue1* before budding and flowering. Time course metabolite profiling during 16-h/8-h light/dark cycle with sampling in the middle of the light period (14:00), one hour before dark (21:00), middle of the dark period (2:00), and one hour before the light period (5:00). Error bars represent S.E. Asterisks indicate significance levels. n ≥ 4. Numbers in brackets indicate deviating replicate numbers.Sample values at each condition are not comparable among each other.

	21:00						2:00						5:00					
	col-0		re-6		Col-0/re-6		col-0		re-6		Col-0/re-6		col-0		re-6		Col-0/re-6	
metabolite	Aver.	S.E.	Aver.	S.E.	p-val.	sig lev.	Aver.	S.E.	Aver.	S.E.	p-val.	sig lev.	Aver.	S.E.	Aver.	S.E.	p-val.	sig lev.
α-alanine	504.02	29.68	614.09	53.83	0.1111	ns	400.31	23.82	416.98	43.24	0.7443	ns	347.57	29.88	435.12	30.12	0.0730	ns
leucine	9.48	2.12	9.01	0.41	0.8337	ns	7.82	0.52	8.00	0.74	0.8468	ns	6.51	0.56	7.84	0.40	0.0886	ns
valine	53.03	3.66	65.39	4.32	0.0605	ns	46.93	1.98	50.94	3.03	0.2996	ns	45.22	2.69	53.21	2.91	0.0744	ns
glutamate	1103.20	53.03	1514.41	79.94	0.0027	**	1232.32	69.11	966.49	38.17	0.0144	*	931.08	18.18	833.81	100.41	0.3684	ns
proline	52.91	7.59	80.02	11.63	0.0868	ns	48.15	10.66	37.83	11.50	0.5290	ns	27.85	9.69	22.94	3.79	0.6496	ns
aspartate	196.54	9.50	272.16	12.50	0.0025	**	191.79	20.06	146.92	8.24	0.0724	ns	118.94	5.56	120.82	13.98	0.9036	ns
isoleucine	13.24	1.97	16.04	0.92	0.2348	ns	7.71	0.51	8.20	0.65	0.5678	ns	6.90	0.79	8.29	0.82	0.2591	ns
lysine	5.407	0.99	2.47	0.31	0.0220	*	6.14	0.77	3.93	0.39	0.0337	*	5.10	0.61	3.03	0.44	0.0256	*
methionine	5.33	0.59	4.91	0.46	0.5857	ns	2.72	0.43	1.42	0.20	0.0423	*	0.98	0.09	1.34	0.16	0.1086	ns
phenylalanine	20.28	2.25	21.78	0.89	0.5531	ns	8.56	0.76	8.22	0.46	0.7082	ns	6.43	0.08	6.95	0.26	0.1342	ns
glycine	101.47	13.16	134.09	13.62	0.1233	ns	36.49	10.56	33.19	5.11	0.7856	ns	18.28	1.83	22.20	2.39	0.2288	ns
serine	274.11	36.64	239.52	18.35	0.4232	ns	126.65	30.82	116.10	8.58	0.7501	ns	64.07	3.28	76.65	11.29	0.3159	ns
(iso)-citric acid	472.47	51.07	463.62	37.03	0.8919	ns	701.80	58.18	320.23	66.12	0.0025	**	645.25	40.57	478.38	33.63	0.0133	*
shikimate	50.20	1.31	57.47	1.61	0.0081	**	42.56	1.38	48.52	1.23	0.0119	*	45.82	1.82	50.44	0.74	0.0471	*
glucose	110.16	15.97	131.07	20.17	0.4400	ns	162.05	32.71	155.21	14.31	0.8529	ns	98.26	7.57	139.78	15.02	0.0573	ns
fructose	41.35	5.26	42.12	5.02	0.9177	ns	30.97	4.90	21.32	3.52	0.1605	ns	22.14	4.59	21.88	2.63	0.9609	ns
xylose	4.37	0.24	4.04	0.53	0.5532	ns	3.87	0.23	4.02	0.24	0.6589	ns	3.83	0.18	4.09	0.31	0.4778	ns
myoinositol	315.37	13.56	288.20	18.12	0.2641	ns	342.45	30.52	340.48	18.50	0.9573	ns	354.08	12.75	320.83	13.66	0.1129	ns
maltose	36.75	2.55	51.18	3.88	0.0145	*	124.72	11.74	159.63	10.94	0.0613	ns	105.40	8.82	125.81	9.11	0.1462	ns
sucrose	4159.79	178.64	4543.90	86.10	0.0888	ns	3648.43	229.99	3692.88	71.45	0.8581	ns	3460.99	90.21	3154.27	132.68	0.0923	ns
raffinose	3.69	0.63	1.94	0.19	0.0285	*	3.19	1.79	4.22	0.73	0.6084	ns	3.00	0.94	2.58	0.30	0.6786	ns
lactate	116.08	19.77	199.12	30.91	0.0535	ns	1456.63	67.04	1636.61	32.39	0.0420	*	1597.44	30.23	1691.41	61.79	0.2091	ns
succinate	36.84	2.68	31.79	1.52	0.1394	ns	43.02	6.32	34.96	3.62	0.3004	ns	47.16	3.30	41.87	2.20	0.2199	ns
fumarate	3083.23	199.18	2847.37	84.57	0.3075	ns	2346.65	224.66	1921.58	282.38	0.2727	ns	1964.16	227.61	1762.51	263.20	0.4656	ns
glycerol	1295.01	49.80	1384.64	28.28	0.4562	ns	1456.63	67.04	1636.61	32.39	0.0420	*	1597.44	30.23	1691.41	61.79	0.2091	ns
glycerate	29.39	3.73	31.79	1.79	0.5774	ns	5.50	0.56	4.81	0.47	0.3754	ns	4.50	0.25	4.51	1.02	0.9904	*
glycolic acid	50.59	3.19	54.16	5.96	0.5756	ns	30.59	1.61	27.13	2.00	0.2146	ns	22.84	0.68	35.32	5.37	0.0348	*
maleic acid	27.88	4.08	29.13	1.92	0.7885	ns	22.31	3.59	11.25	1.76	0.0244	*	15.70	0.86	12.26	1.33	0.0622	ns
malic acid	868.32	88.53	847.09	21.34	0.08215	ns	521.32	60.12	298.28	56.49	0.0268	*	375.39	38.85	264.65	22.65	0.0391	*
hydroxyglutarate	2.21	0.31	2.91	0.34	0.1637	ns	1.74	0.36	1.75	0.31	0.9963	ns	1.91	0.32	2.12	0.573	0.7488	ns

	14:00						21:00						2:00					
	col-0		re-6		Col-0/re-6		col-0		re-6		Col-0/re-6		col-0		re-6		Col-0/re-6	
metabolite	Aver.	S.E.	Aver.	S.E.	p-val.	sig lev.	Aver.	S.E.	Aver.	S.E.	p-val.	sig lev.	Aver.	S.E.	Aver.	S.E.	p-val.	sig lev.
α-alanine	577.54	57.20	678.66	82.17	0.3421	ns	424.28	33.56	603.72	58.28	0.0284	*	521.72	21.14	446.31	39.08	0.6246	ns
leucine	7.84	0.48	9.19	0.67	0.1411	ns	7.08	1.13	9.72	0.76	0.0839	ns	8.61	0.37	10.86	1.35	0.1935	ns
valine	47.18	2.38	56.21	4.79	0.1644	ns	47.05	1.23	46.20	3.28	0.8317	ns	47.05	1.23	62.87	5.58	0.0432	*
glutamate	931.08	18.18	833.81	100.41	0.3684	ns	1320.33	79.20	1375.93	61.99	0.5955	ns	1233.76	105.09	1342.76	65.75	0.4130	ns
proline	38.20	5.44	47.69	10.96	0.4605	ns	47.69	10.96	34.17	4.95	0.2938	ns	56.25	7.31	60.90	5.81	0.6289	ns
aspartate	172.90	8.62	139.96	40.97	0.3437	ns	223.80	10.12	275.19	14.88	0.0290	*	148.30	20.07	200.40	12.50	0.0560	ns
isoleucine	11.97	0.94	16.32	0.97	0.0123	*	9.68	1.03	13.61	0.67	0.0127	*	8.31	0.73	9.64	1.02	0.3471	ns
lysine	5.67	0.38	3.14	0.79	0.0206	*	5.32	0.20	3.10	0.28	0.0002	***	5.44	0.30	3.29	0.43	0.0063	**
methionine	4.34	0.75	3.24	1.02	0.4106	ns	4.59	0.34	5.56	0.46	0.1242	ns	4.59	0.34	5.56	0.46	0.1242	ns
phenylalanine	8.82	0.71	9.08	0.62	0.7851	ns	19.91	0.90	21.44	0.96	0.2816	ns	8.99	0.23	9.05	0.64	0.9435	ns
glycine	132.28	19.92	138.85	17.81	0.8120	ns	183.66	27.81	212.45	21.10	0.4335	ns	55.03	8.28	51.16	11.41	0.8019	ns
serine	274.36	18.27	238.00	50.09	0.4789	ns	336.27	50.15	295.08	39.55	0.5370	ns	152.41	24.81	129.36	23.10	0.5339	ns
(iso)-citric acid	318.67	29.11	289.93	48.04	0.6058	ns	583.52	22.91	636.47	45.42	0.3283	ns	871.09	75.42	766.26	92.74	0.4267	ns
shikimate	48.37	3.57	58.21	3.02	0.0686	ns	44.70	1.51	49.93	2.34	0.0975	ns	49.86	3.41	51.04	5.01	0.8597	ns
glucose	163.50	15.69	153.55	20.87	0.7132	ns	155.78	19.51	232.36	36.76	0.1331	ns	242.48	41.88	207.43	47.69	0.6086	ns
fructose	25.73	4.11	28.01	3.73	0.6926	ns	84.81	27.89	86.67	10.18	0.9564	ns	46.41	8.54	36.04	7.09	0.3768	ns
xylose	4.10	0.35	4.77	0.37	0.2260	ns	3.23	0.46	3.29	0.20	0.9157	ns	3.58	0.13	3.38	0.23	0.5112	ns
myoinositol	394.76	11.17	345.71	25.63	0.1147	ns	356.17	20.38	321.16	20.26	0.2684	ns	385.36	27.51	315.84	21.37	0.0817	ns
maltose	31.13	0.59	46.50	5.25	0.0195	*	35.93	1.93	56.97	6.54	0.0149	*	165.30	17.64	268.11	30.94	0.0315	*
sucrose	2734.67	125.96	2952.61	223.76	0.4784	ns	4245.09	135.30	4335.93	53.28	0.5496	ns	3814.20	179.54	3674.48	149.59	0.5545	ns
raffinose	5.07	0.94	7.17	1.93	0.3291	ns	5.63	0.48	2.99	0.74	0.0257	*	3.13 (3)	0.58	3.72	1.42	0.7704	ns
lactate	1767.87	16.68	1827.54	65.73	0.4045	ns	1320.33	79.20	1375.93	61.99	0.5955	ns	1603.08	45.97	1692.01	68.38	0.3429	ns
succinate	39.52	5.23	32.33	4.68	0.3358	ns	35.84	4.20	27.97	1.87	0.1256	ns	52.74	2.20	41.97	5.76	0.1574	ns
fumarate	1868.59	199.00	2076.53	59.07	0.3458	ns	3494.42	160.45	2927.03	115.35	0.0208	*	2687.66	140.07	2221.97	119.48	0.0384	*
glycerol	1767.87	16.68	1827.54	65.73	0.4045	ns	1320.33	79.20	1375.93	61.99	0.5955	ns	1603.08	45.97	1692.01	68.38	0.3429	ns
glycerate	32.38	1.19	32.43	2.69	0.9689	ns	30.50	2.36	29.81	1.52	0.8122	ns	7.79	0.77	4.86	0.63	0.0206	*
glycolic acid	32.68	2.52	38.85 (4)	4.14	0.2958	ns	36.75	2.60	34.44	1.49	0.4618	ns	42.46	4.08	29.27	1.86	0.0156	*
maleic acid	26.82	3.25	18.13	1.66	0.0444	*	37.43	1.84	31.67	2.45	0.0973	ns	34.73	1.89	22.69	2.18	0.0049	**
malic acid	498.12	36.31	487.20	51.58	0.8669	ns	959.26	34.47	832.59	28.65	0.0277	*	562.24	99.12	461.45	43.62	0.3476	ns
hydroxyglutarate	1.70	0.27	2.25	0.66	0.4614	ns	2.63	0.388	2.00	0.180	0.1803	ns	2.66	0.09	1.69	0.13	0.0007	***

Supplemental Table 10: Steady state purine contents of eight week old rosettes of col-0, *re-6*, and *cue1* before flowering. Plants were grown under 12-h/12-h light/dark cycle at 100 μ E/m^2/s. Samples were taken in the middle of te light period. Error bars represent S.E. Asterisks (*) indicate the significance level. n(col) = 4, n (*re-6*) = 5. ade: adenine; ado: adenosine; gua: guanine; guo: guanosine; hyp: hypoxanthine; ino: inosine; xan: xanthine; xao: xanthosine.

Purine/purine derivate	col-0 [pmol/g]		*re-6* [pmol/g]		p-value	Sig. lev.	*cue1* [pmol/g]		p-value	Sig. lev.
	Aver.	± S.E.	Aver.	± S.E.			Aver.	± S.E.		
Ade	5031.707	445.948	6363.488	482.926	0.0884	ns	8345.488	545.817	0.0027	**
Ado	342.741	51.640	489.659	25.178	0.0289	*	553.061	31.391	0.0082	**
Gua	113.315	29.371	108.753	20.681	0.0074	ns	556.360	102.463	0.0074	**
Guo	3695.770	482.680	3628.998	634.730	0.9385	ns	5157.996	608.424	0.1139	ns
Hyp	229.905	39.539	158.383	17.101	0.1152	ns	462.643	70.209	0.0316	*
Ino	574.058	112.228	495.765	75.866	0.5684	ns	653.694	135.885	0.6764	ns
Xan	1856.396	142.049	1831.015	65.033	0.8659	ns	2952.108	233.565	0.0072	**
Xao	1008.160	33.741	1315.304	148.814	0.1161	ns	3237.691	298.742	0.0003	***
Total auxins	12582.051	528.899	14391.365	697.687	0.1373	ns	21918.587	1120.578	0.0003	***

Supplemental Table 11: Chlorophyll (Chl) concentrations and Chl a/ Chl b ratio of col-0 and *re-6*.

	Average (Col-0)	± S.E.	Average (*re-6*)	± S.E.	p-value	Sig. level
Chl a	0.246	0.009	0.212	0.007	0.0099	**
Chl b	0.080	0.003	0.069	0.002	0.0081	**
Total Chl	0.328	0.012	0.282	0.008	0.0093	**
Chl a/ Chl b	3.068	0.014	3.048	0.022	0.4315	ns

Supplemental Table 12: Gene-specific primers used for cloning. Restriction sites (RS) are underlined, start-ATG and stop codons are in bold. Further properties are indicated in the column "comments". FP = forward primer, RP = reverse primer. Lowercase letters indicate spacer sequence, which are necessary to be in frame with a tag in the final vector.

Name	Sequence in 5`- 3`- orientation	Direction	Comments
CR1	*GGGGACAAGTTTGTACAAAAAAGCAGGCT*ccacc**ATG**GCAGGATGTGCAATG	FP	Italic: attR1
CR2	*GGGGACCACTTTGTACAAGAAAGCTGGGT***TCA**CTGACAACCGCTCAATC	RP	Italic: attR2
CR4	*GGGGACCACTTTGTACAAGAAAGCTGGGT*cCTGACAACCGCTCAATCTTG	RP	Italic: attR2
CR6	*GGGGACAAGTTTGTACAAAAAAGCAGGCT*ccacc**ATG**GGTGGTTCAGGTAGGCAAAG	FP	Italic: attR1
CR19	*GGGGACCACTTTGTACAAGAAAGCTGGGTC***TTA**CCGTTTGGCAGTCATGATAAGAT	RP	Italic: attR2
CR39	TTCAATGTCCCTGCCATGTA	FP	-
CR40	TGAACAATCGATGGACCTGA	RP	-
CR43	GGATATGTCCTGCGGGTAAA	FP	-
CR47	ATTTGTGTACGCCCGACAGT	RP	-
CR48	AAAGATTTCTGGGCGGAGTT	FP	-
CR49	ATTGCCAAATGTTTGAACGA	RP	-
CR51	CTATGGAGGGAGTGCCTTACC	FP	-
CR52	TACCACACGTGCAAGAGACTG	RP	-
CR53	ATTTTGCCGATTTCGGAAC	-	LBb1.3 T-DNA primer
CR116	*GGGGACCACTTTGTACAAGAAAGCTGGGT*cTCTAATCCGCAAAACAGGCA	RP	-
CR161	ATGGCAGGATGTGCAATGAAT	FP	-
CR162	TCACTGACAACCGCTCAATCTT	RP	-
F	ATCTTATCATGACTGCCAAACG	FP	-
R1	ACATGACCCTTTCGATTTTAGC	RP	-
R2	ACCGGGATGTTCTCTTCTGA	RP	-

Supplemental Data

These tables will be provided as EXCEL files in the publication.

Supplemental Data1. Genes co-regulated with *RE* (At2g33786). 500 top hits inferred from the Atted-II database. n.a.: not assigned. *Arabidopsis* genome identifier.

AGI	Name	Annotation
At2g37860	LCD1	LCD1 (LOWER CELL DENSITY 1)
At1g19920	APS2	APS2; sulfate adenylyltransferase (ATP)
At1g33040	NACA5	NACA5 (NASCENT POLYPEPTIDE-ASSOCIATED COMPLEX SUBUNIT ALPHA-LIKE PROTEIN 5)
At5g47630	mtACP3	mtACP3 (mitochondrial acyl carrier protein 3); acyl carrier/ cofactor binding
At3g49680	BCAT3	BCAT3 (BRANCHED-CHAIN AMINOTRANSFERASE 3); branched-chain-amino-acid transaminase/ catalytic
At5g17630	translocator	glucose-6-phosphate/phosphate translocator, putative
At1g31230	AK-HSDH I	AK-HSDH I (ASPARTATE KINASE-HOMOSERINE DEHYDROGENASE I); aspartate kinase/ homoserine dehydrogenase
258365_s_at	n.a.	At5g11880;At3g14390
At5g03300	ADK2	ADK2 (ADENOSINE KINASE 2); adenosine kinase/ copper ion binding / kinase
259138_s_at	n.a.	At5g04130;At3g10270
At5g36950	DegP10	DegP10 (DegP protease 10); catalytic/ protein binding / serine-type endopeptidase/ serine-type peptidase
At2g36230	APG10	APG10 (ALBINO AND PALE GREEN 10); 1-(5-phosphoribosyl)-5-[(5-phosphoribosylamino)methylideneamino]imidazole-4-carboxamide isomerase
At4g30020	subtilase	subtilase family protein
At1g79560	FTSH12	FTSH12 (FTSH PROTEASE 12); ATP-dependent peptidase/ ATPase/ metallopeptidase
At3g52940	FK	FK (FACKEL); delta14-sterol reductase
At3g20790	oxidoreductase	oxidoreductase family protein
At2g22230	dehydratase	beta-hydroxyacyl-ACP dehydratase, putative
At4g15820	n.a.	n.a.
At1g20950	kinase	pyrophosphate--fructose-6-phosphate 1-phosphotransferase-related / pyrophosphate-dependent 6-phosphofructose-1-kinase-related
260172_s_at	n.a.	At5g10330;At1g71920
At2g43360	BIO2	BIO2 (BIOTIN AUXOTROPH 2); biotin synthase
At4g33680	AGD2	AGD2 (ABERRANT GROWTH AND DEATH 2); L,L-diaminopimelate aminotransferase/ transaminase
At4g39120	IMPL2	IMPL2 (MYO-INOSITOL MONOPHOSPHATASE LIKE 2); 3'(2'),5'-bisphosphate nucleotidase/ L-galactose-1-phosphate phosphatase/ inositol or phosphatidylinositol phosphatase/ inositol-1(or 4)-monophosphatase
At4g22930	PYR4	PYR4 (PYRIMIDIN 4); dihydroorotase/ hydrolase/ hydrolase, acting on carbon-nitrogen (but not peptide) bonds, in cyclic amides
At5g65010	ASN2	ASN2 (ASPARAGINE SYNTHETASE 2); asparagine synthase (glutamine-hydrolyzing)
At5g09650	PPa6	AtPPa6 (Arabidopsis thaliana pyrophosphorylase 6); inorganic diphosphatase/ pyrophosphatase
At3g25860	LTA2	LTA2; dihydrolipoyllysine-residue acetyltransferase
At1g56050	GTP-binding	GTP-binding protein-related
At3g13560	hydrolase	glycosyl hydrolase family 17 protein
At2g37790	reductase	aldo/keto reductase family protein
At3g53900	UPP	uracil phosphoribosyltransferase, putative / UMP pyrophosphorylase, putative / UPRTase, putative
At4g26900	HF	AT-HF (HIS HF); imidazoleglycerol-phosphate synthase
At1g54220	transferase	dihydrolipoamide S-acetyltransferase, putative
At4g19710	AK-HSDH II	bifunctional aspartate kinase/homoserine dehydrogenase, putative / AK-HSDH, putative
At5g58480	hydrolase	glycosyl hydrolase family 17 protein
At3g46940	DUT1	deoxyuridine 5'-triphosphate nucleotidohydrolase family
At4g24620	PGI1	PGI1 (PHOSPHOGLUCOSE ISOMERASE 1); glucose-6-phosphate isomerase
At1g64880	ribosome	ribosomal protein S5 family protein
At2g29690	ASA2	ASA2 (ANTHRANILATE SYNTHASE 2); anthranilate synthase
At5g12150	PH	pleckstrin homology (PH) domain-containing protein / RhoGAP domain-containing protein
At4g30330	ribonucleoprotein	small nuclear ribonucleoprotein E, putative / snRNP-E, putative / Sm protein E, putative
263706_s_at	n.a.	At1g31180;At5g14200
At4g23940	protease	FtsH protease, putative
At5g55280	FTSZ1-1	FTSZ1-1; protein binding / structural molecule
At3g49500	RDR6	RDR6 (RNA-DEPENDENT RNA POLYMERASE 6); RNA-directed RNA polymerase/ nucleic acid binding
At1g63940	MDAR6	monodehydroascorbate reductase, putative
At3g29375	XH	XH domain-containing protein
At5g40830	transferase	methyltransferase
At1g52670	biotin/lipoyl attachment	biotin/lipoyl attachment domain-containing protein
At5g23310	FSD3	FSD3 (FE SUPEROXIDE DISMUTASE 3); superoxide dismutase
At1g13560	AAPT1	AAPT1 (AMINOALCOHOLPHOSPHOTRANSFERASE 1); phosphatidyltransferase/ phosphotransferase, for other substituted phosphate groups
At1g53240	malate dehydrogenase (NAD)	malate dehydrogenase (NAD), mitochondrial
At3g52170	DNA binding	DNA binding
At5g49030	OVA2	OVA2 (ovule abortion 2); ATP binding / aminoacyl-tRNA ligase/ catalytic/ isoleucine-tRNA ligase/ nucleotide binding
At2g37500	ArgJ	arginine biosynthesis protein ArgJ family
At3g57220	transferase	UDP-GlcNAc:dolichol phosphate N-acetylglucosamine-1-phosphate transferase, putative
At3g57610	ADSS	ADSS (ADENYLOSUCCINATE SYNTHASE); adenylosuccinate synthase
At2g41950	n.a.	unknown protein
At4g25870	n.a.	unknown protein
At5g19750	peroxisomal membrane 22 kDa	peroxisomal membrane 22 kDa family protein
At2g44640	n.a.	n.a.
At1g16340	KDSA2	ATKDSA2; 3-deoxy-8-phosphooctulonate synthase
At5g10920	arginosuccinase	argininosuccinate lyase, putative / arginosuccinase, putative
At1g18090	nuclease	exonuclease, putative
At2g34640	PTAC12	PTAC12 (PLASTID TRANSCRIPTIONALLY ACTIVE12)
At1g55490	CPN60B	CPN60B (CHAPERONIN 60 BETA); ATP binding / protein binding
At5g48830	n.a.	unknown protein
At5g09240	PC4	transcriptional coactivator p15 (PC4) family protein
At1g76405	n.a.	unknown protein
At2g30200	transferase	[acyl-carrier-protein] S-malonyltransferase/ binding / catalytic/ transferase
At3g25530	GLYR1	GLYR1 (GLYOXYLATE REDUCTASE 1); 3-hydroxybutyrate dehydrogenase/ phosphogluconate dehydrogenase (decarboxylating)
At5g61130	PDCB1	PDCB1 (PLASMODESMATA CALLOSE-BINDING PROTEIN 1); callose binding / polysaccharide binding

AGI	Name	Annotation
At5g20040	IPT9	ATIPT9; ATP binding / tRNA isopentenyltransferase
At3g06930	PRMT4B	protein arginine N-methyltransferase family protein
At3g18110	EMB1270	EMB1270 (embryo defective 1270)
At1g50575	decarboxylase	lysine decarboxylase family protein
At2g19940	oxidoreductase	N-acetyl-gamma-glutamyl-phosphate reductase/ NAD or NADH binding / binding / catalytic/ oxidoreductase, acting on the aldehyde or oxo group of donors, NAD or NADP as acceptor / protein dimerization
At5g63040	n.a.	unknown protein
At4g30810	scpl29	scpl29 (serine carboxypeptidase-like 29); serine-type carboxypeptidase
At3g16060	kinesin motor	kinesin motor family protein
At5g09995	n.a.	unknown protein
At2g14660	n.a.	unknown protein
At5g67150	transferase	transferase family protein
At5g44785	OSB3	OSB3 (ORGANELLAR SINGLE-STRANDED DNA BINDING PROTEIN 3); single-stranded DNA binding
At3g19720	ARC5	ARC5 (ACCUMULATION AND REPLICATION OF CHLOROPLAST 5); GTP binding / GTPase
At3g43610	tubulin binding	tubulin binding
At1g78370	GSTU20	ATGSTU20 (GLUTATHIONE S-TRANSFERASE TAU 20); glutathione transferase
At3g25470	bacterial hemolysin	bacterial hemolysin-related
At4g23740	kinase	leucine-rich repeat transmembrane protein kinase, putative
At4g25890	RPP3A	60S acidic ribosomal protein P3 (RPP3A)
At5g22640	emb1211	emb1211 (embryo defective 1211)
258977_s_at	n.a.	At3g02020;At5g14060
At5g66530	epimerase	aldose 1-epimerase family protein
At3g09820	ADK1	ADK1 (adenosine kinase 1); adenosine kinase/ copper ion binding
At2g18990	TXND9	TXND9 (THIOREDOXIN DOMAIN-CONTAINING PROTEIN 9 HOMOLOG)
At5g62890	permease	permease, putative
At3g24770	CLE41	CLE41 (CLAVATA3/ESR-RELATED 41); protein binding / receptor binding
At3g02870	VTC4	VTC4; 3'(2'),5'-bisphosphate nucleotidase/ L-galactose-1-phosphate phosphatase/ inositol or phosphatidylinositol phosphatase/ inositol-1(or 4)-monophosphatase
At3g15680	Ran-binding	zinc finger (Ran-binding) family protein
At3g58610	isomerase	ketol-acid reductoisomerase
At1g59990	DEAD	DEAD/DEAH box helicase, putative (RH22)
259842_at	n.a.	At1g73602;At1g73600
At4g28706	kinase	pfkB-type carbohydrate kinase family protein
At3g55010	PUR5	PUR5; ATP binding / phosphoribosylformylglycinamidine cyclo-ligase
At5g23740	RPS11-BETA	RPS11-BETA (RIBOSOMAL PROTEIN S11-BETA); structural constituent of ribosome
At4g17520	RNA-binding	nuclear RNA-binding protein, putative
At5g20590	n.a.	unknown protein
248633_at	n.a.	n.a.
At2g31790	transferase	UDP-glucoronosyl/UDP-glucosyl transferase family protein
249424_s_at	n.a.	At5g40080;At5g39800
At4g27080	PDI7	thioredoxin family protein
At1g04520	PDLP2	PDLP2 (PLASMODESMATA-LOCATED PROTEIN 2)
At4g16340	SPK1	SPK1 (SPIKE1); GTP binding / GTPase binding / guanyl-nucleotide exchange factor
At2g46110	KPHMT1	KPHMT1 (KETOPANTOATE HYDROXYMETHYLTRANSFERASE 1); 3-methyl-2-oxobutanoate hydroxymethyltransferase
At1g21880	LYM1	LYM1 (LYSM DOMAIN GPI-ANCHORED PROTEIN 1 PRECURSOR)
At2g19720	rps15ab	rps15ab (ribosomal protein S15A B); structural constituent of ribosome
At3g01120	MTO1	MTO1 (METHIONINE OVERACCUMULATION 1); cystathionine gamma-synthase
At1g18340	transcription	basal transcription factor complex subunit-related
At1g76400	ribophorin I	ribophorin I family protein
At1g15000	scpl50	scpl50 (serine carboxypeptidase-like 50); serine-type carboxypeptidase
At3g04340	emb2458	emb2458 (embryo defective 2458); ATP binding / ATPase/ metalloendopeptidase/ nucleoside-triphosphatase/ nucleotide binding
At4g13430	IIL1	IIL1 (ISOPROPYL MALATE ISOMERASE LARGE SUBUNIT 1); 4 iron, 4 sulfur cluster binding / hydro-lyase/ lyase
At4g36660		unknown protein
At4g13720	HAM1	inosine triphosphate pyrophosphatase, putative / HAM1 family protein
At5g10240	ASN3	ASN3 (ASPARAGINE SYNTHETASE 3); asparagine synthase (glutamine-hydrolyzing)
At3g15380	transporter	choline transporter-related
At5g40150	peroxidase	peroxidase, putative
At4g13170	RPL13aC	60S ribosomal protein L13A (RPL13aC)
At3g16290	EMB2083	EMB2083 (embryo defective 2083); ATP binding / ATP-dependent peptidase/ ATPase/ metalloendopeptidase/ metallopeptidase/ nucleoside-triphosphatase/ nucleotide binding / serine-type endopeptidase
At3g07140	GPI transamidase component Gpi16 subunit	GPI transamidase component Gpi16 subunit family protein
At5g60940	transducin	transducin family protein / WD-40 repeat family protein
At3g48610	phosphoesterase	phosphoesterase family protein
At1g28395	n.a.	unknown protein
At4g15790	n.a.	unknown protein
At1g31860	IE	AT-IE; phosphoribosyl-AMP cyclohydrolase/ phosphoribosyl-ATP diphosphatase
At4g04750	transporter	carbohydrate transmembrane transporter/ sugar:hydrogen symporter
At3g52960	peroxiredoxin type 2	peroxiredoxin type 2, putative
At5g16715	EMB2247	EMB2247 (embryo defective 2247); ATP binding / aminoacyl-tRNA ligase/ nucleotide binding / valine-tRNA ligase
At3g53580	epimerase	diaminopimelate epimerase family protein
At2g35040	AICARFT	AICARFT/IMPCHase bienzyme family protein
At5g46290	KAS1	KAS I (3-KETOACYL-ACYL CARRIER PROTEIN SYNTHASE I); catalytic/ fatty-acid synthase/ transferase, transferring acyl groups other than amino-acyl groups
At3g62060	pectinacetylesterase	pectinacetylesterase family protein
At4g12390	PME1	PME1 (PECTIN METHYLESTERASE INHIBITOR 1); enzyme inhibitor/ pectinesterase/ pectinesterase inhibitor
At3g49470	NACA2	NACA2 (NASCENT POLYPEPTIDE-ASSOCIATED COMPLEX SUBUNIT ALPHA-LIKE PROTEIN 2)
At2g04280	n.a.	unknown protein
At3g18130	RACK1C_AT	RACK1C_AT (RECEPTOR FOR ACTIVATED C KINASE 1 C); nucleotide binding
At2g24970	n.a.	unknown protein
At1g60660	CB5LP	CB5LP (CYTOCHROME B5-LIKE PROTEIN); heme binding
At1g16350	dehydrogenase	inosine-5'-monophosphate dehydrogenase, putative
At1g80850	glycosylase	methyladenine glycosylase family protein
At5g42480	ARC6	ARC6 (ACCUMULATION AND REPLICATION OF CHLOROPLASTS 6); protein binding
At1g49630	PREP2	ATPREP2 (ARABIDOPSIS THALIANA PRESEQUENCE PROTEASE 2); catalytic/ metal ion binding / metalloendopeptidase/ metallopeptidase/ zinc ion binding
At1g66820	glycine-rich	glycine-rich protein
At4g33760	tRNA syn	tRNA synthetase class II (D, K and N) family protein

AGI	Name	Annotation
At3g21300	transferase	RNA methyltransferase family protein
253773_s_at	n.a.	At4g28360;At1g52370
267237_s_at	n.a.	At2g44040;At3g59890
At2g25830	YebC	YebC-related
At1g64790	binding	binding
At2g35155	catalytic	catalytic
At1g55130	endomembrane 70	endomembrane protein 70, putative
At1g09830	PUR2	phosphoribosylamine--glycine ligase (PUR2)
At3g55400	OVA1	OVA1 (OVULE ABORTION 1); ATP binding / aminoacyl-tRNA ligase/ methionine-tRNA ligase/ nucleotide binding
At3g23940	dehydratase	dehydratase family
At4g18460	deacylase	D-Tyr-tRNA(Tyr) deacylase family protein
At3g13180	NOL1	NOL1/NOP2/sun family protein / antitermination NusB domain-containing protein
250282_at		
At3g16480	MPPalpha	MPPalpha (mitochondrial processing peptidase alpha subunit); catalytic/ metal ion binding / metalloendopeptidase/ zinc ion binding
At1g29880	ligase	glycyl-tRNA synthetase / glycine--tRNA ligase
At4g24830	synthase	arginosuccinate synthase family
At4g24780	lyase	pectate lyase family protein
At3g60440	n.a.	
At4g32570	TIFY8	TIFY8 (TIFY DOMAIN PROTEIN 8)
245810_at	n.a.	At1g38065;At1g38131
At5g19670	exostosin	exostosin family protein
At4g25740	RPS10A	40S ribosomal protein S10 (RPS10A)
At5g10560	hydrolase	glycosyl hydrolase family 3 protein
At1g26100	B561	cytochrome B561 family protein
At4g00810	RPP1B	60S acidic ribosomal protein P1 (RPP1B)
At1g07070	RPL35aA	60S ribosomal protein L35a (RPL35aA)
At3g17170	RFC3	RFC3 (REGULATOR OF FATTY-ACID COMPOSITION 3); structural constituent of ribosome
At4g36470	transferase	S-adenosyl-L-methionine:carboxyl methyltransferase family protein
At5g10910	methylase	mraW methylase family protein
At4g26300	emb1027	emb1027 (embryo defective 1027); ATP binding / aminoacyl-tRNA ligase/ arginine-tRNA ligase/ nucleotide binding
At5g26780	SHM2	SHM2 (SERINE HYDROXYMETHYLTRANSFERASE 2); catalytic/ glycine hydroxymethyltransferase/ pyridoxal phosphate binding
At3g27740	CARA	CARA (CARBAMOYL PHOSPHATE SYNTHETASE A); carbamoyl-phosphate synthase (glutamine-hydrolyzing)/ carbamoyl-phosphate synthase/ catalytic
At1g78060	hydrolase	glycosyl hydrolase family 3 protein
At1g67950	RRM	RNA recognition motif (RRM)-containing protein
At5g40810	cytochrome c1	cytochrome c1, putative
At5g27820	L18	ribosomal protein L18 family protein
At3g52390	nuclease	tatD-related deoxyribonuclease family protein
At5g01590	n.a.	unknown protein
At1g21440	mutase	mutase family protein
At1g14810	dehydrogenase	semialdehyde dehydrogenase family protein
At5g41880	POLA3	POLA3; DNA primase
At3g27230	n.a.	n.a.
263601_s_at	n.a.	At4g34570;At2g16370
At5g08610	RH26	DEAD box RNA helicase (RH26)
At2g02500	ISPD	ISPD; 2-C-methyl-D-erythritol 4-phosphate cytidylyltransferase
At5g60670	RPL12C	60S ribosomal protein L12 (RPL12C)
At5g64580	ATPase	AAA-type ATPase family protein
At2g39670	SAM	radical SAM domain-containing protein
At2g31670	n.a.	n.a.
At1g15710	dehydrogenase	prephenate dehydrogenase family protein
At3g22780	TSO1	TSO1 (CHINESE FOR 'UGLY'); transcription factor
At3g66658	ALDH22a1	ALDH22a1 (Aldehyde Dehydrogenase 22a1); 3-chloroallyl aldehyde dehydrogenase/ oxidoreductase
At2g17630	transferase	phosphoserine aminotransferase, putative
At3g04840	RPS3aA	40S ribosomal protein S3A (RPS3aA)
At4g39280	ligase	phenylalanyl-tRNA synthetase, putative / phenylalanine--tRNA ligase, putative
At1g65900	n.a.	unknown protein
At5g19620	OEP80	OEP80 (OUTER ENVELOPE PROTEIN OF 80 KDA)
At1g62330	n.a.	unknown protein
At1g75330	OTC	OTC (ORNITHINE CARBAMOYLTRANSFERASE); amino acid binding / carboxyl- or carbamoyltransferase/ ornithine carbamoyltransferase
At4g09550	GIP1	unknown protein
At2g15290	TIC21	TIC21 (TRANSLOCON AT INNER MEMBRANE OF CHLOROPLASTS 21); copper uptake transmembrane transporter/ iron ion transmembrane transporter/ protein homodimerization
At5g16130	RPS7C	40S ribosomal protein S7 (RPS7C)
At2g18400	ribosome	ribosomal protein L6 family protein
At5g17530	mutase	phosphoglucosamine mutase family protein
At1g21650	binding	ATP binding / protein binding
At5g27740	EMB2775	EMB2775 (EMBRYO DEFECTIVE 2775); DNA binding / nucleoside-triphosphatase/ nucleotide binding
At1g34430	EMB3003	EMB3003 (embryo defective 3003); acyltransferase/ dihydrolipoyllysine-residue acetyltransferase/ protein binding
At5g04510	PDK1	PDK1 (3'-PHOSPHOINOSITIDE-DEPENDENT PROTEIN KINASE 1); 3-phosphoinositide-dependent protein kinase/ kinase/ phosphoinositide binding / protein binding / protein kinase
At5g07320	mitochondrial substrate carrier	mitochondrial substrate carrier family protein
At2g01120	ORC4	ORC4 (ORIGIN RECOGNITION COMPLEX SUBUNIT 4); protein binding
At4g17540	n.a.	unknown protein
At1g14410	WHY1	WHY1 (WHIRLY 1); DNA binding / telomeric DNA binding
At3g02660	emb2768	emb2768 (EMBRYO DEFECTIVE 2768); ATP binding / RNA binding / aminoacyl-tRNA ligase/ nucleotide binding / tyrosine-tRNA ligase
At1g74260	PUR4	PUR4 (purine biosynthesis 4); ATP binding / catalytic/ phosphoribosylformylglycinamidine synthase
At2g47590	PHR2	PHR2 (photolyase/blue-light receptor 2); DNA photolyase
At5g13120	CYP20-2	peptidyl-prolyl cis-trans isomerase cyclophilin-type family protein
At2g01250	RPL7B	60S ribosomal protein L7 (RPL7B)
At2g48120	PAC	PAC (PALE CRESS)
At4g13050	thioesterase	acyl-(acyl carrier protein) thioesterase, putative / acyl-ACP thioesterase, putative / oleoyl-(acyl-carrier protein) hydrolase, putative / S-acyl fatty acid synthase thioesterase, putative
At1g70280	NHL repeat	NHL repeat-containing protein
At5g53620	n.a.	unknown protein
At5g14210	kinase	leucine-rich repeat transmembrane protein kinase, putative
At2g39290	PGP1	PGP1 (PHOSPHATIDYLGLYCEROLPHOSPHATE SYNTHASE 1); CDP-alcohol phosphatidyltransferase/ CDP-diacylglycerol-

		glycerol-3-phosphate 3-phosphatidyltransferase
At2g03350	n.a.	unknown protein
At2g45470	FLA8	FLA8 (FASCICLIN-LIKE ARABINOGALACTAN PROTEIN 8)
At4g09730	DEAD	DEAD/DEAH box helicase, putative
At1g13730	RRM	nuclear transport factor 2 (NTF2) family protein / RNA recognition motif (RRM)-containing protein
At5g48580	FKBP15-2	FKBP15-2; FK506 binding / peptidyl-prolyl cis-trans isomerase
At2g28310	n.a.	unknown protein
At1g48630	RACK1B_AT	RACK1B_AT (RECEPTOR FOR ACTIVATED C KINASE 1 B); nucleotide binding
At1g06950	TIC110	TIC110 (TRANSLOCON AT THE INNER ENVELOPE MEMBRANE OF CHLOROPLASTS 110)
At1g80560	IMD2	3-isopropylmalate dehydrogenase, chloroplast, putative
At5g41760	transporter	nucleotide-sugar transporter family protein
At1g09660	KH quaking	KH domain-containing quaking protein, putative
At1g07370	PCNA1	PCNA1 (PROLIFERATING CELLULAR NUCLEAR ANTIGEN); DNA binding / DNA polymerase processivity factor/ protein binding
At3g12390	alpha-NAC	nascent polypeptide associated complex alpha chain protein, putative / alpha-NAC, putative
At1g34010	n.a.	unknown protein
At2g31170	SYCO ARATH	SYCO ARATH; ATP binding / aminoacyl-tRNA ligase/ cysteine-tRNA ligase/ nucleotide binding
At4g28210	emb1923	emb1923 (embryo defective 1923)
At1g67320	DNA primase	DNA primase, large subunit family
At3g57050	CBL	CBL (cystathionine beta-lyase); cystathionine beta-lyase
At5g61300	n.a.	unknown protein
At4g39460	SAMC1	SAMC1 (S-ADENOSYLMETHIONINE CARRIER 1); S-adenosylmethionine transmembrane transporter/ binding
At5g51560	kinase	leucine-rich repeat transmembrane protein kinase, putative
At2g25840	OVA4	OVA4 (ovule abortion 4); ATP binding / aminoacyl-tRNA ligase/ nucleotide binding / tryptophan-tRNA ligase
At5g04430	BTR1L	BTR1L (BINDING TO TOMV RNA 1L (LONG FORM)); nucleic acid binding / single-stranded RNA binding
At2g05830	translation	eukaryotic translation initiation factor 2B family protein / eIF-2B family protein
At1g16020	n.a.	unknown protein
At5g37290	armadillo/beta-catenin repeat	armadillo/beta-catenin repeat family protein
At3g23070	CFM3A	RNA binding
At1g69700	HVA22C	ATHVA22C
267553_s_at	n.a.	At2g32180;At2g32650
At2g18910	glycoprotein	hydroxyproline-rich glycoprotein family protein
At5g13980	hydrolase	glycosyl hydrolase family 38 protein
At5g49160	MET1	MET1 (METHYLTRANSFERASE 1); methyltransferase
At3g62110	pectinase	glycoside hydrolase family 28 protein / polygalacturonase (pectinase) family protein
At2g28000	CPN60A	CPN60A (CHAPERONIN-60ALPHA); ATP binding / protein binding
At3g08030	n.a.	unknown protein
At5g50420	n.a.	unknown protein
At3g07430	emb1990	emb1990 (embryo defective 1990)
At3g62390	n.a.	unknown protein
At5g26790	n.a.	unknown protein
At1g15080	LPP2	LPP2 (LIPID PHOSPHATE PHOSPHATASE 2); acid phosphatase/ phosphatidate phosphatase
At3g52750	FTSZ2-2	FTSZ2-2; GTP binding / GTPase/ structural molecule
At2g36620	RPL24A	RPL24A (ribosomal protein L24); structural constituent of ribosome
At2g44050	COS1	COS1 (COI1 SUPPRESSOR1); 6,7-dimethyl-8-ribityllumazine synthase
At3g56120	Met-10+ like	Met-10+ like family protein
At3g46740	TOC75-III	TOC75-III (TRANSLOCON AT THE OUTER ENVELOPE MEMBRANE OF CHLOROPLASTS 75-III); P-P-bond-hydrolysis-driven protein transmembrane transporter
At4g34160	CYCD3;1	CYCD3;1 (CYCLIN D3;1); cyclin-dependent protein kinase regulator/ protein binding
At4g17610	tRNA	tRNA/rRNA methyltransferase (SpoU) family protein
At2g21790	RNR1	RNR1 (RIBONUCLEOTIDE REDUCTASE 1); ATP binding / protein binding / ribonucleoside-diphosphate reductase
At1g80690	n.a.	unknown protein
At4g10470	n.a.	unknown protein
At3g56370	kinase	leucine-rich repeat transmembrane protein kinase, putative
At5g35740	hydrolase	glycosyl hydrolase family protein 17
At1g19710	transferase	glycosyl transferase family 1 protein
At1g13380	n.a.	unknown protein
At3g50240	KICP-02	KICP-02; ATP binding / microtubule motor
At4g20270	BAM3	BAM3 (BARELY ANY MERISTEM 3); ATP binding / protein binding / protein kinase/ protein serine/threonine kinase
At5g45590	n.a.	unknown protein
At1g03687	n.a.	n.a.
At1g19800	TGD1	TGD1 (TRIGALACTOSYLDIACYLGLYCEROL 1); lipid transporter
At4g22756	SMO1-2	SMO1-2 (STEROL C4-METHYL OXIDASE 1-2); 4,4-dimethyl-9beta,19-cyclopropylsterol-4alpha-methyl oxidase/ C-4 methylsterol oxidase/ catalytic
At3g07190	n.a.	n.a.
At1g64650	n.a.	n.a.
At5g11690	TIM17-3	ATTIM17-3; P-P-bond-hydrolysis-driven protein transmembrane transporter/ protein transporter
At5g57170	MIF	macrophage migration inhibitory factor family protein / MIF family protein
At5g67070	RALFL34	RALFL34 (ralf-like 34); signal transducer
At2g47940	DEGP2	DEGP2; serine-type endopeptidase/ serine-type peptidase
At5g20980	ATMS3	ATMS3 (methionine synthase 3); 5-methyltetrahydropteroyltriglutamate-homocysteine S-methyltransferase/ methionine synthase
At5g05560	EMB2771	EMB2771 (EMBRYO DEFECTIVE 2771); ubiquitin-protein ligase
At2g40480	n.a.	unknown protein
At3g20390	L-PSP	endoribonuclease L-PSP family protein
At2g29260	dehydrogenase	tropinone reductase, putative / tropine dehydrogenase, putative
At1g48520	GATB	GATB (GLU-ADT SUBUNIT B); carbon-nitrogen ligase, with glutamine as amido-N-donor / glutaminyl-tRNA synthase (glutamine-hydrolyzing)/ ligase
At5g17660	transferase	tRNA (guanine-N7-)-methyltransferase
At2g19670	PRMT1A	PRMT1A (PROTEIN ARGININE METHYLTRANSFERASE 1A); protein-arginine N-methyltransferase
At4g24175	n.a.	unknown protein
At5g46280	MCM3	DNA replication licensing factor, putative
At1g60070	transporter	binding / clathrin binding / protein binding / protein transporter
At1g48230	translocator	phosphate translocator-related
At3g21110	PUR7	PUR7 (PURIN 7); phosphoribosylaminoimidazolesuccinocarboxamide synthase
At5g19370	PPIASE	rhodanese-like domain-containing protein / PPIC-type PPIASE domain-containing protein
At1g21560	n.a.	unknown protein
At1g78180	binding	binding
At4g31210	isomerase	DNA topoisomerase family protein
At3g06680	RPL29B	60S ribosomal protein L29 (RPL29B)
At4g10480	alpha-NAC	nascent polypeptide associated complex alpha chain protein, putative / alpha-NAC, putative
At5g59870	HTA6	HTA6; DNA binding
At3g53190	lyase	pectate lyase family protein
At3g11250	RPP0C	60S acidic ribosomal protein P0 (RPP0C)
At1g67490	GCS1	GCS1 (GLUCOSIDASE 1); alpha-glucosidase

AGI	Name	Annotation
At5g57440	GS1	GS1; catalytic/ hydrolase
At3g16100	RABG3C	ATRABG3C (ARABIDOPSIS RAB GTPASE HOMOLOG G3C); GTP binding
At5g47210	RNA-binding	nuclear RNA-binding protein, putative
At1g47290	3BETAHSD	AT3BETAHSD/D1 (3BETA-HYDROXYSTEROID-DEHYDROGENASE/DECARBOXYLASE ISOFORM 1); 3-beta-hydroxy-delta5-steroid dehydrogenase/ sterol-4-alpha-carboxylate 3-dehydrogenase (decarboxylating)
At1g66430	kinase	pfkB-type carbohydrate kinase family protein
At5g22440	RPL10aC	60S ribosomal protein L10A (RPL10aC)
At1g29900	CARB	CARB (CARBAMOYL PHOSPHATE SYNTHETASE B); ATP binding / carbamoyl-phosphate synthase/ catalytic
At2g29760	OTP81	pentatricopeptide (PPR) repeat-containing protein
At2g20850	SRF1	SRF1 (strubbelig receptor family 1); kinase
At1g67690	metalloendopeptidase	metalloendopeptidase
At3g13030	hAT dimerisation	hAT dimerisation domain-containing protein
At4g13650	PPR	pentatricopeptide (PPR) repeat-containing protein
At5g51100	FSD2	FSD2 (FE SUPEROXIDE DISMUTASE 2); superoxide dismutase
At2g39460	RPL23AA	RPL23AA (RIBOSOMAL PROTEIN L23AA); RNA binding / nucleotide binding / structural constituent of ribosome
At3g06040	L12	ribosomal protein L12 family protein
At2g35780	scpl26	scpl26 (serine carboxypeptidase-like 26); serine-type carboxypeptidase
At2g27130	LTP	protease inhibitor/seed storage/lipid transfer protein (LTP) family protein
At1g62640	KAS III	KAS III (3-KETOACYL-ACYL CARRIER PROTEIN SYNTHASE III); 3-oxoacyl-[acyl-carrier-protein] synthase/ catalytic/ transferase, transferring acyl groups other than amino-acyl groups
At5g64816	n.a.	unknown protein
At4g00370	ANTR2	ANTR2; inorganic phosphate transmembrane transporter/ organic anion transmembrane transporter
At2g29570	PCNA2	PCNA2 (PROLIFERATING CELL NUCLEAR ANTIGEN 2); DNA binding / DNA polymerase processivity factor
At4g26760	MAP65-2	MAP65-2
251331_s_at	n.a.	At3g61650;At5g05620
At3g45850	kinesin motor	kinesin motor protein-related
At2g04845	GNAT	GCN5-related N-acetyltransferase (GNAT) family protein
At4g30000	DHPS	dihydropterin pyrophosphokinase, putative / dihydropteroate synthase, putative / DHPS, putative
At3g49670	BAM2	BAM2 (BARELY ANY MERISTEM 2); ATP binding / protein binding / protein kinase/ protein serine/threonine kinase
At4g05210	transferase	bacterial transferase hexapeptide repeat-containing protein
At1g11130	SUB	SUB (STRUBBELIG); protein binding / receptor signaling protein serine/threonine kinase
At1g44900	MCM2	ATP binding / DNA binding / DNA-dependent ATPase
At2g05990	MOD1	MOD1 (MOSAIC DEATH 1); enoyl-[acyl-carrier-protein] reductase (NADH)/ enoyl-[acyl-carrier-protein] reductase/ oxidoreductase
At5g46580	PPR	pentatricopeptide (PPR) repeat-containing protein
At4g38660	thaumatin	thaumatin, putative
At5g49555	oxidase	amine oxidase-related
At3g59760	OASC	OASC (O-ACETYLSERINE (THIOL) LYASE ISOFORM C); ATP binding / cysteine synthase
At5g06050	dehydration-responsive	dehydration-responsive protein-related
258218_at	n.a.	At3g17998;At3g18000
At1g70310	SPDS2	SPDS2 (spermidine synthase 2); spermidine synthase
At1g10522	n.a.	unknown protein
At1g20410	n.a.	unknown protein
At5g07090	RPS4B	40S ribosomal protein S4 (RPS4B)
At5g02870	RPL4D	60S ribosomal protein L4/L1 (RPL4D)
At5g59500	n.a.	unknown protein
At3g16260	TRZ4	TRZ4 (TRNASE Z 4); 3'-tRNA processing endoribonuclease/ catalytic
At5g63310	NDPK2	NDPK2 (NUCLEOSIDE DIPHOSPHATE KINASE 2); ATP binding / nucleoside diphosphate kinase/ protein binding
At5g50110	n.a.	n.a.
At2g33430	DAL1	DAL1 (DIFFERENTIATION AND GREENING-LIKE 1)
At5g19260	n.a.	unknown protein
At4g12880	plastocyanin-like	plastocyanin-like domain-containing protein
At4g30620	n.a.	unknown protein
At3g48110	EDD1	EDD1 (EMBRYO-DEFECTIVE-DEVELOPMENT 1); glycine-tRNA ligase
At2g47580	U1A	U1A (SPLICEOSOMAL PROTEIN U1A); RNA binding / nucleic acid binding / nucleotide binding
At4g05450	MFDX1	adrenodoxin-like ferredoxin 2
At2g25870	hydrolase	haloacid dehalogenase-like hydrolase family protein
At3g62120	tRNA syn	tRNA synthetase class II (G, H, P and S) family protein
At3g20320	TGD2	TGD2 (TRIGALACTOSYLDIACYLGLYCEROL2); lipid transporter/ phospholipid binding
At5g08020	RPA70B	RPA70B (RPA70-KDA SUBUNIT B); DNA binding / nucleic acid binding
At1g70370	PG2	BURP domain-containing protein / polygalacturonase, putative
At5g63980	SAL1	SAL1; 3'(2'),5'-bisphosphate nucleotidase/ inositol or phosphatidylinositol phosphatase
At1g79260	n.a.	unknown protein
At2g26930	CDPMEK	ATCDPMEK (4-(CYTIDINE 5'-PHOSPHO)-2-C-METHYL-D-ERITHRITOL KINASE); 4-(cytidine 5'-diphospho)-2-C-methyl-D-erythritol kinase
At5g52650	RPS10C	40S ribosomal protein S10 (RPS10C)
At5g50375	CPI1	CPI1 (CYCLOPROPYL ISOMERASE); cycloeucalenol cycloisomerase
At2g42770	peroxisomal membrane 22 kDa	peroxisomal membrane 22 kDa family protein
At4g32520	SHM3	SHM3 (SERINE HYDROXYMETHYLTRANSFERASE 3); catalytic/ glycine hydroxymethyltransferase/ pyridoxal phosphate binding
At5g59850	RPS15aF	40S ribosomal protein S15A (RPS15aF)
At4g39620	EMB2453	EMB2453 (embryo defective 2453)
At1g04020	BARD1	BARD1 (BREAST CANCER ASSOCIATED RING 1); DNA binding / transcription coactivator
At3g13070	transporter	CBS domain-containing protein / transporter associated domain-containing protein
At5g42130	mitochondrial substrate carrier	mitochondrial substrate carrier family protein
At5g61000	RPA70D	replication protein, putative
At1g79850	RPS17	RPS17 (RIBOSOMAL PROTEIN S17); structural constituent of ribosome
At2g30695	n.a.	n.a.
At5g10390	histone H3	histone H3
At1g36390	chaperonin	co-chaperone grpE family protein
At1g69200	kinase	kinase
At5g40480	EMB3012	EMB3012 (embryo defective 3012)
At3g25660	transferase	glutamyl-tRNA(Gln) amidotransferase, putative
At5g14100	NAP14	ATNAP14; transporter
At1g63130	PPR	pentatricopeptide (PPR) repeat-containing protein
At2g28740	HIS4	HIS4; DNA binding
At1g56670	hydrolase	GDSL-motif lipase/hydrolase family protein
At4g38160	pde191	pde191 (pigment defective 191)
At1g15690	AVP1	AVP1; ATPase/ hydrogen-translocating pyrophosphatase
At4g16155	dehydrogenase	dihydrolipoyl dehydrogenase
At2g27810	NAT12	xanthine/uracil permease family protein

AGI	Name	Annotation
At5g54880	DTW	DTW domain-containing protein
At1g09200	histone H3	histone H3
At1g01080	ribonucleoprotein	33 kDa ribonucleoprotein, chloroplast, putative / RNA-binding protein cp33, putative
At1g18250	LP-1	ATLP-1
At3g63170	isomerase	chalcone isomerase
At1g69420	zinc finger	zinc finger (DHHC type) family protein
At3g06730	TRX P	thioredoxin family protein
At2g20450	RPL14A	60S ribosomal protein L14 (RPL14A)
At5g16870	hydrolase	aminoacyl-tRNA hydrolase
At3g03710	RIF10	RIF10 (resistant to inhibition with FSM 10); 3'-5'-exoribonuclease/ RNA binding / nucleic acid binding / polyribonucleotide nucleotidyltransferase
At4g26230	RPL31B	60S ribosomal protein L31 (RPL31B)
At4g02060	PRL	PRL (PROLIFERA); ATP binding / DNA binding / DNA-dependent ATPase/ nucleoside-triphosphatase/ nucleotide binding
At4g32915	n.a.	n.a.
At1g20540	transducin	transducin family protein / WD-40 repeat family protein
At3g61780	emb1703	emb1703 (embryo defective 1703)
At4g16390	n.a.	n.a.
At4g17390	RPL15B	60S ribosomal protein L15 (RPL15B)
At5g15770	GNA1	AtGNA1 (Arabidopsis thaliana glucose-6-phosphate acetyltransferase 1); N-acetyltransferase/ glucosamine 6-phosphate N-acetyltransferase
At1g65010	n.a.	unknown protein
At1g43190	ribonucleoprotein	polypyrimidine tract-binding protein, putative / heterogeneous nuclear ribonucleoprotein, putative
At1g77750	ribosome	30S ribosomal protein S13, chloroplast, putative
At5g10170	MIPS3	MIPS3 (MYO-INOSITOL-1-PHOSTPATE SYNTHASE 3); binding / catalytic/ inositol-3-phosphate synthase
At1g06960	ribonucleoprotein	small nuclear ribonucleoprotein U2B, putative / spliceosomal protein, putative
At2g32170	n.a.	n.a.
At5g64670	L15	ribosomal protein L15 family protein
At2g32060	RPS12C	40S ribosomal protein S12 (RPS12C)
At4g28100	n.a.	unknown protein
At2g25270	n.a.	unknown protein
At1g10510	emb2004	emb2004 (embryo defective 2004)
At5g13280	AK-LYS1	AK-LYS1 (ASPARTATE KINASE 1); aspartate kinase
At5g67100	ICU2	ICU2 (INCURVATA2); DNA-directed DNA polymerase
At3g06650	ACLB-1	ACLB-1; ATP citrate synthase
At2g32400	GLR5	GLR5 (GLUTAMATE RECEPTOR 5); intracellular ligand-gated ion channel
At2g31840	n.a.	
At1g44835	YbaK	YbaK/prolyl-tRNA synthetase family protein
At2g40316	n.a.	unknown protein
At3g54750	n.a.	unknown protein
At5g05990	MAM33	mitochondrial glycoprotein family protein / MAM33 family protein
At5g14460	transporter	pseudouridine synthase/ transporter
At1g64580	PPR	pentatricopeptide (PPR) repeat-containing protein
At2g27590	n.a.	unknown protein
At1g16780	pyrophosphatase	vacuolar-type H+-translocating inorganic pyrophosphatase, putative
At4g34290	BAF60b	SWIB complex BAF60b domain-containing protein
At1g08640	n.a.	unknown protein
At2g22870	EMB2001	EMB2001 (embryo defective 2001); GTP binding
At5g07590	WD-40 repeat	WD-40 repeat protein family
At1g03560	PPR	pentatricopeptide (PPR) repeat-containing protein
At2g44650	CHL-CPN10	CHL-CPN10 (CHLOROPLAST CHAPERONIN 10); chaperone binding
At3g16080	RPL37C	60S ribosomal protein L37 (RPL37C)
At4g38220	hydrolase	aminoacylase, putative / N-acyl-L-amino-acid amidohydrolase, putative
At3g55170	RPL35C	60S ribosomal protein L35 (RPL35C)
At5g20080	reductase	NADH-cytochrome b5 reductase, putative
At1g65060	4CL3	4CL3; 4-coumarate-CoA ligase
At3g12930	n.a.	
At3g55920	rotamase	peptidyl-prolyl cis-trans isomerase, putative / cyclophilin, putative / rotamase, putative
At3g20050	TCP-1	ATTCP-1; ATP binding / protein binding / unfolded protein binding
At2g23950	kinase	leucine-rich repeat family protein / protein kinase family protein
At3g02060	DEAD	DEAD/DEAH box helicase, putative
At4g16265	NRPB9B	NRPB9B; DNA binding / DNA-directed RNA polymerase/ nucleic acid binding / transcription regulator/ zinc ion binding
At2g30460	n.a.	
At3g63410	APG1	APG1 (ALBINO OR PALE GREEN MUTANT 1); 2-methyl-6-phytyl-1,4-benzoquinone methyltransferase/ S-adenosylmethionine-dependent methyltransferase/ methyltransferase
At2g05920	subtilase	subtilase family protein
At5g55580	transcription	mitochondrial transcription termination factor family protein / mTERF family protein
At1g74690	IQD31	IQD31 (IQ-domain 31); calmodulin binding
At1g27400	RPL17A	60S ribosomal protein L17 (RPL17A)
At5g11480	GTP binding	GTP binding
At2g19680	ATP synthase	mitochondrial ATP synthase g subunit family protein
At2g40550	ETG1	ETG1 (E2F TARGET GENE 1)
At4g18060	clathrin binding	clathrin binding
260118_s_at	n.a.	At1g33940;At5g18700
At3g02900	n.a.	unknown protein
At5g61170	RPS19C	40S ribosomal protein S19 (RPS19C)
At5g12860	DiT1	DiT1 (dicarboxylate transporter 1); oxoglutarate:malate antiporter
At1g73230	NAC	nascent polypeptide-associated complex (NAC) domain-containing protein
At4g02790	GTP-binding	GTP-binding family protein
267187_s_at	n.a.	At3g59970;At2g44160
At1g71440	PFI	PFI (PFIFFERLING)
At3g15390	SDE5	SDE5 (silencing defective 5)
264419_s_at	n.a.	At5g33320;At1g43310
At5g58420	RPS4D	40S ribosomal protein S4 (RPS4D)
At3g10160	DFC	DFC (DHFS-FPGS HOMOLOG C); tetrahydrofolylpolyglutamate synthase
At4g17770	TPS5	ATTPS5; protein binding / transferase, transferring glycosyl groups / trehalose-phosphatase
At3g05560	RPL22B	60S ribosomal protein L22-2 (RPL22B)
At5g61420	MYB28	MYB28 (myb domain protein 28); DNA binding / transcription factor
At2g26730	kinase	leucine-rich repeat transmembrane protein kinase, putative
At5g65810	n.a.	unknown protein

At4g34980	SLP2	SLP2; serine-type peptidase
At1g09750	DNA-binding	chloroplast nucleoid DNA-binding protein-related
At3g10140	RECA3	RECA3 (recA homolog 3); ATP binding / DNA binding / DNA-dependent ATPase/ nucleoside-triphosphatase/ nucleotide binding

Supplemental Data 2. Genes co-regulated with *RE* (At2g33786). Own co-regulational analysis. AGI: *Arabidopsis* genome identifier.

AGI	Annotation
At5g57230	expressed protein|
At5g56280	COP9 signalosome subunit 6 / CSN subunit 6 (CSN6A)| identical to CSN complex subunit 6A (Arabidopsis thaliana) GI:18056665, COP9 complex subunit 6 (Arabidopsis thaliana) GI:15809663; contains Pfam profile PF01398: Mov34/MPN/PAD-1 family; identical to cDNA
At1g18070	EF-1-alpha-related GTP-binding protein, putative| similar to EF-1-alpha-related GTP-binding protein gi|1009232|gb|AAA79032
At5g67220	nitrogen regulation family protein| similar to unknown protein (gb|AAF51525.1) ; contains Pfam domain PF01207: Dihydrouridine synthase (Dus); similar to (SP:P45672) NIFR3-like protein (SP:P45672) (Azospirillum brasilense)
At1g80410	acetyltransferase-related| low similarity to acetyltransferase Tubedown-1 (Mus musculus) GI:8497318, N-TERMINAL ACETYLTRANSFERASE GB:P12945 from (Saccharomyces cerevisiae); contains Pfam profile PF00515 TPR Domain
At5g36950	DegP protease contains similarity to DegP2 protease GI:13172275 from [Arabidopsis thaliana]
At1g32580	plastid developmental protein DAG, putative| similar to DAG protein, chloroplast precursor (Garden snapdragon) SWISS-PROT:Q38732
At1g74260	purL-FGAM synthase
At4g25550	expressed protein|
At5g47320	40S ribosomal protein S19 ; supported by cDNA: gi_15028320_gb_AY045963.1_
At1g29880	glycyl tRNA synthetase, putative similar to glycyl tRNA synthetase GI:577711 from [Homo sapiens];supported by full-length cDNA: Ceres:29666.
At3g20330	pyrB-ATCase
At5g58370	expressed protein|
At4g16700	Phosphatidylserine Decarboxylase
At1g69210	expressed protein|
At5g54580	RNA recognition motif (RRM)-containing protein
At4g32520	glycine hydroxymethyltransferase, putative / serine hydroxymethyltransferase, putative / serine/threonine aldolase, putative| similar to serine hydroxymethyltransferase (Chlamydomonas reinhardtii) GI:17066746; contains Pfam profile PF00464: serine hydroxy
At3g10050	threonine ammonia-lyase / threonine dehydratase / threonine deaminase (OMR1)| identical to SP|Q9ZSS6 Threonine dehydratase biosynthetic, chloroplast precursor (EC 4.3.1.19, formerly EC 4.2.1.16) (Threonine deaminase) (TD) {Arabidopsis thaliana}
At5g08420	expressed protein|
At4g18590	expressed protein|
At4g16265	DNA-directed RNA polymerase II, putative| similar to SP|P36958 DNA-directed RNA polymerase II 15.1 kDa polypeptide (EC 2.7.7.6) {Drosophila melanogaster}; contains Pfam profile PF02150: RNA polymerases M/15 Kd subunit
At5g54970	expressed protein|
At5g52220	expressed protein| ; expression supported by MPSS
At3g46940	deoxyuridine 5'-triphosphate nucleotidohydrolase family| contains Pfam profile: PF00692 deoxyuridine 5'-triphosphate nucleotidohydrolase
At3g14740	PHD finger family protein| similar to zinc-finger protein BR140 (PIR|JC2069)(Homo sapiens); contains PHD-finger domain PF00628
At4g34265	expressed protein|
At5g16870	expressed protein|
At4g37660	ribosomal - like protein ribosomal protein L12, Liberobacter africanum, U09675;supported by full-length cDNA: Ceres:41011.
At3g58470	expressed protein| several hypothetical proteins - Saccharomyces cerevisiae
At3g57220	UDP-GlcNAc:dolichol phosphate N-acetylglucosamine-1-phosphate transferase, putative
At1g59600	expressed protein
At4g39120	inositol monophosphatase family protein| low similarity to Mono-phosphatase (Streptomyces anulatus) GI:1045231; contains Pfam profile PF00459: Inositol monophosphatase family
At1g47210	cyclin family protein| similar to A-type cyclin (Catharanthus roseus) GI:2190259; contains Pfam profile PF00134: Cyclin, N-terminal domain
At2g42710	hypothetical protein predicted by genefinder
At1g64580	pentatricopeptide (PPR) repeat-containing protein| low similarity to fertility restorer (Petunia x hybrida) GI:22128587; contains Pfam profile PF01535: PPR repeat
At1g65470	chromatin assembly factor-1 (FASCIATA1) (FAS1)| identical to FAS1 (Arabidopsis thaliana) GI:4887626
At3g56810	expressed protein|
At2g37790	aldo/keto reductase family protein| similar to chalcone reductase (Sesbania rostrata)(GI:2792155), and aldose reductase ALDRXV4 (Xerophyta viscosa)(GI:4539944), (Hordeum vulgare)(GI:728592)
At1g15000	serine carboxypeptidase precursor, putative similar to GB:AAD42963 from [Matricaria chamomilla]
At5g17630	AtXPT
At2g23350	polyadenylate-binding protein, putative / PABP, putative|
At3g23940	dehydratase family
At1g31860	PRS-hisIE
At5g10920	argininosuccinate lyase, putative / arginosuccinase, putative| similar to argininosuccinate lyase (Nostoc punctiforme) GI:7672743; contains Pfam profile PF00206: Lyase
At3g14390	diaminopimelate decarboxylase, putative / DAP carboxylase, putative| similar to diaminopimelate decarboxylase (Arabidopsis thaliana) GI:6562332; contains Pfam profiles PF02784: Pyridoxal-dependent decarboxylase pyridoxal binding domain, PF00278: Pyridoxal
At3g58610	ketol-acid reductoisomerase| identical to ketol-acid reductoisomerase, chloroplast precursor (EC 1.1.1.86) (Acetohydroxy-acid reductoisomerase) (Alpha-keto-beta-hydroxylacil reductoisomerase) (Swiss-Prot:Q05758) (Arabidopsis thaliana)
At1g80560	3-isopropylmalate dehydrogenase, chloroplast, putative| strong similarity to 3-ISOPROPYLMALATE DEHYDROGENASE PRECURSOR GB:P29102 SP|P29102 from (Brassica napus)
At3g53580	diaminopimelate epimerase family protein| contains Pfam profile PF01678: Diaminopimelate epimerase
At3g05130	expressed protein| ; expression supported by MPSS
At1g03687	DTW domain-containing protein
At4g13720	inosine triphosphate pyrophosphatase, putative / HAM1 family protein
At3g60210	chloroplast chaperonin 10, putative| similar to chloroplast chaperonin 10 GI:14041813 from (Arabidopsis thaliana)
At2g44040	dihydrodipicolinate reductase family protein| weak similarity to SP|Q52419 Dihydrodipicolinate reductase (EC 1.3.1.26) (DHPR) {Pseudomonas syringae} ; contains Pfam profiles PF01113: Dihydrodipicolinate reductase N-terminus, PF05173: Dihydrodipicolinate r
At2g33330	33 kDa secretory protein-related| contains Pfam PF01657: Domain of unknown function, duplicated in 33 KDa secretory proteins
At4g26900	imidazole glycerol phosphate synthase hisHF, chloroplast / IGP synthase / ImGPP synthase / IGPS
At3g57610	purA-adenyosuccinate synthase
At2g35040	purH-AICAR transformylase+IMPcyclohydrolase
At1g75330	ornithine carbamoyltransferase, chloroplast / ornithine transcarbamylase / OTCase (OTC)| identical to SP|O50039 Ornithine carbamoyltransferase, chloroplast precursor (EC 2.1.3.3) (OTCase) (Ornithine transcarbamylase) {Arabidopsis thaliana}
At2g37500	arginine biosynthesis protein ArgJ family| contains Pfam profile: PF01960 ArgJ family
At2g43090	aconitase C-terminal domain-containing protein| contains Pfam profile PF00694: Aconitase C-terminal domain
At4g38100	hypothetical protein ;supported by full-length cDNA: Ceres:21.
At2g37860	expressed protein|reticulata
At5g13280	aspartate kinase| identical to aspartate kinase (Arabidopsis thaliana) GI:4376158
At3g26420	glycine-rich RNA-binding protein| similar to RNA-binding protein (RZ-1) GB:BAA12064 (Nicotiana sylvestris); contains Pfam profile: PF00076 RNA recognition motif. (a.k.a. RRM, RBD, or RNP domain)
At1g45170	expressed protein
At1g76405	expressed protein|
At1g55805	BolA-like family protein
At2g11890	expressed protein|

Literature

Al-Whaibi MH (2011) Plant heat-shock proteins: A mini review. Journal of King Saud University - Science **23:** 139-150

Anastasiou E, Lenhard M (2007) Growing up to one's standard. Current Opinion in Plant Biology **10:** 63-69

Ascough GD, Novák O, Pěnčík A, Rolčík J, Strnad M, Erwin JE, Van Staden J (2009) Hormonal and cell division analyses in *Watsonia lepida* seedlings. Journal of Plant Physiology **166:** 1497-1507

Bahassi EM, Salmon MA, Van Melderen L, Bernard P, Couturier M (1995) F plasmid CcdB killer protein - *ccdB* gene mutants coding for non-cytotoxic proteins which retain their regulatory functions. Molecular Microbiology **15:** 1031-1037

Bajguz A, Piotrowska A (2009) Conjugates of auxin and cytokinin. Phytochemistry **70:** 957-969

Barczak AJ, Zhao JM, Pruitt KD, Last RL (1995) 5-fluoroindole resistance identifies tryptophan synthase beta subunit mutants in *Arabidopsis thaliana*. Genetics **140:** 303-313

Barth C, Conklin PL (2003) The lower cell density of leaf parenchyma in the *Arabidopsis thaliana* mutant *lcd1-1* is associated with increased sensitivity to ozone and virulent *Pseudomonas syringae*. Plant Journal **35:** 206-218

Bartlem D, Lambein I, Okamoto T, Itaya A, Uda Y, Kijima F, Tamaki Y, Nambara E, Naito S (2000) Mutation in the threonine synthase gene results in an over-accumulation of soluble methionine in *Arabidopsis*. Plant Physiology **123:** 101-110

Batoko H, Zheng HQ, Hawes C, Moore I (2000) A Rab1 GTPase is required for transport between the endoplasmic reticulum and Golgi apparatus and for normal Golgi movement in plants. Plant Cell **12:** 2201-2217

Bernard P, Couturier M (1992) Cell killing by the F plasmid ccdb protein involves poisoning of DNA-topoisomerase II complexes. Journal of Molecular Biology **226:** 735-745

Boston RS, Viitanen PV, Vierling E (1996) Molecular chaperones and protein folding in plants. Plant Molecular Biology **32:** 191-222

Bräutigam A, Weber APM (2009) Proteomic Analysis of the Proplastid Envelope Membrane Provides Novel Insights into Small Molecule and Protein Transport across Proplastid Membranes. Molecular Plant **2:** 1247-1261

Breuers FK, Braeutigam A, Geimer S, Welzel UY, Stefano G, Renna L, Brandizzi F, Weber APM (2012) Dynamic remodeling of the plastid envelope membranes: a tool for chloroplast envelope in vivo localizations. Frontiers in Plant Science **3:** article 7, 1-10

Brugière N, Dubois F, Masclaux C, Sangwan RS, Hirel B (2000) Immunolocalization of glutamine synthetase in senescing tobacco (*Nicotiana tabacum* L.) leaves suggests that ammonia assimilation is progressively shifted to the mesophyll cytosol. Planta **211:** 519-527

Bukhov N, Carpentier R (2004) Alternative Photosystem I-driven electron transport routes: mechanisms and functions. Photosynthesis Research **82:** 17-33

Byrne ME (2005) Networks in leaf development. Current Opinion in Plant Biology **8:** 59-66

Byrne ME (2012) Making leaves. Current Opinion in Plant Biology **15:** 24-30

Casson SA, Lindsey K (2003) Genes and signalling in root development. New Phytologist **158:** 11-38

Chivasa S, Slabas AR (2012) Plant extracellular ATP signalling: new insight from proteomics. Molecular Biosystems **8:** 445-452

Chomczynski P, Sacchi N (1987) Single-Step Method Of RNA Isolation By Acid Guanidinium Thiocyanate Phenol Chloroform Extraction. Analytical Biochemistry **162:** 156-159

Chomczynski P, Sacchi N (2006) The single-step method of RNA isolation by acid guanidinium thiocyanate-phenol-chloroform extraction: twenty-something years on. Nat. Protocols **1:** 581-585

Clough SJ, Bent AF (1998) Floral dip: a simplified method for *Agrobacterium*-mediated transformation of *Arabidopsis thaliana*. Plant Journal **16:** 735-743

Colon-Carmona A, You R, Haimovitch-Gal T, Doerner P (1999) Spatio-temporal analysis of mitotic activity with a labile cyclin-GUS fusion protein. Plant Journal **20:** 503-508

Craciun A, Jacobs M, Vauterin M (2000) *Arabidopsis* loss-of-function mutant in the lysine pathway points out complex regulation mechanisms. FEBS Letters **487:** 234-238

Curtis MD, Grossniklaus U (2003) A Gateway Cloning Vector Set for High-Throughput Functional Analysis of Genes in Planta. Plant Physiology **133:** 462-469

De Smet I, Jürgens G (2007) Patterning the axis in plants - auxin in control. Current Opinion in Genetics and Development **17:** 337-343

Dimitrov P, Zucker SW (2006) A constant production hypothesis guides leaf venation patterning. Proceedings of the National Academy of Sciences **103:** 9363-9368

Emanuelsson O, Nielsen H, Brunak S, von Heijne G (2000) Predicting subcellular localization of proteins based on their N-terminal amino acid sequence. Journal of Molecular Biology **300:** 1005-1016

English A, Patel K, Loraine A (2010) Prevalence of alternative splicing choices in *Arabidopsis thaliana*. Bmc Plant Biology **10:** 102

Eveland AL, Jackson DP (2012) Sugars, signalling, and plant development. Journal of Experimental Botany **63:** 3367-3377

Ferro M, Brugiere S, Salvi D, Seigneurin-Berny D, Court M, Moyet L, Ramus C, Miras S, Mellal M, Le Gall S, Kieffer-Jaquinod S, Bruley C, Garin J, Joyard J, Masselon C, Rolland N (2010) AT_CHLORO, a comprehensive chloroplast proteome database with subplastidial localization and curated information on envelope proteins. Molecular and Cellular Proteomics **9:** 1063-1084

Fiehn O (2006) Metabolite profiling in *Arabidopsis*. Salinas J, Sanchez-Serrano JJ (eds) Arabidopsis Protocols **2nd edition**

Fischer K, Kammerer B, Gutensohn M, Arbinger B, Weber A, Häusler RE, Flügge UI (1997) A new class of plastidic phosphate translocators: A putative link between primary and secondary metabolism by the *phosphoenolpyruvate/phosphate* antiporter. Plant Cell **9:** 453-462

Fischer WN, Kwart M, Hummel S, Frommer WB (1995) Substrate specificity and expression profile of amino acid transporters (AAPss) in *Arabidopsis*. Journal of Biological Chemistry **270:** 16315-16320

González-Bayón R, Kinsman EA, Quesada V, Vera A, Robles P, Ponce MR, Pyke KA, Micol JL (2006) Mutations in the *RETICULATA* gene dramatically alter internal architecture but have little effect on overall organ shape in *Arabidopsis* leaves. Journal of Experimental Botany **57:** 3019-3031

Gowik U, Bräutigam A, Weber KL, Weber APM, Westhoff P (2011) Evolution of C_4 photosynthesis in the genus *Flaveria*: how many and which genes does it take to make C_4? Plant Cell **23:** 2087-2105

Grefen C, Donald N, Hashimoto K, Kudla J, Schumacher K, Blatt MR (2010) A ubiquitin-10 promoter-based vector set for fluorescent protein tagging facilitates temporal stability and native protein distribution in transient and stable expression studies. The Plant Journal**:** 355-365

Guyer D, Patton D, Ward E (1995) Evidence for cross-pathway regulation of metabolic gene-expression in plants. Proceedings of the National Academy of Sciences of the United States of America **92:** 4997-5000

Hibberd JM, Quick WP (2002) Characteristics of C_4 photosynthesis in stems and petioles of C_3 flowering plants. Nature **415:** 451-454

Hirner B, Fischer WN, Rentsch D, Kwart M, Frommer WB (1998) Developmental control of H+/amino acid permease gene expression during seed development of *Arabidopsis*. Plant Journal **14:** 535-544

Hoffmann WA, Poorter H (2002) Avoiding bias in calculations of relative growth rate. Annals of Botany **90:** 37-42

Höfgen R, Willmitzer L (1988) storage of competent cells for *Agrobacterium* transformation. Nucleic Acids Research **16:** 9877-9877

Holloway PJ (1983) some variations in the composition of suberin from the cork layers of higher plants. Phytochemistry **22:** 495-502

Horváth I, Glatz A, Nakamoto H, Mishkind ML, Munnik T, Saidi Y, Goloubinoff P, Harwood JL, Vigh L (2012) Heat shock response in photosynthetic organisms: Membrane and lipid connections. Progress in Lipid Research **51:** 208-220

Hung WF, Chen LJ, Boldt R, Sun CW, Li HM (2004) Characterization of *Arabidopsis* glutamine phosphoribosyl pyrophosphate amidotransferase-deficient mutants. Plant Physiology **135:** 1314-1323

Janacek SH, Trenkamp S, Palmer B, Brown NJ, Parsley K, Stanley S, Astley HM, Rolfe SA, Quick WP, Fernie AR, Hibberd JM (2009) Photosynthesis in cells around veins of the C_3 plant *Arabidopsis thaliana* is important for both the shikimate pathway and leaf senescence as well as contributing to plant fitness. Plant Journal **59:** 329-343

Jansen M, Gilmer F, Biskup B, Nagel KA, Rascher U, Fischbach A, Briem S, Dreissen G, Tittmann S, Braun S, De Jaeger I, Metzlaff M, Schurr U, Scharr H, Walter A (2009) Simultaneous phenotyping of leaf growth and chlorophyll fluorescence via GROWSCREEN FLUORO allows detection of stress tolerance in *Arabidopsis thaliana* and other rosette plants. Functional Plant Biology **36:** 902-914

Javelle M, Vernoud V, Rogowsky PM, Ingram GC (2011) Epidermis: the formation and functions of a fundamental plant tissue. New Phytologist **189:** 17-39

Jeter CR, Tang WQ, Henaff E, Butterfield T, Roux SJ (2004) Evidence of a novel cell signaling role for extracellular adenosine triphosphates and diphosphates in *Arabidopsis*. Plant Cell **16:** 2652-2664

Jing YJ, Cui DY, Bao F, Hu ZB, Qin ZX, Hu YX (2009) Tryptophan deficiency affects organ growth by retarding cell expansion in *Arabidopsis*. Plant Journal **57:** 511-521

Johnson GN (2005) Cyclic electron transport in C_3 plants: fact or artefact? Journal of Experimental Botany **56:** 407-416

Joshi V, Laubengayer KM, Schauer N, Fernie AR, Jander G (2006) Two *Arabidopsis* threonine aldolases are nonredundant and compete with threonine deaminase for a common substrate pool. Plant Cell **18:** 3564-3575

Kangasjärvi S, Nurmi M, Tikkanen M, Aro EM (2009) Cell-specific mechanisms and systemic signalling as emerging themes in light acclimation of C_3 plants. Plant Cell and Environment **32:** 1230-1240

Kichey T, Le Gouis J, Sangwan B, Hirel B, Dubois F (2005) Changes in the cellular and subcellular localization of glutamine synthetase and glutamate dehydrogenase during flag leaf senescence in wheat (*Triticum aestivum* L.). Plant and Cell Physiology **46:** 964-974

Kim MC, Chung WS, Yun D-J, Cho MJ (2009) Calcium and calmodulin-mediated regulation of gene expression in plants. Molecular Plant **2:** 13-21

Kinsman EA, Pyke KA (1998) Bundle sheath cells and cell-specific plastid development in *Arabidopsis* leaves. Development **125:** 1815-1822

Knappe S, Löttgert T, Schneider A, Voll L, Flügge UI, Fischer K (2003) Characterization of two functional *phosphoenolpyruvate/phosphate translocator (PPT)* genes in *Arabidopsis*-AtPPT1 may be involved in the provision of signals for correct mesophyll development. Plant Journal **36:** 411-420

Koncz C, Schell J (1986) The promoter of TL-DNA gene 5 controls the tissue-specific expression of chimeric genes carried by a novel type of *Agrobacterium* binary vector. Molecular and General Genetics **204:** 383-396

Kurepa J, Smalle JA (2008) Structure, function and regulation of plant proteasomes. Biochimie **90:** 324-335

Kwart M, Hirner B, Hummel S, Frommer WB (1993) Differential expression of two related amino acid transporters with differing substrate specificity in *Arabidopsis thaliana*. The Plant Journal **4:** 993-1002

Ladwig F, Stahl M, Ludewig U, Hirner AA, Hammes UZ, Stadler R, Harter K, Koch W (2012) Siliques Are Red1 from *Arabidopsis* acts as a bidirectional amino acid transporter that is crucial for the amino acid homeostasis of siliques. Plant Physiology **158:** 1643-1655

Lam HM, Coschigano K, Schultz C, Melo-Oliveira R, Tjaden G, Oliveira I, Ngai N, Hsieh MH, Coruzzi G (1995) Use of *Arabidopsis* mutants and genes to study amide amino acid biosynthesis. Plant Cell **7:** 887-898

Last RL, Bissinger PH, Mahoney DJ, Radwanski ER, Fink GR (1991) Tryptophan mutants in *Arabidopsis*: the consequences of dublicated tryptophan synthase ß genes. Plant Cell **3:** 345-358

Leegood RC (2008) Roles of the bundle sheath cells in leaves of C_3 plants. Journal of Experimental Botany **59:** 1663-1673

Leonard NJ, Hecht SM, Skoog F, Schmitz RY (1969) Cytokinins: synthesis, mass spectra, and biological activity of compounds related to zeatin. Proceedings of the National Academy of Sciences of the United States of America **63:** 175-182

Lepistö A, Kangasjärvi S, Luomala EM, Brader G, Sipari N, Keränen M, Keinänen M, Rintamäki E (2009) Chloroplast NADPH-thioredoxin reductase interacts with photoperiodic development in *Arabidopsis*. Plant Physiology **149:** 1261-1276

Lepistö A, Rintamäki E (2012) Coordination of plastid and light signaling pathways upon development of *Arabidopsis* leaves under various photoperiods. Molecular Plant **5:** 799-816

Lewis NG, Yamamoto E (1990) Lignin: occurence, biogenesis and biodegradation. Annual Review of Plant Physiology and Plant Molecular Biology **41:** 455-496

Li HM, Culligan K, Dixon RA, Chory J (1995) *CUE1*: a mesophyll cell-specific positive regulator of light-controlled gene-expression in *Arabidopsis*. Plant Cell **7:** 1599-1610

Matsubara S (1980) Structure-activity relationships of cytokinins. Phytochemistry **19:** 2239-2253

Mattsson J, Ckurshumova W, Berleth T (2003) Auxin signaling in *Arabidopsis* leaf vascular development. Plant Physiology **131:** 1327-1339

Mersereau M, Pazour GJ, Das A (1990) Efficient transformation of *Agrobacterium tumefaciens* by electroporation. Gene **90:** 149-151

Mitchell DE, Gadus MV, Madore MA (1992) Patterns of assimilate production and translocation in muskmelon (*Cucumis melo* L) I. Diurnal Patterns. Plant Physiology **99:** 959-965

Mizukami Y (2001) A matter of size: developmental control of organ size in plants. Current Opinion in Plant Biology **4:** 533-539

Mok DWS, Mok MC (2001) Cytokinin metabolism and action. Annual Review of Plant Physiology and Plant Molecular Biology **52:** 89-118

Mollá-Morales A, Sarmiento-Mañús R, Robles P, Quesada V, Pérez-Pérez JM, González-Bayón R, Hannah MA, Willmitzer L, Ponce MR, Micol JL (2011) Analysis of *ven3* and *ven6* reticulate mutants reveals the importance of arginine biosynthesis in *Arabidopsis* leaf development. The Plant Journal **65:** 335-345

Muralla R, Sweeney C, Stepansky A, Leustek T, Meinke D (2007) Genetic dissection of histidine biosynthesis in *Arabidopsis*. Plant Physiol. **144:** 890-903

Nolte KD, Koch KE (1993) Companion-cell specific localization of sucrose synthase in zones of phloem loading and unloading. Plant Physiology **101:** 899-905

Novák O, Hauserová E, Amakorová P, Doležal K, Strnad M (2008) Cytokinin profiling in plant tissues using ultra-performance liquid chromatography-electrospray tandem mass spectrometry. Phytochemistry **69:** 2214-2224

Novák O, Hényková E, Sairanen I, Kowalczyk M, Pospíšil T, Ljung K (2012) Tissue-specific profiling of the *Arabidopsis thaliana* auxin metabolome. The Plant Journal**:** 1-14

Novák O, Tarkowski P, Tarkowská D, Doležal K, Lenobel R, Strnad M (2003) Quantitative analysis of cytokinins in plants by liquid chromatography - single-quadrupole mass spectrometry. Analytica Chimica Acta **480:** 207-218

Obayashi T, Kinoshita K, Nakai K, Shibaoka M, Hayashi S, Saeki M, Shibata D, Saito K, Ohta H (2007) ATTED-II: a database of co-expressed genes and cis elements for identifying co-regulated gene groups in *Arabidopsis*. Nucleic Acids Research **35:** D863-D869

Obayashi T, Nishida K, Kasahara K, Kinoshita K ATTED-II Updates: Condition-Specific Gene Coexpression to Extend Coexpression Analyses and Applications to a Broad Range of Flowering Plants. Plant and Cell Physiology **52:** 213-219

Ort DR (1986) Energy transduction in oxygenic photosynthesis, an overview of structure and mechanism. *In* LA Steahlin, CJ Arntzen, eds, Encyclopedia of Plant Physiology (New Series), Vol 19. Springer Verlag, Berlin, pp 179-196

Ouyang J, Shao X, Li J (2000) Indole-3-glycerol phosphate, a branchpoint of indole-3-acetic acid biosynthesis from the tryptophan biosynthetic pathway in *Arabidopsis thaliana*. The Plant Journal **24:** 327-333

Overmyer K, Kollist H, Tuominen H, Betz C, Langebartels C, Wingsle G, Kangasjarvi S, Brader G, Mullineaux P, Kangasjärvi J (2008) Complex phenotypic profiles leading to ozone sensitivity in *Arabidopsis thaliana* mutants. Plant Cell and Environment **31:** 1237-1249

Pérez-Pérez JM, Rubio-Díaz S, Dhondt S, Hernández-Romero D, Sánchez-Soriano J, Beemster GTS, Ponce MR, Micol JL (2011) Whole organ, venation and epidermal cell morphological variations are correlated in the leaves of *Arabidopsis* mutants. Plant, Cell and Environment **34:** 2200-2211

Porra RJ, Thompson WA, Kriedemann PE (1989) Determination of accurate extinction coefficients and simultaneous equations for assaying chlorophylls a and b extracted with four different solvents: verification of the concentration of chlorophyll standards by atomic absorption spectroscopy. Biochimica et Biophysica Acta **975:** 384-394

Powell AE, Lenhard M (2012) Control of Organ Size in Plants. Current Biology **22:** R360-R367

Radwanski ER, Barczak AJ, Last RL (1996) Characterization of tryptophan synthase alpha subunit mutants of *Arabidopsis thaliana*. Molecular and General Genetics **253:** 353-361

Reddy ASN (2001) Calcium: silver bullet in signaling. Plant Science **160:** 381-404

Rédei GP, Hironyo Y (1964) Linkage studies. Arabidopsis Information Service **1:** 9-10

Reed RC, Brady SR, Muday GK (1998) Inhibition of auxin movement from the shoot into the root inhibits lateral root development in *Arabidopsis*. Plant Physiology **118:** 1369-1378

Rentsch D, Hirner B, Schmelzer E, Frommer WB (1996) Salt stress-induced proline transporters and salt stress-repressed broad specificity amino acid permeases identified by suppression of a yeast amino acid permease-targeting mutant. Plant Cell **8:** 1437-1446

Rodriguez CMS, Petersen M, Mundy J (2010) Mitogen-activated protein kinase signaling in plants. Annual Review of Plant Biology **61:** 621-649

Rosar C, Kanonenberg K, Nanda AM, Mielewczik M, Bräutigam A, Novák O, Strnad M, Walter A, Weber APM (2012) The leaf reticulate mutant *dov1* is impaired in the first step of purine metabolism. Molecular Plant doi:10.1093/mp/sss045

Rubio V, Bustos R, Irigoyen M, Cardona-López X, Rojas-Triana M, Paz-Ares J (2009) Plant hormones and nutrient signaling. Plant Molecular Biology **69:** 361-373

Ruuhola T, Ossipov V, Lempa K, Haukioja E (2003) Amino acids during development of mountain birch leaves. Chemoecology **13:** 95-101

Sakakibara H (2006) Cytokinins: Activity, biosynthesis, and translocation. *In* Annual Review of Plant Biology, Vol 57, pp 431-449

Sambrook J, Russell DW, Irwin N, Janssen KA (2001) Molecular Cloning: a laboratory manual, Ed third edition. Cold Spring Harbor Laboratory Press, Cold Spring Harbor, New York

Sanchez-Calderon L, Lopez-Bucio J, Chacon-Lopez A, Cruz-Ramirez A, Nieto-Jacobo F, Dubrovsky JG, Herrera-Estrella L (2005) Phosphate starvation induces a determinate developmental program in the roots of Arabidopsis thaliana. Plant and Cell Physiology **46:** 174-184

Santner A, Estelle M (2009) Recent advances and emerging trends in plant hormone signalling. Nature **459:** 1071-1078

Santner A, Estelle M (2010) The ubiquitin-proteasome system regulates plant hormone signaling. The Plant Journal **61:** 1029-1040

Savaldi-Goldstein S, Peto C, Chory J (2007) The epidermis both drives and restricts plant shoot growth. Nature **446:** 199-202

Schmid J, Amrhein N (1995) Molecular organization of the shikimate pathway in higher plants. Phytochemistry **39:** 737-749

Schmitz RY, Skoog F, Bock RM, Leonard NJ, Hecht SM (1972) Comparison of cytokinin activities of naturally occurring ribonucleosides and corresponding bases. Phytochemistry **11:** 1603-1610

Schobert C, Lucas W, Franceschi V, Frommer W (2004) Intercellular transport and phloem loading of sucrose, oligosaccharides and amino Acids. *In:* Photosynthesis. R Leegood, T Sharkey, S Caemmerer, eds, Vol 9. Springer Netherlands, pp 249-274

Schwacke R, Schneider A, van der Graaff E, Fischer K, Catoni E, Desimone M, Frommer WB, Flugge UI, Kunze R (2003) ARAMEMNON, a novel database for *Arabidopsis* integral membrane proteins. Plant Physiology **131:** 16-26

Serrato AJ, Pérez-Ruiz JM, Spínola MC, Cejudo FJ (2004) A novel NADPH thioredoxin reductase, localized in the chloroplast, which deficiency causes hypersensitivity to abiotic stress in *Arabidopsis thaliana*. Journal of Biological Chemistry **279:** 43821-43827

Shen WJ, Forde BG (1989) Eefficient transformation of *Agrobacterium* spp by high voltage electroporation. Nucleic Acids Research **17:** 8385-8385

Simpson CG, Lewandowska D, Fuller J, Maronova M, Kalyna M, Davidson D, McNicol J, Raczynska D, Jarmolowski A, Barta A, Brown JWS (2008) Alternative splicing in plants. Biochemical Society Transactions **36:** 508-510

Stähr P (2010) Untersuchungen an *Arabidopsis thaliana*-Mutanten mit einer Defizienz der plastidären Phosphoenolpyruvat/Phosphat-Translokatoren (PPT1 und PPT2): Plastidäres Phosphoenolpyruvat steuert Stoffwechsel- und Entwicklungsprozesse. Ph.D. . University of Cologne, Cologne

Stepansky A, Leustek T (2006) Histidine biosynthesis in plants. Amino Acids **30:** 127-142

Streatfield SJ, Weber A, Kinsman EA, Häusler RE, Li JM, Post-Beittenmiller D, Kaiser WM, Pyke KA, Flügge UI, Chory J (1999) The *phosphoenolpyruvate/phosphate translocator* is required for phenolic metabolism, palisade cell development, and plastid-dependent nuclear gene expression. Plant Cell **11:** 1609-1621

Sun J, Zhang CL, Deng SR, Lu CF, Shen X, Zhou XY, Zheng XJ, Hu ZM, Chen SL (2012) An ATP signalling pathway in plant cells: extracellular ATP triggers programmed cell death in *Populus euphratica*. Plant Cell and Environment **35:** 893-916

Syed NH, Kalyna M, Marquez Y, Barta A, Brown JWS (2012) Alternative splicing in plants - coming of age. Trends in Plant Science **17:** 616-623

Tao Y, Ferrer J-L, Ljung K, Pojer F, Hong F, Long JA, Li L, Moreno JE, Bowman ME, Ivans LJ, Cheng Y, Lim J, Zhao Y, Ballaré CL, Sandberg G, Noel JP, Chory J (2008) Rapid synthesis of auxin via a new tryptophan-dependent pathway is required for shade avoidance in plants. Cell **133:** 164-176

Thomas C, Rajagopal A, Windsor B, Dudler R, Lloyd A, Roux SJ (2000) A role for ectophosphatase in xenobiotic resistance. Plant Cell **12:** 519-533

Tsugeki R, Fedoroff NV (1999) Genetic ablation of root cap cells in *Arabidopsis*. Proceedings of the National Academy of Sciences of the United States of America **96:** 12941-12946

Tsukaya H (2006) Mechanism of leaf-shape determination. *In* Annual Review of Plant Biology, Vol 57, pp 477-496

Tsukaya H (2008) Leaf development. *In* The Arabidopsis Book, Vol null. The American Society of Plant Biologists, pp 1-23

Turgeon R (2010) The role of phloem loading reconsidered. Plant Physiology **152:** 1817-1823

Tzin V, Galili G (2010) New insights into the shikimate and aromatic amino acids biosynthesis pathways in plants. Molecular Plant **3:** 956-972

Van der Graaff E, Hooykaas P, Lein W, Lerchl J, Kunze G, Sonnwald U, Boldt R (2004) Molecular analysis of "de novo" purine biosynthesis in solanaceous species and in *Arabidopsis thaliana*. Frontiers in Bioscience **9:** 1803-1816

Vierstra RD (2009) The ubiquitin-26S proteasome system at the nexus of plant biology. Nat Rev Mol Cell Biol **10:** 385-397

Vogt T (2010) Phenylpropanoid biosynthesis. Molecular Plant **3:** 2-20

Voll L, Häusler RE, Hecker R, Weber A, Weissenböck G, Fiene G, Waffenschmidt S, Flügge UI (2003) The phenotype of the *Arabidopsis cue1* mutant is not simply caused by a general restriction of the shikimate pathway. Plant Journal **36:** 301-317

Voll LM, Allaire EE, Fiene G, Weber APM (2004) The *Arabidopsis phenylalanine insensitive growth* mutant exhibits a deregulated amino acid metabolism. Plant Physiology **136:** 3058-3069

Walch-Liu P, Liu L-H, Remans T, Tester M, Forde BG (2006) Evidence that L-glutamate can act as an exogenous signal to modulate root growth and branching in *Arabidopsis thaliana*. Plant and Cell Physiology **47:** 1045-1057

Walter A, Scharr H, Gilmer F, Zierer R, Nagel KA, Ernst M, Wiese A, Virnich O, Christ MM, Uhlig B, Junger S, Schurr U (2007) Dynamics of seedling growth acclimation towards altered light conditions can be quantified via GROWSCREEN: a setup and procedure designed for rapid optical phenotyping of different plant species. New Phytologist **174:** 447-455

Westfall CS, Herrmann J, Chen Q, Wang S, Jez JM (2010) Modulating plant hormones by enzyme action: The GH3 family of acyl acid amido synthetases. Plant signaling and behavior **5:** 1607-1612

Wiese A, Christ MM, Virnich O, Schurr U, Walter A (2007) Spatio-temporal leaf growth patterns of *Arabidopsis thaliana* and evidence for sugar control of the diel leaf growth cycle. New Phytologist **174:** 752-761

Zhang XR, Henriques R, Lin SS, Niu QW, Chua NH (2006) *Agrobacterium*-mediated transformation of *Arabidopsis thaliana* using the floral dip method. Nature Protocols **1:** 641-646

Zrenner R, Stitt M, Sonnewald U, Boldt R (2006) Pyrimidine and purine biosynthesis and degradation in plants. Annual Review of Plant Biology **57:** 805-836

Zybailov B, Rutschow H, Friso G, Rudella A, Emanuelsson O, Sun Q, van Wijk KJ (2008) Sorting Signals, N-Terminal Modifications and Abundance of the Chloroplast Proteome. Plos One **3:** e1994

The authors` contributions to Manuscript 3

C.R. wrote the manuscript, performed the genetic complementation of *re* (Figure 1), protein localization studies (Figure 2) and determined the plant growth rate and photosynthetic performance in cooperation (Figure 3) with **M.M. C.R.** determined plant hormone (Figure 6) and purine levels (Figure 9) in cooperation with **O.N**. and **M.S.** Cytokinin-, and auxin-reporter assays (Figure 7), polar metabolite profiling (Figure 8) and lysine complementation (Figure 10) was done by **C.R.** All experiments depicted as Supplemental Figures, except for phylogenetic analysis, was accomplished by **C.R.** The phylogenetic tree was calculated by **A.B.**

P.S. performed the microarray analysis together with **A.B.**, **J.S.**, and **R.H.** (Figure 5).

J.S. performed the microarray analysis together with **A.B.**, **P.S.**, and **R.H.** (Figure 5).

M.M. determined plant growth rates and photosynthetic capacity (Figure 1) in cooperation with **C.R. M.M.** established diel growth patterns (Figure 4).

A.B. did the phylogenetic analysis (Supplemental Figure 3) and analyzed the microarray data (Figure 5).

O.N. determined cytokinin-, auxin- and purine concentrations in cooperation with **C.R.** (Figure 6 and Figure 9).

A.B. and **A.P.M.W.** participated in drafting the manuscript.

VII. Addendum

Experiments and data that were neither published nor included in the *Manuscripts* are presented in this section. These data and tools will be useful for future studies. The *Addendum* is subdivided into two parts: (i) the characterization of *reticulata* and (ii) the transcriptional profiling of mesophyll (M) and bundle sheath (BS) cells. The latter project intended to use laser microdissection (LMD) coupled to deep-sequencing to establish a transcriptional profile of the *Arabidopsis* M and BS. The *Addendum* starts with the hypothesis of RE being a novel amino acid transporter. The chapters are streamlined to this hypothesis and deal with the aim of the experiment, the results and include a short discussion. Future experiments with the appropriate tools are shortly discussed.

1. Results of the RETICULATA project

1.1 RE - a potential novel amino acid transporter

There is strong evidence that *re* is involved in amino acid metabolism (Manuscripts 1 and 3). Briefly, this is: all evenly reticulated plants are deregulated in amino acid metabolism; *CUE1*, affected in aromatic amino acid synthesis, is epistatic to *RE* and thus *RE* is likely involved in the same pathway; *RE* is co-regulated with amino acid metabolism genes; *re* shows altered amino acid patterns; *re* has lowered lysine levels; and the basic amino acids lysine and arginine revert the *re* phenotype. Consistent with the plastidic synthesis of most amino acids and the plastid envelope localized RE protein, which contains transmembrane regions, it is tempting to hypothesize that RE is an amino acid transporter for basic amino acids.

Only little is known about amino acid transporters in plants (Tegeder, 2012). The majority of identified transporters is localized to the plasma membrane of the root epidermis/cortex, and the phloem of siliques and seeds (Tegeder, 2012) for uptake from the soil (Lee et al., 2007; Lehmann et al., 2011; Svennerstam et al., 2011; Tegeder, 2012) and import into the developing seed/embryo (Sanders et al., 2009; Tegeder, 2012), respectively. Since amino acids are largely synthesized in shoot and root plastids (Mills et al., 1980; Galili, 1995; Slocum, 2005; Tegeder and Weber, 2006; Rentsch et al., 2007), they need to be exported to reach their destinations, such as being loaded into the phloem to be delivered from source to sink tissues. Much like transporters in phloem loading have not been identified (Rennie and Turgeon, 2009; Tegeder, 2012) and little is known about exporters (Chen et al., 2001; Dundar and Bush, 2009; Tegeder, 2012), the knowledge about plastidic amino acid transporters is very scarce (Pohlmeyer et al., 1997; Pohlmeyer et al., 1998; Kleffmann et al., 2004; Tegeder, 2012). A need for plastid amino acid transporters is crucial

for plant life, because amino acids are building blocks of proteins, nucleotides, hormones, primary/secondary metabolites, and are centrally involved in complex metabolic networks integrating nitrogen-, carbon-, sulfur-, and phosphorus metabolism (Scheible et al., 2004; Nikiforova et al., 2005; Nikiforova et al., 2006; Tegeder and Weber, 2006; Gutiérrez et al., 2007; Vidal and Gutiérrez, 2008).

Our group hypothesizes that amino acid metabolism is compartmentalized between M and vein associated tissues, largely occurring in the latter tissue, particularly in the BS (Manuscripts 1 and 3), corroborated by *RE*`s vein-associated expression (González-Bayón et al., 2006; Figure 7). The BS is a perfectly located unit combining morphology with physiology, because this metabolic active cell layer is physically connected to the pipeline system of the plant and thereby at the nexus of metabolic processes. Here, I speculate about the physiological role of RE. Assuming amino acid synthesis is prominent in the BS chloroplast, RE might export amino acids for phloem loading. The lowered lysine contents in *re* leaves (Manuscript 3: Figure 8) might be due to a decreased export of lysine causing its accumulation in the plastid stroma. This, in turn, provokes a feedback inhibition of lysine biosynthesis as previously described (Galili, 1995).

RE is highly expressed in the meristematic tissues of the shoot and root (González-Bayón et al., 2006), where it might be central in amino acid metabolism. Most amino acids for protein synthesis are not provided via the phloem to the sink tissues in *Arabidopsis thaliana*, and thus need to be synthesized in meristematic tissues (Weibull and Melin, 1990; Zhu et al., 2005; Bräutigam and Weber, 2009). Shoot meristems mainly contain photosynthetically non-active proplastids. However, proplastids are biochemical factories providing the dividing and growing meristem with nucleotides, fatty acids, lipids, and branched chain and aromatic amino acids (Bräutigam and Weber, 2009). Proplastids are well equipped with enzymes of amino acid biosynthesis (Baginsky et al., 2004) and transporters associated with amino acid metabolism (Bräutigam and Weber, 2009). Amino acid synthesis is increased in proplastids, as indicated by transcriptional analysis (Bräutigam and Weber, 2009). The organelle is provided with carbon skeletons for amino acid biosynthesis via carbon transporters of the envelope (Bräutigam and Weber, 2009), namely the triosephosphate/phosphate translocator (TPT) (Loddenkötter et al., 1993), the glucose-6-phosphate/ phosphate translocator (GPT) (Kammerer et al., 1998), and the phosphoenolpyruvate/phosphate translocator (PPT) (Fischer et al., 1997). The pentose-phosphate translocator (XPT) (Eicks et al., 2002) was not detected in the proplastid envelope (Bräutigam and Weber, 2009). The defect in the vein associated isoform PPT1 leads to the reticulated *cue1* phenotype (Streatfield et al., 1999; Knappe et al., 2003). N for stromal amino acid biosynthesis is likely donated from glutamate, which is provided by the two-translocator system DiT1/DiT2 (Weber and Flügge, 2002; Renné et al., 2003; Bräutigam and Weber, 2009). Amino acids are exported via transporters

of the outer envelope (OE): OEP16 (Pohlmeyer et al., 1997) and OEP24 (Pohlmeyer et al., 1998), and a putative basic amino acid transporter (Bräutigam and Weber, 2009). However, transporters of the inner envelope (IE) are unknown to date. A homologue of RE was found in the IE and OE of proplastids in the meristem (Bräutigam and Weber, 2009), suggesting RE might export amino acids over the envelope. A dual localization to both IE and OE is likely, because the transiently expressed protein formed rings with half-moon shape around the plastids and builts up stromules (Manuscript 3: Figure 2), characteristic for IE and OE proteins, respectively (Breuers et al., 2012). OEP16, detected in the IE and OE, has an intriguingly similar structural similarity to RE (Pohlmeyer et al., 1997; Pudelski et al., 2012) and *oep16 Arabidopsis* mutants are debalanced in amino acid contents (Pudelski et al., 2012). The proposed function of RE as an exporter is applicable to proplastids and chloroplasts, because both plastid types synthesize amino acids and RE homologues were found in proplastid and chloroplast envelope proteomes (Bräutigam et al., 2008; Bräutigam and Weber, 2009).

An alternative function of RE might be that of a plastidic amino acid importer, providing bulk amino acids to the meristem for growth and development. The basic amino acid transporter CAT8, expressed at the root meristem and in young leaves, is supposed to be involved in the allocation of the highly abundant amino acids glutamine and glutamate to developing tissues (Su et al., 2004).

RE has two splice forms: RE_{long} and RE_{short} (Manuscript 3: Supplemental Figure 1). (Genotyping of positively transformed *re-6* with RE_{short} has to be performed (Manuscript1: Figure 1).) The splice variants could have regulatory functions with RE_{short} either being non-functional or taking over other functions. An *Arabidopsis* ureide permease has two splice forms with the shorter not mediating transport (Schmidt et al., 2006). Transporters regulated by splicing are known (Kumar et al., 2011; Cotsaftis et al., 2012). The organ and tissue specific occurrence of RE_{long} and RE_{short} will be assessed by quantitative real-time PCR (qRT-PCR) (Udvardi et al., 2008; Rieu and Powers, 2009).

1.2 Protein structure, localization and conclusions

RE, specific to the green lineage of plants (González-Bayón et al., 2006), belongs to a family in *Arabidopsis* with seven additional members and has orthologs in dicots, monocots, moss, fern, and green alga (Manuscript 3: Supplemental Figure 3). These proteins contain the domain of unknown function (DUF) 3411, which is characterized by two to four hydrophobic TM-domains dependent on the prediction program (Figure 1; Schwacke et al., 2003). Both RE_{long} and RE_{short} contain the DUF3411, which is truncated at the C-terminus of RE_{short} (Figure 1). All eight DUF3411 *Arabidopsis* proteins are predicted by

proteomics to be plastid localized. Six proteins were found in mature chloroplasts (Bräutigam et al., 2007; Bräutigam et al., 2008) and two in meristematic proplastids (Bräutigam and Weber, 2009) (Table 1). The function of the DUF3411 proteins is not understood.

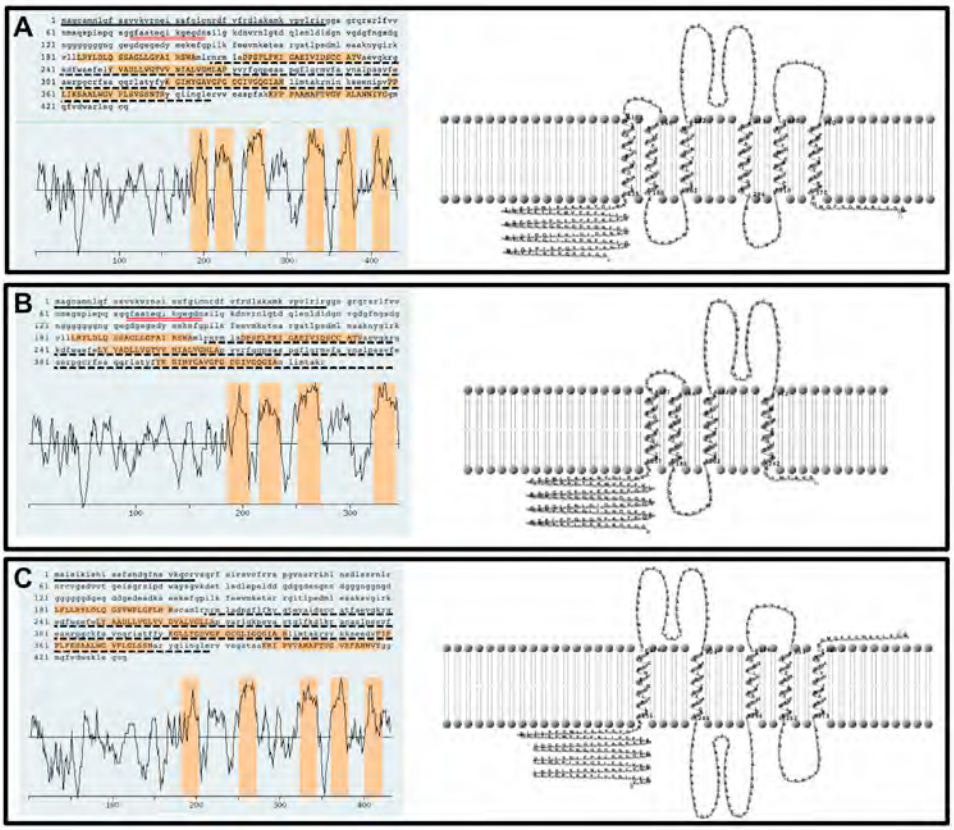

Figure 1. Predicted protein structures of RE_{long}, RE_{short}, and RER-1. Predicted transmembrane α-helix spans of RE_{long} **(A)**, RE_{short} **(B)**, and RER-1 **(C)**, each with predicted N-terminal cTP (left panel). The cTPs are underlined. Dotted lines show the DUF3411. Red, double lines indicate RE_{AB} epitope. Protein structures of RE_{long} **(A)**, RE_{short} **(B)**, and RER-1 **(C)** each lacking the predicted cTP (right panel).

Gene expression data from the public Arabidopsis eFP Browser (Winter et al., 2007) indicate that five proteins are expressed in young meristematic tissues, while the two thylakoid localized proteins and the gene product of At2g40400 are expressed in mature tissues (Supplemental Figure 1, Table 1). All eight proteins share high similarity (Figure 3). The protein with the highest similarity of RE in *Arabidopsis* is RE-related1 (RER1) (At5g22790) with 61.3% identity, not including the predicted cTPs. A tissue specific expression profile is not available for RER1 on the efp translatome browser (Mustroph et al., 2009; Supplemental Figure 1).

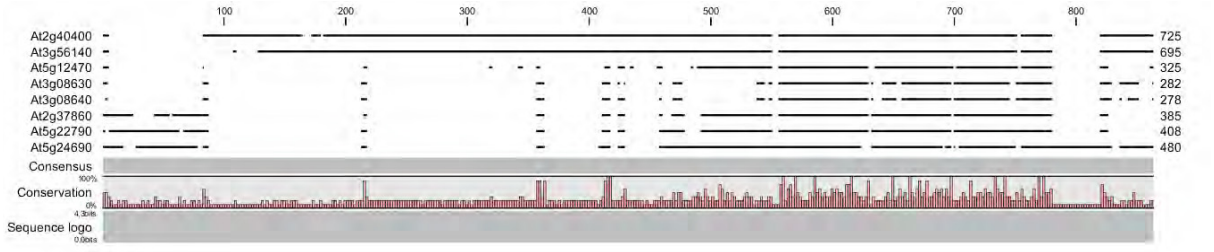

Figure 2. Alignment of the eight DUF3411 proteins from *Arabidopsis thaliana*.

Table 1. *Arabidopsis thaliana* proteins with DUF3411. IE: Inner Envelope, OE: Outer Envelope; na: not assigned; puf: protein of unknown function.

Arabidopsis genome identifier	name	annotation	localization by proteomics	localization by fluoreszent protein-fusions	highest expression
At2g37860	RE, LCD	reticulata	Chloroplast; IE/OE	IE/OE	shoot apex
At5g22790	RE-R	reticulata-related	Chloroplast; IE	na	Shoot apex, young seeds
At3g08630	na	puf	proplastid	na	young seeds, roots
At3g08640	na	puf	na	na	late seeds, dry seeds
At5g12470	na	puf	chloroplast	na	Imbibed seeds
At5g24690	na	puf	Chloroplast; IE	na	leaves
At2g40400	na	puf	Chloroplast, thylakoid	na	cotyledons
At3g56140	na	puf	Chloroplast; thylakoid	na	overall

1.3 The chloroplast ultrastructure is unaltered in *re-6* mesophyll cells

While M chloroplasts of ATase2 mutants lack their thylakoid structure (Kinsman and Pyke, 1998; Hung et al., 2004), chloroplasts of the evenly reticulated mutant *trp2* are not affected in their ultrastructure (Jing et al., 2009). Like these mutants, *re* is disturbed in M development and deficient in a plastid envelope protein (González-Bayón et al., 2006; Manuscript 3: Figure 2). Thus, we investigated the ultrastructure of M chloroplasts by electron microscopy (EM). Chloroplasts of col-0 and *re-6* did not differ on the ultrastructural level (Figure 3C-F). Grana and stroma thylakoids were fully developed in *re-6*, indicating that the mutation of *RE* does influence the construction and assembly of grana. This observation is in good agreement with previous findings that the *re* phenotype does not result from perturbed plastid development but from alteration in internal leaf structure (González-Bayón et al., 2006). M cells of *re* appeared normal and contained chloroplasts similar in quantity and morphology compared to those of wild type (González-Bayón et al., 2006; Figure 3). An aberrant M structure in *re-6* was confirmed (Figure 3B). EM microscopy will be used to investigate morphological differences between BS and M chloroplasts in *re-6*. *Dov1* has wild-type like M chloroplasts but vesicular, thylakoid less BS chloroplasts (Kinsman and Pyke, 1998).

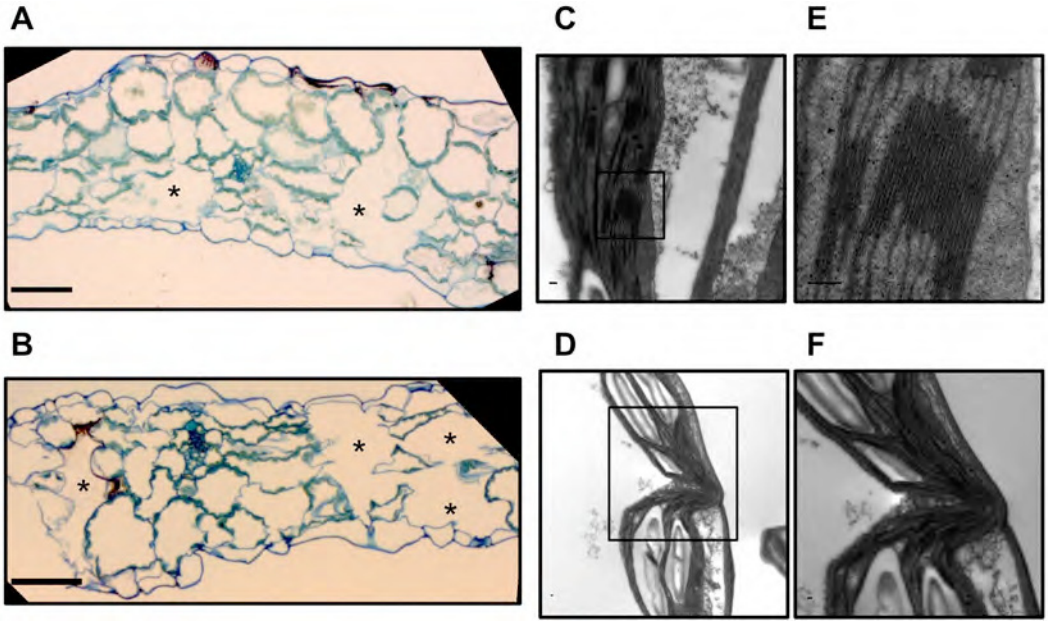

Figure 3. Cross sections **(A, B)** and M chloroplast ultrastructure **(C-F)** of the sixth rosette leaf of col-0 and *re-6*. **(A)** col-0 leaf. **(B)** *re-6* leaf. Ultrastructure of M chloroplast of col-0 **(C, E)** and *re-6* **(D, F)**. Boxes in **(B)** and **(D)** are magnified in **(E)** and **(F)**, respectively. Asterisks indicate airspaces. Scale bars correspond to 50 µm **(A, B)** and to 100 nm **(C-F)**.

1.4 Yeast complementation studies

To test whether RE is an amino acid transporter, yeast strains defective in multiple amino acid transporters were transformed with RE and LHT1 (Lysine Histidine Transporter1) in various expression domains, with translational stop and C-terminal eYFp for localization studies. LHT1 was used as a positive control (Hirner et al., 2006), namely $PMA1_{pro}$::LHT1 and $PMA1_{pro}$::LHT1::eYFP. All constructs were driven by the constitutive promoter $PMA1_{pro}$ (Rentsch et al., 1995). Despite yeast has been used as a heterologous expression system for many metabolite transporters (Su et al., 2004), expressing plastid targeted proteins in yeast is challenging, because the cTP negatively affects protein expression and may interfere with the delivery and integration into the yeast cell membrane (Bouvier et al., 2006). Thus, the cTP of RE was omitted, giving rise to $PMA1_{pro}$::$RE_{long,\Delta TP}$ and $PMA1_{pro}$::$RE_{long,\Delta TP}$::eYFP. To facilitate delivery of RE to the plasma membrane, RE was N-terminally tagged in additional constructs with the positively charged 6xHis-tag, giving rise to $PMA1_{pro}$::6*His::$RE_{long,\Delta TP}$, and $PMA1_{pro}$::6*His::$RE_{long,\Delta TP}$::eYFP. The positive charge might foster the incorporation into the negatively charged cell membrane.

The yeast strain JT16 was used to demonstrate that an *Arabidopsis* integral membrane protein transports histidine (Tanaka and Fink, 1985; Hsu et al., 1993) and LHT1 transports lysine and histidine (Chen and Bush, 1997). In 22Δ6AAL, defective in lysine uptake and synthesis, lysine transport by LHT1 was demonstrated (Tegeder et al., 2000). 22Δ8AA, defective in eight amino acid transport systems, is deficient in the uptake of proline,

glutamate, citrulline and GABA (Tegeder et al., 2000), and arginine and aspartate (Su et al., 2004). This strain was used to demonstrate that LHT1 transports other amino acids such as aspartate, proline, glutamate, citrulline, and GABA (Hirner et al., 2006) next to lysine and histidine. Amino acid transport is not specific, particularly for the broad specificity AAP transporters in *Arabidopsis* and pea, which transport basic, neutral, acidic amino acids and citrulline (Urquhart and Joy, 1981; Fischer et al., 1995; Tegeder et al., 2000).

Since 22Δ8AA lacks most amino acids transporters, it was chosen for complementation approaches. 22Δ8AA was transformed with LHT and RE constructs, which were located to the plasma membrane and found in the yeast membrane fraction (Figure 4 C, D). $PMA1_{pro}$::LHT1 restored the growth of 22Δ8AA on sole proline, ornithine, citrulline and GABA media (Figure 4A and 4B). The same results were found by (Hirner et al., 2006). However, we could not confirm that LHT1 rescued 22Δ8AA growth on sole aspartate and glutamate as published by Hirner et al., 2006. 22Δ8AA transformed with an empty vector control and all other vector constructs grew on aspartate, glutamate, and arginine (Figure 4A, 4B). Growth of an empty vector control on 3mM asparate was observed (Fischer et al., 2002). LHT1 was assessed as a positive control in our hands. RE, in either expression domain used, was not able to revert the phenotype (Figure 4A and 4B). LHT1 expressed in 22Δ8AA did not grow on histidine and lysine media (Figure 4B). Taken together, there is no evidence that RE transports proline, ornithine, citrulline or GABA. The inability of RE rescuing the growth of 22Δ8AA on various amino acids might also be due to inactivity of the transporter under the tested conditions, e.g. the protein lacking the cTP might not correspond to the native conformation.

JT16 was transformed with the same constructs. Neither of the transformed yeasts grew on lysine and histidine media (data not shown). 22Δ6AAL caused problems when transformed cells were selected on the appropriate selection media (data not shown). Thus far, I did not demonstrate that RE is an active transporter. Further studies, using these mutant strains will be performed (see Outline).

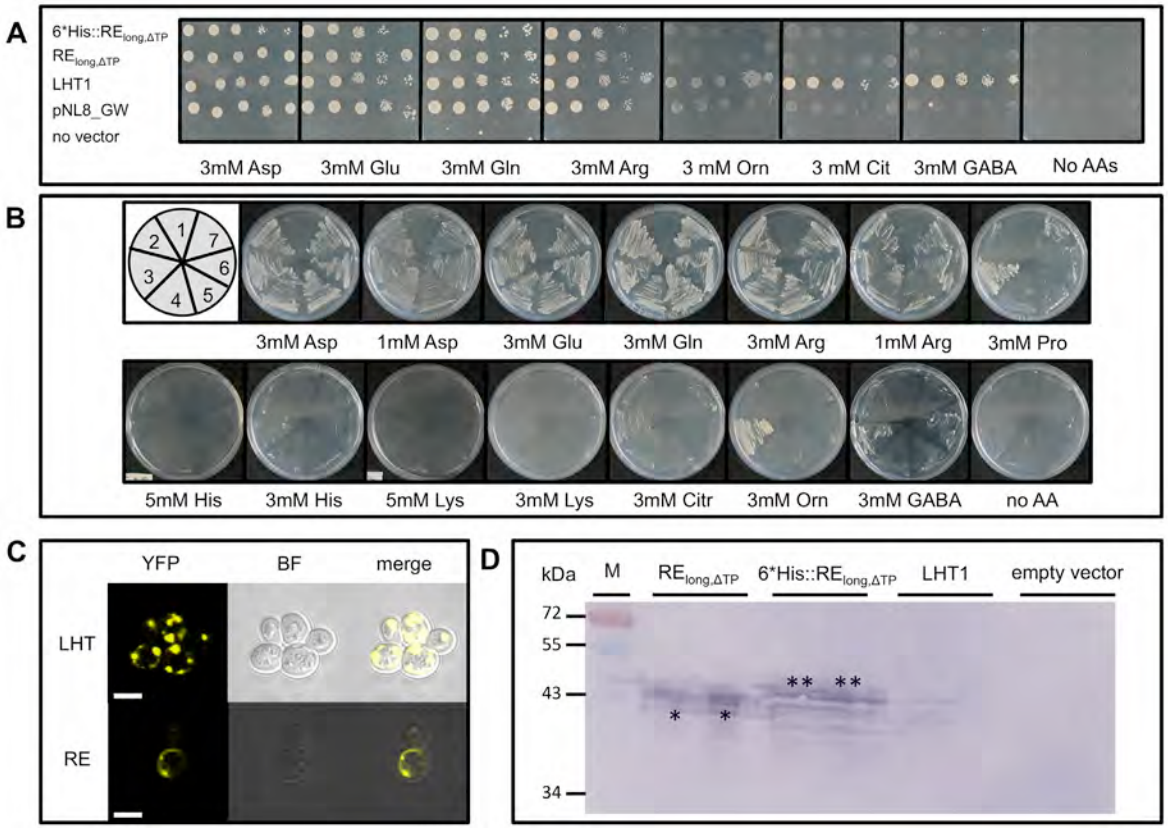

Figure 4. 22Δ8AAL transfomed with RE and LHT1, grown on medium containing single amino acids, cellular localization of LHT and RE, and cofirmation of protein expression. **(A)** 22Δ8AA transformed with appropriate vectors and grown for five days on YNB medium with single amino acids. Yeast was dropped on the plates in a dilution series from right to left. **(B)** 22Δ8AA transformed with appropriate vectors, grown for five days on YNB medium with single amino acids. (1): non-transformed 22Δ8AA, (2): pNL8_GW (empty vector control), (3) LHT1, (4) LHT1::eYFP, (5) $RE_{long,\Delta TP}$, (6) 6*His::$RE_{long,\Delta TP}$, (7) 6*His:: $RE_{long,\Delta TP}$::eYFP. All constructs are driven by the constitutive $PMA1_{pro}$. **(C)** Cellular localization in 22Δ8AA yeast cells to the plasma membrane. The upper row shows the localization of LHT1::eYFP, the lower row that of 6*His::$RE_{long,\Delta TP}$. Scale bar corresponds to 5µm. BF: bright field. (C) Western Blot of $RE_{long,\Delta TP}$, 6*His::$RE_{long,\Delta TP}$, LHT1, and empty vector control. 1(st) antibody: AB_{RE}, 2(nd) antibody: donkey-anti-rabbit-AP-conjugated. M: size marker. *: expected size: 41.3 kDa. **: expected size: 42.5 kDa.

1.5 RE was overexpressed in yeast and a cell-free system

RE_{long} and RE_{short}, both lacking the predicted cTP, were heterologously expressed in the bakers yeast (*Saccharomyces cerevisiae*) strain InvSC (Invitrogen™) using the pDEST galactose inducible GATEWAY® vector system (Invitrogen™). Additionally, expression was performed in cell-free wheat germ extract (Nozawa et al., 2007). The cTP was omitted as it is known to cause reduced expression in yeast (Bouvier et al., 2006) and is not functional in RE, because the cTP is cleaved off in the plastid (Keegstra and Cline, 1999).

RE_{long} and RE_{short} were each expressed taglessly and with C-Terminal-His-tags. In a Western Blot, the proteins were detected with an antibody against RE (AB_{RE}; see next paragraph) and a second goat-anti-rabbit AP-conjugated antibody (AB). All lanes were

loaded with equal protein amounts. The expected band sizes were detected (Figure 5). $RE_{long,\Delta cTP}$::6xHis has a calculated mass of 45.8 kDa and 43.3 kDa for the yeast and WGE expressed protein, respectively. $RE_{short,\Delta cTP}$::6xHis is predicted to be 36.5 kDa and 34.0 kDa if expressed in yeast and WGE, respectively.

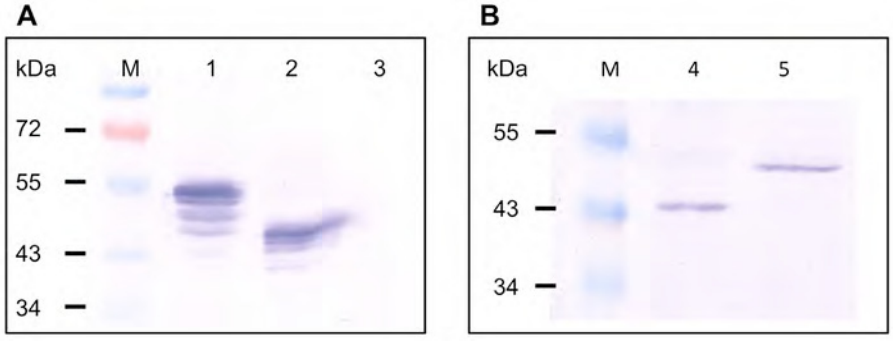

Figure 5. Western Blot of heterologously expressed RE_{long} and RE_{short}. **(A)** Heterologous expression in yeast. 1. $RE_{long,\Delta cTP}$::6xHis. 2. $RE_{short\Delta cTP}$::6xHis. 3. Empty vector control. **(B)** Heterologous expression in wheat germ extract. 4. $RE_{short\Delta cTP}$::6xHis. 5. $RE_{long,\Delta cTP}$::6xHis. 1(st) AB: AB_{RE}, 2(nd) AB: AP-conjugated anti-rabbit AB. M: size marker.

1.6 Raising an antibody against RE

A polypeptide anti-RE antibody (AB_{RE}) was raised against the amino acids 73 to 86 (including the cTP) at the N-terminal part of RE (Figure 1) by Agrisera, Sweden (Campbell et al., 2003). These amino acids were predicted not to span the plastid envelope (Schwacke et al., 2003). AB_{RE} binding was tested by Western blotting of $RE_{long,\Delta cTP}$::6xHis, expressed in yeast (see above, Figure 6). An anti-His antibody (Figure 6A) and AB_{RE} (Figure 6B) were used as first antibodies, and an Alkaline Phosphatase (AP)-conjugated anti-mouse antibody (Figure 6A) and an AP-conjugated anti-rabbit antibody (Figure 6B) as secondary antibodies, respectively. The second combination was also applied on the pre-serum (Figure 6C). Signals at 46 kDa were detected for both the anti-His antibody and AB_{RE}, no band was detected on the pre-serum. The detected sizes corresponded to the calculated size of 45.8 kDa (http://web.expasy.org/compute_pi).

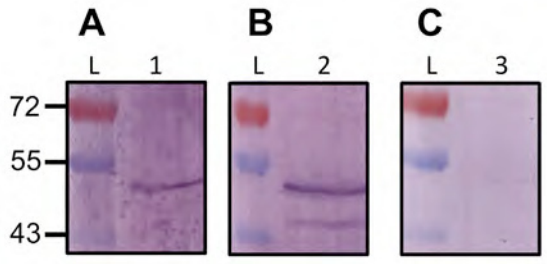

Figure 6. Testing AB_{RE} on heterologously yeast expressed RE_{long}::6x-His **(A, B)** and on pre-serum **(C)**. **(A)** 1(st) AB: mouse anti-His-AB, 2(nd) AB: AP-conjugated anti-mouse AB. **(B)** 1(st) AB: AB_{RE}, 2(nd) AB: AP-conjugated anti-rabbit AB. **(C)** 1(st) AB: AB_{RE}, 2(nd) AB: AP-conjugated anti-rabbit AB. Signals in **(A)** and **(B)** show band at ca. 46 kDa.

1.7 Inducible *re-6* complementation and overexpressor lines

Re`s phenotype is restricted to smaller and reticulated leaves (González-Bayón et al., 2006; Mansuscript 3: Figure 3). The reticulation is detectable in leaf primordia, in cotyledons and in early development of the first true leaves (González-Bayón et al., 2006). To investigate at which developmental stage *RE* exerts its function, *RE* driven by inducible promoters was introduced into the *re-6* genetic background. Two inducible promoters were used: the XVE estradiol inducible promoter in the pAB117 vector, which bases on pmDC7 (Curtis and Grossniklaus, 2003), and the heat shock promoter (hsp) of the pmDC30 vector (Curtis and Grossniklaus, 2003). pAB117, was provided by Dr. Andrea Bleckmann and Prof. Dr. Rüdiger Simon, HHU Düsseldorf. Non-tagged RE was cloned into pAB117, giving rise to XVE::RE, was transformed into *re-6*, delivering nine lines. Non-tagged RE, RE_{long}, and RE_{short} was cloned into pmDC30, yielding hsp::RE, hsp::RE_{long}, and hsp::RE_{short}, respectively. hsp::RE_{long}, and hsp::RE_{short} were transformed into *re-6* plants. The heat shock inducible lines can be used for laser guided promoter induction in distinct tissues (Halfon et al., 1997). In the context of a *signaling phenotype* of *re*, an induction in a tissue natively not expressing RE, might rescue the phenotype. This would appoint to a signaling role of RE.

1.8 RE is expressed around the veins

RE is expressed around the veins (González-Bayón et al., 2006). The exact tissue specific expression under the used promoter construct remains elusive. However, the exact expression is crucial in the context of the BS generating a metabolic signal (Manuscript1: signaling hypothesis). Thus, we amplified three promoter sequences: $P_{short,re}$, $P_{intermediate,re}$, $P_{long,re}$, with $P_{short,re}$ corresponding to the sequence chosen by (González-Bayón et al., 2006). Longer sequences were used since they might contain additional regulatory elements that better reflect native expression. All three promoter constructs showed similar GUS-staining patterns in the pmDC163 vector: a high level of GUS-expression was observed along the veins and at the hydathodes of ca. seven week-old col-0 plants (Figure 7), confirming previous results (Gonzales-Bayon et al., 2006). To pinpoint RE`s exact tissue specific expression by circumventing GUS-bleeding, GFP and nucleus-targeted GFP-constructs were cloned. Promoter-GFP constructs in the pmDC107 vector (Curtis and Grossniklaus, 2003) were transformed into the col-0 background, but the plants did not show GFP signals. Three nucleus targeted promoter-GFP constructs were cloned, two in the pGREEN-II-H4-GFP ($P_{short,re}$,::H4-GFP; $P_{intermediate,re}$::H4-GFP) and one in the pAB146 vector background ($P_{long,re}$,::VENUS-H2-GFP). Transformed col-0 plants did not survive selection. The promoter::GUS lines could be used for tissue specific expression profiling as described by (Sessions et al., 1999; Engelmann et al., 2008; Wiludda et al., 2012). The same start as

chosen for $P_{extralong,re}$ until *RE´S* stop codon was used to create native promoter complementation constructs in the pmDC99 background (Curtis and Grossniklaus, 2003).

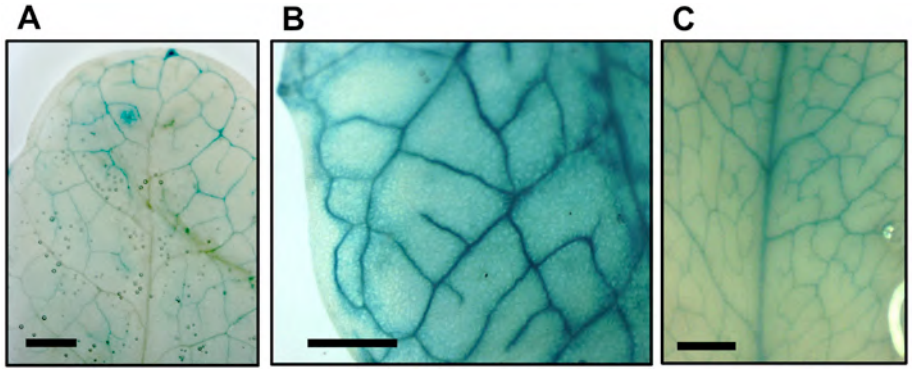

Figure 7. Histochemical GUS-assay of *col-0* plants harboring three different promoter constructs. Leaf magnifications of the 4(th) rosette leaves of six week old plants are shown. **(A)** $P_{short,re}$. **(B)** $P_{intermediate,re}$. **(C)** $P_{long,re}$. The scale bars correspond to 1 mm.

1.9 Generation of stable GFP lines

RE, RE_{long}, and RE_{short} were C-terminally fused to GFP to investigate both intracellular localization and potential genetic complementation in stably transformed *re-6* plants. The same vector constructs in pmDC83 (Curtis and Grossniklaus, 2003) were used for transient expression and protein localization in tobacco (Manuscript 3: Figure 2). Stable *Arabidopsis thaliana re-6* lines harboring 35S::RE::GFP, 35S::RE_{long}::GFP, 35S::RE_{short}::GFP, 35S::$RE_{\Delta cTP}$::GFP, and 35S::$RE_{long,\Delta cTP}$::GFP were generated. More than five independent lines each were generated. *Re-6* transformed with 35S::RE and 35S::RE_{long} showed wild-type like fully green leaves (Manuscript 3: Figure 1). However, stably transformed *re-6* with 35S::RE::GFP and 35S:: RE_{long}::GFP remained reticulated and no GFP signals were detected (data not shown). Thus, the 35S promoter could have been silenced as previously observed (Elmayan and Vaucheret, 1996; Elmayan et al., 1998; Ho et al., 1999; Hull et al., 2000; Mishiba et al., 2005) and/or the GFP tag interfered with RE´s function.

1.10 Fatty acid composition of *re-6*

FAs are synthesized as palmatic acid (C16:0) or oleic acid (C18:1) within the plastid, exported, and activated to acyl-CoAs at the ER, converted to phosphatidic acids and desaturated to Δ3-trans hexadeconoic acid (C16:1), hexadecatrienoic acid (C16:3), linoleic acid (C18:2), and α-linoleneic acid (C18:3) (Browse and Sommerville, 1991; Ohlrogge and Browse, 1995; Benning, 2009; Li-Beisson et al., 2010). To asses if these plastidic metabolic pathways are affected, *re-6* was profiled for changed fatty acids (FAs) profiles. While 16C FAs were at the wild-type level in *re-6*, 18:0, 18:1, 18:2, but not 18:3-FAs, were significantly

increased in *re-6* (Figure 3) by 39.1% (p=0.0333), 49.6% (0.0108), and 56.0 % (p= 0.0214), respectively. The level of glycerol, the carbohydrate backbone of FAs (Browse and Sommerville, 1991; Li-Beisson et al., 2010), was not changed in *re-6* (Manuscript 3: Supplemental Figures 6 and 7). The increased levels of free FAs in the mutant could be caused by either (i) a direct or indirect influence of RE on the plastid localized FA biosynthesis or on (ii) a secondary change of the lipid acid composition.

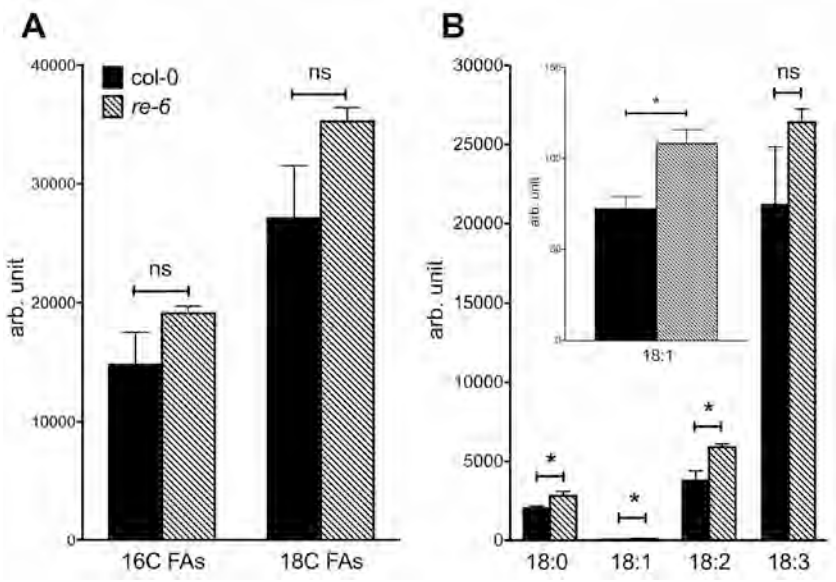

Figure 13. Free fatty acid levels of eight-week old vegetative col-0 and *re-6* rosettes. Plants were grown under 16-h/8-h light/dark cycle at 100µE/m^2/s^1. Samples were taken in middle of light period. Arbitrary units (arb. unit) are shown. **(A)** Total free C16 and C18 fatty acids (16C FAs and 18 C FAs, respectively). **(B)** Unsaturated (18:0) and saturated (18:1, 18:2, 18:3) FAs. The inlay shows 18:1 FAs. Error bars represent S.E. Asterisks indicate significance levels. n(col-0) = 5 , n(*re-6*) = 4.

1.11 *Re-6* is a null mutant

The most experiments performed in this project were carried out with the T-DNA insertion line *re-6*, because it allows easy genotyping, is in the common genetic background col-0, and can be cultivated on MS plates without germinating deficiencies as compared to *re-2*. *Re-2*, initially used as a second line, showed growth deficiencies on MS plates if not supplemented with sucrose. Crosses of *re-6* into *re-2* were reticulated in the F1 generation, i.e. they are allelic (Figure 9 A). As assumed by (González-Bayón et al., 2006), *re-6* is a null mutant (Figure 9 B). PCR on *re-6* cDNA did not show signals if amplification was performed with the primers for RE_{long} (CR161/CR162) and RE_{short} (CR161/CR173), but signals were detected on col-0 cDNA (Figure 9 B).

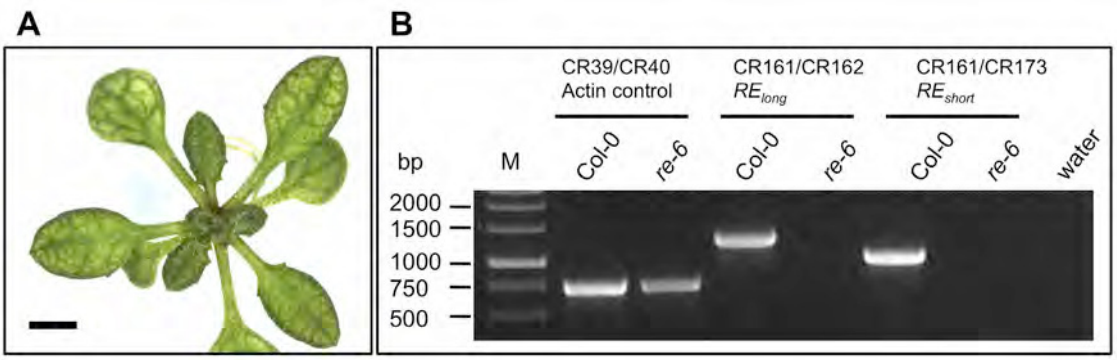

Figure 9. Reticulated leaf phenotype of *re-2* X *re-6* F1 plants and RT-PCR showing *re-6* is a null mutant. **(A)** Plant rosette of three week old plant. Error bar represents 2mm. **(B)** PCR on cDNA showing that *re-6* is a null mutant. *re-6* neither contains RE_{long} nor RE_{short}-transcripts.

1.12 Outline for experiments to decipher the role of *re*

1.12.1 Testing whether RE transports amino acids

Yeast complementation will be continued with a focus on 22Δ6LL. Additionally, heterologously expressed RE will be reconstituted into proteoliposomes for uptake experiments (Hoyos et al., 2003; Linka et al., 2008). Alternatively, *Xenopus* oocytes (Lee et al., 2007; Svennerstam et al., 2008; Haferkamp and Linka, 2012) or the bilayer method (Harsman et al., 2011; Haferkamp and Linka, 2012) could be used for transport studies. LHT1 will be fused to a cTP, and will be transiently expressed in *re-6*. Despite potential different transport mechanisms between LHT1 (proton coupled) and RE, *re-6* might be complemented. Previous experiments indicated that RE forms dimers (data not shown). For confirmation, heterologously expressed protein will be investigated by native gels and Western Blots. The formation of homo-, di- or oligomers will back the hypothesis that RE is a transporter.

1.12.2 RE generates a metabolic signal

If RE generates a mobile signal, such as a metabolite, the tissue specific expression of RE should be replaceable. Cell-autonomy will be tested by expressing RE_{long} under the control of epidermal-, xylem, phloem- or BS-specific promoters. The plants will be tested for complementing the phenotype. Appropriate promoters are discussed in Chapter 2. To further asses potential metabolites that are changed in *re*, an unbiased metabolic profiling approach will be applied (Fiehn et al., 2000; Krueger et al., 2011; Svatos, 2011), including genetically complemented *re-6* lines and overexpressor plants.

If RE is exerts other functions than transporting, further approaches will be used. Due to it`s plastid localization, RE might interact with proteins. A global approach to identify potential interaction partner is the split-ubiquitin (Pasch et al., 2005) or pulldown approaches (Smith et al., 2004; Chou et al., 2006).

2. Tissue specific transcriptional profiling of the *Arabidopsis* bundle sheath and mesophyll

Almost all processes studied by biologists are tissue and cell specific. However, most experimental methods do not discriminate between tissue and cell types. Thus, the conclusions are “tampered” by the mixture of cell types. This is particularly valid for the unbiased methods of *omics*-techniques, such as transcriptomis, proteomics and metabolomics. In the age of systems biology, capturing data at cellular resolution is of utmost importance. Within the last decade, laser microdissection (LMD) has been established as a powerful tool to isolate pure cell populations from heterogenous tissues. LMD is visually guided by a microscope, which is coupled to a laser that cuts and harvests the tissue/cells of interest. The tissues can either be identified by histochemical staining or cell location of histological appearance (Nelson et al., 2006). First successfully applied to human and animal tissues (Emmert-Buck et al., 1996; Inada and Wildermuth, 2005; Esposito, 2007), this technique is also adaptable to plants. However, only few studies were presented by plant biologists during the last decade (Asano et al., 2002; Kerk et al., 2003; Nakazono et al., 2003; Inada and Wildermuth, 2005; Jiao et al., 2009; Wuest et al., 2010; Schmid et al., 2012). LMD is the method of choice over other cell-isolation systems, such as cell sorting by flow cytometry. LMD allows rapid cell/tissue isolation, fixatives “freeze” the tissue at it`s steady-state not inducing stress responses, and no molecular marker is needed to identify the appropriate tissue (Kehr, 2003; Day et al., 2005; Inada and Wildermuth, 2005; Lee et al., 2005; Nelson et al., 2006).

For our purpose we intended to couple LMD to a downstream processes of RNA isolation, cDNA-synthesis, and deep sequencing. This procedure essentially has to fulfill two requirements: (i) high quality tissue integrity and (ii) fixation of RNA that allows isolation of sufficient RNA amounts for subsequent deep sequencing. These two constraints are hardly to equilibrate due to very delicate structural integrity of the *Arabidopsis* leaf tissue (Inada and Wildermuth, 2005). Cryosectioning, widely used for animal tissues, is not applicable to plant tissues due to high vacuolization (Inada and Wildermuth, 2005), but was used in a modified manner (Asano et al., 2002; Nakazono et al., 2003). Paraffin tissue preparation with prior RNA-fixation provides a high histological integrity and high-quality RNA (Schmid et al., 2012). Thus, we chose the following principal steps for fixation and LMD, which were modified and changed during establishing the method for our laboratory: harvesting leaf tissue by cutting it into small peaces (ca. 0.4 x 0.4 cm^2), preferentially including parts of the midrib, that gives stability. The leaf samples were fixed in 4:1 ethanol-acetic acid at 4°C over night and dehydrated by an ethanolic dilution series. The ethanol was replaced by xylole before paraffin fixation. The paraffin embedded leaf tissue was cross sectioned and transferred onto special PEN (poly ethylene naphthalate) coated glass slides to perform LMD. To shorten the

time of manually performed paraffin tissue preparation, which takes about five to eight days, we used an automated vacuum tissue processor (Leica ASP300S). This circumvents degradation of nucleic acids as observed in the conventional paraffin method (Jackson, 1991; Inada and Wildermuth, 2005). However, paraffin preparation methods fail to provide the structural integrity of plant cross sections. Thus, Inada and Wildermuth, 2005 adapted a rapid microwave paraffin preparation method (Schichnes et al., 1998) to LMD, resulting in well-defined internal leaf structure. Contact to Prof. Ritter (Organic Chemistry, HHU Düsseldorf) revealed that his group possesses the technical equipment, such as special microwaves, to apply this method. However, this method was not applied, because (i) RNA amount and integrity achieved with the normal paraffin method was high enough, at least when cross-sections were scraped of the slide for RNA isolation, and (ii) focus of the research shifted to other projects.

The preparation method that we used (Material and Methods) delivered leaf cross sections of high integrity (Figure 10A, 10B), comparable to the quality published by (Inada and Wildermuth, 2005). Although the paraffinized tissue integrity was well, RNA isolation firstly gave no RNA when the method as presented by (Wuest et al., 2010) was used. If the paraffin-cross-section-ribbons, however, were stretched out on the glass slides using methanol (Schmid et al., 2012) instead of water, RNA yield increased. However, it is noteworthy that RNA was isolated from cross-sections and not from tissue cut by the laser. RNA quality was tested with an Agilent 2100 Bioanalyzer (Agilent) (Masotti and Precke, 2006; Buhtz et al., 2008) at the Biologisch-Medizinische Forschungszentrum (BMFZ), HHU Düsseldorf. RNA quality met a standard sufficient for qRT-PCR and sequencing (Figure 10C).

If RNA was isolated from BS and M tissues, purity and contamination should be assessed by PCR markers. The following markers could be used for qRT-PCR: chloroplastic carbonic anhydrase (Jacobson et al., 1975; Brandt et al., 2002; Kerk et al., 2003; Inada and Wildermuth, 2005) and/or the promoter of the rubisco small subunit (pRBCS1A) (Mustroph et al., 2009) for M cells; the very-long-chain fatty acid-condensating enzyme CUT1 (Inada and Wildermuth, 2005) and/or the promoter of the cuticular wax gene (pCER5) for epidermal cells; the promoter of the sulfate transporter (pSULTR2;2) for BS cells (Mustroph et al., 2009); the promoter of the sucrose transporter2 (pSUC2) for phloem companion cells (Mustroph et al., 2009), and the promoter of the K^+-channel (pKAT1) for leaf guard cells (Mustroph et al., 2009). Actin2 or ubiquitin5 (Czechowski et al., 2004; Inada and Wildermuth, 2005) are adequate for assessing cDNA quality in each tissue. Before cuttings, it would be helpful to identify the tissues, such as xylem and phloem by safranin and astrablue staining (Braune et al., 2007). The BS could be identified by visual comparison to stained GLDPA-driven GUS constructs (Wiludda et al., 2012).

Laser microdissection was done with the Zeiss Microdissection system (Zeiss Palm Microbeam, Palm RoboSoftware 4.3 SP1) as described in Material and Methods.

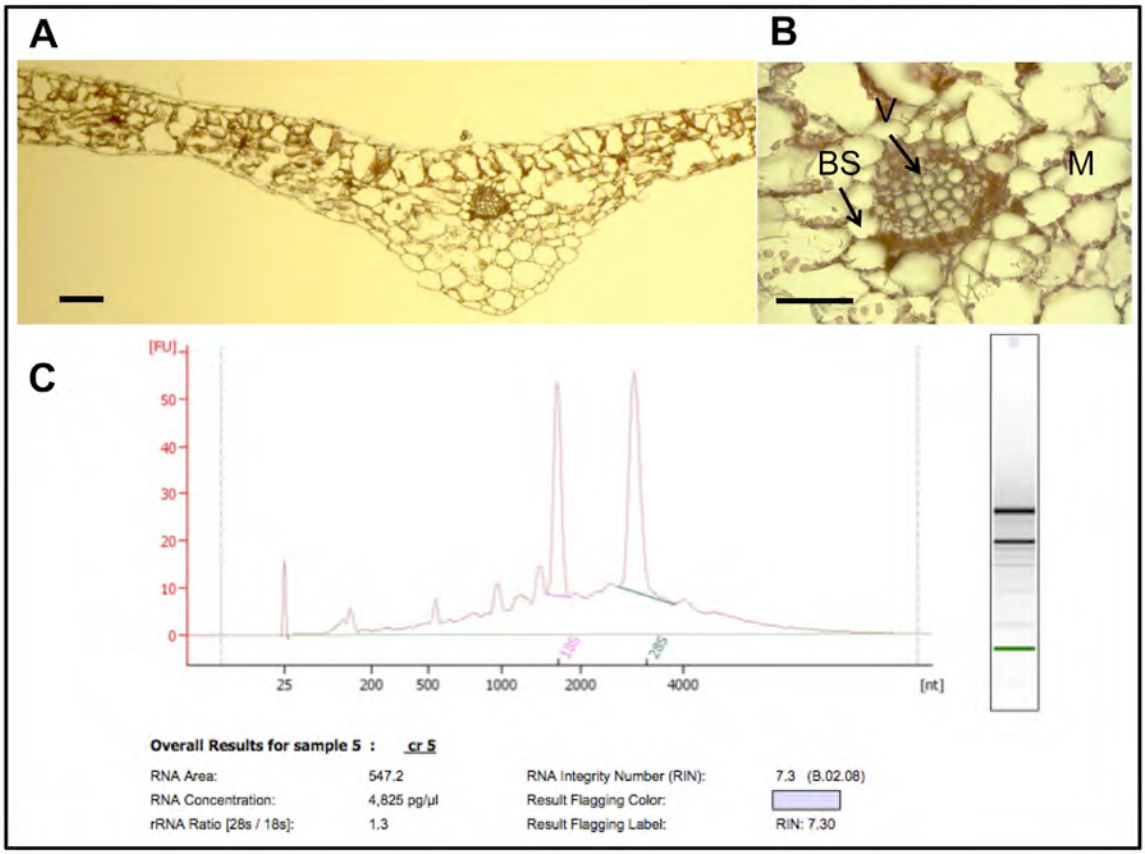

Figure 10. Cross-sections of col-0 leaves and RNA-quality control. **(A)** Cross-section (14 µm) of a four week old 4(th) rosette leaf. Tissue structures are preserved. Scale bar: 100 µm. **(B)** Magnification of (A). Scale bar 50 µm. **(C)** RNA-quality control on an Agilent Bioanalyzer 2100 Picochip. 28S and 18S peaks are prominent, as also seen on the gel pictogramm on the right hand site. RIN (RNA inegrity number) of 7.3 states a good quality RNA. M: mesophyll; V: vasculature; BS: bundle sheath.

3. Material and Methods

Cloning Procedures and DNA sequencing

For general cloning, DNA sequences were amplified from cDNA and gDNA using a proofreading polymerase (Phusion Polymerase, New England Biolabs). PCR procucts were purified from Agarose gels using the QIAquick Gel Extraction Kit (Qiagen). For cDNA synthesis, RNA was extracted as described (Chomczynski and Sacchi, 1987; Chomczynski and Sacchi, 2006), DNase digested, and subjected to cDNA synthesis using either Superscript II or Superscript III (Invitrogen).The PCR primers used are listed in Supplemental Table 2. Depending on the cloning strategy, the PCR products were subcloned in pJET 1.2 (Fermentas) or recombined into pDONR207 (Invitrogen). Classical cloning steps were performed by standard molecular techniques (Sambrook et al., 2001). Subsequent Gateway™ recombination steps were performed by LR reactions as described by the manufacturer (Invitrogen). The explicit steps are described in the corresponding section. All vectors were controlled by restriction digest and sequencing (GATC Biotech).

SDS-Gelelectrophoresis and Western Blotting

10% SDS-PAGEs and immunoblot analyses were performed as described (Sambrook et al., 2001). The following antibody combinations were used for immunodetection on Western Blots: (i) mouse penta-His antibody (Quiagen) (1:2500 dilution) / alkaline phosphatase (AP)-conjugated anti-mouse IgG (1:2500 dilution)(Promega); (ii) serum rabbit anti RE antibody (AB_{RE}) (1:2500 dilution) / AP-conjugated donkey anti rabbit antibody (Promega) (1:2500 dilution). To estimate molecular protein masses, the PageRuler™ Prestained Protein Ladder (Fermentas) was used.

Heterologous protein expression in yeast and crude membrane extraction

Arabidopsis col-0 cDNA was PCR amplified using a proofreading polymerase (Phusion, New England Biolabs) with the primer combinations CR6/CR4 and CR6/CR5 to receive $RE_{long,\Delta cTP}$ and $RE_{short\Delta cTP}$, respectively. The PCR products were recombined into pDONR207 with BP-clonase (Invitrogen). Each insert in the pDONR207 entry vector was recombined with LR-clonase into the yeast expression vector pYES-DEST52 (Invitrogen) to be in frame with the C-terminal 6xHis-tag. pYES-DEST52 is under the control of the galactose-inducible GAL4 promoter. The resulting contructs, $RE_{long,\Delta cTP}$::6xHis and $RE_{short\Delta cTP}$::6xHis, were transformed into the *Saccharomyces cerevisiae* strain INVSc1 (Invitrogen) by the lithium chloride method (Schiestl and Gietz, 1989). Transformants were selected on synthetic complete minimal agar plates lacking uracil (SC-U). Heterologous expression and subsequent crude membrane extraction was performed as described (Bouvier et al., 2006).

Cell-free heterologous protein expression in wheat germ extract

RE in different expression domains was expressed in a cell-free wheat germ extract (WGE) system as (Bernhardt et al., 2012). The Gateway compatible expression vector pDEST-LL5 was generated by introducing attR1 and attR2 sites into a pEU3a-C-His vector (CellFree Sciences; http://cfsciences.com). pDEST-LL5 was generated by Dr. Andrea Bräutigam und Lisa Leson. $RE_{long,\Delta cTP}$ and $RE_{short,\Delta cTP}$ were amplified on cDNA with the primer combination CR6/4 and CR6/CR5, respectively, and recombined into pDEST-LL5 via pDONR207 (Invitrogen). Templates for *in vitro* transcription were PCR-amplified from both pDEST-LL5 constructs with primers P73/P74. The PCR products were purified with QIAquick Gel Extraction Kit (Quiagen). *In vitro* translation was performed as described (Nozawa et al., 2007).

Gateway vector creation for yeast complementation studies and complementation studies

The vector pNL8GW was derived from pNL8 (Linka, 2001), which itself bases on pDR195 (Rentsch et al., 1995). pNL8GW contains the Gateway LR cassette upstream of a constitutive promoter of the plasma membrane H^+-ATPase ($PMA1_{pro}$) from *Saccharomyces cerevisiae* (Rentsch et al., 1995), and a C-terminal YFP. pNL8 was opened with XhoI. A PCR was performed on pmDC32 (Curtis and Grossniklaus, 2003) using the primers CR145/CR146, each primer containing a XhoI restriction site as underlined in the sequences (Supplemental Table 2). The PCR amplificate was ligated into the XhoI-opened pNL8 to gain pNL8GW. Three yeast strains were used to test for potential amino acid transport activity of RE_{long}: JT16 (Hsu et al., 1993; Chen and Bush, 1997), 22Δ6LL (Fischer et al., 2002), and 22Δ8AA (Fischer et al., 2002; Hirner et al., 2006). All mutants strains are multiple knock outs for amino transporters with the following phenotypes: JT16: MATα, hip1-614, his 4-401, ura3-52, ino1, and can1 (Tanaka and Fink, 1985; Chen and Bush, 1997); 22Δ6LL: MATα, gap1, put4, uga4, ura3, can1, lyp1, and alp1 (Tegeder et al., 2000); and 22Δ8AA: MATα, gap1, put4, uga4, ura3, can1, lyp1, and alp1, hip1, and dip5 (Tegeder et al., 2000). JT 16 was maintained on YPD medium + 3mM histidine or S1 medium + 0.2% uracil without sorbitol (Tanaka and Fink, 1985; Hsu et al., 1993; Chen and Bush, 1997), 22Δ6LL on $SC_{complete}$ + 100mg/L Lys-Val (adapted to (Fischer et al., 2002)), and 22Δ8AA on YPD (Mechthild Tegeder, personal communication). For yeast complementation studies, the ORFs of At2g37860 (RE) and At5g40780 (LHT1) were amplified from col-0 cDNA by PCR. LHT was used as a positive control with the same coding sequence as described (Hirner et al., 2006). The following constructs were achieved via recombination in pDONR207 subseqzent and recombination in the final vector pNL8GW, each driven by the constitutive promoter $PMA1_{pro}$ (Rentsch et al., 1995): $PMA1_{pro}$::LHT1 (CR147/CR148), $PMA1_{pro}$::LHT1::eYFP

(CR147/CR149), $PMA1_{pro}$::$RE_{long,\Delta TP}$ (CR6/CR2), $PMA1_{pro}$::$RE_{long,\Delta TP}$::eYFP (CR6/CR4), $PMA1_{pro}$::6*His::$RE_{long,\Delta TP}$ (CR150/CR2), and $PMA1_{pro}$::6*His::$RE_{long,\Delta TP}$::eYFP (CR150/CR4). All three yeast strains were transformed with these constructs and pNL8GW as a negative control using the lithium chloride method (Schiestl and Gietz, 1989). Positive JT16 transformants were selected on SC medium without uracil (SC-U) + 20 mM His + 0.002% Inosine (Hsu et al., 1993) Mechthild Tegeder, personal communication). Positively transformed 22Δ6LL were selected on SC medium without uracil + 100 mg/L Lys-Val (adapted from (Fischer et al., 2002), and 22Δ8AA were selected on SC without uracil (Hirner et al., 2006). SC medium contains 0.17% (w/w) yeast nitrogen base (YNB without amino acids and without $(NH_4)_2SO_4$, 0.5% (w/w) $(NH_4)_2SO_4$,2% (w/w) glucose and 2g/L dropout mix. Transformed colonies were tested by yeast colony PCR following zymolase digestion (Amberg et al., 2006) and by Western-Bloting. To test for complementation, single transformed 22Δ8AA colonies were individualized on SC-U without $(NH_4)_2SO_4$, containing one amino acid as sole nitrogen source (Hirner et al., 2006). Transformed 22Δ8AA yeast cells used for the droptest were washed twice in 1xTE (10 mM Tris-HCl/ 1mM EDTA/ pH 7.5) before applying on the plates. For the first spot, 5µl of a yeast suspension of OD_{600}= 1 was applied. The subsequent spots were diluted by 1:10 for each further spot. The yeast was grown at 30°C for five days. All experiments were repeated with independent colonies of independent transformation batches. Transformed JT16 cells were tested for complementation on S1 media (0.17% (w/w) YNB with 0.5% (w/w) $(NH_4)_2SO_4$, 2% (w/w) glucose, 0.0002% (w/w) inosine) (Chen and Bush, 1997) with additional histidine and lysine concentrations. Transformed 22Δ6LL were tested for complementation on 0.17% (w/w) YNB without amino acids + 0.5% (w/w) $(NH_4)_2SO_4$, 2% (w/w) glucose and appropriate lysine concentrations (adapted to (Fischer et al., 2002)).

Confocal microscopic analysis

22Δ8AA yeast cells transformed with $PMA1_{pro}$::LHT1::eYFP and $PMA1_{pro}$::6*His::$RE_{long,\Delta TP}$::eYFP were fixed in 3% agarose on a glass slide. The agarose yeast mix was tightly covered with a cover glass. Yeast cells were analyzed with a Zeiss LSM 510 META confocal laser-scanning microscope as described by (Breuers et al., 2012). YFP was excited with an Argon-laser at 500nm and emission was collected at 542 nm. Pictures were processed and merged using the freeware GIMP 2.8. (http://www.gimp.org).

Transmission electron microscopy

The forth leaves of four week old col-0 and *re-6* plants were used for transmission electron microscopy. Plants were grown at 16-h light/ 8-h dark with a photosynthetically

active radiation of 100 µE/m^2/s. Leaf material was fixed in 0.1 M phosphate buffer (pH 7.4) and 2.5% glutaraldehyde for 3 h. The samples were incubated in 2% osmiumtetroxide for 2 h and in 2% uranylacetate for 30 min. Subsequent treatment was performed as described in (Richard et al., 2009).

Promoter constructs in col-0

The promoter sequences were amplified on col-0 gDNA by CR8/CR9, CR8/CR10, and CR 151/CR138 to give rise to $P_{short,re}$, $P_{intermediate,re}$, and $P_{long,re}$, respectively. The sequences were recombined into pmDC163 (Curtis and Grossniklaus, 2003) via pDONR207, to create translational C-terminal GUS fusions. $P_{short,re}$ includes 966 bp of the intergenic region of the upstream gene and 156 bp of the first exon (-966/156nt), $P_{intermediate,re}$ the same intergenic region plus 735 bp into the second exon (-966/735nt), and $P_{long,re}$ spans the sequence from -2986 until + 156 of the first exon (-2986/156nt). $P_{short,re}$ corresponds to the promoter sequence used by (González-Bayón et al., 2006). The promoter constructs were stably transformed in col-0 and selected on Hygromycin containing (30 µg/mL) 1 MS medium (Murashige and Skoog, 1962). 19 independent plant lines were generated for $P_{short,re}$, eight for $P_{intermediate,re}$ and five for $P_{long,re}$. $P_{short,re}$ and $P_{intermediate,re}$ were cloned into pGREEN-H4-GFP ((Hellens et al., 2000), Marcel Lafos, personal communication) and $P_{long,re}$ into pAB146 (Andrea Bleckmann, personal communication). Both vectors are Gateway compatible.

Generating heat shock and estradiol inducible *re-6* complementation and overexpressor lines

Gene products were PCR amplified from col-0 gDNA and cDNA with the primers CR1/CR2. The short splice variant of re, RE_{short}, was amplified with the primers CR1/CR19 on cDNA. The PCR-products were recombined into pDONR207, and then into the destination vector pmDC30 (Curtis and Grossniklaus, 2003) for heat shock induction and into pAB117 (pABindGFP) for estradiol induction (Bleckmann et al., 2010; Breuers et al., 2012). pAB117 (pABindGFP) was derived from pmDC7 (Curtis and Grossniklaus, 2003) by Andrea Bleckmann (Bleckmann et al., 2010). Propagation in *E.coli*, transformation into *Agrobacterium tumefaciens*, and transfection of *Arabidopsis thaliana* was done as described in Manuscript 3.

Fatty acid analysis

Aerial tissue of seven week-old *re-6* and col-0 rosettes before budding and induction of flowering was used. Plant rosettes were harvested in the middle of the light period of 16-h light/8-h dark light cycle and quick frozen in liquid nitrogen. Ground leaf material was used for lipid extraction. Lipids were isolated and fatty acids were converted to methyl esters (Browse

et al., 1986). The subsequent detection was performed by gas chromatography – electron impact – time of flight – mass spectrometry (GC-EI-TOF-MS) with the fatty acid 17:0 as an internal standard (Bernhardt et al., 2012).

Alignment of protein sequences

Homologous protein sequences of different organisms were inferred from publicly available databases. Alignment of the sequences was performed with CLC Genomic Workbench (www.clcbio.com). The settings were chosen as follows: default alignment, gap open cost 10, gap extension 1, and end gap cost as any other.

Prediction of protein structures

Protein structures were predicted by using the consensus sequence provided on http://aramemnon.uni-koeln.de/ (Schwacke et al., 2003). Proteins were graphically presented using TMRPres2D (http://bioinformatics.biol.uoa.gr/TMRPres2D/; (Spyropoulos et al., 2004).

Plant growth conditions/ Confirmation of T-DNA insertion in *re-6*/ Statistical Analysis/ GUS-staining / gDNA isolation / Polymerase Chain Reaction / Agarose Gel Electrophoresis

Done as described in Manuscript 3

Plant material for LMD

Arabidopsis thaliana col-0 plants were grown under controlled conditions in climate chambers. The day/night cycle was chosen as 12-h light/ 12-h dark with a photosynthetically active radiation of 100 µE/m^2/s. *Arabidopsis thaliana* seeds were surface sterilized with chlorine gas in a desiccator as described (Desfeux et al., 2000), spotted on solid 1 Murashige and Skoog (MS)-medium with vitamins containing 0.8% (w/w) plant agar (Murashige and Skoog, 1962), and stratified at 4°C for four days. All plant material was germinated and grown in 1 MS medium and transferred on soil at the first true leaf stadium. Plants were further grown for three weeks under the same conditions. Mature leaves were cut into small squares of about 0.4 cm x 0.4 cm with a sharp new razor blade and directly transferred into tissue fixation solution.

Tissue preparation for LMD

Principally, the methods were performed as described by (Kleber and Kehr, 2006). However, modifications were necessary for our conditions, particularly due to the fragile *Arabidopsis thaliana* leaves. A helpful and detailed description of parts of this section is

presented by (Inada and Wildermuth, 2005). All material used had to be RNAase free and if not acquired as such was treated with RNAse inhibitor (RNase-ExitusPlus™, AppliChem) and carefully cleaned with ethanol and/or chloroform. For fixation of leaf pieces, freshly prepared Farmer`s fixative, i.e. 4:1 ethanol:acetic acid, was used as described (Kerk et al., 2003; Inada and Wildermuth, 2005; Yu et al., 2007). 4:1 ethanol: acetic acid worked the best for *Arabidopsis* leaf tissue. The fixative was cooled to 4°C on ice. The leaf pieces were carefully transferred into the fixative, and incubated for ten to twelve hours. The tissue was transferred from 1.5 mL reaction vials to tissue cassettes for dehydration in a graded ethanol series. The ethanol was replaced by the clearing agent xylene (xylene isomers, Carl Roth). Xylene removes ethanol and is miscible with paraffin (Para Plast Plus, Sigma-Aldrich and Carl Roth). These steps were performed in the following order in an automated vacuum tissue processor (Leica ASP300S): 4:1 ethanol:acetic acid (4h, RT); 50% ethanol (1h, RT); 70% ethanol (1h, RT); 95% ethanol, 0.1% eosin Y (1h, RT); 100% ethanol, 0.1% eosin Y (1h, RT); 100% ethanol, 0.1% eosin Y (1h, RT); 100% ethanol (1h, RT); 100% xylene (1h, RT); 100% xylene (1h, RT); 100% xylene (1h, 37°C); paraffin (10min, 62°C); paraffin (10min, 62°C); paraffin (10h, 62°C). The last step was set to a long period in order to avoid that the Leica ASP300S pumps out the paraffin and the sample gets destroyed. The sample was transferred to a paraffin bath at 62°C, solidified paraffin was remolten, and the tissue fixed in paraffin in plastic weigh boats in a water bath at room temperature (RT). Almost all steps were performed at RT because the Leica ASP300S is unable to cool down. Eosin Y (Sigma-Aldrich) stained the tissue so that is was visible in the paraffin blocks. Leaf sections in paraffin blocks were prepared in order to cross-section the tissue with a rotary microtome (12 to 14 µm). To get intact sections, new microtome blades were used. The paraffin ribbons, including the leaf sample, were floated on ca. 80 µL methanol (Schmid et al., 2012). The ribbon was stretched with a soft paintbrush on DNase/RNase free PEN (poly ethylene naphthalate) coated microscope slides (Carl Zeiss MicroImaging) following activation with UV-light as described by the manufacturer. Slides were dried on a 42°C warm plate to ensure evaporation of methanol and adhesion to the microscope slide. Dried paraffin was removed by carefully dumping the slide in fresh xylene for some minutes (ca. 10 min) and air dried. It was important to minimize xylene incubation time because longer treatment changed the “structure” of the PEN coat on the class slides, leading to dissociation of the PEN-foil from the slide when performing laser cutting. Similar observations were made by (Inada and Wildermuth, 2005). Deparaffinization was performed immediately before microdissection.

Laser microdissection

The Zeiss Microdissection system (Zeiss Palm Microbeam, Palm RoboSoftware 4.3 SP1) was used for isolation of tissues from prepared tissue cross sections. Deparaffinized slides with tissue were placed on the stage and visualized by a digital camera on a computer screen using the software provided by the manufacturer. Cells to cut out were encircled with an electronic pen on a touch pad and cut with a laser beam. Settings were chosen for 14 µm thick cross sections as follows: energy = 50, focus between 50 and 60, Delta (catapulting) = 10. Tissue fractions were sampled in a DNase/RNAase free 0.2 mL LMD cap. Tubes of the same size were also used by pipetting 80 µL of RLT buffer (Quiagen) into the lid. Cutting was performed for maximum 1 hour per sampling. The samples in the tubes were directly transferred on ice and stored at -80°C.

RNA preparation, quality control and cDNA synthesis

Before starting with RNA isolation, tissue samples were homogenized by QIashredder columns as described by the manufacturer (Quiagen). RNA was isolated using the RNeasy Plant Mini Kit (Quiagen), following the manufacturer´s instructions. Optional on-column-DNAse treatment was performed as described by the manufacturer (Quiagen). RNase was eluted with 16 µL RLT-buffer, immediately placed on ice and stored at -80°C till further use. Quality control was assessed by RNA microchips (Agilent 2100 Bioanalyzer Agilent; (Masotti and Precke, 2006) at the Biologisch-Medizinische Forschungszentrum (BMFZ), HHU Düsseldorf. cDNA was not synthesized. Appriate kits for high quality cDNA synthesis for subsequent deep-sequencing might be: Ovation® RNA-Seq System (Nugen®).

Supplemental Figures

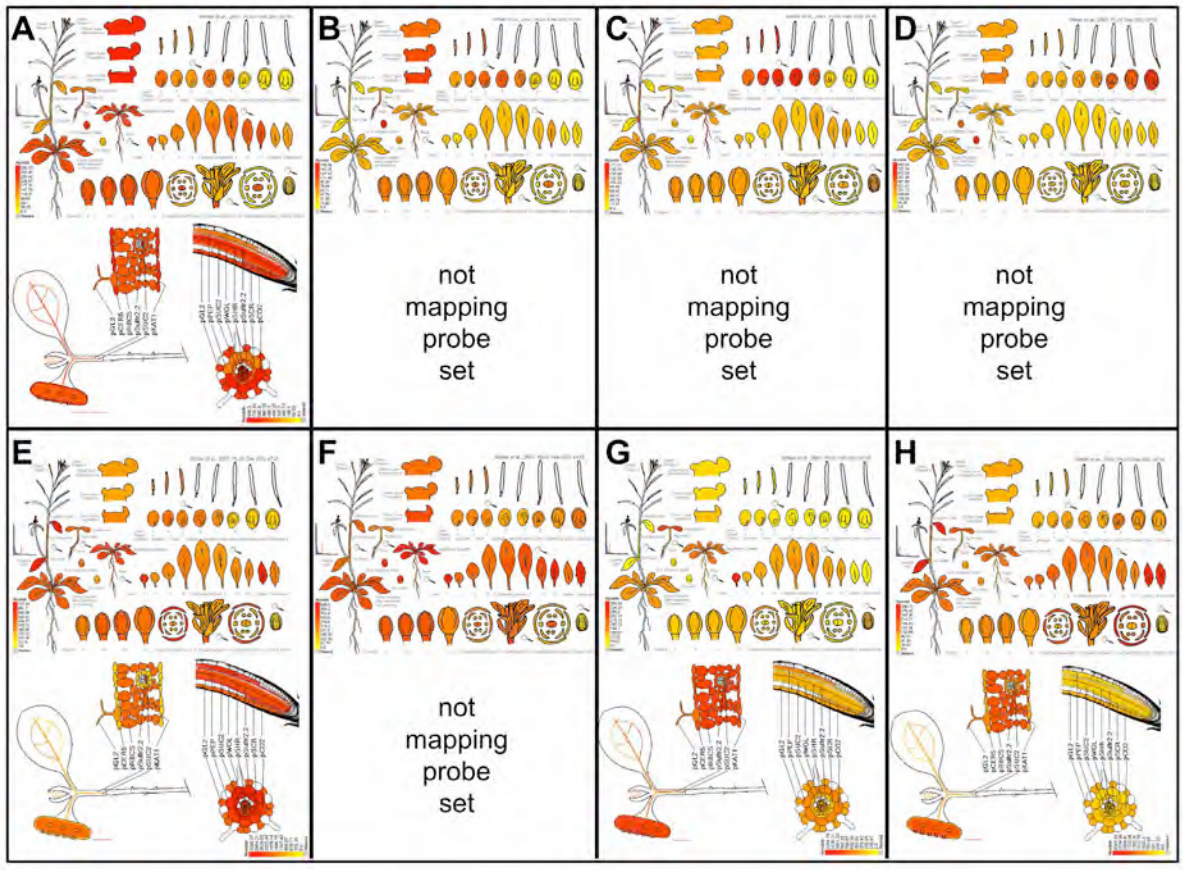

Supplemental Figure 1. Tissue and cell specific expression profiles of *Arabidopsis* genes encoding proteins with DUF3411, inferred from the efp- and efp translatome browser, respectively. **(A)** At2g37860 (RE). **(B)** At5g22790 (RER-1). **(C)** At3g08630. **(D)** At3g08640. **(E)** At5g12470. **(F)** At5g24690. **(G)** At2g40400. **(H)** At3g56140.

Supplemental Tables

Supplemental Table 1. Relative fatty acid levels of col-0 and *re-6* plant rosettes.

Fatty Acid	col-0		re-6		p-value	Sig. Lev.
	Average	± S.E.	Average	± S.E.		
C16:0	10579.20	1810.40	13814.28	443.35	0.1655	ns
C16:1	276.00	55.62	373.74	27.77	0.1916	ns
C16: 3	3931.54	861.47	4922.78	149.22	0.3480	ns
Total C16	14786.74	2725.52	19110.8	600.66	0.2103	ns
C18:0	2030.32	150.37	2824.42	281.80	0.0333	*
C18:1	72.26	6.96	108.10	7.70	0.0108	*
C18:2	3788.61	616.52	5910.63	191.95	0.0214	*
C18:3	21174.28	3692.33	26401.90	847.56	0.2587	ns
Total C18	27065.48	4454.94	35245.02	1154.81	0.1564	ns
Total Fatty acids	41852.22	7178.05	54355.82	1744.60	0.1749	ns

Supplemental Table 2. Gene-specific primers used for cloning. Restriction sites (RS) are underlined. start-ATG and stop codons are in bold. Further properties are indicated in the column “comments”. FP: forward primer; RP: reverse primer. Lowercase letters indicate spacer sequences, which are necessary to be in frame with a tag in the final vector.

Name	Sequence in 5`- 3`- orientation	Direction	RS	Comments
CR1	*GGGGACAAGTTTGTACAAAAAAGCAGGCT*ccaccAT GGCAGGATGTGCAATG	FP	-	Italic: attR1 ccacc: Kozac-seq.
CR2	*GGGGACCACTTTGTACAAGAAAGCTGGGT*TCACT GACAACCGCTCAATC	RP	-	Italic: attR2
CR4	*GGGGACCACTTTGTACAAGAAAGCTGGGT*cCTGA CAACCGCTCAATCTTG	RP	-	Italic: attR2
CR5	*GGGGACCACTTTGTACAAGAAAGCTGGGT*ccCGTT TGGCAGTCATGATAA	RP	-	Italic: attR2
CR6	*GGGGACAAGTTTGTACAAAAAAGCAGGCT*ccaccAT GGGTGGTTCAGGTAGGCAAAG	FP	-	Italic: attR1 ccacc: Kozac-seq.
CR8	*GGGGACAAGTTTGTACAAAAAAGCAGGCT*ccaccAG CTGGTCAGATGCAAGGAT	FP	-	Italic: attR1 ccacc: Kozac-seq.
CR9	*GGGGACCACTTTGTACAAGAAAGCTGGGT*cCCTAC CTGAACCACCTCTAATCC	RP	-	Italic: attR2
CR10	*GGGGACCACTTTGTACAAGAAAGCTGGGT*cGAAA GATGGATCAGCCAACATT	RP	-	Italic: attR2
CR19	*GGGGACCACTTTGTACAAGAAAGCTGGGT*CTTAC CGTTTGGCAGTCATGATAAGAT	RP	-	Italic: attR2
CR39	TTCAATGTCCCTGCCATGTA	FP	-	Actin2 primer
CR40	TGAACAATCGATGGACCTGA	RP	-	Actin2 primer
CR53	ATTTTGCCGATTTCGGAAC	-	-	LBb1.3 T-DNS primer
CR94	AAACCTGTTGATGCCACAGAC	FP	-	Screening primer for SALK_073985(RER1)
CR95	TAAACCCAACTGATCAAACGC	RP	-	Screening primer for SALK_073985(RER1)
CR138	*GGGGACCACTTTGTACAAGAAAGCTGGGT*ggCCTA CCTGAACCACCTCTAATCC	RP	-	Italic: attR2
CR139	*GGGGACCACTTTGTACAAGAAAGCTGGGT*ggGAAA GATGGATCAGCCAACATT	RP	-	italic: attR2
CR145	AGAGACTCGAGAAACAAGTTTGTACAAAAAAGCTG	FP	XhoI	AGAGA: digest protection caps
CR146	AGAGACTCGAGccCCACTTTGTACAAGAAAGCTGA AC	RP	XhoI	AGAGA: digest protection caps
CR147	GGGGACAAGTTTGTACAAAAAAGCAGGCTccaccAT GGTAGCTCAAGCTCCTCATG	FP	-	ccacc: Kozac-seq.
CR148	*GGGGACCACTTTGTACAAGAAAGCTGGGT*cTTATG AGTAAAACTTGTATCCTTTTGCTT	FP	-	-
CR149	*GGGGACCACTTTGTACAAGAAAGCTGGGT*cTGAGT AAAACTTGTATCCTTTTGCTT			
CR150	GGGGACAAGTTTGTACAAAAAAGCAGGCTccaccAT GgggCATCATCACCATCACCATggtgctGGTGGTTCA GGTAGGCAAAG	-	-	6*HIS-tag ggg: Gylcin-spacer ggtgct: Gly-Ala-spacer ccacc: Kozac-seq.
CR151	*GGGGACAAGTTTGTACAAAAAAGCAGGCT*ccGAGT TGCGGAGTTTTCCAGA	FP	-	
P74	CACATACGATTTAGGTGACACTATAGAA	FP	-	-
P75	GATAATCTCATGACCAAAATCCCTTA	RP	-	-

4. Acknowledgement and Funding

The work was supported by the “Sonderforschungsbereich 590 – Inhärente und adaptive Differenzierungsprozesse”, funded by the Deutsche Forschungsgemeinschaft. The author, Christian Rosar, was supported by the “Studienstiftung des deutschen Volkes”. The yeast strains JT16, 22Δ6LL, and 22Δ8AA were kindly provided by Prof. Dr. Mechthild Tegeder (Washington State University). I thank Dr. Andrea Bleckmann and Prof. Dr. Rüdiger Simon for the vectors pAB117 and pAB146, Sarah Vigelius and Dr. Nicole Linka for pNL8, Dr. Marcel Lafos and Dr. Daniel Schubert for pGREENII-H4-GFP, and Lisa Leson and Dr. Andrea Bräutigam for pDEST-LL5. Thanks go to Ferdi Grawe (Institute for Genetics, HHU Düsseldorf; Prof. Dr. Thomas Klein) for electron microscopy, Dr. Daniel Schubert for allowance to use the stereomicroscope, and Frederique K.H. Breuers for support with confocal microscopy. I appreciate technical assistance by Katrin L. Weber and Elisabeth Klemp with GC/MS-analysis of metabolites and by Manuel Wagner for plant work. I thank Steffen Jäger for assistance with photographic documentation of plants and Simon Schliesky for protein alignment.

5. References

Amberg DC, Burke DJ, Strathern JN (2006) Yeast colony PCR. Cold Spring Harbor Protocols 2006: pdb.prot4170

Asano T, Masumura T, Kusano H, Kikuchi S, Kurita A, Shimada H, Kadowaki K (2002) Construction of a specialized cDNA library from plant cells isolated by laser capture microdissection: toward comprehensive analysis of the genes expressed in the rice phloem. Plant Journal **32:** 401-408

Baginsky S, Siddique A, Gruissem W (2004) Proteome analysis of tobacco bright yellow-2 (BY-2) cell culture plastids as a model for undifferentiated heterotrophic plastids. Journal of Proteome Research **3:** 1128-1137

Benning C (2009) Mechanisms of lipid transport involved in organelle biogenesis in plant cells. *In* Annual Review of Cell and Developmental Biology **25**: 71-91

Bernhardt K, Wilkinson S, Weber APM, Linka N (2012) A peroxisomal carrier delivers NAD plus and contributes to optimal fatty acid degradation during storage oil mobilization. Plant Journal **69:** 1-13

Bleckmann A, Weidtkamp-Peters S, Seidel CAM, Simon R (2010) Stem cell signaling in *Arabidopsis* requires CRN to localize CLV2 to the plasma membrane. Plant Physiology **152:** 166-176

Bouvier F, Linka N, Isner J-C, Mutterer J, Weber APM, Camara B (2006) *Arabidopsis* SAMT1 defines a plastid transporter regulating plastid biogenesis and plant development. The Plant Cell Online **18:** 3088-3105

Brandt S, Kloska S, Altmann T, Kehr J (2002) Using array hybridization to monitor gene expression at the single cell level. Journal of Experimental Botany **53:** 2315-2323

Braune W, Leman A, Taubert H (2007) Pflanzenanatomisches Praktikum I, Ed 9. Spektrum Akademischer Verlag, Heidelberg

Bräutigam A, Hoffmann-Benning S, Weber A (2007) Comparative proteomics of C_3 and C_4 mesophyll chloroplast envelopes and the characterization of a novel transport protein, Mep1. Photosynthesis Research **91:** PS1022

Bräutigam A, Shrestha RP, Whitten D, Wilkerson CG, Carr KM, Froehlich JE, Weber APM (2008) Low-coverage massively parallel pyrosequencing of cDNAs enables proteomics in non-model species: Comparison of a species-specific database generated by pyrosequencing with databases from related species for proteome analysis of pea chloroplast envelopes. Journal of Biotechnology **136:** 44-53

Bräutigam A, Weber APM (2009) Proteomic analysis of the proplastid envelope membrane provides novel insights into small molecule and protein transport across proplastid membranes. Molecular Plant **2:** 1247-1261

Breuers FK, Braeutigam A, Geimer S, Welzel UY, Stefano G, Renna L, Brandizzi F, Weber APM (2012) Dynamic remodeling of the plastid envelope membranes: a tool for chloroplast envelope in vivo localizations. Frontiers in Plant Science **3:** doi: 10.3389/fpls.2012.00007

Browse J, McCourt PJ, Somerville CR (1986) Fatty acid composition of leaf lipids determined after combined digestion and fatty acid methyl ester formation from fresh tissue. Analytical Biochemistry **152:** 141-145

Browse J, Sommerville C (1991) Glycerolipid biosynthesis: biochemistry and regulation. Annual Review of Plant Physiology and Plant Molecular Biology **42:** 467-505

Buhtz A, Springer F, Chappell L, Baulcombe DC, Kehr J (2008) Identification and characterization of small RNAs from the phloem of *Brassica napus*. The Plant Journal **53:** 739-749

Campbell DA, Cockshutt AM, Porankiewicz-Asplund J (2003) Analysing photosynthetic complexes in uncharacterized species or mixed microalgal communities using global antibodies. Physiologia Plantarum **119:** 322-327

Chen L, Ortiz-Lopez A, Jung A, Bush DR (2001) ANT1, an aromatic and neutral amino acid transporter in *Arabidopsis*. Plant Physiology **125:** 1813-1820

Chen LS, Bush DR (1997) LHT1, a lysine- and histidine-specific amino acid transporter in *Arabidopsis*. Plant Physiology **115:** 1127-1134

Chomczynski P, Sacchi N (1987) Single-step method of RNA isolation by acid guanidinium thiocyanate phenol chloroform extraction. Analytical Biochemistry **162:** 156-159

Chomczynski P, Sacchi N (2006) The single-step method of RNA isolation by acid guanidinium thiocyanate-phenol-chloroform extraction: twenty-something years on. Nat. Protocols **1:** 581-585

Chou M-L, Chu C-C, Chen L-J, Akita M, Li H (2006) Stimulation of transit-peptide release and ATP hydrolysis by a cochaperone during protein import into chloroplasts. The Journal of Cell Biology **175:** 893-900

Cotsaftis O, Plett D, Shirley N, Tester M, Hrmova M (2012) A two-staged model of Na^+ exclusion in rice explained by 3D modeling of HKT transporters and alternative splicing. Plos One **7**

Curtis MD, Grossniklaus U (2003) A gateway cloning vector set for high-throughput functional analysis of genes in planta. Plant Physiology 133: 462-469

Czechowski T, Bari RP, Stitt M, Scheible W-R, Udvardi MK (2004) Real-time RT-PCR profiling of over 1400 *Arabidopsis* transcription factors: unprecedented sensitivity reveals novel root- and shoot-specific genes. The Plant Journal **38:** 366-379

Day RC, Grossniklaus U, Macknight RC (2005) Be more specific! Laser-assisted microdissection of plant cells. Trends in Plant Science **10:** 397-406

Desfeux C, Clough SJ, Bent AF (2000) Female reproductive tissues are the primary target of *Agrobacterium*-mediated transformation by the *Arabidopsis* floral-dip method. Plant Physiology **123:** 895-904

Dundar E, Bush DR (2009) BAT1, a bidirectional amino acid transporter in *Arabidopsis*. Planta **229:** 1047-1056

Eicks M, Maurino V, Knappe S, Flugge UI, Fischer K (2002) The plastidic pentose phosphate translocator represents a link between the cytosolic and the plastidic pentose phosphate pathways in plants. Plant Physiology **128:** 512-522

Elmayan T, Balzergue S, Béon F, Bourdon V, Daubremet J, Guénet Y, Mourrain P, Palauqui J-C, Vernhettes S, Vialle T, Wostrikoff K, Vaucheret H (1998) *Arabidopsis* mutants impaired in cosuppression. The Plant Cell Online **10:** 1747-1757

Elmayan T, Vaucheret H (1996) Expression of single copies of a strongly expressed 35S transgene can be silenced post-transcriptionally. The Plant Journal **9:** 787-797

Emmert-Buck MR, Bonner RF, Smith PD, Chuaqui RF, Zhuang ZP, Goldstein SR, Weiss RA, Liotta LA (1996) Laser capture microdissection. Science 274: 998-1001

Engelmann S, Wiludda C, Burscheidt J, Gowik U, Schlue U, Koczor M, Streubel M, Cossu R, Bauwe H, Westhoff P (2008) The gene for the P-subunit of glycine decarboxylase from the C_4 species *Flaveria trinervia*: Analysis of transcriptional control in transgenic *Flaveria bidentis* (C_4) and *Arabidopsis* (C_3). Plant Physiology **146:** 1773-1785

Esposito G (2007) Complementary techniques: Laser capture microdissection - Increasing specificity of gene expression profiling of cancer specimens. Microarray Technology and Cancer Gene Profiling **593:** 54-65

Fiehn O, Kopka J, Dörmann P, Altmann T, Trethewey RN, Willmitzer L (2000) Metabolite profiling for plant functional genomics. Nature Biotechnology **18:** 1157-1161

Fischer K, Kammerer B, Gutensohn M, Arbinger B, Weber A, Häusler RE, Flügge UI (1997) A new class of plastidic phosphate translocators: A putative link between primary and secondary metabolism by the *phosphoenolpyruvate/phosphate* antiporter. Plant Cell **9:** 453-462

Fischer WN, Kwart M, Hummel S, Frommer WB (1995) Substrate specificity and expression profile of amino acid transporters (AAPss) in *Arabidopsis*. Journal of Biological Chemistry **270:** 16315-16320

Fischer WN, Loo DDF, Koch W, Ludewig U, Boorer KJ, Tegeder M, Rentsch D, Wright EM, Frommer WB (2002) Low and high affinity amino acid H^+-cotransporters for cellular import of neutral and charged amino acids. Plant Journal **29:** 717-731

Galili G (1995) regulation of lysine and threonine synthesis. Plant Cell **7:** 899-906

González-Bayón R, Kinsman EA, Quesada V, Vera A, Robles P, Ponce MR, Pyke KA, Micol JL (2006) Mutations in the *RETICULATA* gene dramatically alter internal architecture but have little effect on overall organ shape in *Arabidopsis* leaves. Journal of Experimental Botany **57:** 3019-3031

Gutiérrez R, Lejay L, Dean A, Chiaromonte F, Shasha D, Coruzzi G (2007) Qualitative network models and genome-wide expression data define carbon/nitrogen-responsive molecular machines in *Arabidopsis*. Genome Biology **8:** R7

Haferkamp I, Linka N (2012) Functional expression and characterisation of membrane transport proteins. Plant Biology **14:** 675-690

Halfon MS, Kose H, Chiba A, Keshishian H (1997) Targeted gene expression without a tissue-specific promoter: Creating mosaic embryos using laser-induced single-cell heat shock. Proceedings of the National Academy of Sciences of the United States of America **94:** 6255-6260

Harsman A, Bartsch P, Hemmis B, Krüger V, Wagner R (2011) Exploring protein import pores of cellular organelles at the single molecule level using the planar lipid bilayer technique. European Journal of Cell Biology **90:** 721-730

Hellens RP, Edwards EA, Leyland NR, Bean S, Mullineaux PM (2000) pGreen: a versatile and flexible binary Ti vector for Agrobacterium-mediated plant transformation. Plant Molecular Biology **42:** 819-832

Hirner A, Ladwig F, Stransky H, Okumoto S, Keinath M, Harms A, Frommer WB, Koch W (2006) *Arabidopsis* LHT1 is a high-affinity transporter for cellular amino acid uptake in both root epidermis and leaf mesophyll. Plant Cell **18:** 1931-1946

Ho M-W, Ryan A, Cummins J (1999) Cauliflower mosaic viral promoter - a recipe for disaster? Microbial Ecology in Health and Disease **11:** 194-197

Hoyos ME, Palmieri L, Wertin T, Arrigoni R, Polacco JC, Palmieri F (2003) Identification of a mitochondrial transporter for basic amino acids in *Arabidopsis thaliana* by functional reconstitution into liposomes and complementation in yeast. Plant Journal **33:** 1027-1035

Hsu LC, Chiou TJ, Chen LS, Bush DR (1993) Cloning a plant amino acid transporter by functional complementation of a yeast amino acid transport mutant. Proceedings of the National Academy of Sciences of the United States of America **90:** 7441-7445

Hull R, Covey SN, Dale P (2000) Genetically modified plants and the 35S promoter: assessing the risks and enhancing the debate. Microbial Ecology in Health and Disease **12:** 1-5

Hung WF, Chen LJ, Boldt R, Sun CW, Li HM (2004) Characterization of *Arabidopsis* glutamine phosphoribosyl pyrophosphate amidotransferase-deficient mutants. Plant Physiology **135:** 1314-1323

Inada N, Wildermuth MC (2005) Novel tissue preparation method and cell-specific marker for laser microdissection of *Arabidopsis* mature leaf. Planta **221:** 9-16

Jackson D (1991) *In situ* hybridization in plants. *In* DJ Bowles, SJ Gurr, M McPherson, eds, Molecular plant pathology: a practical approach. Oxford University Press, New York, pp 163-174

Jacobson BS, Fong F, Heath RL (1975) Carbonic-anhydrase of spinach - studies on its location, inhibition, and physiological function. Plant Physiology **55:** 468-474

Jiao YL, Tausta SL, Gandotra N, Sun N, Liu T, Clay NK, Ceserani T, Chen MQ, Ma LG, Holford M, Zhang HY, Zhao HY, Deng XW, Nelson T (2009) A transcriptome atlas of rice cell types uncovers cellular, functional and developmental hierarchies. Nature Genetics **41:** 258-263

Jing YJ, Cui DY, Bao F, Hu ZB, Qin ZX, Hu YX (2009) Tryptophan deficiency affects organ growth by retarding cell expansion in *Arabidopsis*. Plant Journal **57:** 511-521

Kammerer B, Fischer K, Hilpert B, Schubert S, Gutensohn M, Weber A, Flügge U-I (1998) Molecular characterization of a carbon transporter in plastids from heterotrophic tissues: the glucose 6-phosphate/phosphate antiporter. The Plant Cell Online **10:** 105-117

Keegstra K, Cline K (1999) Protein import and routing systems of chloroplasts. The Plant Cell Online **11:** 557-570

Kehr J (2003) Single cell technology. Current Opinion in Plant Biology **6:** 617-621

Kerk NM, Ceserani T, Tausta SL, Sussex IM, Nelson TM (2003) Laser capture microdissection of cells from plant tissues. Plant Physiology **132:** 27-35

Kinsman EA, Pyke KA (1998) Bundle sheath cells and cell-specific plastid development in *Arabidopsis* leaves. Development **125:** 1815-1822

Kleber R, Kehr J (2006) Preparation and quality assessment of RNA from cell-specific samples obtained by laser microdissection. *In* J Salinas, JJ Sanchez-Serrano, eds, Arabidopsis Protocols, Vol 2nd edition. Humana Press, Totowa, New Jersey, pp 367-377

Kleffmann T, Russenberger D, von Zychlinski A, Christopher W, Sjolander K, Gruissem W, Baginsky S (2004) The *Arabidopsis thaliana* chloroplast proteome reveals pathway abundance and novel protein functions. Current Biology **14:** 354-362

Knappe S, Löttgert T, Schneider A, Voll L, Flügge UI, Fischer K (2003) Characterization of two functional *phosphoenolpyruvate/phosphate translocator (PPT)* genes in *Arabidopsis*-AtPPT1 may be involved in the provision of signals for correct mesophyll development. Plant Journal **36:** 411-420

Krueger S, Giavalisco P, Krall L, Steinhauser M-C, Büssis D, Usadel B, Flügge U-I, Fernie AR, Willmitzer L, Steinhauser D (2011) A topological map of the compartmentalized *Arabidopsis thaliana* leaf metabolome. Plos One **6:** e17806

Kumar S, Asif M, Chakrabarty D, Tripathi R, Trivedi P (2011) Differential expression and alternative splicing of rice sulphate transporter family members regulate sulphur status during plant growth, development and stress conditions. Functional and Integrative Genomics **11:** 259-273

Lee JY, Levesque M, Benfey PN (2005) High-throughput RNA isolation technologies. New tools for high-resolution gene expression profiling in plant systems. Plant Physiology **138:** 585-590

Lee YH, Foster J, Chen J, Voll LM, Weber APM, Tegeder M (2007) AAP1 transports uncharged amino acids into roots of *Arabidopsis*. Plant Journal **50:** 305-319

Lehmann S, Gumy C, Blatter E, Boeffel S, Fricke W, Rentsch D (2011) In planta function of compatible solute transporters of the AtProT family. Journal of Experimental Botany **62:** 787-796

Li-Beisson Y, Shorrosh B, Beisson F, Andersson MX, Arondel V, Bates PD, Baud S, Bird D, Debono A, Durrett TP, Franke RB, Graham IA, Katayama K, Kelly AA, Larson T, Markham JE, Miquel M, Molina I, Nishida I, Rowland O, Samuels L, Schmid KM, Wada H, Welti R, Xu C, Zallot R, Ohlrogge J (2010) Acyl-lipid metabolism. The Arabidopsis book / American Society of Plant Biologists **8:** e0133-e0133

Linka N (2001) Evolution nicht-mitochondrialer Nukleotid-Transporter. Technische Universität Kaiserslautern. PhD-thesis.

Linka N, Theodoulou FL, Haslam RP, Linka M, Napier JA, Neuhaus HE, Weber APM (2008) Peroxisomal ATP import is essential for seedling development in *Arabidopsis thaliana*. Plant Cell **20:** 3241-3257

Loddenkötter B, Kammerer B, Fischer K, Flügge UI (1993) Expression of the functional mature chloroplast triose phosphate translocator in yeast internal membranes and purification of the histidine-tagged protein by a single metal-affinity chromatography step. Proceedings of the National Academy of Sciences **90:** 2155-2159

Masotti A, Precke T (2006) Analysis of small RNAs with the Agilent 2100 Bioanalyzer. Nature Methods **3**

Mills WR, Lea PJ, Miflin BJ (1980) photosynthetic formation of the aspartate family of amino acids in isolated-chloroplasts. Plant Physiology **65:** 1166-1172

Mishiba K-i, Nishihara M, Nakatsuka T, Abe Y, Hirano H, Yokoi T, Kikuchi A, Yamamura S (2005) Consistent transcriptional silencing of 35S-driven transgenes in gentian. The Plant Journal **44:** 541-556

Murashige T, Skoog F (1962) A revised medium for rapid growth and bio assays with tobacco tissue cultures. Physiologia Plantarum **15:** 473-497

Mustroph A, Zanetti ME, Jang CJH, Holtan HE, Repetti PP, Galbraith DW, Girke T, Bailey-Serres J (2009) Profiling translatomes of discrete cell populations resolves altered cellular priorities during hypoxia in *Arabidopsis*. Proceedings of the National Academy of Sciences of the United States of America **106:** 18843-18848

Nakazono M, Qiu F, Borsuk LA, Schnable PS (2003) Laser-capture microdissection, a tool for the global analysis of gene expression in specific plant cell types: Identification of genes expressed differentially in epidermal cells or vascular tissues of maize. Plant Cell **15:** 583-596

Nelson T, Tausta SL, Gandotra N, Liu T (2006) Laser microdissection of plant tissue: What you see is what you get. *In* Annual Review of Plant Biology **57:** 181-201

Nikiforova VJ, Bielecka M, Gakière B, Krueger S, Rinder J, Kempa S, Morcuende R, Scheible WR, Hesse H, Hoefgen R (2006) Effect of sulfur availability on the integrity of amino acid biosynthesis in plants. Amino Acids **30:** 173-183

Nikiforova VJ, Daub CO, Hesse H, Willmitzer L, Hoefgen R (2005) Integrative gene-metabolite network with implemented causality deciphers informational fluxes of sulphur stress response. Journal of Experimental Botany **56:** 1887-1896

Nozawa A, Nanamiya H, Miyata T, Linka N, Endo Y, Weber APM, Tozawa Y (2007) A cell-free translation and proteoliposome reconstitution system for functional analysis of plant solute transporters. Plant and Cell Physiology **48:** 1815-1820

Ohlrogge J, Browse J (1995) Lipid biosynthesis. Plant Cell **7:** 957-970

Pasch JC, Nickelsen J, Schünemann D (2005) The yeast split-ubiquitin system to study chloroplast membrane protein interactions. Applied Microbiology and Biotechnology **69:** 440-447

Pohlmeyer K, Soll J, Grimm R, Hill K, Wagner R (1998) A high-conductance solute channel in the chloroplastic outer envelope from pea. The Plant Cell Online **10:** 1207-1216

Pohlmeyer K, Soll J, Steinkamp T, Hinnah S, Wagner R (1997) Isolation and characterization of an amino acid-selective channel protein present in the chloroplastic outer envelope membrane. Proceedings of the National Academy of Sciences of the United States of America **94:** 9504-9509

Pudelski B, Schock A, Hoth S, Radchuk R, Weber H, Hofmann Jr, Sonnewald U, Soll J, Philippar K (2012) The plastid outer envelope protein OEP16 affects metabolic fluxes during ABA-controlled seed development and germination. Journal of Experimental Botany **63:** 1919-1936

Renné P, Dreßen U, Hebbeker U, Hille D, Flügge U-I, Westhoff P, Weber APM (2003) The *Arabidopsis* mutant *dct* is deficient in the plastidic glutamate/malate translocator DiT2. The Plant Journal **35:** 316-331

Rennie EA, Turgeon R (2009) A comprehensive picture of phloem loading strategies. Proceedings of the National Academy of Sciences **106:** 14162-14167

Rentsch D, Laloi M, Rouhara I, Schmelzer E, Delrot S, Frommer WB (1995) *NTR1* encodes a high affinity oligopeptide transporter in *Arabidopsis*. Febs Letters **370:** 264-268

Rentsch D, Schmidt S, Tegeder M (2007) Transporters for uptake and allocation of organic nitrogen compounds in plants. Febs Letters **581:** 2281-2289

Richard M, Muschalik N, Grawe F, Özüyaman S, Knust E (2009) A role for the extracellular domain of crumbs in morphogenesis of *Drosophila* photoreceptor cells. European Journal of Cell Biology **88:** 765-777

Rieu I, Powers SJ (2009) Real-time quantitative RT-PCR: design, calculations, and statistics. The Plant Cell Online **21:** 1031-1033

Sambrook J, Russell DW, Irwin N, Janssen KA (2001) Molecular cloning: a laboratory manual, third edition. Cold Spring Harbor Laboratory Press, Cold Spring Harbor, New York

Sanders A, Collier R, Trethewy A, Gould G, Sieker R, Tegeder M (2009) AAP1 regulates import of amino acids into developing *Arabidopsis* embryos. The Plant Journal **59:** 540-552

Scheible W-R, Morcuende R, Czechowski T, Fritz C, Osuna D, Palacios-Rojas N, Schindelasch D, Thimm O, Udvardi MK, Stitt M (2004) Genome-wide reprogramming of primary and secondary metabolism, protein synthesis, cellular growth processes, and the regulatory infrastructure of *Arabidopsis* in response to nitrogen. Plant Physiology **136:** 2483-2499

Schichnes D, Nemson J, Sohlberg L, Ruzin SE (1998) Microwave protocols for paraffin microtechnique and *in situ* localization in plants. Microscopy and Microanalysis **4:** 491-496

Schiestl RH, Gietz RD (1989) High efficiency transformation of intact yeast cells using single stranded nucleic acids as a carrier. Current Genetics **16:** 339-346

Schmid MW, Schmidt A, Klostermeier UC, Barann M, Rosenstiel P, Grossniklaus U (2012) A powerful method for transcriptional profiling of specific cell types in eukaryotes: laser-assisted microdissection and RNA sequencing. Plos One **7:** e29685

Schmidt A, Baumann N, Schwarzkopf A, Frommer WB, Desimone M (2006) Comparative studies on ureide permeases in *Arabidopsis thaliana* and analysis of two alternative splice variants of AtUPS5. Planta **224:** 1329-1340

Schwacke R, Schneider A, van der Graaff E, Fischer K, Catoni E, Desimone M, Frommer WB, Flugge UI, Kunze R (2003) ARAMEMNON, a novel database for *Arabidopsis* integral membrane proteins. Plant Physiology **131:** 16-26

Sessions A, Weigel D, Yanofsky MF (1999) The *Arabidopsis thaliana MERISTEM LAYER 1* promoter specifies epidermal expression in meristems and young primordia. The Plant Journal **20:** 259-263

Slocum RD (2005) Genes, enzymes and regulation of arginine biosynthesis in plants. Plant Physiology and Biochemistry **43:** 729-745

Smith MD, Rounds CM, Wang F, Chen K, Afitlhile M, Schnell DJ (2004) AtToc159 is a selective transit peptide receptor for the import of nucleus-encoded chloroplast proteins. The Journal of Cell Biology **165:** 323-334

Spyropoulos IC, Liakopoulos TD, Bagos PG, Hamodrakas SJ (2004) TMRPres2D: high quality visual representation of transmembrane protein models. Bioinformatics **20:** 3258-3260

Streatfield SJ, Weber A, Kinsman EA, Häusler RE, Li JM, Post-Beittenmiller D, Kaiser WM, Pyke KA, Flügge UI, Chory J (1999) The *phosphoenolpyruvate/phosphate translocator* is required for phenolic metabolism, palisade cell development, and plastid-dependent nuclear gene expression. Plant Cell **11:** 1609-1621

Su YH, Frommer WB, Ludewig U (2004) Molecular and functional characterization of a family of amino acid transporters from arabidopsis. Plant Physiology **136:** 3104-3113

Svatos A (2011) Single-cell metabolomics comes of age: new developments in mass spectrometry profiling and imaging. Analytical Chemistry **83:** 5037-5044

Svennerstam H, Ganeteg U, Nasholm T (2008) Root uptake of cationic amino acids by Arabidopsis depends on functional expression of amino acid permease. New Phytologist **180:** 620-630

Svennerstam H, Jämtgård S, Ahmad I, Huss-Danell K, Näsholm T, Ganeteg U (2011) Transporters in *Arabidopsis* roots mediating uptake of amino acids at naturally occurring concentrations. New Phytologist **191:** 459-467

Tanaka J, Fink GR (1985) The histidine permease gene (Hip1) Of *Saccharomyces cerevisiae*. Gene **38:** 205-214

Tegeder M (2012) Transporters for amino acids in plant cells: some functions and many unknowns. Current Opinion in Plant Biology **15:** 315-321

Tegeder M, Offler CE, Frommer WB, Patrick JW (2000) Amino acid transporters are localized to transfer cells of developing pea seeds. Plant Physiology **122:** 319-325

Tegeder M, Offler CE, Frommer WB, Patrick JW (2000) Amino acid transporters are localized to transfer cells of developing pea seeds. Plant Physiology **122:** 319-326

Tegeder M, Weber APM (2006) Metabolite transporters in the control of plant primary metabolism. *In* WC Plaxton, MT McManus, eds, Control of Primary Metabolism in Plants, Vol 22. Blackwell Publishing, Oxford, pp 85-120

Udvardi MK, Czechowski T, Scheible W-R (2008) Eleven Golden Rules of Quantitative RT-PCR. The Plant Cell Online **20:** 1736-1737

Urquhart AA, Joy KW (1981) Use of phloem exudate technique in the study of amino acid transport in pea plants. Plant Physiology **68:** 750-754

Vidal EA, Gutiérrez RA (2008) A systems view of nitrogen nutrient and metabolite responses in *Arabidopsis*. Current Opinion in Plant Biology **11:** 521-529

Weber A, Flügge U-I (2002) Interaction of cytosolic and plastidic nitrogen metabolism in plants. Journal of Experimental Botany **53:** 865-874

Weibull J, Melin G (1990) Free amino acid content of phloem sap from *Brassica* plants in relation to performance of *Lipaphis erysimi* (Hemiptera: *Aphididae*). Annals of Applied Biology **116:** 417-423

Wiludda C, Schulze S, Gowik U, Engelmann S, Koczor M, Streubel M, Bauwe H, Westhoff P (2012) Regulation of the photorespiratory GLDPA Gene in C_4 *Flaveria*: An intricate interplay of transcriptional and posttranscriptional processes. The Plant Cell Online **24:** 137-151

Winter D, Vinegar B, Nahal H, Ammar R, Wilson GV, Provart NJ (2007) An "Electronic Fluorescent Pictograph" browser for exploring and analyzing large-scale biological data sets. Plos One **2:** 1-12

Wuest SE, Vijverberg K, Schmidt A, Weiss M, Gheyselinck J, Lohr M, Wellmer F, Rahnenfuehrer J, von Mering C, Grossniklaus U (2010) *Arabidopsis* female gametophyte gene expression map reveals similarities between plant and animal gametes. Current Biology **20:** 506-512

Yu YY, Lashbrook CC, Hannapel DJ (2007) Tissue integrity and RNA quality of laser microdissected phloem of potato. Planta **226:** 797-803

Zhu X, Shaw PN, Pritchard J, Newbury J, Hunt EJ, Barrett DA (2005) Amino acid analysis by micellar electrokinetic chromatography with laser-induced fluorescence detection: Application to nanolitre-volume biological samples from *Arabidopsis thaliana* and *Myzus persicae*. Electrophoresis **26:** 911-919

The authors` contributions to the Addendum

C.R. performed all experiments. Andrea Bräutigam established Table 1. Protein alignment (Figure 2) was performed by Simon Schliesky.

VIII. Acknowledgements / Danksagungen

Ich danke:

Prof. Dr. Andreas Weber für die Möglichkeit, meine Doktorarbeit an seinem Institut durchführen zu können und für die hilfreiche Betreuung, Unterstützung und stete Diskussionsbereitschaft.

Prof. Dr. Rüdiger Simon für die Möglichkeit, die LMD-Experimente an seinem Institut durchführen zu können und die hilfreichen Anregungen als Kommissionsmitglied und darüber hinaus. Nicht zu vergessen, die Übernahme des Koreferats als 2. Berichterstatter.

Prof. Dr. Peter Westhoff für die Anregungen und fruchtbaren Diskussionen im Rahmen der "Committee Meetings".

Dr. Andrea Bräutigam für die Betreuung, die hilfreichen Diskussionen, die "Deals" und für die Unterstützung bei den Publikationen/Manuskripten.

Manuel Wagner für die Unterstützung im Labor.

Dr. Nicole Linka und **Dr. Marc Linka** für ihre freundliche Hilfe bei diversen Projekten und die ständig "offenen Ohren".

Dr. Fabio Facchinelli für das Korrekturlesen und für lustige Pokerabende.

Dr. Dunia del Carpio für die gemeinsame Zeit am LMD-Projekt.

Katrin Weber, **Elisabeth Klemp** und **Maria Graf** für die MS-Experimente.

Dr. Marion Eisenhuth für Diskussionen und die gemeinsamen Fitness-Kurse.

Freddy Breuers für die Hilfe am Fokalen, die äußerste Hilfsbereitschaft, die Gespräche und die lustige Zeit.

Sarah Vigelus für die tolle Zeit als Labornachbarin und dafür dass du "da" warst/bist.

Dr. Thea Pick und **Katja Paas** für die schöne Zeit im Büro.

Und allen langjährigen und anderen Kollegen, wie **Manuel Sommer**, **Christian Bordych**, **Jan Wiese**, **Kristin Bernhardt**, **Nils Jaspert**, **Alexandra Meier**, **Canan Külahoglu**, und **allen**, die ich vergessen habe.

Allen, die an den **Publikationen** und den **Manuskripten beteiligt** waren.

Den **Gärtnern** für die Betreuung meiner Pflanzen.

Meinen **Freunden**, allen voran **Michael Ostertag**, **Stefan Herwig**, **Dr. Matthias Bauch** und **Dr. Steffi Stieb**, für die Unterstützung an schlechten und das Mitfreuen an freudigen Tagen, danke!

Meinen **Eltern** für das Verständnis und die Unterstützung.

Hannah Mohr für die Liebe und das Verständnis.

Der **Studienstiftung des deutschen Volkes** für das Stipendium und ihre Unterstützung.